Subplate populations in normal and pathological cortical development

Franziska Oeschger

Lincoln College

University of Oxford

A thesis submitted for the degree of

Doctor of Philosophy

Hilary 2011

Abstract

Subplate populations in normal and pathological cortical development

Franziska Oeschger

Lincoln College

A thesis submitted for the degree of Doctor of Philosophy

Hilary 2001

The subplate layer of the cerebral cortex is comprised of a heterogeneous population of cells and contains some of the earliest-generated neurons. Subplate plays a fundamental role in cortical development. In the embryonic brain, subplate cells contribute to the guidance and areal targeting of corticofugal and thalamic axons. At later stages, these cells are involved in the maturation and plasticity of the cortical circuitry and the establishment of functional modules. In my thesis, I aimed to further characterize the embryonic murine subplate by establishing a gene expression profile of this population at embryonic day 15.5 (E15.5) using laser capture microdissection combined with microarrays. I found over 250 transcripts with presumed higher expression in the subplate at E15.5. Using quantitative RT-PCR, in situ hybridization and immunohistochemistry, I have confirmed specific expression in the E15.5 subplate for 13 selected genes which have not been previously associated with this compartment. In the reeler mutant, the expression pattern of a majority of these genes was shifted in accordance with the altered position of subplate cells. These genes belong to several functional groups and likely contribute to the maturation and electrophysiological properties of subplate cells and to axonal growth and guidance. The roles of two selected genes - cadherin 10 (Cdh10) and Unc5 homologue c (Unc5c) - were explored in more detail. Preliminary results suggest an involvement of Cdh10 in subplate layer organization while Unc5c could mediate the waiting period of subplate corticothalamic axons in the internal capsule. Finally, I compared the expression of a selection of subplate-specific genes (subplate markers) between mouse and rat and found some surprising species differences. Confirmed subplate markers were used to monitor subplate injury in a rat model of preterm hypoxia-ischemia and it appeared that deep cortical layers including subplate showed an increased vulnerability over upper layers. Further characterization of subplate-specific genes will allow us to broaden our understanding of molecular mechanisms underlying subplate properties and functions in normal and pathological development.

Acknowledgments

During the 3.5 years of my DPhil, I've had the privilege to work with a number of extraordinary colleagues. They all have supported me and this thesis in numerous ways - by advising on my plans, discussing my hypotheses, sharing their knowledge and skills, listening to my worries and always giving me a helping hand when needed. I am deeply thankful for their kindness and generosity.

Zoltán Molnár gave me the opportunity to join his research group and Oxford University. With his kind, honest and generous approach, he provided a friendly and stimulating working and learning environment. His optimism and trust have helped me at numerous times to overcome my skepticism and to progress further.

Wei-Zhi Wang has taught me many of the techniques and skills underlying this thesis and collaborated with me on several projects. We have spent uncountable hours together microdissecting hundreds of tissue samples, sectioning dozens of brains, coverslipping boxes of slides and extracting tiny amounts of RNA. Wei-Zhi's patience and diligence helped to surmount many technical challenges and to bring difficult projects to completion.

Anna Hoerder-Suabedissen has given thoughtful advice on many conceptual and technical aspects of this thesis. Her critical and careful thinking has helped me at many times to refine my approach and hypotheses. She also often lent a helping hand and generously shared material and data.

Amanda Cheung has helped me with the animal and slice culture work used in this thesis. Thanks to her skills and dedication, I had the opportunity to expand my project and to get insight into a different set of very useful techniques.

Vanessa Ginet has greatly contributed to the hypoxia-ischemia work – both by providing one of the models and through enthusiastic and knowledgeable advice.

Sheena Lee provided the microarray service and shared her expertise during the optimization of the laser capture microdissection and the validation of the data.

Tamara Sirrey, Lisa Bluy, Helen Stolp, Tom Lickiss, Navneet Vasistha, Shinichi Kondo and Fernando García-Moreno all generously supported me with advice, suggestions and a helping hand.

The staff of the Department of Physiology, Anatomy and Genetics has provided technical support and a safe working environment throughout my DPhil.

During my time in Oxford, I've been supported by Lincoln College and its staff. In particular, my college advisor Dr Dennis has lent a patient ear and given thoughtful advice in the early stages of my DPhil. My stay in Oxford wouldn't have been possible without the generous financial support of the Berrow Foundation.

My husband, parents and siblings, sister-in-law, family and friends in Switzerland and Oxford have been my source of strength and happiness. My husband Oleg has supported me all the way. He patiently fixed my computer problems, advised on software and web tools and helped me with my illustrations and thesis publishing. More importantly, though, he listened to my worries, gave me the confidence to overcome my fears and encouraged me to enjoy my time in Oxford to the fullest. His trust and love have carried me every day.

Collaborations

The work described in this thesis is largely my own but was greatly helped by the following contributions:

- The optimization of the laser capture microdissection protocol (Chapter 2) as well as the microdissection of samples for the microarray and qRT-PCR (Chapter 3) was a joint effort between Dr Wei-Zhi Wang and me. We contributed equally to all the steps including tissue collection, section preparation, laser microdissection and RNA extraction.

- Quality of RNA from laser microdissected samples was assessed by Ms Sheena Lee from the OXION microarray facility, Oxford (Chapters 2 & 3). Ms Lee also performed the microarray experiment, i.e. the preparation of cDNA, hybridization and raw data analysis (Chapter 3).

- Initial qRT-PCR for the confirmation of microarray data was planned and performed with the help of Dr Wang, later experiments and all data analyses were done by me (Chapter 3).

- Brains for in situ hybridization and immunohistochemistry were often collected with the help of Dr Wang. The large majority of brains were cut by me but some sections were provided by Dr Wang or Dr Amanda Cheung (Chapters 5 & 7).

- All perfusions were either performed by Prof Zoltán Molnár or Dr Cheung (Chapters 5 & 7) or perfused brains were sent to me from abroad (Chapter 8).

- Reeler mutant brains were provided by Prof André Goffinet, Université catholique de Louvain, Brussels. Free-floating sections of P8 reeler mutant brains were cut by Dr Anna Hoerder-Suabedissen (Chapter 4).

- Gad67-GFP brains were provided by Dr Sonia Rakic and Prof John Parnavelas, University College London, UK (Chapter 5).

- About half of the RNA probes for in situ hybridizations were generated by Dr Wang, sometimes with my assistance. The other half was designed and generated by me, often

with her help (Chapters 4, 5, 6 & 7). The RNA probe against Tbr2 was provided by Mr Navneet Vasistha (Chapter 6 Part I).

- In situ hybridization experiments were often performed with a helping hand from Dr Wang. The in situ hybridizations on E15.5 mouse against Nt5dc2, NeuroD1, Sema6d and 1190002N15Rik were done by Dr Wang (Chapter 4). Dr Wang also provided the images for MoxD1 and Ddc expression in mouse in Fig7_2 (Chapter 7).

- The extracortical expression patterns of subplate-enriched genes were described with the help of Dr Fernando García-Moreno (Chapter 5).

- Cdh10 expression in the neuroblastoma cell line was assessed by Dr Tamara Sirrey (Chapter 6 Part I).

- Silencing constructs against Cdh10 were designed and prepared by Dr Cheung with the help of Dr Sirrey and Ms Lisa Bluy. EYFP and DsRed constructs were provided by Prof Nobuhiko Yamamoto, Ossaka, Japan. In vitro electroporation, slice cultures and manual dissections of electroporated tissues were done jointly between Dr Cheung and me. All in utero electroporations were performed by Dr Cheung in the laboratory of Prof Yamamoto with a helping hand from members of his lab. Dr Cheung also collected the brains and helped to screen brains for electroporated cells (Chapter 6 Part I).

- DiI crystals for tracing experiments were placed into the embryonic brains by Dr Hoerder-Suabedissen (Chapter 6 Part II).

- The preterm hypoxia-ischemia models were either prepared by Dr Vanessa Ginet in the laboratory of Prof Peter Clarke, University of Lausanne (Model 1) or by Ms Anne Sheldon in the laboratory of Prof Donna Ferriero, University of California, San Francisco, USA (Model 2).

Important note:

- Chapter 2 was published in: Wang WZ*, Oeschger FM*, Lee S, Bitoun E and Molnár Z. High quality RNA from multiple brain regions simultaneously acquired by laser capture microdissection. BMC Mol Biol. 2009 Jul 6;10:69 *joint first authorship (see Appendix).

- Chapter 7 was largely incorporated into: Wang WZ, Oeschger FM, Montiel JF, García-Moreno F, Hoerder-Suabedissen A, Krubitzer L, Ek J, Saunders N, Reim K, Villalón A and Molnár Z. Comparative aspects of subplate zone studies with gene expression in sauropsids and mammals. In press in Cerebral Cortex (see Appendix).

Contents

Abbreviations

A1	primary auditory cortex
ABC	avidin-biotinylated enzyme complex
Abca8a	ATP-binding cassette, sub-family A (ABC1), member 8a
AMPA	α-amino-3-hydroxy-5-methyl-4-isoxazolepropionic acid
ASD	autism spectrum disorder
ATP	adenosine triphosphate
BDNF	brain-derived neurotrophic factor
BrdU	bromodeoxyuridine
CCA	common carotid artery
Cdh10/18	cadherin 10/18
cDNA	complementary DNA
CNS	central nervous system
CP	cortical plate
Cplx3	complexin 3
Csmd3	CUB and Sushi multiple domains 3
CTA	corticothalamic afferent
Ctgf	connective tissue growth factor
DAB	diaminobenzamide
DAPI	4',6-diamidino-2-phenylindole
Dcc	deleted in coleorectal cancer
Ddc	dopa decarboxylase
DiI	1,1'-didodecyl-3,3,3',3'-tetra-methylindocarbocyanine perchlorate
DNA	deoxyribonucleic acid
DTB	diencephalic-telencephalic boundary
E	embryonic day
ECM	extracellular matrix
eGFP	enhanced GFP
Er81	ets variant gene 1
EtOH	ethanol
FACS	fluorescent-activated cell sorting
Fgf	fibroblast growth factor
FoxP2	forkhead box P2
GABA	γ-Aminobutyric acid
Gabra5	GABA-A receptor, subunit α5

Gad65/67	glutamate decarboxylase 65/67
GFP	green fluorescent protein
HI	hypoxia-ischemia
IC	internal capsule
IHC	immunohistochemistry
ISEL	in situ end labeling
ISH	in situ hybridization
IZ	intermediate zone
KAT-I	kynurenine aminotransferase I
Kcnt2	potassium channel, subfamily T, member 2
KO	knock-out
LCM	laser capture microdissection
LGE	lateral ganglionic eminence
LGN	lateral geniculate nucleus
LTD	long-term depression
LTP	long-term potentiation
M1	primary motor cortex
MAP2	microtubule associated protein 2
MBP	myelin basic protein
MGE	medial ganglionic eminence
MGN	medial geniculate nucleus
MoxD1	monooxygenase DBH-like 1
MRI	magnetic resonance imaging
mRNA	messenger RNA
MZ	marginal zone
NeuN	neuronal nuclei
NMDA	N-Methyl-D-aspartic acid
Nurr1	nuclear receptor related 1
Ogfrl1	opioid growth factor receptor like 1
P	postnatal day
$p75^{NTR}$	neurotrophin receptor p75
PBS	phosphate-buffered saline
PCR	polymerase chain reaction
PFA	paraformaldehyde
Pls3	plastin 3/T-plastin
PP	preplate
PR	progesterone receptor
PSPB	pallial-subpallial boundary
PVL	periventricular leukomalacia
qRT-PCR	quantitative RT-PCR

Rcan2	regulator of calcineurin 2
RIN	RNA integrity number
RNA	ribonucleic acid
RT	room temperature
RT-PCR	reverse transcription PCR
S1	primary somatosensory cortex
Slc8a2	solute carrier family 8 (sodium/calcium exchanger), member 2
SP	subplate
SRK	shaking-rat Kawasaki
STDP	spike timing-dependent plasticity
Sv2b	synaptic vesicle 2b
SVZ	subventricular zone
Tbr2	T-brain gene 2
TBS	Tris-buffered saline
TCA	thalamocortical afferent
TE	Tris-EDTA
tPA	tissue plasminogen activator
TRH	thyrotropin releasing hormone
tRN	thalamic reticular nucleus
TUNEL	terminal deoxynucleotidyl transferase dUTP nick end labeling
Unc5c	unc5 homologue c
UV	ultraviolet
V1	primary visual cortex
VB	ventrobasal thalamus
VZ	ventricular zone
WT	wild-type
Zdhhc2	zinc finger, DHHC domain containing 2

Chapter 1 Introduction

1.1 Development of the neocortex

The neocortex is unique to mammals and is responsible for higher cognitive functions including the processing and interpretation of sensory information, the control of voluntary movement and conscious thought. The mature cortex contains approximately 20 billion neurons in human[1,2] and 14 million neurons in mouse[3], and about 1.5 times more glial cells (oligodendrocytes, astrocytes and microglia)[1,2,3]. There are two basic neuronal cell types – the glutamatergic excitatory neurons which constitute the large majority of cortical neurons and the GABAergic inhibitory neurons which make up about 20% of cortical neurons. These two basic neuron classes are very heterogeneous and can be further subdivided based on morphology, electrophysiological properties, connectivity and gene expression (reviewed in[4,5]).

1.1.1 Radial and tangential compartmentalization of the neocortex

The neocortex can be radially subdivided into six layers which differ in neuronal cell type composition, density and connectivity (Fig 1_1 a). The deep cortical layers VI and V contain projection neurons responsible for the output to subcortical structures including the thalamus, basal ganglia, superior colliculus and pons. Neurons in the upper layers II and III provide mainly cortico-cortical connectivity with ipsi- and contralateral cortical areas. Neurons in layer IV receive the major inputs into the cortex relayed through the thalamus[6]. In the tangential dimension, the neocortex is organized into functional areas which can be distinguished based on cytoarchitecture, gene expression and connectivity (Fig 1_1 b). In all mammals, there are four primary cortical areas – the primary somatosensory (S1), auditory (A1), visual (V1) and motor (M1) cortices. These primary areas are connected to higher-order areas underlying more complex processing and integration. In the human cortex, Brodmann originally identified 44 histologically distinct areas[7] which were further refined and subdivided by Economo and Koskinas into more than a hundred cortical fields[8] (Fig 1_1b). Many of them have since been correlated to diverse cortical functions[9,10].

The development of the neocortex proceeds from a simple epithelium of apparently homogeneous cells to a highly organized structure containing a huge diversity of neuronal cell types which are specifically connected to other cortical and extracortical neurons. It is now widely accepted that the specification of neuronal cell types and the establishment of both laminar and areal organization are controlled by both intrinsic and extrinsic mechanisms[11,12].

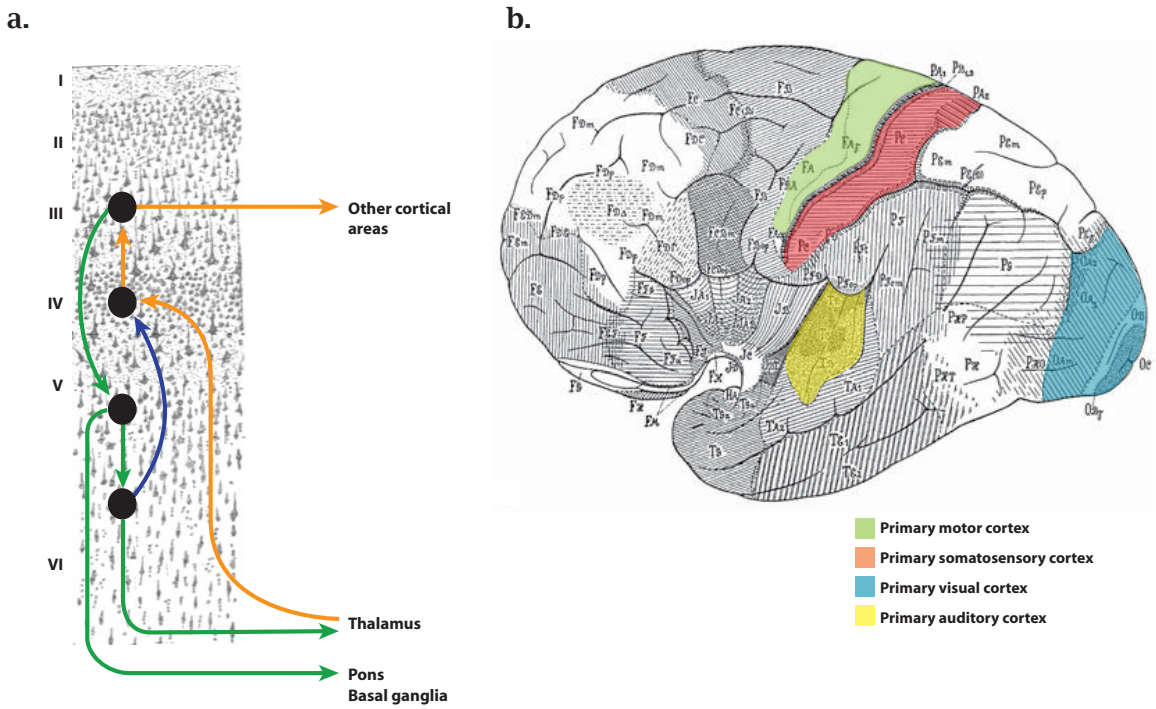

Figure 1_1: **Laminar and areal organization of the neocortex.** a. The six layers of the neocortex and the canonical cortical circuitry. A drawing by Cajal, 1889 of the cresyl-violet stained adult human motor cortex illustrates the radial division into six layers. A schema of the canonical cortical circuitry according to Douglas and Martin, 2004[6] is superimposed. Input from the thalamus is mostly received by neurons in layer IV and then relayed to layers II/III and further to other cortical areas. Projections back to the thalamus mostly originate from layer VI and output to other subcortical targets from layer V. b. The areal organization of the human neocortex. An illustration by Economo and Koskinas, 1925[8] of the adult human neocortex distinguishes more than 100 cortical fields. Highlighted in color are the primary cortical areas - somatosensory (red), motor (green), auditory (yellow) and visual (blue).

1.1.2 Establishment of laminar identity

The laminar identity of a neuron is tightly linked to its birth-date. Cortical neurons are generated in an inside-out order with layer VI neurons being born first and layer II neurons last[13]. Each neuronal progenitor can give rise to every laminar cell type but its competence becomes progressively restricted to upper layer neurons over time[14,15,16]. This temporal restriction is at least partially governed by cell-intrinsic mechanisms as isolated neuronal progenitors and embryonic stem cells in culture sequentially generate neurons expressing markers of the different cortical layers[17,18]. However, extrinsic factors can also influence the laminar identity, and progenitors can be at least partially reprogrammed under certain conditions[16,19,20]. Among others, the brain-derived neurotrophic factor (BDNF) has been identified as one of the key environmental cues capable of altering laminar fate. The application of BDNF to neuronal progenitors at E13.5 in the mouse led to the production of deep layer neurons instead of layer IV neurons while the blocking of BDNF changed their cell fate to layer II/III neurons[20]. It has been proposed that some of the extrinsic cues are provided as feedback signals

from postmitotic neurons to inhibit further production of a particular cell type[16,21,22]. In addition, there is some evidence that cortical afferents can influence the cell-cycle progression of neuronal progenitors[23,21]. At least in culture, thalamocortical axons have been shown to release a diffusible factor which promotes the production of both glia and neurons by shortening the cell-cycle length[23] and accelerates radial migration[24]. This raises the possibility that activity could modulate the laminar cytoarchitecture of the neocortex.

1.1.3 Arealization in the tangential dimension

Just like the laminar organization, the arealization of the cortex in the tangential dimension is governed by both intrinsic and extrinsic factors. Cortical regionalization is initiated by gradients of diffusible signalling molecules (morphogens) released from early patterning centres including the commissural plate, cortical hem and cortical antihem[12,25]. These gradients of morphogens induce graded expression of transcription factors (e.g. Emx2, Pax6, Coup-Tf1) in the cortical neuroepithelium (Fig 1_2 a). Loss and gain of function studies for these transcription factors demonstrate that they are crucial for areal patterning as alterations in their expression leads to substantial changes in size and position of cortical areas[26,27, 28, 29, 30, 31] (Fig 1_2 b). The graded expression of transcription factors results in the subsequent area-specific expression of other molecular markers such as cadherins and ephrins. The early area-specific expression of these molecules is independent of thalamic input as they appear unaltered in mutant mice where thalamocortical connections are defective[32, 33,34]. These studies strongly suggest that the initial arealization of the cortex is established by intrinsic mechanisms. However, the areal architecture is plastic and can be modulated and refined by thalamocortical afferents. For instance, manipulations of the sensory input to the cortex by visual deprivation or whisker removal change the cytoarchitecture in primary sensory areas (see section 1.5.5 for further details). Similarly, early ablation of thalamic nuclei alters the size of the corresponding cortical area[35]. Rewiring experiments further suggest that the modality of the sensory input determines certain area-specific spezialiation[36, 37]. For instance, when retinal inputs were rewired into the auditory thalamus in developing ferrets, the primary auditory cortex developed visual orientation-selective cells and an orientation map[37]. This suggests that the initial cortical patterns established by intrinsic mechanisms will be modulated and adapted depending on the sensory input relayed by thalamocortical afferents.

1.1.4 Connections between thalamus and neocortex

The establishment of connections between the developing thalamus and cortex is a difficult task. Axons have to travel a long distance in a highly dynamic environment and cross at least two important emerging boundaries - the diencephalic-telencephalic boundary (DTB) and

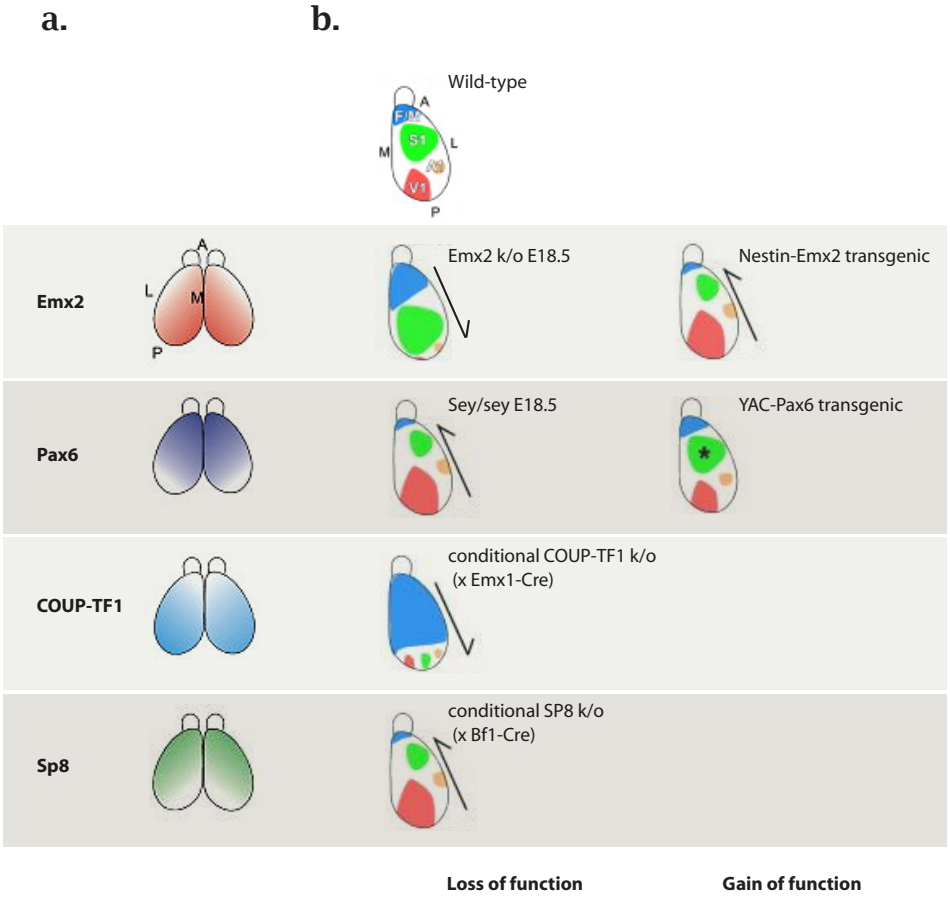

Figure 1_2: **Gradients of transcription factors and their influence on arealization.** a. The transcription factors Emx2, Pax6, Coup-TF1 and Sp8 are expressed in different anterior-posterior and medial-lateral gradients in the embryonic mouse brain. b. Knock-down or overexpression of these transcription factors lead to shifts in the size and/or position of the primary cortical areas (blue = motor, M1; green = somatosensory, S1; yellow = auditory, A1; red = visual, V1). A: anterior; P: posterior; M: medial; L: lateral. Reproduced from O'Leary et al., 2007[12].

the pallial-subpallial boundary (PSPB). In addition, connections have to be established in a topographic manner between thalamic nuclei and their reciprocal cortical areas (Fig 1_3 a). To accomplish this task, thalamocortical axons are directed along their way by a sequence of "guideposts" constituted by gradients of guidance molecules, intermediate target cells and scaffolds (Fig 1_3 b; reviewed in [38, 39,40]).

Attractive and repellent secreted factors expressed in the ventral forebrain initially guide the thalamic axons through the ventral forebrain. Netrin-1 is a guidance molecule expressed in the mantle zone of the internal capsule and attracts corticopetal axons from the anterior thalamus[41,42]. Inversely, chemorepellant signals are present in the hypothalamus and at the midline and prevent thalamic axons from aberrantly invading these regions[43,44].

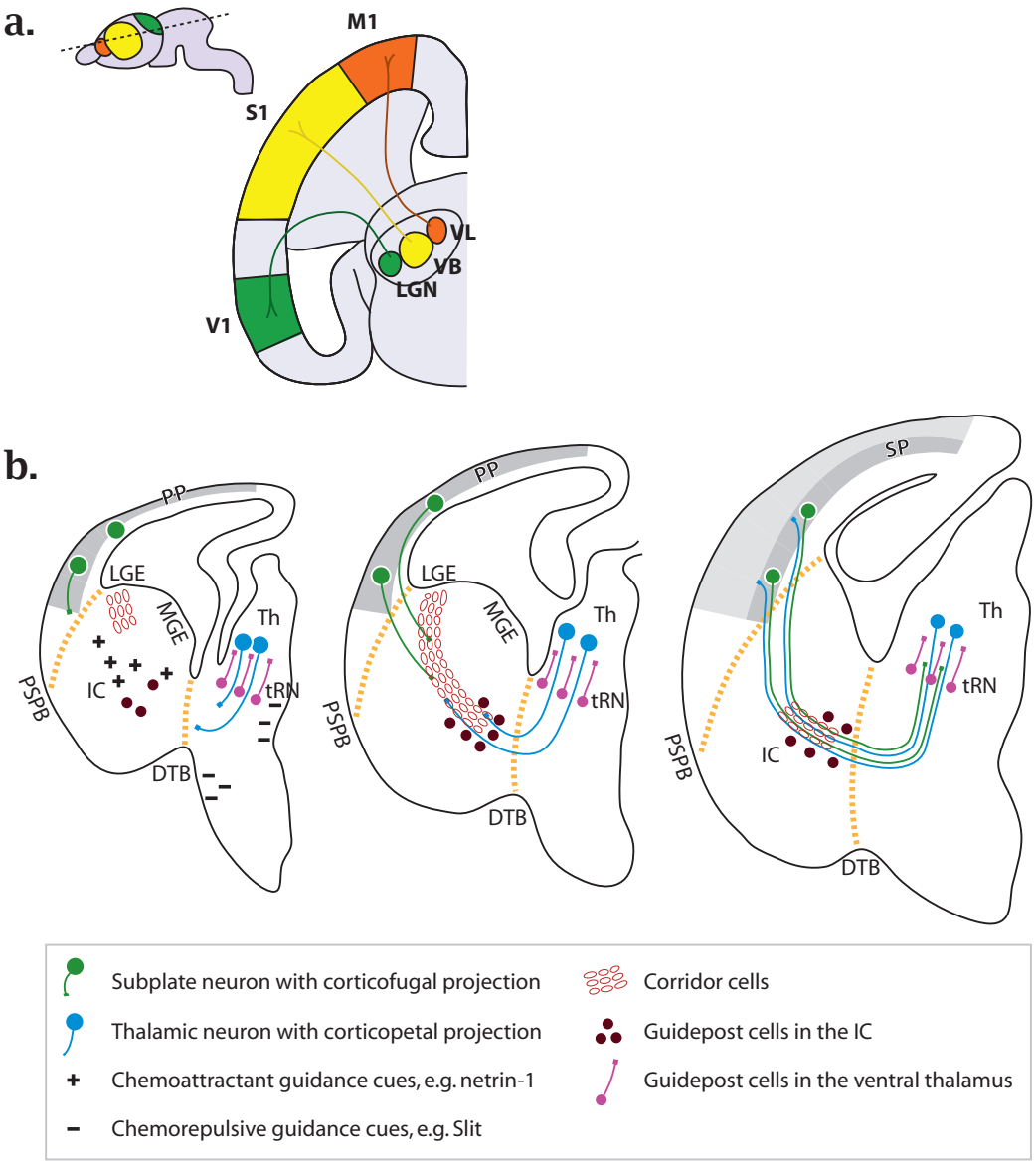

Figure 1_3: **Establishment of connections between the neocortex and the thalamus**. a. Topography of thalamocortical axons. Specific connections between thalamic nuclei and primary cortical areas are illustrated on a horizontal E18.5 mouse section. The plane of the slice is shown in the top left corner. The lateral geniculate nucleus (LGN) projects to the visual cortex (V1; green), the ventrobasal nucleus (VB) to the somatosensory cortex (S1; yellow) and the ventrolateral nucleus (VL) to the motor cortex (M1; orange). Reproduced from Garel and Rubenstein, 2004[39]. b. Signaling molecules, guidepost cells and scaffolds guiding thalamocortical afferents (TCAs). This schema depicts coronal sections through the rodent forebrain at different embryonic stages. TCAs are guided by repulsive cues in the hypothalamus and at the midline and attractive cues in the internal capsule (IC). Neurons in the thalamic reticular nucleus (tRN) might provide an early scaffold for the initial outgrowth from the thalamus (Th). In the IC, TCAs interact with guidepost cells and corridor cells originating from the lateral ganglionic eminence (LGE). A scaffold provided by corticofugal axons from the subplate (SP) guides TCAs across the pallial-subpallial boundary (PSPB). DTB: diencephalic-telencephalib boundary; MGE: medial ganglionic eminence; PP: preplate. Adapted from Hanashima et al., 2007[40].

Several cell populations in the ventral forebrain have been involved in guiding thalamic afferents to their target. Neurons in the thalamic reticular nucleus (tRN) are the first to send axons towards the thalamus and have been suggested to provide a scaffold for the outgrowing thalamic axons[45, 46]. Within the internal capsule, at least two different cell populations have been involved in channelling thalamocortical axons towards the dorsal telenencephalon and in assisting their crossing of the DTB[45,47,48,49, 50]. "Guidepost cells" (including perireticular thalamic neurons[45]) in the ganglionic eminences have been proposed as intermediate targets for both corticothalamic and thalamocortical fibers and to provide fiber scaffolds towards the cortex and the thalamus, respectively[45,47,40]. Another cell population, the "corridor cells", migrate from the lateral ganglionic eminence (LGE) towards the medial ganglionic eminence (MGE) and create a permissive bridge for thalamocortical axons[49,40]. In the conditional Celsr3 x Dlx5/6 knock-out mice, the cadherin Celsr3 is deleted specifically from the ventral telencephalon but not from the cortex or the thalamus. In these animals, all corticofugal and thalamocortical tracts in the internal capsule are defective[51]. This strongly supports an important role for cells of the ventral telencephalon ("guidepost cells" and "corridor cells") in the establishment of thalamocortical connections[50].

Finally, once thalamic axons have entered the internal capsule, early "pioneer" corticofugal axons from the subplate provide a scaffold for thalamic axons to cross the PSPB and reach their appropriate cortical target area (see section 1.5.2). Inversely, the thalamic afferents provide a scaffold for corticofugal fibers and are necessary for their guidance to the thalamus[52].

Subplate cells have been discovered nearly forty years ago in human[53] and have since been characterized and studied in many other mammalian species. Besides a role in the guidance of thalamocortical axons, other functions of subplate neurons have started to become elucidated. The subplate is the subject of this thesis and will be discussed in detail in the following paragraphs with a particular focus on the rodent.

1.2 Developmental time-course of subplate

1.2.1 Formation of the subplate

Subplate neurons are among the earliest-born cells in the cerebral cortex. In the mouse, they are generated between E10.5 and E12.5[54]. Like the other cortical layers, the subplate contains a majority of glutamatergic projection neurons and a minority of GABAergic interneurons[55]. The glutamatergic subplate neurons are generated by dorsal progenitors in the pallial neuroepithelium (Fig 1_4). From there, they migrate a short distance radially to accumulate and form the cell-dense preplate (or primordium plexiform zone)[56, 57]. During the next cell

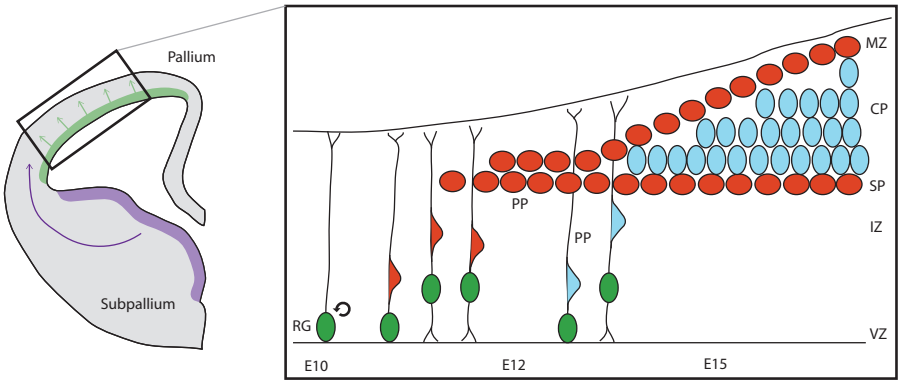

Figure 1_4: **Pallial neurogenesis and radial migration.** Cortical glutamatergic neurons are generated by neuroprogenitors in the pallial ventricular zones (depicted in green in the schema on the left). Around E10.5, progenitors in the ventricular zone (also called radial glia, RG) divide assymetrically to generate the first neurons. RG extend a process to the pial surface along which the newly generated posmitotic neurons migrate. The early-born neurons (from E10.5 to E12.5) form the cell-dense preplate (PP). The next cohort of neurons migrates radially into the preplate where they accumulate and start forming the cortical plate (CP). The emergence of the CP splits the PP into two zones: the subplate (SP) and the marginal zone (MZ).More neurons are added to the CP in an inside-out order, forming layer VI first and layer II/III last.

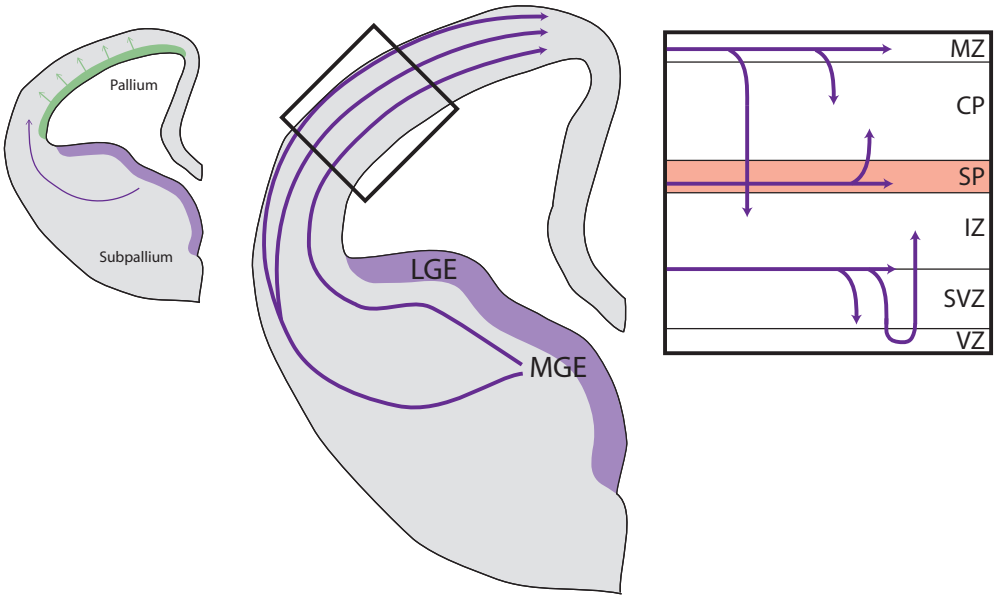

Figure 1_5: **Subpallial neurogenesis and tangential migration**. Cortical GABAergic interneurons largely originate from the ganglionic eminences (GEs) in the subpallium (purple). They migrate tangentially into the cortex along three routes: in the marginal zone (MZ), in the subplate (SP) and in the border zone between the intermediate zone (IZ) and subventricular zone (SVZ). From the MZ, interneurons migrate inwards into the cortical plate (CP). Interneurons from the SP and SVZ/IZ either enter the CP directly or after a short detour to the ventricular zone (VZ). MGE: medial ganglionic eminence; LGE: lateral ganglionic eminence. Adapted from Métin et al., 2006[93].

divisions of the dorsal progenitors, glutamatergic neurons of the future layer VI are generated. This new cohort of neurons accumulates within the preplate and starts to form the cortical plate in an inside-out order (i.e. later-born neurons migrate past earlier-born neurons and reside closer to the pial surface)[13]. The formation of the cortical plate will eventually split the preplate into two layers: the marginal zone (future layer I) and the subplate[56, 58,59]. In the mouse, the splitting of the preplate begins around E13 in the most anterior and lateral areas of the cortex and is completed in the whole rostro-caudal and medio-lateral expanse by E15.

The GABAergic subplate neurons in contrast are largely generated by progenitors in different compartments of the ganglionic eminences in the subpallium at approximately the same time as their glutamatergic counterparts[60,61,62]. These interneurons then migrate tangentially over a long distance to their final destination (Fig 1_5).

1.2.2 Embryonic subplate

The embryonic rodent subplate is a heterogeneous and highly dynamic compartment. Compared to neurons in the cortical plate, embryonic subplate neurons are relatively mature. This is reflected in their often complex morphology (polymorphous, multipolar)[63] and their expression of markers of mature neurons such as microtubule associated protein 2 (MAP2)[64]. As early as E15, subplate neurons have established synapses[65,66,55] of which at least some display mature features such as numerous vesicles and asymmetric membrane thickening[67]. Consistently, embryonic subplate neurons specifically express some receptors for neurotransmitters including GABA A receptors[68] and the vesicular glutamate transporter VGLUT2[69].

Early subplate projections

Subplate neurons start projecting corticofugal axons towards the ventral telencephalon at the early preplate stage and they arrive in the internal capsule one day later (around E13 in the mouse)[63,55]. At E14, these axons accumulate within the internal capsule before continuing towards the thalamus which at least some of them reach around E15/16 [70, 55,71,72]. However, whether subplate axons actually enter and innervate the thalamic nuclei is debated[73]. Subplate cells also extend axons across the cortical plate and into the marginal zone[74,75]. The precise developmental time-frame of the formation of these axons has not been established, but in rats, they are present from at least P0 onwards[74]. Subplate cells project extensively to other subplate cells in the same hemisphere and, in very small numbers, callosally to the contralateral hemisphere[70,76]. Ipsilateral subplate connections as well as projections towards the midline can already be observed at the preplate stage even though fibres do not cross the corpus callosum until late embryonic stages (E17 in the mouse)[63,55,76].

Early afferents to subplate

The embryonic subplate zone is the major target of early subcortical afferents. By E15, monoaminergic afferents have reached the subplate where they defasciculate and establish a dense network[70,77]. These include dopaminergic fibres from the mesencephalon and noradrenergic and serotonic fibres from the brainstem. Thalamocortical afferents reach the internal capsule at E13 and start innervating the subplate by E14/E15[70,63]. The innervation of the visual cortex appears to be delayed by two days indicating an important anterior-posterior developmental gradient[78]. Synapses between subplate and thalamic afferents become visible at E16 in the mouse subplate[71], and functional connectivity has been demonstrated from E19 onwards in the rat[79]. In contrast to thalamic and monoaminergic afferents, cholinergic fibres from the basal forebrain probably only innervate the subplate at late embryonic stages. Cholinergic fibres and functional cholinergic synapses have been shown to be present in the subplate from P0 onwards, at least in rat[80, 81,82,83]. In addition to subcortical afferents, fibres from the overlying cortical plate project through the embryonic subplate and often extend side-branches[70].

Enrichment in extracellular matrix and plasma proteins

The embryonic rodent subplate is very rich in extracellular matrix (ECM) and contains high quantities of proteins associated with the ECM including laminin, fibronectin and chondroitin sulfate proteoglycans[57,84,85,86]. The source of these molecules is not clear but it has been suggested that they can be both secreted by subplate neurons (Kondo et al., in preparation) and glial cells[85,86].

In addition, the embryonic rodent and human subplate specifically contains a number of plasma proteins such as alpha 2HS-glycoprotein and $\alpha_2$zinc-binding globulin[87,88,89]. Similarly, immunoglobulin-like proteins are specifically present in the subplate and marginal zone of developing rats and cats [90,91]. Some of these proteins are probably absorbed from the cerebrospinal fluid or the blood while others are synthesized *in situ*, i.e. by the cortical cells themselves[87,91].

Compartment for neuron migration

The embryonic subplate zone contains a large number of migrating neurons. Radially migrating glutamatergic neurons have to cross the subplate zone on their way to the cortical plate. In addition, the subplate is one out of three main streams of tangentially migrating GABAergic interneurons originating from the subpallium[92, 93] (Fig 1_5).

1.2.3 Postnatal subplate

By the end of the first postnatal week, both radial and tangential migration of cortical neurons is largely completed, and from then on, the subplate zone mainly contains residential subplate cells. However, subplate neurons themselves are a heterogeneous population. As in other cortical layers, approximately 75%-85% are glutamatergic excitatory neurons while the remaining 15-25% are GABAergic interneurons[92].

Morphology of postnatal subplate cells

Postnatal subplate neurons have varied morphologies and sizes. Their cell bodies are horizontally or vertically orientated or radially symmetrical. They can be multipolar or have a primary dendrite extending vertically towards the pial surface, vertically towards the white matter or horizontally[94, 95]. At early postnatal ages, the primary dendrite of many subplate neurons extends all the way to the marginal zone while at later postnatal stages, all dendrites branch in layer IV or below, indicating an important rearrangement during the first postnatal week[95].

During a similar developmental time-frame, a rearrangement of subplate neurites within layer IV of the barrel cortex has been described in the Golli-tau-eGFP mouse[96]. In these transgenic animals, subplate and to a lesser extent layer VI neurons express enhanced green fluorescent protein (eGFP)[72]. At late embryonic and early postnatal stages, eGFP-positive neurites extend into the putative barrel hollows while after the first postnatal week, these neurites shift to concentrate in the barrel septa[96]. Changing the sensory input during the first postnatal week by removing the whiskers in a single row delayed the rearrangement of the neurites in the corresponding position[96]. It is currently unknown whether the eGFP-positive neurites are axons or dendrites and further studies would be needed to understand the functional significance of this rearrangement.

Projections of postnatal subplate neurons

Postnatal subplate neurons project to at least three different target sites in the mouse: through the internal capsule to the thalamus, through the corpus callosum to the contralateral cortex and within the ipsilateral cortex. A minority of subplate neurons were found to send collateral axons to more than one target[95]. In addition, subplate neurons in the early postnatal cortex are connected to an average of eight to ten neighbouring neurons through gap junctions leading to extensive electrical coupling[97].

The large majority of the long-ranging projection neurons in subplate are glutamatergic[98], but interestingly, a small subset appears to be GABAergic[95]. GABAergic cells in the subplate could be backlabeled from the corpus callosum, the internal capsule and the distant ipsilateral cortex in the postnatal mouse[95]. In the adult mouse, cat and monkey, GABAergic neurons with projections to the distal ipsilateral cortex were mainly found to be localized in the white matter remnants of subplate and layer VI (mouse and cat) or layer III (monkey)[99, 100,101].

Transitory circuitry between thalamus, subplate and layer IV neurons

A subset of postnatal subplate neurons are involved in a transitory circuitry connecting thalamic afferents and layer IV[102, 103, 104, 105] (Fig 1_6). This microcircuit has first been proposed in the visual cortex of newborn cats where white matter stimulation elicited a short-latency response in subplate followed by a long-latency response in layer IV[103]. This suggests that in the early postnatal cortex thalamocortical afferents directly activate subplate neurons (monosynaptic connection) which then relay the input to layer IV neurons (disynaptic connection). Similar observations have subsequently been made in the neonatal rodent cortex. Stimulations of the thalamus in the newborn rat led to an activation of subplate cells while the same stimulations after the first postnatal week elicited a direct response in layer IV[106]. In the neonatal mouse auditory cortex, functional excitatory synapses between the medial geniculate nucleus (MGN) and subplate neurons and between subplate neurons and layer IV neurons were demonstrated using photostimulation[105]. Interestingly, functional excitatory and inhibitory input from layer IV into subplate neurons has recently been observed suggesting the presence of a feed-back loop (Viswanathan and Kanold, submitted).

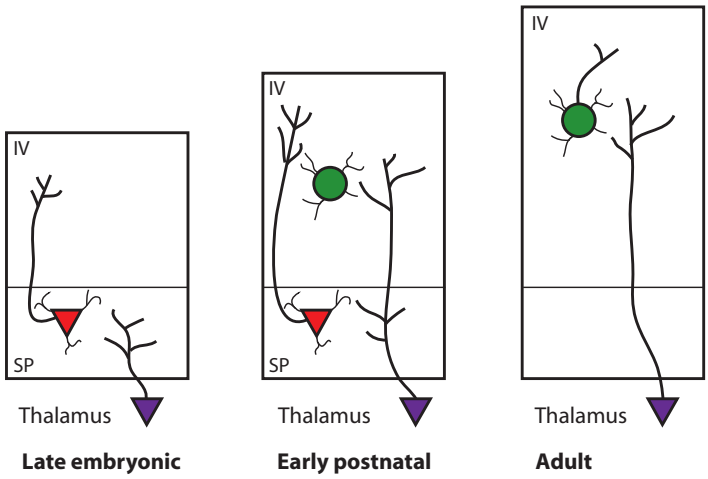

Figure 1_6. **Developing circuitry between thalamic, subplate and layer IV neurons.** In the late embryonic brain, thalamic neurons (purple) establish functional synapses with subplate (SP) neurons (red). These connections are maintained at early postnatal stages. Postnatal SP neurons project to neurons in layer IV (green), resulting in a transitory circuitry between thalamus, SP and layer IV. At later postnatal stages, thalamic axons form direct connections with layer IV neurons establishing the mature circuitry. Adapted from Kanold, 2004[104].

Cholinergic and glycinergic inputs

In addition to the glutamatergic input of thalamocortical afferents, postnatal subplate neurons are modulated by cholinergic and glycinergic inputs[82,107]. In newborn rats, cholinergic afferents are largely confined to the subplate zone[80, 81]. Consistently, acetylcholine can excite a majority of subplate neurons of diverse morphologies through nicotinergic acetylreceptors at early postnatal ages[82]. Similarly, at this stage, glycine or glycinergic agonists can depolarize subplate neurons[107]. In the developing cortex, endogeneous glycine and glycine agonists (especially taurine) are probably released nonsynaptically from cortical neurons[108] and have a modulatory effect on neuronal activity.

Cell death in the postnatal subplate

In carnivores and primates, subplate neurons are largely transient and the majority dies during the first postnatal weeks through apoptosis[109, 110] (see also section 1.4.2). In rodents, however, the transient nature of subplate neurons is debated. In the mouse, cells labelled with BrdU at E11, E12 or E13 had almost completely disappeared from the subplate at P21 while labelled cells in the cortical layers were largely retained[111,54]. In the rat, however, the number of subplate cells labelled with ^{3}H-thymidine at E12, E13 or E14 (equivalent to E11-E13 in the mouse) did not decrease between P1 and P63[112]. In contrast to this study, Robertson et al. found a decrease of ~70% of subplate neurons labelled at E14 in the adult rat which was moderately more than the 50% neuronal loss in the upper layers III and IV labelled at E18[113]. A similar reduction of ~ 60% was found between P2 and P30 in the rat when counting NeuN-labelled subplate neurons[114]. More in agreement with findings in the mouse, Al Ghoul and Miller described a complete absence of subplate cells labelled at E12 by P21 in the rat[115].

1.2.4 Adult subplate

As described in the previous paragraph, several but not all studies suggest a largely transient nature of subplate neurons in rodents and maybe more so in mice than in rats[111, 54, 115]. However, based on histology, the presence of a clearly-defined subplate layer (or layer VIb or layer VII) separated from the overlying layer VI has been described in the adult cortex of both rodent species[116]. In addition, several molecular markers of the embryonic and/or early postnatal subplate are still expressed in the adult subplate both in mouse[117] and rat[118, 119,120]. If all or nearly all early-born neurons indeed died during postnatal development as suggested by some[111, 54, 115], this adult subplate layer would have to comprise a different cell population than the embryonic or early postnatal subplate. However, ^{3}H-thymidine injections at E13 labelled cells situated in the cytoarchitectonically-defined subplate in three-week old rats[121]. Further studies would be needed to completely resolve this issue.

The adult rodent subplate has been poorly characterized. Adult subplate neurons are mostly horizontally orientated with dendrites projecting towards the pial surface and/or horizontally but not towards the white matter[114]. In the mouse, adult subplate neurons have been shown to be electrophysicologically active and functionally integrated into the cortical network[114]. Like neurons in layers II/III and V, adult subplate cells form many long-ranging and local corticocortical connections which run primarily in the cell-sparse plexus between subplate and layer VI[121, 75, 122]. In addition, adult subplate neurons possibly receive inputs from collaterals of thalamocortical and other subcortical fiber systems[114]. In contrast, retrograde tracing from large areas of the thalamus (ventrobasal thalamus or posterior thalamus) did not label any adult rodent subplate cells indicating that adult subplate neurons do not innervate the thalamus or only to a limited extent[75, 122].

1.3 Gene expression in the subplate

1.3.1 Traditional immunohistochemical markers

A range of traditional immunohistochemical markers for the subplate zone has been described and they are usually linked to one of the following characteristics of subplate: the early maturation, the presence of migrating interneurons or the accumulation of developing fibres.

MAP2, a cytoskeleton protein expressed in mature neurons, is specifically localized in the early embryonic subplate of rodents[64,55] and cats[123] and can be used for a brief period to identify this layer[123].

Calbindin, calretinin, neuropeptide Y and somatostatin have all been associated with the developing subplate, often in several species[124, 55, 125, 123, 126, 127.] However, all or almost all cells expressing these genes have been identified as GABAergic interneurons[128, 129, 130] which are migrating within the embryonic subplate zone (see Fig 1_5). The exception is calretinin[124, 125]: In the mature cortex, the majority of calretinin-expressing cells are GABAergic. However, in the developing cortex, an important proportion of calretinin-positive cells in the subplate and marginal zone are negative for GABA, both in mouse[124] and human[125]. This suggests that calretinin is expressed in at least two cell populations – transiently in developing glutamatergic subplate neurons and more permanently in GABAergic cortical interneurons.

Finally, several adhesion molecules including L1, J1 and NCAM are found at high levels in the subplate zone at certain developmental stages [131, 132, 133]. However, all of these proteins are also present in the developing cortical and/or thalamic axons[132, 134] which are accumulating in the embryonic subplate and thus explain at least partially the abundance of these proteins in this zone.

1.3.2 Specifically expressed genes in subplate cells

In addition to these traditional immunohistological labels, a number of other molecules have been described as specifically expressed in subplate cells. In search for a subplate-specific antibody, Naegele et al. used a homogenate of early postnatal cat subplate to immunize mice[135]. The resulting antibody was termed SP1 and specifically labels both GABAergic and non-GABAergic subplate neurons in the cat. After the first two postnatal weeks, SP1 expression declines and then disappears, possibly due to the cell death of subplate neurons[135].

Alz-50 is an antibody which binds to neurofibrillary tangles and many other neuronal components in brains of Alzheimer's disease patients but not in healthy age-matched controls[136]. In the normal developing brain of human foetuses and infants, however, many Alz-50-positive cells were observed, especially in the subplate and marginal zones[137]. Similarly, in the neonatal rat brain, Alz-50 labels numerous subplate and white matter cells and sparse cells in the cortical plate[138, 139]. As the immunoreactivity of Alz-50 disappears at the end of the second postnatal week, Alz-50 has been proposed to label neurons destined to undergo apoptosis[139,115.]

The neurotrophin receptor p75 ($p75^{NTR}$) has been described to be exclusively expressed in the developing subplate of cats[140] and rats[141,142,143]. In the rat subplate, $p75^{NTR}$ is expressed in a posterior-high anterior-low gradient[141,143.] The specific expression of $p75^{NTR}$ has been used in a number of studies to ablate subplate through injection of an immunotoxin[144, 145] or to isolate subplate neurons through immunopurification[142,146,147]. In other systems, signalling through $p75^{NTR}$ is involved in the regulation of neuronal death and survival[148]. In cultured subplate neurons, $p75^{NTR}$ appears to promote cell survival through the regulation of the ceramide pathway[142]. However, in the $p75^{NTR}$ knock-out mouse, the numbers of subplate neurons are unaltered. Instead, subplate growth cones are smaller and have less filopodia in the knock-out animals indicating a role for $p75^{NTR}$ in determining growth cone morphology[143].

Kynurenine aminotransferase I (KAT-I) is an enzyme producing kynurenic acid, the only known endogeneous antagonist of the NMDA receptor. KAT-I has been shown to be exclusively expressed in the embryonic and early postnatal rat subplate[149]. As kynurenic acid protects neurons from excitotoxicity[150], this suggests that KAT-I could play a role in regulating subplate neuron survival.

Recently, the progesterone receptor (PR) has been found to be strongly expressed in the rat subplate between E18 and P10 with a peak of expression around P2[151]. Based on this temporal expression pattern, PR could be involved in regulating the synapse formation between thalamocortical afferents and subplate neurons. In cerebellar Purkinje cells, progesterone promotes dendritic growth and synaptogenesis through a PR-dependent mechanism[152]. Alternatively, PR could also play a role in regulating cell survival as progesterone alters the expression of pro- and anti-apoptotic factors[151].

1.3.3 Microarray-based subplate gene expression analyses

Over the last few years, more comprehensive gene expression studies of the subplate have been conducted. Osheroff and Hatten have performed a microarray analysis of preplate cells destined to become subplate in the E12 mouse cortex[153]. They found four prominent categories of genes expressed in the very early subplate cell population: cell adhesion and axogenesis; vesicle formation and exocytosis; transcriptional regulation; steroid synthesis and signalling. Further analysis suggested that the estrogen signaling pathway might be particularly important in the subplate, perhaps regulating subplate maturation and neurite formation. Two genes were confirmed to be specifically expressed in the preplate at E12 and in the subplate at E14 – the calcium-binding protein hippocalcin and the glutamate transporter EAAC1. Both of these genes are involved in synaptic function[153].

In our own laboratory, a microarray screen of the E18.5 and P8 subplate has been performed[95,117]. At E18.5, many of the subplate-enriched genes appear to be involved in transcriptional regulation and neuron fate commitment and in axon extension. Genes coding for proteins in the bone morphogenic protein (BMP) and Notch signalling pathways were expressed at high levels in subplate at both E18.5 and P8. Interestingly, genes involved in the regulation of apoptosis or cell survival were not particularly highlighted for the postnatal subplate[95]. From the P8 gene expression profiling, six genes with subplate-specific expression were confirmed: nuclear receptor related 1 (Nurr1), connective tissue growth factor (Ctgf), transmembrane protein Tmem163, monooxygenase DBH-like 1 (MoxD1), complexin 3 (Cplx3) and dopa decarboxylase (Ddc)[117]. Ctgf and Nurr1 had been previously described to be localized in the subplate of adult rats[119], mice and monkeys[154]. These different postnatal subplate markers were found to be expressed in distinct yet overlapping subplate subpopulations[117], which further emphasizes the heterogeneous nature of the postnatal subplate. More studies will be needed to correlate gene expression to cell morphology, electrophysiological properties and hodology.

1.4 Comparative aspects of subplate cells

1.4.1 Evolutionary origin of subplate cells

The subplate zone has first been discovered in humans[53] and shortly after in rodents[155], monkeys[156] and carnivores[109]. Besides human and a few model species including rat, mouse, ferret, cat and macaque, little is known about subplate in other species or lineages. As the development of subplate is tightly linked to the development of the six-layered cerebral cortex (see section 1.2.1), the subplate is often considered a unique mammalian feature[110]. Moreover, based on cytoarchitecture, a distinct subplate cannot be found in the developing marsupial

cortex[157] suggesting that subplate is not only exclusive to mammals but more specifically to placental mammals.

In contrast, some authors (including our own group) have proposed an ancestral evolutionary origin of at least a subpopulation of subplate neurons. Morphological and gene expression studies indicate that the three-layered dorsal cortex of reptiles and the hyperpallium of birds contain cells equivalent to the deep layers of mammals including subplate[158, 120]. The function of these subplate-equivalent cells in sauropsids (i.e. reptiles and birds) has not been studied. Based on their location, it has been suggested that as in mammals, they could play a role in guiding and organizing the thalamocortical inputs[120,159].

1.4.2 Expansion of subplate in higher-order mammals

Among different mammalian lineages subplate varies greatly in size, and species with larger and more complex cortices generally have a thicker subplate zone[160]. In rodents, the subplate is very thin throughout the entire period of cortical development and involves a layer of two or three cells just above the intermediate zone/white matter. In cats, the subplate is much more substantial and is wider than the cortical plate during a significant proportion of development[109]. Finally, in the developing human, the subplate is extremely large compared to rodents. At the peak of its size (around the end of the second trimester), the human subplate is at least four times wider than the cortical plate[110]. The carnivore and primate subplate is not only larger than the rodent subplate but also appears to contain distinct sub-compartments. In the cat, an upper cell-dense and a lower loosely-packed subplate zone can be distinguished based on cytoarchitecture[109]. Similarly, in human, an upper and a lower subplate have been described where different subplate subpopulations distinguished by gene expression preferentially reside[110,161]. Whether these different subplate cell types also differ in their birth-dates, connectivity and/or function remains to be elucidated.

In contrast to rodents where the subplate is generated during the very first cycles of cell division and constitutes a remnant of the preplate, neurons are added continuously to the subplate in primates until about midgestation[162,163]. A large proportion of the primate subplate is therefore not early-born as in rodents but generated in parallel with neurons of the cortical plate. Consequently, the early-birthdate is not a sufficient criterion to define subplate cells in all species and additional factors such as location, gene expression and connectivity have to be used to delineate this cell population.

Different species do not only differ in the size and complexity of subplate, but probably also in the survival of subplate neurons. In rodents, the transient nature of subplate is still debated (see section 1.2.3) but many studies suggest that an important proportion of subplate

neurons survive into adulthood[112, 113, 114, 121]. In contrast, in carnivores, the large majority of subplate neurons degenerates during the first postnatal weeks[109]. Similarly, in primates, the subplate zone is resolved during late foetal and early postnatal development[110]. Only a fraction of neurons survives into adulthood where they form the superficial white matter neurons[156,110,164.]

It has been proposed that the increased size and complexity of the subplate in some mammalian lineages (in particular in primates) could be linked to increased cortico-cortical connectivity[110]. In the human cortex, the subplate is thickest and persists longest in areas with greater cortico-cortical connectivity such as the frontal cortex and other associative areas[110,165]. In addition, after analyzing the presence of an adult subplate in 144 mammalian species, Reep has suggested that the timing of apoptosis in subplate and the timing of establishment of cortico-cortical connections are correlated[116]. This suggests that subplate neurons could be crucial for establishing and supporting cortico-cortical connectivity but no direct evidence for such a role has been shown so far.

1.5 Functions of subplate

1.5.1 Pioneering of the corticofugal pathway

Subplate neurons pioneer the corticofugal pathway in carnivores[166, 167], rodents[63, 168,55] and humans[125]. Subplate neurons already extend axons towards the internal capsule at the preplate stage and thus before most neurons of layers VI and V (the main subcortically projecting neurons in the mature cortex) have completed their migration. Axons from subplate neurons are also the first to reach the thalamus[166, 63], but whether and when they actually innervate the thalamic nuclei is debated in rodents[73]. In monkeys, corticofugal axons from the visual cortex rapidly extend towards the thalamus but then accumulate and "wait" outside the lateral geniculate nucleus (LGN) for about two weeks before finally innervating it[169]. In cats but not rodents, subplate neurons also pioneer the pathway to the superior colliculus[166] and possibly to other subcortical targets including the pons and spinal cord[170].

Corticofugal axons from the subplate could serve as a substrate for axons of cortical layers V and VI and guide them to their correct subcortical targets as has been demonstrated for pioneer systems in lower vertebrates and invertebrates[171, 172]. Indeed, ablation studies in the embryonic cat visual cortex have shown that in the absence of subplate, the descending projections failed to innervate the LGN, the superior colliculus and the pons in a subset of animals[167]. These findings suggest that subplate axons play a role in the guidance and target selection of cortical efferents even though other signals are probably also involved[170].

1.5.2 Guidance of thalamocortical axons to the cortex

Interactions between subplate and thalamocortical axons

Corticofugal axons from the subplate and corticopetal axons from the thalamus develop in parallel and enter the internal capsule at the same time from opposite sides[166, 173, 63, 174]. This observation underlies the "handshake hypothesis" which proposes that thalamic and early corticofugal projections from subplate meet, fasciculate and guide each other to their appropriate targets[175, 170, 176] (Fig 1_7). Indeed, tracing studies in rats have shown that thalamic and subplate axons intermingle in the internal capsule ("handshake") and then grow along each other in the intermediate zone[168, 174]. This view is not shared by all, as some studies have found that the two fiber systems grow in distinct compartments, at least in hamster and cat[177,167]. This discrepancy could be due to species-differences or caused by the technical difficulty to precisely label corresponding regions of thalamus and subplate at an early embryonic age[174]. Despite this controversy, there is a lot of functional evidence for the handshake hypothesis from ablation studies and from the analysis of mutant animals[175,178,179, 106, 180,51, 52] (see the following sections for details).

Once the thalamocortical afferents reach the cortex, they do not immediately grow into the cortical plate but instead accumulate in the subplate. This "waiting period" can last from several weeks in primates and cats[181, 182, 173] to only two or three days in rodents[183, 174, 179]. Due to its short time-frame, the waiting period in rodent has been contested by some[184, 78]. However, it is now widely accepted that in rodents only a small subset of thalamic fibres penetrate the deep cortical plate immediately while the majority waits within subplate for at least two days[174,179].

Establishment of topographic connectivity

The mechanisms through which specific interactions between the subplate and the thalamic fibre system are established are not fully elucidated. The timing of outgrowth of both thalamic and subplate axons follows the rostrolateral-to-caudomedial gradient of cortical maturation[185]. This spatiotemporal gradient or "chronotopy" also determines the sequence in which specific groups of fibres arrive and are able to interact in the internal capsule[176, 174] (Fig 1_7). It is also conceivable that axons of corresponding regions express specific guidance or adhesion cues which increases their specific interaction although no such molecules have been identified so far[176].

It has been noted that thalamocortical afferents growing towards the cortex appear to send collaterals to the subplate and sometimes lower cortical plate of inappropriate cortical

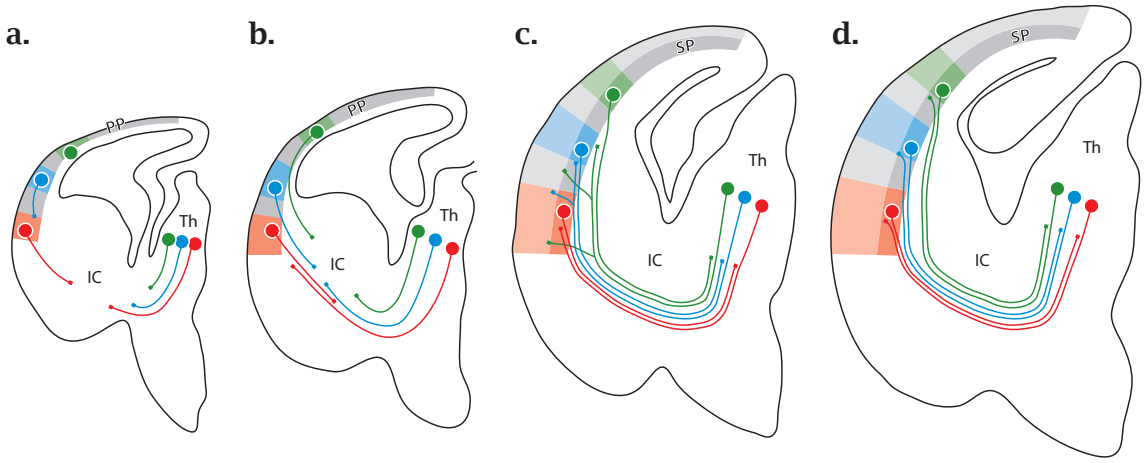

Figure 1_7. **A role for subplate in the establishment of thalamocortical topography.** This schema illustrates how thalamocortical topography could be established based on the chronotopy in axonal growth and the expression of signaling molecules in the cortex. The drawings depict coronal sections through the rodent forebrain at different embryonic stages. a. Neurons in the preplate (PP) and in the thalamus (Th) start sending out axons towards the internal capsule (IC) in a chronological sequence. In the PP, ventral axons are growing before dorsal axons and in the Th, medial axons before lateral axons. b. Corticofugal axons from subplate (SP) and corticopetal axons from the Th meet and fasciculate in the IC according to the chronological sequence of their growth. c. While growing towards the cortex, thalamic axons send out collaterals to different cortical areas. d. Only collaterals to the correct cortical target area, possibly defined by signaling molecules, will be maintained. Adapted from Molnár and Blakemore, 1995[176].

areas[186,173]. This observation led to the proposal that such collaterals are "sampling" different cortical areas in order to select their appropriate target[170]. This suggests that in addition to the specific interactions between subplate and thalamic axons, signalling molecules expressed in the subplate and/or cortical plate could contribute to establish the correct thalamocortical topography (Fig 1_7).

Interestingly, for some fibre pathways major topographic rearrangements have been described[187, 188,189]. For instance, in the geniculate-striate pathway of the cat, medially and laterally placed fibres run separately in the optic radiation but then cross and exchange position just before reaching the cortex[188]. It has been suggested that this crossing occurs in the subplate zone[189], possibly during the waiting period, but the underlying mechanisms are currently unknown.

Even though many details remain to be elucidated, an important role of subplate in attracting and guiding thalamic afferents to the cortex has been confirmed in several species[175,178,179,106], and evidence will be discussed in the following sections.

Ablation studies in the cat

In embryonic cats, subplate was ablated in the visual cortex at a stage when thalamic axons had just arrived below the cortex[175,178]. In the absence of subplate neurons, thalamic afferents from the LGN failed to innervate the visual cortex and instead grew past it in the intermediate zone. Even at postnatal and adult stages, LGN afferents were not present in the visual cortex of ablated animals and many axons were found to have withdrawn or atrophied[178]. Similar findings were also made in the auditory cortex where after ablation of subplate, afferents from the MGN grew past their target area and often displayed abnormal trajectories in the dorsal and posterior cortex[178]. These results demonstrate that the presence of subplate cells is required for the selection and innervation of the appropriate cortical field by thalamic afferents.

Evidence from mutant and transgenic rodents

The reeler mouse and the shaking-rat Kawasaki (SRK) both carry a mutation in the gene encoding reelin, an important regulator of neuronal migration. In these mutant animals, the neurons of the cortical plate fail to split the preplate into subplate and marginal zone and instead accumulate below these early-born cells. The preplate remains above the developing cortical plate and is therefore termed "superplate"[58,179,106]. In the reeler mouse and SRK, thalamocortical afferents do not "wait" below the cortical plate as in normal animals. Instead, they immediately penetrate and run diagonally through the cortical plate and accumulate in the superplate[179,106]. The thalamic axons run in close association with the corticofugal axons from the superplate, both in the intermediate zone and when crossing the cortical plate[179]. This behaviour of thalamic axons in the reelin mutants is particularly striking as usually the cortical plate is not permissive for fibre ingrowth at such an early developmental stage[190,191].

In Tbr1 knock-out mouse cortices, early corticofugal axons grow normally into the internal capsule but but then fail to continue towards the thalamus. In these mice, thalamic axons never reach the cortex but are instead deviated into the external capsule and towards the amygdala[180]. As Tbr1 is not expressed in the thalamus, this observation indicates that the correct positioning of early corticofugal axons is a prerequisite for the correct pathfinding of thalamocortical afferents. Together with the work in cat, the reeler mouse and the SRK, this strongly suggests that early corticofugal subplate axons provide a scaffold along which thalamocortical afferents are guided to the cortex.

Guidance cues within subplate

In addition to a subplate scaffold, guidance cues for thalamic axons might be expressed in the subplate and/or cortical plate (see above), a view which is supported by the work of

Shimogori and Grove[192]. In their studies, the misexpression of fibroblast growth factor 8 (Fgf8), a patterning gene normally expressed in the anterior telencephalon, led to a shift or partial duplication of the primary somatosensory cortex (S1)[193, 192].The expression of the guidance molecule ephrin A5 followed this shift. Thalamic axons from the ventrobasal thalamus (VB) were also shifted correspondingly, leading to a change in the barrel patterns. In the cases where S1 was duplicated, afferents from VB bifurcated and separated into two bundles within subplate in order to innervate the non-shifted and shifted S1, respectively. When Fgf8 was misexpressed only in the cortical plate but not in the subplate, VB axons became skewed: they first innervated the non-shifted subplate and layer VI and then turned to enter layer IV in the shifted cortical plate[192]. These findings suggest that positional information both in the subplate and cortical plate, probably in the form of guidance molecules such as ephrins, cadherins and neurotrophins[38,194], sequentially influence the growth of thalamic axons.

1.5.3 Synchronization of neuronal activity

During the waiting period, thalamocortical afferents form functional excitatory synapses with subplate neurons[102, 94, 79, 105]. In addition, subplate also receives intracortical inhibitory and excitatory input[94] and cholinergic and glycinergic input[107,83] (see section 1.2.3). This suggests that subplate could function as a temporary centre which integrates and synchronizes neuronal activity from different inputs and distributes it to the developing cortical plate[62,195,196].

In dissociated neuronal cultures, Voigt et al. have found that a particular population of large GABAergic neurons is crucial for generating synchronous oscillatory network activity. Using birthdating and morphology, they suggest that *in vivo*, these neurons primarily reside within the subplate zone[62]. Indeed, electrical stimulation of subplate in cortical slices elicits synchronized oscillatory activity[197]. Consistently, in the absence of an intact subplate on the slice, synchronous oscillations induced by carbachol (a cholinergic agonist) are not generated[97,198]. This early network activity appears to be propagated through gap-junctions[97]. Similarly, it has been proposed that subplate together with the claustrum could function as a pacemaker zone generating synchronous activity waves in the cortex[199]. Interestingly, the rodent claustrum and subplate share a number of molecular markers including Nurr1, Cplx3 and MoxD1[120] but whether these genes are related to oscillatory activity is unknown.

In vivo, oscillatory activity occurs in the cortex during the first days after birth in the rat and can be either spontaneous or evoked by stimulation of the periphery[200,201]. The subplate appears to play an important role in generating at least a subset of these early activity patterns[201]. In the somatosensory cortex, such oscillations synchronize a network of 200-400μm in diameter, approximately the dimensions of a barrel in the barrel field. It has therefore been suggested that these early activity patterns could serve as a template for the development

of the cortical barrels present in the mature cortex[201]. Similarly, it has been shown that in the visual cortex synchronous rhythmic activity is necessary for the correct development of cortical maps[202,203]. In addition to patterning, synchronized oscillations might be involved in regulating cell death and neuronal migration[196].

In any case, it seems likely that the subplate is not a passive waiting compartment for subcortical afferents but plays an important role in integrating and synchronizing early activity in the developing cortex.

1.5.4 Maturation of the cortical circuitry

In the neonatal cortex, subplate neurons are involved in a transitory circuitry connecting thalamic afferents and layer IV neurons (see section 1.2.3 and Fig 1_6). This transient input from subplate into layer IV appears to be important for the maturation of the thalamocortical synapses. Ablation of the subplate in the visual cortex of newborn cats prevented the normally observed developmental increase of glutamate receptor subunit GluR1 expression in layer IV neurons. This low receptor expression was accompanied by functionally weak thalamocortical synapses in layer IV. For instance, the amplitude of excitatory postsynaptic currents evoked in layer IV neurons after stimulation of the thalamic afferents was decreased by 80% when subplate had been ablated[144]. In contrast, abnormally high frequencies of spontaneous synaptic activity were observed indicating that the visual cortex had become functionally uncoupled from the LGN and thus the evoked visual activity[144,195].

It has been suggested that subplate inputs could strengthen the developing thalamocortical synapses in layer IV through spike timing-dependent plasticity (STDP)[145,204] (Fig 1_8 a,b). STDP is based on the rule that a synapse is strengthened when presynaptic activity precedes postsynaptic activity while a synapse is weakened when presynaptic activity follows postsynaptic activity[205]. In the presence of subplate, weak monosynaptic thalamic inputs onto layer IV neurons are followed by strong disynaptic inputs relayed through subplate. The postsynaptic activity in layer IV neurons will thus be slightly delayed compared to the presynaptic activity in the thalamic axon and the synapse will be potentiated (long-term potentiation, LTP; Fig 1_8 b)[145, 204].

The input of the postnatal subplate onto the cortex also appears to be important for the maturation of inhibitory cortical connections that underlie the decrease in spontaneous activity normally observed[145,195]. In the absence of subplate, the normal developmental increase of the ionotropic GABA-A receptor subunits α1 and γ 2and the decrease of α2 were prevented in layer IV specifically. Consistent with this impaired maturation of the GABAergic synapses, currents evoked by the GABA agonist muscimol were reduced by 85% in layer IV neurons after subplate ablation[145].

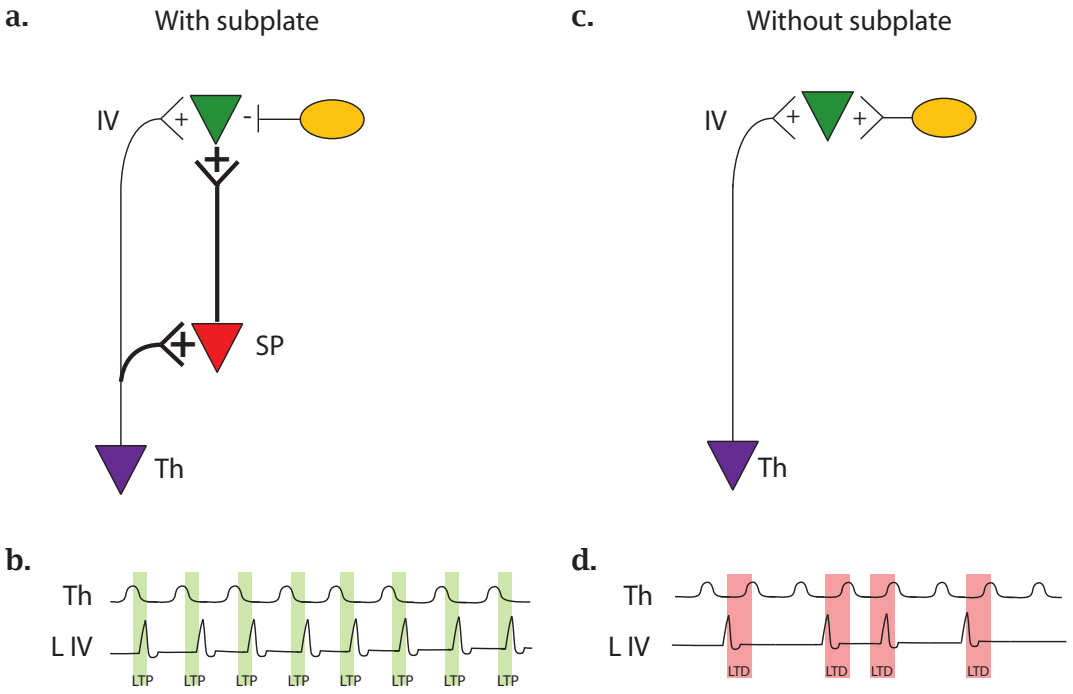

Figure 1_8. **A role for subplate in regulating maturation and plasticity of the cortical circuitry.** This schema illustrates how the subplate could influence the strengthening of the thalamocortical synapse through spike timing-dependant plasticity (STDP) as proposed by Kanold et al., 2003[144] and Kanold and Shatz, 2006[145]. a. In the early postnatal brain, spiny stellate cells in layer IV (green) receive weak monosynaptic thalamic input and strong disynaptic thalamic input relayed through the subplate (SP; red). b. Action potentials in the thalamic neuron (purple) will always precede depolarization in the layer IV stellate cells resulting in long-term potentiation (LTP) of the thalamus-layer IV synapse. c. In the absence of subplate, layer IV stellate cells only receive weak monosynaptic thalamic input. In addition, the inhibitory system (yellow) remains immature leading to high spontaneous activity in layer IV. d. Action potentials in the thalamus are unable to drive layer IV stellate cells. Activity in the thalamus and in layer IV is therefore uncorrelated. If we assume a longer time window for long-term depression (LTD) than LTP, this will lead to a weakening of the thalamus-layer IV synapse. Adapted from Ohshiro and Weliky, 2006[203].

Expression levels of the Cl^- transporter KCC2 also remained low in layer IV but not in other cortical layers[145]. KCC2 is crucially involved in determining the intracellular Cl^- levels and thus the effect of GABA on the neuron. Early in development, when KCC2 is not expressed, intracellular Cl^- is high and GABA has a depolarizing effect. Later in development, as KCC2 expression increases, intracellular Cl^- becomes low and GABA has a hyperpolarizing effect[206]. Consistently, after ablation of subplate, GABA had a depolarizing effect on neurons in layer IV but not in layers II/III in the two- to three-week old cat[145].

The precise mechanisms through which subplate neurons regulate the maturation of inhibitory circuitry in the cortex have not been identified. It has been proposed that the excitatory input from subplate into layer IV drives the increase of KCC2 and GABA-A receptors in

these cells[145]. Indeed, blockage of all glutamatergic activity in the developing cortex prevented the normal developmental increase in KCC2 expression[145]. BDNF might also play a role in regulating this maturation processes as it can decrease KCC2 expression levels[207] and was found to be altered following subplate ablation[208].

Taken together, these studies suggest an important involvement of subplate in the maturation of cortical circuits through at least two processes: 1) The input from subplate into layer IV strengthens the excitatory thalamocortical synapse, probably through STDP; 2) Subplate influences the maturation of inhibition in layer IV which decreases spontaneous intracortical activity. Together, these developmental changes will lead to a strengthening of the coupling between thalamus and cortical layer IV.

1.5.5 Establishment of cortical columns

Many cortical areas, especially the primary sensory cortices, are organized into vertical columns in which neurons respond to the same characteristics of a stimulus[209,210]. Many types of such columns have been identified cytoarchitectonically and functionally, but the most studied are the ocular dominance and orientation columns in the visual cortex and the whisker barrels in the somatosensory cortex. In the visual cortex of many but not all mammals, the thalamic inputs from the two eyes segregate into ocular dominance columns where neurons respond predominantly to the left eye or the right eye[210]. In addition, neurons in the visual cortex are tuned to a specific orientation of a visual stimulus, and neurons with the same orientation preference are organized into orientation columns[210]. In the somatosensory cortex of most rodents, thalamic afferents from a given whisker terminate in a discrete area of layer IV leading to the formation of a barrel pattern. The thalamic axons cluster within the barrel hollows while layer IV neurons aggregate around these axons forming the barrel septa[211].

In the absence of subplate in the early postnatal visual cortex of the cat, thalamic axons from the LGN representing the left and right eye do not segregate and ocular dominance columns fail to form[212,144]. Similarly, orientation selectivity is weaker and orientation maps disrupted or absent after the ablation of subplate[144]. Finally, a preliminary study suggests that the ablation of subplate in the rat somatosensory cortex on the day of birth leads to a disruption of the barrel pattern[198].

The formation of these different cortical columns is dependent on sensory information and neuronal activity. For instance, during the critical period, monocular deprivation induces abnormal patterns of ocular dominance columns with a reduction of columns representing the deprived eye and an increase in columns representing the nondeprived eye[210,213]. Similarly, the removal of an individual whisker leads to an absence of the corresponding barrel[214]. In

the absence of subplate, thalamic inputs into the cortex are weak and cortical activity remains largely uncoupled from thalamic and thus retinal or whisker activity (see previous paragraph). This disconnection could underlie the failure in neuronal tuning and the disruption of column formation[212,195.] Alternatively, a recent model suggests that columnar patterns are first mapped onto the subplate which then serves as a template for other cortical layers[215]. According to this hypothesis, ocular dominance and orientation columns are initially established within the subplate during the waiting period of thalamic axons. Next, these patterns are formed in layer IV and then layers II/III with the help of "teaching inputs" from subplate. Consistent with this model, recent work in the auditory cortex of developing ferrets suggests that tuning maps are first present in the subplate before becoming established in layer IV (P. Kanold, unpublished observation). Further studies in other cortical areas, in particular the visual cortex, could corroborate these findings[215].

1.5.6 Regulation of developmental plasticity

Influence of subplate on STDP between thalamus and layer IV neurons

Linked to a role in the maturation of the cortical circuitry and column formation, subplate has also been involved in directing developmental plasticity. As described above, in the newborn cortex, monocular deprivation during the critical period normally leads to an expansion of the columns representing the open eye and a reduction of the columns representing the closed eye[210,213]. However, in the absence of subplate, a paradoxical shift towards the deprived eye has been observed[145]. This unexpected finding could be explained by the model illustrated in Fig 1_8[145,204,195]. In the absence of subplate, the thalamic input into the cortex is weak, inhibitory circuits remain immature and the spontaneous cortical activity is high[144] (see previous paragraphs). This leads to a decorrelation between thalamic and cortical activities so that the arrival of thalamic inputs into layer IV neurons is random relative to the postsynaptic activity (Fig 1_8 d). In the proposed model, STDP has a longer time window for synaptic depression (LTD) than for synaptic potentiation (LTP). This leads to a bias towards synaptic depression if the timing between pre- and postsynaptic activity is random which has shown to be the case at least for L2/3 pyramidal neurons in the rat[216]. In this scenario, the more active inputs from the nondeprived eye will undergo more frequent LTDs compared to those of the less active deprived eye which would explain the paradoxical shift.

Remodeling of the extracellular matrix

In addition to influencing the cortical circuitry directly, subplate could modulate cortical plasticity through remodelling of the ECM. Based on morphology and marker expression, it has been proposed that the postnatal rodent subplate cells are highly secretory and produce high

levels of proteins associated with the ECM (e.g. Ctgf, neuroserpin, neurotrypsin) (Kondo et al., in preparation). The ECM has been identified as a key component in the regulation of structural plasticity (reviewed in[217,218]). For instance, remodelling of the ECM by the serine protease tissue plasminogen activator (tPA) is necessary for the ocular dominance plasticity to occur during the critical period[219]. Similarly, the degradation of chondroitin sulphate proteoglycans in the adult cortex by injection of chondroitinase-ABC allowed for ocular dominance plasticity even after the normal closure of the critical period[220].

Consistently, several of the secreted proteins associated with subplate have been shown to be acting on components of the ECM and/or to be involved in the regulation of structural plasticity. The serine protease neurotrypsin cleaves the ECM component agrin in an activity-dependant manner and promotes the formation of dendritic filopodia and possibly new synapses in the hippocampus[221]. The expression of neuroserpin, an inhibitor of tPA and possibly other serine proteases, is increased following depolarization which suggests a possible role in the regulation of neuronal plasticity[222].

Subplate neurons could thus play a role in remodelling the ECM and influencing plasticity in the developing and maybe even mature cortex. Further studies would be needed to confirm this hypothesis.

1.6 Subplate in neurodevelopmental disorders

1.6.1 Vulnerability of subplate to preterm hypoxia-ischemia

Hypoxia-ischemia is the most common cause for perinatal brain injury both in the term and preterm infants[223, 224]. In preterm infants, perinatal brain injury is mainly localized in the cerebral white matter. The spectrum of injury ranges from focal cystic (macroscopic) and non-cystic (microscopic) lesions in the deep periventricular white matter characteristic for periventricular leukomalacia (PVL) to more diffuse disturbances in the central white matter [225, 226, 224].

There is increasing evidence, however, that perinatal brain injury in premature infants is not limited to the white matter but also involves cortical and subcortical grey matter. Volumetric magnetic resonance imaging (MRI) studies have shown that premature infants exhibit reduced volumes of the cerebral cortex, thalamus, basal ganglia and hippocampus at term equivalence[227, 228, 229]. Similarly, a neuropathological study of preterm infants with white matter damage has found neuronal loss and gliosis in the thalamus, basal ganglia and to a lesser extent in the cerebral cortex[230]. Infants with PVL also showed an increase in markers of

oxidative and nitrative stress in the overlying grey matter including subplate and Cajal-Retzius cells[231]. In addition, the expression of the chloride transporters NKCC1 and KCC2 was significantly reduced not only in the white matter but also in the subplate and cortical plate[232]. Therefore the terms "encephalopathy of prematurity" [233] or "perinatal panencephalopathy"[230] have been suggested to describe more accurately the scope of cerebral pathology observed in preterm infants.

There is some evidence that subplate neurons could be specifically vulnerable to insults at the preterm stage. A recent study using cell cultures suggests that purified subplate cells are more vulnerable to oxygen-glucose deprivation than cells derived from the cortical plate[147]. Similarly, in a rat model of hypoxia-ischemia, subplate neurons appeared selectively vulnerable to the insult while other cortical layers remained largely unaffected[234]. In human preterm infants, perinatal injury has been shown in MRI to sometimes extend from the white matter into the subplate zone [235].

The process underlying the possible specific vulnerability of subplate is not yet understood but several mechanisms have been proposed. Firstly, subplate neurons mature earlier than neurons in other cortical layers and thus show earlier a mature expression of the glutamate receptors NMDA-R1[236] and AMPA[237,238], at least in some species. It is well established that advanced neuronal maturity is correlated with greater vulnerability, in particular to excitotoxicity[239,240,241]. This maturation-dependant vulnerability has been used to specifically ablate subplate through excitotoxin-injections in the embryonic cat[175]. Interestingly, cultured rat subplate neurons and human subplate neurons in preterm infants (25-37GW) specifically expresses high levels of GluR2-lacking AMPA receptors[147,238]. This receptor configuration exhibits an increased Ca^{2+} permeability and has been shown to be a major mediator of hypoxic-ischemic injury and epilepsy[242,243,244], suggesting a possible mechanism for a selective subplate vulnerability in the preterm human. In addition, the subplate's position deep in the cerebral cortex could contribute to its increased susceptibility to hypoxia-ischemia. Together with the underlying white matter, the subplate is at the end zone of penetrating arteries which are only partially developed before the end of term. In the fetal sheep, the cerebral blood flow is almost twice as low in the white matter and subplate zones and as in the cortical plate and the ventricular zone[245]. This suggests that for these layers there is a minimal margin of safety for cerebral blood flow fluctuations which are very common in preterm infants on intensive care[225]. Alternatively, the specific vulnerability in the subplate could be due to a greater susceptibility to programmed cell death, as the subplate is a largely transient structure, at least in human[110]. Finally, subplate damage could be a secondary effect of lesions in other cortical or subcortical structures[246]. For instance, inflammatory and degenerative processes taking place in the white matter could cause secondary damage in the bordering subplate. In addition, degeneration of thalamic and cortical axons could lead to subsequent cell death in

the highly connected subplate neurons. In co-culture experiments, it has been demonstrated that subplate cells survive better in the presence of thalamic explants suggesting that thalamic afferents provide crucial trophic support to subplate cells[247].

1.6.2 Subplate abnormalities in schizophrenia

Schizophrenia is a form of psychosis which affects approximately 0.7% of the adult population[248]. Schizophrenia can manifest itself with many symptoms including positive symptoms (e.g. hallucinations, delusions, disordered thoughts), negative or deficit symptoms (e.g. blunted emotions, anhedonia, asociality) and cognitive symptoms (e.g reduced long-term and working memory). It is now widely accepted that schizophrenia is a developmental neuronal disorder which primarily affects the cortical circuitry[249]. Many factors, both genetic and environmental, have been linked to the development of schizophrenia.

Interestingly, insults such as maternal viral and bacterial infection in particularly in the second trimester have been shown to lead to an increased risk for developing schizophrenia in later life[250,251]. The second trimester is also the peak of subplate development, and pathological changes in subplate neurons could thus contribute to the development of schizophrenia. Hypoxia or hypoxia-ischemia during the prenatal and perinatal period is another risk factor for schizophrenia[252,253]. As discussed above, the subplate might be particularly vulnerable to hypoxic-ischemic insults at certain developmental stages.

Consistent with a potential involvement of subplate in schizophrenia, increased numbers of interstitial white matter neurons have been reported in the prefrontal, parietal, temporal, cingulate and parahippocampal cortices of schizophrenic patients[254,255,256, 257,258,259,260, 261] . Interstitial white matter neurons can be divided into two populations: superficial and deep interstitial neurons[164]. The superficial interstitial neurons are mainly localized in the gyral white matter and are the remnants of the subplate. In contrast, the deep interstitial neurons are remnants of the deep foetal interstitial neurons and are found in the periventricular white matter. Several studies have reported increased numbers of superficial interstitial neurons (the remnants of the subplate) but not of deep interstitial neurons in several cortical areas[255, 256, 257, 258, 259]. This increase would most likely be caused by an abnormally decreased rate of apoptosis of subplate neurons. In contrast, other studies have shown a shift in the distribution of interstitial white matter neurons from the superficial to the deep white matter, possibly caused by a migration defect of subplate neurons[262,263, 261]. These discrepancies between different studies could at least partially be due to different subtypes of schizophrenia examined. For instance, Kirkpatrick et al. have shown an increase in superficial white matter neurons in the brains of deficit schizophrenic patients (i.e. patients showing negative symptoms) but not in non-deficit schizophrenic patients[256,257].

Very little is known about the function of surviving subplate neurons in the adult human cortex. Based on their position at the interface between afferents and cortical neurons, Kostovic et al. have proposed that superficial interstitial neurons could modulate or gate the input from subcortical and cortical structures into the cortex[264]. They propose among others that an abnormally high number of inhibitory superficial interstitial neurons in the prefrontal cortex could lead to an increased overall inhibition of the prefrontal cortex. This could then result in a functional disconnection between the limbic and prefrontal cortex and thus the executive and emotional brain, a feature characteristic for schizophrenia.

1.6.3 Involvement of subplate in autism

Autism spectrum disorders (ASDs) comprise a variety of behavioural abnormalities which include language delays, impairments in social interactions and repetitive or stereotyped behaviours. ASDs are considered neurodevelopmental disorders, and structural abnormalities have been identified in the brains of ASD patients in many MRI and postmortem studies. The majority of these changes have been found in noncortical regions, in particular in the limbic system and cerebellum[265, 266, 267,268 , 269]. In the cerebral cortex, increased cortical thickness, abnormal layering, dysplasias and altered inter- and intracolumnar spacing have been reported in some but not all cases[267,270, 271,272, 273, 274].

There is some limited evidence of an involvement of subplate neurons in the development of autism. Similar to schizophrenia, an increase in superficial white matter neurons has been described in a subset of ASD patients[267,273, 274]. These supernumerary cells in the subplate zone lead to a poor differentiation of the boundary between layer VI and the white matter[275]. The origin of these additional superficial white matter cells is currently unclear. Firstly, they could constitute cortical neurons which did not migrate properly. Indeed, migration defects have been proposed to be present in autism as a subset of patients presents polymicrogyria, macrogyria, heteroplasia or schizencephaly[276]. In addition, ASD patients show an impairment in the reelin signalling pathway[277], and certain polymorphisms in the reelin gene increase the susceptibility to ASD[278,279,280]. Alternatively, the increase in superficial white matter neurons could also be caused by incomplete apoptosis of subplate neurons, similarly to what has been proposed for some cases of schizophrenia[275].

1.7 Aims of this thesis

From studies in various species over the last sixty years, it has become evident that the subplate is an important player in cortical development[170,110,195]. At different developmental stages, subplate cells fulfil different developmental roles (Fig 1_9). For instance, embryonic subplate cells are involved in the guidance of corticofugal and thalamocortical axons[167, 175]; early postnatal subplate neurons probably play a role in generating oscillatory activity[97,201] and in the maturation of the thalamocortical circuitry[104,145]; adult subplate could be important in supporting cortico-cortical connectivity[110] (see sections 1.5.2, 1.5.3, 1.5.4 and 1.2.4). While some of these roles are widely documented (e.g. guidance of thalamocortical afferents to the cortex) others remain poorly characterized (e.g. regulation of plasticity between thalamic afferents and layer 4 neurons) or are largely hypothetical at this stage (e.g. guidance of tangentially migrating interneurons). Moreover, very little is known about the molecular mechanisms underlying these functions. Recent studies by our laboratory and others have started to profile the gene expression of the murine subplate at different developmental stages (E12[153], E18.5[95], P8[117] and adult (Belgard et al., submitted)). One long-term goal of this effort is to correlate the changing gene expression patterns to the changing functions of subplate across development (Fig 1_9). This approach will hopefully allow us to identify key molecules and pathways underlying the characteristics and roles of subplate. In addition, new hypotheses on currently unknown functions or properties of subplate might emerge from such an analysis.

The first aim of my thesis is to contribute to this effort by expanding the gene expression analysis to the embryonic E15.5 mouse subplate (Chapters 2 – 6). This developmental stage is important as it is the time when thalamic axons start accumulating and forming area-specific connections within subplate[176].

- In Chapter 2, I will optimize a laser capture microdissection protocol to successfully isolate RNA from the embryonic subplate and the overlying cortical plate.

- In Chapter 3, a microarray analysis will be performed to compare gene expression between subplate and cortical plate at E15.5. The quality of the microarray data will be assessed using quantitative RT-PCR and publicly available gene expression datasets.

- In Chapter 4, a selection of genes identified as higher expressed in subplate on the microarray will be validated using in situ hybridization or immunohistochemistry. Analysis of reeler mutant brains (where the relative position of subplate and cortical plate is inverted) will be used as an additional method of validation.

- In Chapter 5, I will study in detail the temporal expression profile and extracortical expression patterns of validated selected genes. Genes will also be assessed for their potential co-localization with markers for GABAergic neurons. Based on these findings, hypotheses on the potential function of these genes in subplate will be discussed.

- In Chapter 6, I will explore some methods to alter expression levels of two selected subplate-specific genes (Cdh10 and Unc5c) in order to gain further insight into their function.

The gene expression profiling of subplate does not only allow us to gain insight into subplate function and molecular mechanisms, but can also provide us with molecular markers to specifically identify, monitor and manipulate these cells in normal and pathological development. From the P8 microarray analysis, several such molecules have been found which can be used to label different subplate subpopulations at postnatal stages in the mouse[117]. The second aim of my thesis is to make use of some of the newly identified subplate markers to study subplate cell populations in pathological development (Chapters 7 and 8).

- In Chapter 7, I will analyse the expression of a selection of murine subplate markers in the postnatal and adult rat, the most commonly used species for disease models.

- In Chapter 8, confirmed markers will be used to monitor subplate in a rat model of preterm hypoxia-ischemia. The vulnerability of two different subplate subpopulations will be described and compared to cells in other cortical layers and the white matter.

Each experimental chapter will contain a Methods sections detailing the relevant experimental procedures.

A general discussion (Chapter 9) will summarize the major findings of this thesis and put them into the wider context of the literature and ongoing research in our own laboratory.

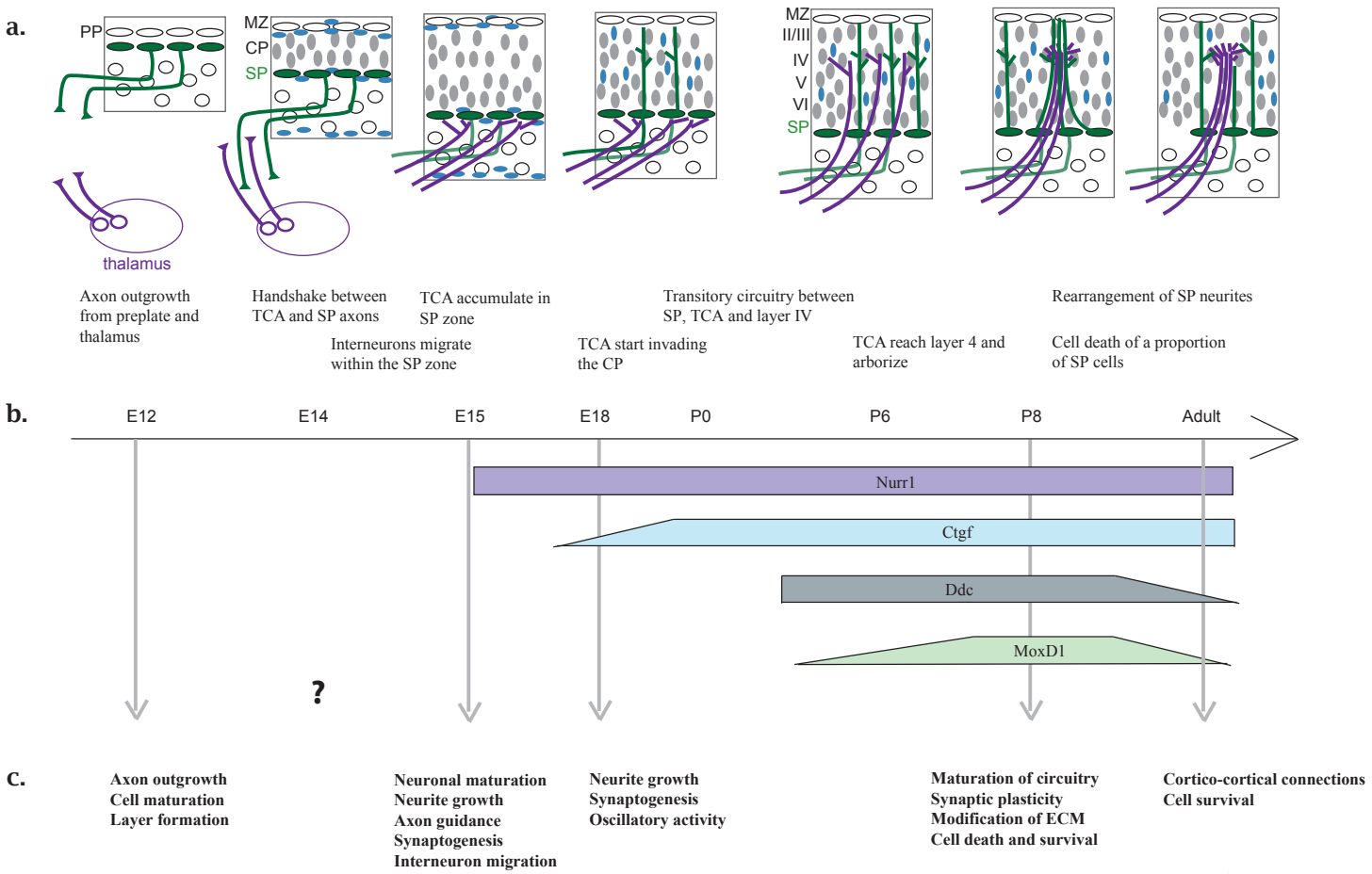

Figure 1_9. **Correlating changing expression in subplate properties and functions with gene expression.** This illustration gives an overview how cellular and functional changes in the developing subplate (SP) (a) could be reflected by gene expression (b) and molecular mechanisms (c). a. Schema showing the development of the mouse SP zone from E12 to adult and its integration in the cortical circuitry. Embryonic SP axons (green) pioneer the corticofugal pathway and interact with thalamocortical afferents (TCAs, purple) in the internal capsule (handshake) guiding them across the pallial subpallial boundary. Interneurons (blue) migrate within the developing SP zone. Early postnatal SP neurons establish a transitory circuitry with TCA and layer 4 neurons influencing the maturation and plasticity of the cortical circuitry. At the end of the first postnatal week, SP neurites are rearranged in the barrel field and a subset of SP cells dies through apoptosis. b. Examples of expression patterns of SP-specific genes identified by the P8 gene expression profiling. Nurr1 is expressed in the SP from E15 onwards and Ctgf from E18. Moxd1 and Ddc are only found in the postnatal SP. Data on gene expression in the embryonic SP is incomplete. c. Functions and developmental processes linked to the SP zone at E12, E15, E18, P8 and adult (the five time-points where gene expression studies are performed).

Chapter 2 Optimization of Laser Capture Microdissection for E15.5 subplate

2.1 Introduction

The aim of the first part of my thesis is to establish a gene expression profile for the embryonic E15.5 subplate (see section 1.7). The first step towards this goal is to separate the subplate cell population from the rest of the embryonic brain. Different methods have been employed in the past to specifically isolate the subplate at various developmental stages. A previous study in our laboratory has used manual dissection to cut out the embryonic E18.5, the postnatal P8 and the adult subplate[95,117]. For this, brains were cut into 150µm- thick sections on a vibrating microtome and subplate was dissected with a microknife based on its location directly above the white matter from transilluminated sections. Subsequent gene expression analysis using microarrays suggested that this method yielded relatively pure cell populations for the P8 and adult subplate. In contrast, E18.5 samples appeared to contain a large amount of white matter contamination (Anna Hoerder-Suabedissen, unpublished observation).

Immunopurification of the E17 rat subplate using an anti-$p75^{NTR}$ antibody has been described, either using immunopanning[142] or magnetic-activated cell separation[147]. According to the authors, the expression of the neurotrophin receptor $p75^{NTR}$ is restricted to the subplate in the embryonic E17 rat cortex. Both methods were reported to yield approximately 90% pure population of subplate neurons based on $p75^{NTR}$ expression, BrdU-birthdating and expression of the neuronal marker tau[142,147].

Finally, fluorescent-activated cell sorting (FACS) has been used to separate different subpopulations from the embryonic E12 mouse preplate using GFP-expressing mouse lines[153]. Due to the unavailability of a transgenic mouse line which expresses GFP specifically in the very early embryonic subplate cells, a gene expression profile was obtained indirectly, by comparing gene expression in all preplate neurons with Cajal-Retzius cells only[153].

None of the above-described methods seems optimal for isolating the embryonic E15.5 mouse subplate towards my aim. Manual dissection of unstained tissue would likely yield impure cells populations as subplate at this stage is thin and very difficult to distinguish from the underlying unmyelinated intermediate zone. Immunopurification requires a subplate-specific antigen which in addition has to be localized on the cell membrane in order to be targeted with an antibody. To my knowledge, the only such antigen described as specifically expressed in the embryonic subplate is $p75^{NTR}$ [281,142]. Gene expression data on

AllenBrainAtlas[282,283] indicates, however, that in the E15.5 mouse cortex, $p75^{NTR}$ is not only expressed in the subplate but also in the lower cortical plate. This could constitute a difference between mouse and rat, even though a careful analysis of the expression data provided by DeFreitas et al. indicates that there are also some labelled cells in the cortical plate in the E17 rat[142]. Several transgenic mouse lines which express GFP in the subplate are available – Edg2-GFP, Ctgf-GFP and Golli-tau-eGFP[72,284]. However, Edg2 and Ctgf are only expressed in the murine subplate from late embryonic or postnatal stages onwards[117] and therefore cannot be used to label the early embryonic subplate. Expression of Golli-tau-eGFP appears in the preplate as early as E12.5[72]. However, in these mice, GFP expression is not entirely restricted to subplate as a proportion of labelled cells are also found in layer VI and very occasionally in layer V[72].

In light of the limitations of previously described methods for subplate purification, I decided to try using laser capture microdissection (LCM) to isolate the E15.5 subplate. Several laser microdissection systems have been developed and commercialized which vary mainly in the type of laser used (infrared or ultraviolet (UV)) and the way the dissected tissue is collected[285]. LCM has initially been developed and optimized for the separation of tumours from the surrounding healthy tissue[286,287,288,289]. Since then it has also been successfully adapted to collect single neurons as well as cell groups in the central nervous system (CNS) both in rodents[290,291,292,293,294,295] and human[296,297,298,299,300,301,302,303,304]. Most commonly, cells are isolated from ethanol-fixed cryosections (Fig 2_1) or formalin-fixed paraffin sections. However, recent developments in the technology have made it possibly to also isolate live cells from culture systems.

Our laboratory has access to a PALM Microbeam IP 230V Z (Zeiss) which is a UV-based laser system[305]. With this set-up, the tissue can be visualized under a microscope and individual cells or cell populations can be identified and selected for microdissection via a software interface. The selected tissue is then isolated by photo volatilization ("cutting") of the cells surrounding the selected area. Finally, the excised cells are collected by a defocused UV laser pulse which creates a gaseous expansion beneath the tissue catapulting it upwards into a collection tube (Figure 2_1).

The main challenge when using laser capture microdissection for gene expression profiling is to obtain RNA of good quality[287,306,289]. RNA can easily be degraded by endogenous and exogenous RNAses. The key to preventing RNA degradation is to minimize the exposure time of the tissue to conditions where RNAses are most readily active, i.e. 1) an aqueous environment and 2) room temperature. However, to be able to identify the embryonic subplate, tissue sections have to be stained which requires the exposure of the tissue to water solutions as well as other chemicals. Secondly, in order to analyze gene expression in subplate, I need to

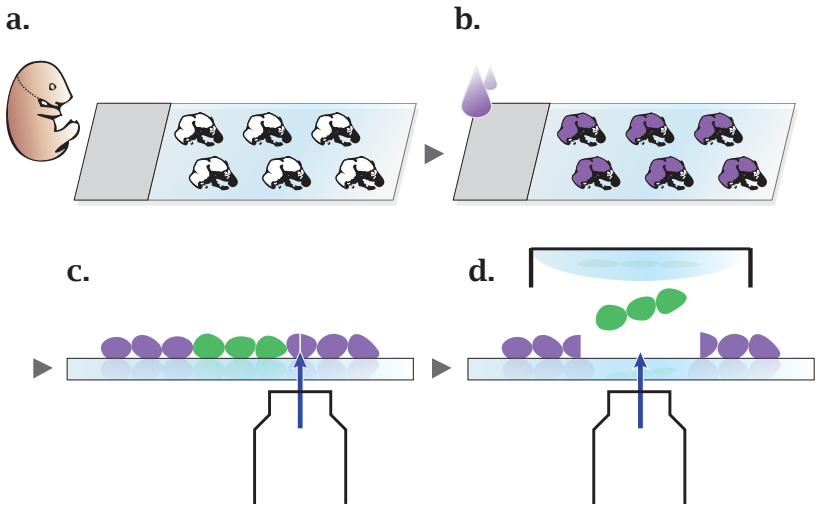

Figure 2_1. **UV-laser capture microdissection from embryonic mouse cryosections.** a. Heads of mouse embryos are fresh-frozen and cryosectioned. b. Sections are ethanol-fixed, stained and dehydrated. c. Cells surrounding the selected area are volatilized by the UV-laser beam. d. A defocused UV laser pulse creates an air expansion underneath the selected area catapulting the selected cells into the collection tube.

compare it to at least one reference cell group. A rigorous experimental design requires that these different cell groups are collected from the same tissue sections. Dissecting out multiple areas from each section, however, will increase the exposure time of the tissue to room temperature.

The aim of this chapter is to optimize each step in the laser capture microdissection protocol for the embryonic E15.5 cortex in order to minimize RNA degradation and to obtain RNA of sufficient quality from all samples.

2.2 Methods

2.2.1 RNase-free experimental environment

All procedures were performed in an RNase-free environment. Working surfaces were treated with RNase decontamination solution (RNaseZap, Ambion) and rinsed with RNase-free water. Glassware was baked at 200°C for 4h to inactivate RNase. Certified RNase-free plastic ware was used in each process. All solutions were made from chemicals of molecular biology grade and RNase-free water. No additional RNase inhibitors were added into the individual solutions.

2.2.2 Tissue preparation

Time-pregnant mice were killed by cervical dislocation. Whole heads of E15.5 mice were flash-frozen directly in isopentane on dry-ice. Nineteen embryos from 6 litters were used for the optimization. Once hardened, the heads were embedded in O.C.T compound (Tissue-Tek) and stored at -80°C. The tissue was sectioned (10µm or 20µm) on a cryostat (Jung CM3000, Leica) and mounted on membrane-coated 1mm PEN slides (Zeiss). Before use, the slides had been treated with RNaseZap and UV irradiation at 320nm for 30min as recommended by the manufacturer. Once the first section had been mounted, the slide was kept inside the cryochamber (-18°C) while the next section was cut. Four to six sections were mounted in this way on each slide. Two slides were prepared at a time and processed in parallel. Sections were allowed to air-dry for at least 2min before fixation in 95% EtOH for 30sec, both in the cryochamber.

2.2.3 Staining procedures

Hematoxylin and hematoxylin and eosin (H&E) staining were performed as previously reported for LCM samples[285]. Sections were rinsed with 70% EtOH and then with H_2O, stained with Mayer's hematoxylin (Sigma) for 15sec, rinsed with H_2O followed by 70% EtOH, stained with Accustain Eosin Y (Sigma) for 10sec (for H&E only), dehydrated with 95% EtOH, 10sec, 100% EtOH, 40sec, and cleared with xylene, 60sec.For cresyl violet staining, sections were rehydrated in 95% EtOH, 75% EtOH, 70% EtOH, stained in cresyl violet for 30–45sec and dehydrated in 75% EtOH, 95% EtOH, 100% EtOH, 100% EtOH, 30sec each. 0.1% cresyl violet was prepared in H_2O and 1% cresyl violet in H_2O or 70% EtOH, filtered and stored at 4°C for up to one month.100% EtOH was stored with desiccant beads (Molecular sieves 4 Å beads, 8–12mm mesh, Sigma) to prevent any rehydration. After dehydration, sections were air-dried and either processed immediately or stored in a box with desiccant at -80°C for up to several weeks.

2.2.4 Immunohistochemistry

Frozen sections were postfixed in 4% paraformaldehyde (PFA) in PBS for 20min and quenched in 1.5% hydrogen peroxide for 30 min. Sections were then blocked for 2h at RT with 5% donkey serum (Sigma) in TBS with 0.1% Triton-X100 (BDH) and incubated with goat anti-Nurr1 1:200 (AF2156, R&D Systems) in 1% donkey serum in TBS at 4°C overnight. Biotinylated donkey anti-goat 1:200 (Abcam) in 1% donkey serum in TBS was applied for 2h at RT and reacted with avidin-biotinylated enzyme complex (ABC) using the Vectastain Elite kit (Vector) and diaminobenzidene (DAB) according to the manufacturer's instructions.

2.2.5 Laser capture microdissection

LCM was performed using a PALM Microbeam IP 230V Z (Zeiss).

Slides which had been stored at -80°C were transported and kept in a box with desiccant on dry ice. Slides were subsequently dried one at a time in a 50ml Falcon tube with desiccant at RT. From each section, four areas (anterior and posterior subplate and lower cortical plate, Fig. 2_3) were cut and catapulted into separate caps (0.6 ml Eppendorf tube). Caps either contained 50µl of RNA stabilization solution (RNAlater, Ambion) or 50µl lysis buffer (RLT, RNeasy micro Kit, Qiagen). Tubes were kept on ice with the cap down until all areas were collected. The approximate time required to collect all four areas from one slide (4–6 sections) was 40min. In order to avoid bias due to RNA degradation, the order in which the four different cell populations were dissected was changed on every slide. The tissue strips that were in RNA stabilization solution were directly stored at -80°C with the cap down. Strips in lysis buffer were vortexed for 45sec, spun down and stored at -80°C.

2.2.6 RNA extraction, quantification and quality control

Cell groups collected in lysis buffer were defrosted on ice and pooled with the same cell lysates from different brains. Tissues stored in RNA stabilization solution were defrosted on ice and stabilization solution was replaced with lysis buffer under a dissecting microscope using a syringe. After 5min incubation, the samples were vortexed for 45sec and spun down. Then the same cell lysates derived from different brains were pooled (see Fig 2_5 j for numbers).

Total RNA was extracted using the RNeasy micro kit (Qiagen) following the manufacturer's instruction. On-column DNase digestion step was performed. RNA quantities were determined using spectrophotometry (Nanodrop ND-1000, Labtech). RNA integrity after LCM was analyzed both on RNA 6000 Pico Chips (Agilent Technologies) and by reverse-transcription PCR (RT-PCR).

Approximately 20ng of total RNA were used as a template for reverse transcription using Superscript III reverse transcriptase together with random hexamers (Invitrogen) following the manufacturer's instructions. Long PCR fragments corresponding to the regions of the mouse Nurr1 (subplate marker), Tbr1 (cortical plate marker) and β-actin cDNAs were amplified using the following sets of forward (F) and reverse (R) primers:

Nurr1 (1244 bp): F 5'-catggacctcaccaacactg-3'; R 5'- ctgggttggacctgtatgct-3'

Tbr1 (1204 bp): F 5'- tctcgaccactgacaacctg-3'; R 5'- gcgtagttgctcacgaactg-3'

β-actin (677 bp): F 5'- agccatgtacgtagccatcc-3'; R 5'- acatctgctggaaggtggac-3'

2.3 Results

To study the gene expression in the E15.5 subplate, I decided to isolate four different cell populations from sagittal cryosections of the E15.5 head: the anterior and posterior subplate and the anterior and posterior lower cortical plate (see Fig 2_2 and Chapter 3 for further details). The following four steps in the LCM protocol were optimized in order to obtain RNA of the best possible quality: tissue staining, section thickness, storage of slides and collection buffer. RNA quality was assessed using the RNA integrity number (RIN), a software algorithm developed by Agilent Technologies, which evaluates RNA quality on a scale from 1 (degraded) to 10 (intact) based on several features of the electrophoretic RNA trace[307]. RIN has been reported as the most reliable method for evaluating RNA quality in LCM samples[290].

2.3.1 Identification of the subplate on stained sections

Four different protocols for staining cryosections were compared – hematoxylin, hematoxylin and eosin (H&E), 0.1% cresyl violet and 1% cresyl violet (Fig 2_3). Either hematoxylin only (Fig 2_3 a) or H&E (Fig 2_3 b) resulted in a faint and nearly uniform staining pattern throughout the cortex, and the different cortical layers were difficult to distinguish. Cresyl violet staining gave overall a better contrast and more morphological details than the

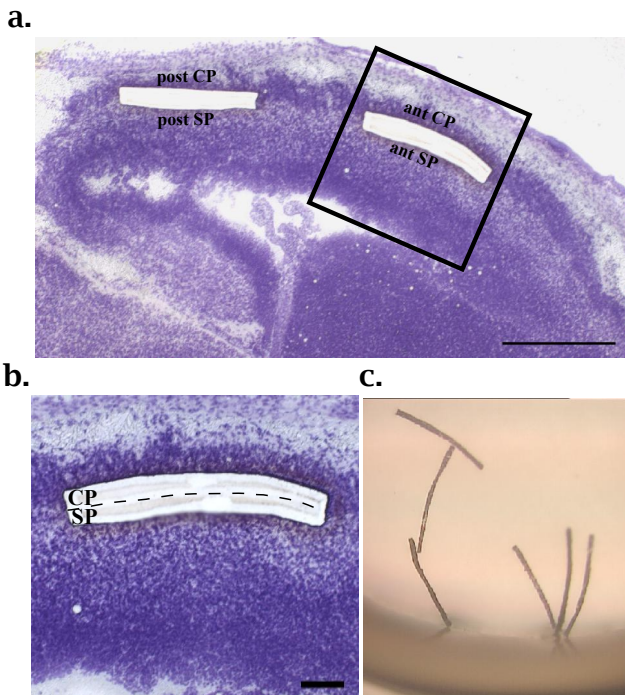

Figure 2_2. **The four cell populations isolated by laser capture microdissection.** a. Cresyl-violet stained cryosection after subplate (SP) and lower cortical plate (CP) from anterior and posterior cortex have been isolated. b. High magnification of the anterior cortex showing the border between SP and CP. c. Microdissected tissue strips in RNA stabilization solution visualized in the cap of the collection tube. Scalebars: a. 500µm. b. 100 µm.

hematoxylin stains. This staining allowed me to reliably identify the dense and darkly stained cortical plate compared to the more cell-sparse and lightly stained subplate below (Fig 2_3 c, d, f). The lower border of subplate, however, was indistinguishable from the intermediate zone based on the staining pattern alone. Immunohistochemistry on adjacent sections against the subplate marker Nurr1 labelled an approximately 40µm-thick band of cells directly below the cortical plate (Fig 2_3 e). For the microdissections, I therefore defined the subplate as a cell band of 40µm just below the lower border of the dark-stained cortical plate, and the lower cortical plate as a 40µm thick cell band just above this border (Figure 2_2).

I found that to achieve satisfactory staining results, 1% cresyl violet required a shorter incubation time (~30sec) than 0.1% cresyl violet (~2min). It has been previously reported that RNAse inhibitors were incompatible with cresyl violet[308] and that ethanol-based staining solutions improve RNA integrity[287]. Therefore, I also prepared 1% cresyl violet in 70% EtOH. I found that this ethanolic staining solution took longer to dissolve but provided equally good results as the water-based solution.

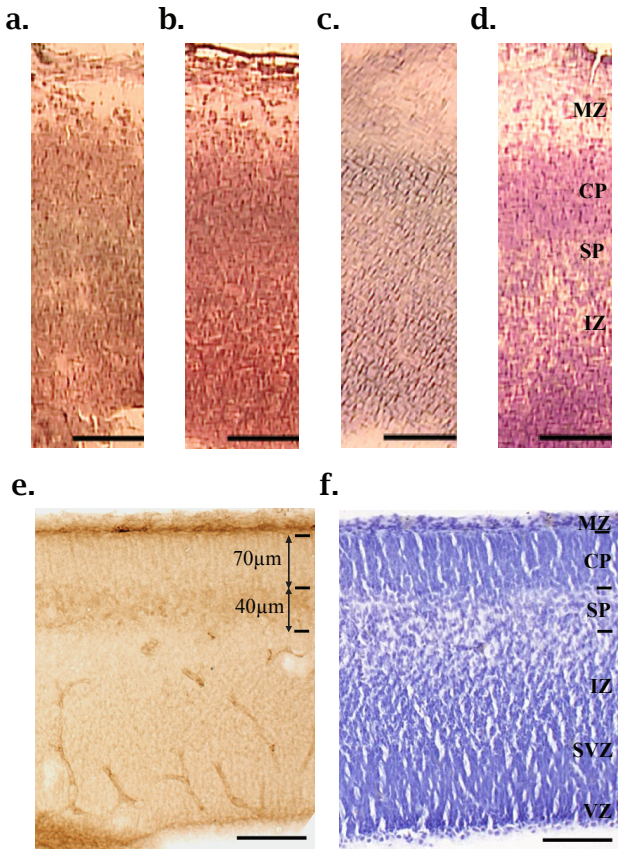

Figure 2_3. **Comparison of different staining methods to identify the subplate.** a. Hematoxylin. b. Hematoxylin and Eosin (H&E). c. 0.1% cresyl violet in H_2O. d. 1% cresyl violet in H_2O. 1% cresyl violet (d) provides the best morphological details and allows clear distinction between cortical plate (CP) and subplate (SP). e, f. Position of the SP in the E15.5 mouse cortex. Depth and width of the SP layer on cresyl violet stained sections (e) was confirmed with immunohistochemistry against Nurr1 (f). Scalebars: 100µm. MZ: marginal zone; IZ: intermediate zone; SVZ: subventricular zone; VZ: ventricular zone.

2.3.2 Section thickness

Manufacturer's guidelines and many protocols recommend using relatively thin sections of 5–12µm[293,295]. I tested two different cryosection thicknesses for LCM: 10µm and 20µm. Cresyl violet staining resulted in equally clear morphological details for sections with both thicknesses (Fig 2_4 a, d). During LCM, I used slightly higher laser energy to cut the 20µm sections than the 10µm (UV energy of 76 points vs. 72 points, respectively), and cut around the cell group two or three times. With these minor adaptations, both cutting and catapulting were consistently successful (Fig 2_4 b, c, e, f). I did not notice any increase in burnt or damaged tissue on the 20µm sections compared to the 10µm sections, neither after cutting nor after catapulting.

2.3.3 Tissue storage

Next, I tested whether storage of sections at -80°C before LCM would noticeably impair RNA quality as previously suggested[291,295] by comparing two approaches. For the first, two slides were prepared at a time, and cell groups were microdissected immediately after staining and dehydration. For the second approach, stained and dehydrated slides were stored in a box with desiccant at -80°C for several days. I noted that condensation accumulated on slides when they were brought from -80°C to RT, which might impair RNA integrity due to RNase activity in rehydrated tissue. This problem could be simply prevented by allowing the slides to warm up in a tube containing desiccant beads. RNA of similar quality was obtained from both approaches with an average RIN of 4.5 for unstored sections and of 4.1 for stored sections (Fig 2_5 a, b).

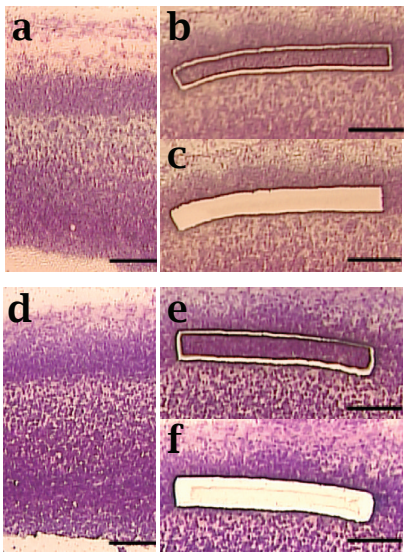

Figure 2_4. **Comparison of cryosection thicknesses.** a-c. 10µm cryosections d-f. 20µm cryosections. The tissue morphology on 10 µm (a) and 20µm (d) sections is of similar quality when stained with 1% cresyl violet. Increasing thickness from 10µm (b, c) to 20µm (e, f) does not cause increased tissue damage during laser cutting (b, e) and catapulting (c, f) even though slightly higher laser energy is needed. Scalebars: 100µm. MZ: marginal zone; CP: cortical plate; SP: subplate; SVZ: subventricular zone; VZ: ventricular zone.

2.3.4 Collection buffer

Collecting samples from multiple regions of the same brain section and pooling samples from several slides increases the time the tissue is in the harvesting tube. I compared collection of tissue in RNA stabilization solution and lysis buffer. Samples preserved in stabilization solution yielded better RNA quality (average RIN = 4.2) than when dissected tissue was collected directly in lysis buffer (average RIN = 3.5) (Fig 2_5 c, d).

2.3.5 Final RNA quality

Based on these observations, I decided on a final protocol which is summarized in Figure 2_6 . Using this protocol, RNA of excellent quality from all four cell groups (anterior and posterior subplate and cortical plate, Fig 2_5 e-h) was obtained. Importantly the variability between samples was also reduced (Fig 2_5 j). The four cell groups collected had RINs ranging from 8.0 to 8.9, indicating that RNA is of high quality for downstream applications[308]. To confirm this result, I tried to amplify long fragments from selected genes (β-actin, Nurr1 and Tbr1) by RT-PCR. The presence of long transcripts is an additional indicator of the RNA integrity. From all four samples, a 677 bp long β-actin PCR product was generated (Fig 2_5 i). Nurr1 is specifically present in the subplate at E15.5 while Tbr1 (T-box brain gene 1) is strongly expressed in the deep layers of the cerebral cortex throughout development[309]. A 1244 bp long cDNA fragment of Nurr1 and a 1204 bp long fragment of Tbr1 were amplified from the subplate and the cortical plate samples, respectively.

2.3.6 RNA quantity

RNA yields from LCM samples are difficult to evaluate as concentrations are usually below the detection limit of spectrophotometers (10ng/µl), and bioanalyzers only give an inaccurate estimate of quantity at this concentration. In order to estimate RNA quantities more reliably, I microdissected and pooled 20µm-thick strips from approximately 140 sections. RNA extracted from this large number of tissue samples was successfully quantified by spectrophotometry, and I obtained yields of total RNA between 120ng (subplate) and 180ng (cortical plate) per sample.

2.4 Discussion

One of the major difficulties when using LCM for gene expression profiling is to obtain RNA of good quality for subsequent gene expression analysis. This is particularly challenging in my study as multiple cell groups are dissected simultaneously from the same tissue sections which increases the time required for microdissection disproportionally. To address

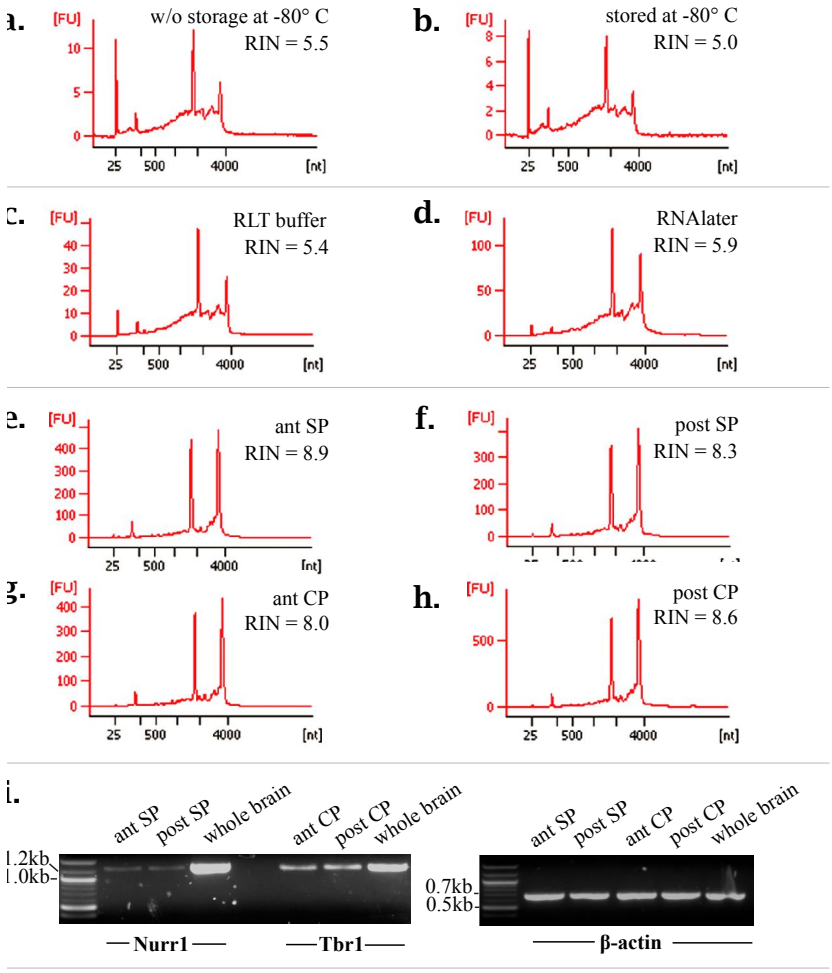

j.

Experimental condition	Mean *n* of strips / sample	Mean RIN (SD)
Without storage	13	4.5 (1.2)
Stored at -80°C	14	4.1 (1.0)
RLT lysis buffer	33	3.5 (1.3)
RNAlater	33	4.2 (1.7)
Optimized protocol	80	8.5 (0.4)

Figure 2_5. **RNA quality after different processing conditions**. a-h. Electropherogram traces of RNA analyzed on Agilent RNA 6000 Pico Chips. For each approach, the RNA trace with the highest RIN out of four samples is shown. The y-axis of the electropherograms represents fluorescence units (FU) and the x-axis represents the nucleotide length of the RNA (nt). The peaks of the 18S and 28S rRNA fragments are clearly visible. a,b After staining and dehydration, cryosections were either processed immediately by LCM (a), or they were stored at -80°C for several days before LCM (b). Storage of sections only had a minor effect on RNA integrity but greatly improved the flexibility of the workflow. c,d Microdissected cell groups were either harvested in lysis buffer (c) or RNA stabilization solution (d). Stabilization solution slightly improved the RNA integrity and in addition allowed visualization of the dissected strips. e-h. The final optimized protocol yields RNA of excellent quality with RINs > 8 from all four microdissected cell groups: anterior subplate (SP) (e), posterior SP (f), anterior cortical plate (CP) (g), posterior CP (h). i. RT-PCR analysis of selected long transcripts. A 1244 bp fragment of Nurr1 was amplified from anterior and posterior SP; a 1204 bp fragment of Tbr1 was amplified from anterior and posterior CP; a 677 bp long fragment of β-actin transcript was amplified from all four samples. Total RNA from the whole E15.5 brain was used as a positive control. The presence of long transcripts in all samples confirms that the RNA is largely undegraded. j. Summary of the different experimental conditions, the average number of strips processed per area, and the average and standard deviation (SD) of the RINs among the four groups after LCM.

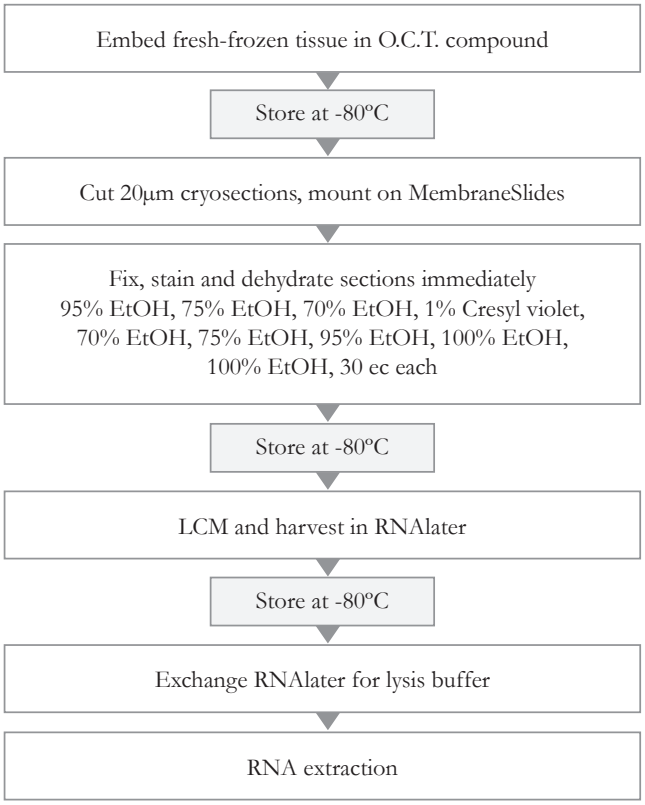

Figure 2_6. **Flow diagram of the optimized protocol.** All steps are performed in an RNase-free environment. Fresh-frozen whole heads are stored at -80°C for up to several months. Heads are cryosectioned to 20µm, and four to six sections are mounted on a membrane-coated PEN slide. Sections are fixed in 95% EtOH, rehydrated with 75% and 70% EtOH, stained with 1% cresyl violet in 70% EtOH and dehydrated with 70%, 75%, 95%, 100%, 100% EtOH, 30sec each. Slides are stored at -80°C up to several weeks in a box with desiccant beads. Four cell groups from the same section are microdissected, harvested in individual tubes with RNA stabilization solution and stored at -80°C. Stabilization solution is replaced with lysis buffer and cell lysates from different brains are pooled before RNA extraction.

these issues, I have analyzed and optimized four crucial steps in the LCM procedure: tissue staining, section thickness, storage of sections and harvesting and storage of microdissected samples.

The ability to identify the subplate and to distinguish it from the cortical plate is a prerequisite for the planned study. A good staining should allow me to clearly visualize the histological structure but at the same time minimize RNA degradation. Therefore, all staining protocols have to be very short to reduce the time the tissue is exposed to room temperature, aqueous solutions and chemical components. I found that staining with 1% cresyl violet needed the shortest staining time (30secs) while at the same time provided the best histological details. This staining protocol allows me to distinguish between cortical plate and subplate, but not between subplate and intermediate zone. Based on Nurr1 staining, I defined subplate as a 40µm thick band below the cortical plate. The absence of a clear histological border between subplate and intermediate zone, however, makes the identification and dissection of subplate somewhat subjective.

In most studies, LCM is performed on very thin sections (5–12µm). I found that it was possible to increase the section thickness to 20µm without impairing staining quality and cutting and catapulting efficiency. The time necessary for laser-cutting increased because I had to cut

around each strip at least twice. However, this did not considerably increase the overall time per slide as cutting is automated and very rapid. Doubling the section thickness allowed me to half the number of sections and thus the number of slides, which is both time- and cost-effective.

Previous studies have reported that cryosections should be processed by LCM immediately after staining to avoid RNA degradation[291,295]. This approach may be ideal, but it is difficult to manage, especially as in my case LCM and histology facilities are not in the same building. I found that storage of sections had only a minor effect on RNA integrity. I therefore subsequently stored sections at -80°C up to several weeks which allowed a much more flexible work management.

To minimize the number of slides used I placed 4-6 sections on each slide and it took me 30–40min to harvest four cell groups from all sections on a slide. For tissue collection, one tube was placed on the laser microdissector at RT while the three tubes for the other three cell groups were kept on ice. In each LCM session, six to eight slides were processed, and samples were collected in the same four tubes. Under these circumstances, I found that RNA stabilization solution preserved RNA better and yielded slightly better RNA quality than when dissected tissue was collected directly in lysis buffer. In addition, the stabilization solution allowed me to visualize and to confirm the number of dissected strips after tissue harvesting and before RNA extraction. I estimate that approximately 10% of microdissected tissue was not successfully captured in the harvesting cap.

Although recently developed amplification methods make it possible to analyze degraded samples, it is likely that part of the gene expression information will be lost, especially from less abundant transcripts[308]. Even more importantly, RNA quality has to be consistent between different cell populations in order to allow unbiased comparison. By using my final protocol, I have consistently obtained RNAs with RINs > 8 from all dissected cell groups. In addition, long transcripts (> 1.2 kb) of layer-specific genes were amplified from all four samples by RT-PCR. These findings confirm that RNA quality obtained by this protocol is well suited for subsequent microarray analysis.

Currently, there is no reliable method for measuring low concentrations of RNA (< 10ng/µl). In order to estimate the RNA yield, I microdissected a large number of strips and quantified the extracted RNA by spectrophotometry. I found an approximate yield of 1.3ng of total RNA per cortical plate strip and 0.8ng per subplate strip, which is consistent with the different cell densities of these two layers. With the recent development of very efficient amplification methods, it has become possible to perform microarray analysis on very small quantities of total RNA, starting from as little as a 250-300pg[310,311]. However, with decreasing

sample size, amplification from less abundant genes becomes unreliable due to stochastic effects[312,313]. In order to avoid loss of information on rare transcripts, it is desirable to use at least 10–20ng of RNA as starting material (Sheena Lee, personal communication). Based on my estimates of RNA recovery, this corresponds to at least 20–30 microdissected strips in the optimized experimental conditions.

2.5 Conclusion

I have optimized a protocol for LCM which allows me to identify and isolate subplate and lower cortical plate in the anterior and posterior E15.5 murine cortex. RNA of high quality (RIN > 8) was obtained from all four simultaneously microdissected cell groups. In addition, I estimate a yield of approximately 0.8 to 1.2ng of RNA per tissue strip. This indicates that both RNA quality and quantity isolated by this method is well suited for a downstream microarray study.

Chapter 3 Gene expression profiling of the embryonic E15.5 subplate

3.1 Introduction

The embryonic E15.5 subplate is a highly dynamic and heterogeneous compartment which not only contains postmigratory subplate neurons but also radially migrating excitatory neurons, tangentially migrating interneurons, developing blood vessels and a rich ECM. The subplate neurons themselves are undergoing many developmental processes including cell maturation, synapse formation and axonal and dendritic growth. E15.5 is an important developmental time point for subplate as it is the time of the accumulation of thalamic axons within subplate and the establishment of the first area-specific thalamocortical connections[176].

The early embryonic subplate cells could be involved in some or all of the following developmental functions: the guidance of monoaminergic and thalamocortical afferents to the cortex, the guidance of corticofugal projections from layers V and VI to the thalamus, the establishment of an early circuitry with the thalamic afferents, the production of the ECM, the development of blood vessels and the guidance of tangentially migrating interneurons[170,110,195]. Of these potential roles of subplate, its involvement in the guidance of corticofugal axons and thalamocortical afferents is the most characterized and best established (for more details on the embryonic subplate and its potential functions see sections 1.2.2, 1.5.1 and 1.5.2). Although several molecules have been suggested to be involved in this process (e.g. the adhesion molecules L1, J1 and NCAM[132] or the guidance molecule ephrin A5[194, 192]), our understanding of underlying molecular mechanisms remains incomplete. Other proposed functions of subplate such as the guidance of tangentially migrating interneurons remain mostly speculative at this stage[314,315].

A few genes have been identified in the past to be specifically expressed in the embryonic mouse subplate cells. These include MAP2[64], the neurotransmitter receptors GABRA-A[68] and VGLUT2[69] and the calcium binding protein calretinin[124]. Many other historical markers of the embryonic subplate appear not to be expressed in subplate cells themselves but rather in migrating interneurons (somatostatin[127], calbindin[92]) or in fibers growing through the subplate zone (L1 and NCAM[132,134]).

Recently, more extensive gene expression studies of the subplate have been conducted (see also section 1.3.3). Osheroff and Hatten have performed a microarray analysis of preplate cells destined to become subplate in the E12 mouse cortex[153]. They have identified two genes which were specifically expressed in the preplate at E12 and in the subplate at E14

–hippocalcin and EAAC1. The expression pattern of these genes at later developmental stages was not investigated. However, gene expression data on AllenBrainAtlas[283] suggest that at least in the adult mouse, these two genes are ubiquitously expressed in the entire forebrain.

In our own laboratory, a microarray screen of the P8 subplate has been performed and six genes with subplate-specific expression were described (Nurr1, Ctgf, Tmem163, MoxD1, Cplx3 and Ddc)[117]. Of these genes, only Nurr1 is expressed in the early embryonic mouse subplate (see Fig 2_3 e) while the onset of expression of all other genes is at late embryonic or postnatal stages[117] (Fig 1_9). Taken together, these observations further underline the dynamic nature of the embryonic and early postnatal subplate.

The goal of this chapter is to establish a comprehensive gene expression profile of the embryonic E15.5 subplate using LCM combined with microarray-based expression analysis. I hope to achieve two aims with this: 1) to correlate at least some of the expressed genes with established or postulated functions of the embryonic subplate in order to gain more insight into the underlying molecular mechanisms and 2) to identify embryonic molecular markers for subplate which in the future can be used to label and manipulate these cells at an important developmental time-point.

3.2 Methods

3.2.1 Tissue preparation and laser capture microdissection

Tissue was prepared and samples isolated using the optimized LCM protocol described in Chapter 2 (Fig 2_6). For the microarray, four litters of E15.5 embryos from time-pregnant C57/Bl6 mice were used as four biological replicates. Litter size varied from 8-10 embryos. Microdissected samples were pooled from the 3-4 first collected embryos from each litter. From each individual embryo, between 20 and 40 tissue strips were collected resulting in an average of nearly 90 microdissected strips per sample. For quantitative RT-PCR (qRT-PCR) two additional sample sets were collected from individual animals from two different litters.

3.2.2 RNA quality and quantity

RNA was extracted using the RNeasy micro kit (Qiagen) following the manufacturer's instruction. For each of the samples, RNA quality was assessed using RNA 6000 Pico Chips on a BioAnalyzer (Agilent Technologies). All samples had RINs ranging from 7.6 to 9.0 indicating that minimal degradation had occurred. Absolute RNA quantity could not be assessed as the RNA concentrations were below the limit of the spectrophotometer. Therefore, the measurements indicated by the BioAnalyzer were used as a relative estimate of the RNA

quantities in the different samples. According to these estimates, the lowest RNA quantity was 20ng and half of this (i.e. 10ng) was used as starting material for the microarray.

3.2.3 Preparation of cDNA and hybridization on Affymetrix microarrays

RNA was reverse-transcribed and the cDNA was amplified using the Ovation™ Pico system (NuGEN) according to manufacturer's instruction. This method is based on the Ribo-SPIA® technology developed by NuGEN. First strand cDNA was synthesized using reverse transcriptase and DNA/RNA chimeric polyT and random primers. The RNA portion of the primer contains a specific sequence which will be used as a priming site in the amplification step. The RNA strand was fragmented and second strand cDNA was produced using DNA polymerase. Next, the RNA portion of the first strand cDNA was digested with RNase H thus exposing the priming site on the second strand cDNA. Using new DNA/RNA chimeric primers complementary to that site and DNA polymerase, cDNA was synthesized. Repetition of this cycle led to rapid linear amplification of the original sequences. Two no-template controls were processed together with the samples and no significant amplification due to contamination was found. Amplified double-stranded cDNA was transformed into single-stranded sense cDNA using the Ovation Exon Module (NuGEN). Sense cDNA was then fragmented and labelled with biotin using the FL-Ovation™ cDNA Biotin Module V2 (NuGEN). Successful fragmentation was confirmed for all samples on the BioAnalyzer showing a peak sequence length of around 200nt.

Fragmented and labelled single-stranded sense cDNA was hybridized to Affymetrix Mouse Gene 1.0 ST arrays at 45°C overnight. Arrays were washed and stained with Streptavidin-Phycoerythrin using the GeneChip® Hybridization, Wash and Stain Kit (Affymetrix) according to manufacturer's instruction. The microarrays were scanned on the Affymetric GeneChip Scanner 8000.

3.2.4 Microarray data analysis

All data processing was performed using Affymetrix software or Agilent GeneSpring GX (Agilent Technologies). First the images of the scanned chips were processed and an intensity value was assigned to each individual probe. Next, background was estimated using generic background probes, i.e. a selection of probes which are not present in the mouse genome. Background probes were grouped into 26 bins according to their G/C content (ranging from 0 G/C to 25 G/C per 25-mer probe) and the median intensity for each bin was calculated. For each mouse gene probe the G/C content was assessed in the same way and the median background intensity corresponding to the same G/C content was substracted from the probe's intensity value. The background-adjusted intensity values were normalized between

different chips using quantile normalization. This method ensures that the distributions of intensities across different chips are identical by replacing the value of each quantile on each chip with the average value of that quantile across all chips.

Each transcript on the Affymetrix Mouse Gene 1.0 ST array is represented by approximately 27 probes constituting a probe set. Intensity values were summarized from these individual probes using the Probe Logarithmic Error Intensity Estimate (PLIER). PLIER uses the experimental data across all arrays to determine the feature response for each probe. The feature response consists of a set of parameters describing systematic differences between probes binding to the same target caused for example by different thermodynamic properties or binding efficiencies. PLIER calculates the overall probe set intensity by weighing the intensity values of each individual probes according to their feature responses.

Summarized signal intensities of each probe set were compared between the following samples using paired Welch's t-tests without correction for multiple testing:

1) Anterior subplate vs Anterior cortical plate

2) Posterior subplate vs Posterior cortical plate

3) Anterior subplate vs Posterior subplate

Genes with a fold-change ≥ 1.4 and a p-value < 0.05 were considered as differentially expressed.

3.2.5 Quality controls

Two types of positive controls were used to monitor the quality of the microarray experiment. First, four polyadenylated prokaryotic sense RNAs (dap, lys, phe, try from *B. subtilis*) were mixed with the sample RNA before reverse transcription (polyA controls). Second, four prokaryotic or viral single stranded sense cDNAs (bioB, bioC and bioD from *E.coli* and cre from P1 bacteriophage) were used as controls for the hybridization step (hybridization controls). The polyA and hybridization controls contain known amounts of RNA and cDNA, respectively, and their relative abundance was faithfully represented in the calculated signal intensities. This suggests that all steps of the microarray experiments were performed correctly without introduction of bias.

Several metrics proposed by Affymetrix were calculated to further evaluate the quality of the microarrays. The "Pos vs neg AUS" metric represents the difference between positive and negative controls on the arrays and was within the optimal range for all our arrays. The overall probe set mean and standard deviations were very consistent between different arrays indicating that the normalization between chips had been performed successfully.

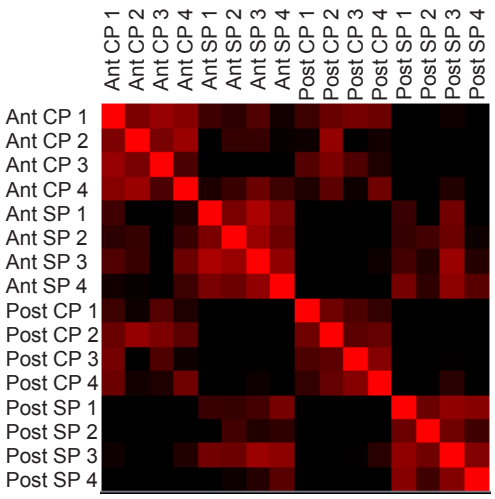

Figure 3_1. **Heatmap of the correlation analysis across all 16 samples.** Bright red squares denote a Pearson Correlation coefficient of 1, black squares a coefficient of 0. The heatmap indicates that the strongest correlations are between replicates of the same cell populations. There is also moderate correlation between samples from the anterior subplate (Ant SP) and posterior subplate (Post SP) and the anterior cortical plate (Ant CP) and posterior cortical plate (Post CP), respectively.

Finally, a correlation analysis across all 16 arrays was performed where the Pearson Correlation Coefficient was calculated for each pair of arrays and visualized as a heatmap (Fig 3_1). As expected the heatmap shows the greatest correlation between replicates of the same cell population indicating that the microdissections have been performed consistently between the different litters.

3.2.6 Quantitative RT-PCR

The remaining RNA from two replicates of the microarray as well as RNA from two new sample sets were used for qRT-PCR. cDNA was generated using Superscript III reverse transcriptase and random hexamers (Invitrogen) according to manufacturer's instructions. No template controls were included for each reaction.

Primers for qRT-PCR were designed to amplify specific intron-spanning sequences of 120-150 bp (Table 3_1) using Roche's Universal ProbeLibrary Assay design centre and Primer3 software. The qRT-PCR reaction was performed using 100nM of forward and reverse primers and Power Sybr Green reagent (Applied Biosystems) on an ABI Prism® 7000 Sequence Detection System (Applied Biosystems). PCR conditions were 95°C for 10min followed by 40 or 50 two-step cycles of 95°C for 15sec and 60°C for 1min. Each primer set was verified to amplify a single PCR product by melt-curve analysis following qRT-PCR and by agarose gel electrophoresis.

Three commonly used house-keeping genes (beta-tubulin 2c (tbb2c), peptidylprolyl isomerase A (ppia) and beta-actin (actb)) were initially selected based on the microarray data where they showed stable expression levels across all samples. They were further validated by qRT-PCR

Gene	Forward primer	Reverse primer	Amplicon length (bp)
2610017I09Rik	tgtgcccgggactgtaag	cataccacttgatgaaggctca	140
Abca8a	cctttatcccaggccttctt	tcctcttcaaaaccgtccag	140
Actb	ttctttgcagctccttcgtt	atggaggggaatacagccc	149
Cacna2d1	aatggctatgtcttattgcatcc	tcattttatttcgaatctccacttt	127
Cdh9	acaaccctcctcggttcc	tatattccagctcggcgttc	129
Csmd3	ggttctgagccacctacaatatg	gggagcactaaatcctcggta	129
Epha3	tggctccttggacagtttct	gttgcgagcagcaaggtc	142
Kcnip4	gctgattgaagcaggtttagaag	gaatctgaagctctttcttggtg	128
Nr4a2	tcagagcccacgtcgatt	gatctccatagagccggtca	143
Nr4a3	tgcagagcctgaaccttgat	tggtcctttaagctgcttgtg	136
Ppia	gtcaaccccaccgtgttct	agccaaatcctttctctccag	139
Sema6d	agaaatcgccgtggaacata	ccgagccttaaggaaggaag	128
Slit1	ccccgaggtgtatttggag	gcgagactctggatcttgttg	146
Tbb2c	cttcgggcagatcttcagac	ggcagtcacagctctcagc	149
Unc5c	aggcagtgcagggacaat	ccagggcataggtactgagg	129

Table 3_1. **Primer sequences for quantitative RT-PCR.**

on additional samples of anterior and posterior subplate and cortical plate where all three genes showed very similar relative expression levels (relative standard deviation < 10%). Tbb2c was subsequently chosen as the endogenous reference gene as it showed similar expression levels as the genes of interest.

Each reaction was performed in triplicates and ran with no-template controls for each primer pair. Tbb2c was included on every qRT-PCR plate. LinRegPCR v11.4 software was used to determine baseline fluorescence and PCR efficiencies which were around 90% for all genes except for Slit1 (82%) and Nr4a3 (98%) and to calculate the starting concentrations (N_0) of each sample taking these two parameters into account [316,317]. LinRegPCR uses the following formula: N_0 = Nt / (Emean^Ct). Ct stands for the number of cycles needed to reach Nt, a fluorescence threshold set within the linear amplification phase of the PCR reaction. Emean is the mean PCR efficiency of the amplicon.N_0 values were normalized to Tbb2c. Fold-changes were determined by dividing normalized N_0 values of anterior subplate:anterior cortical plate and posterior subplate:posterior cortical plate. Fold-changes were considered as significant if they were significantly different from 1 (one-sample, one-tailed t-test, $p<0.05$).

3.2.7 Gene ontology analysis

The Database for Annotation, Visualization and Integrated Discovery (DAVID) bioinformatics software was used to categorize the subplate gene expression data[318]. All genes were linked to Gene Ontology terms describing biological processes (GO_BP)[319] and to pathways described in the KEGG Pathway Database[320]. Genes expressed in the subplate were analyzed for enriched terms by comparison with a background gene list containing all 28,869 genes on the Affymetrix Mouse Gene 1.0 ST array using EASE Score (a modified Fisher Exact test). Terms with a p-value <0.05 were considered as significantly enriched and similar terms were clustered into functional annotation groups using DAVID's fuzzy heuristic clustering algorithm.

3.3 Results

3.3.1 Gene expression analysis using microarrays

In order to establish a gene expression profile of the embryonic E15.5 subplate, a microarray screen was performed. In the previous chapter, I identified the E15.5 subplate as a 40μm thick band just below the developing cortical plate (Fig 2_3). As a reference to the subplate, a population of cells in the adjacent lower cortical plate (corresponding to future layer VI) of equivalent width was used (Fig 2_2). As it has been postulated that the embryonic subplate might be involved in setting up the topography of the cortical connectivity, I further decided to analyze differential gene expression in the subplate across the anterior-posterior axis. The following four cell populations were thus isolated by laser capture microdissection: Anterior and posterior subplate and anterior and posterior cortical plate (see Fig 2_2). Using microarrays, transcripts levels were compared between different samples as shown in Figure 3_2.

3.3.2 Subplate-enriched genes

In a first instance, I compared transcript levels between the anterior subplate and the anterior cortical plate and the posterior subplate and the posterior cortical plate (Fig 3_2). Combining results from these two comparisons, I found a total of 334 genes which were higher expressed in subplate while 327 genes were higher expressed in the lower cortical plate (fold changes ≥ 1.4, Supplementary Table S_1). 116 genes were up-regulated in the anterior subplate only, 97 in the posterior subplate only and 121 in both anterior and posterior subplate. The maximal fold-changes for subplate–enriched genes were relatively robust with a maximal fold-change of 5.4, an average fold-change of 1.7 and 60 genes (18%) with a fold-change ≥ 2.0.

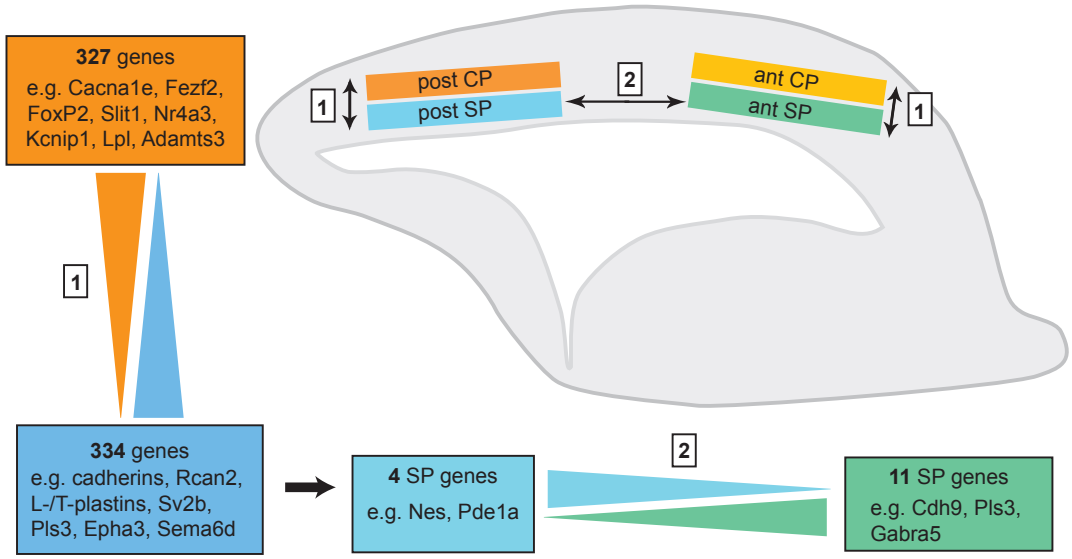

Figure 3_2. **Comparisons of microarray-based gene expression levels between different cell populations.** Transcript levels were compared between the anterior subplate (ant SP) and anterior cortical plate (ant CP) and between the posterior SP (post SP) and posterior CP (post CP) (1). Combinedly, 327 genes were higher expressed in the SP and 334 were higher expressed in the CP. The expression levels of all 334 transcripts with higher expression in the SP were then compared between anterior and posterior SP (2). Eleven SP-enriched genes had a higher anterior expression and four genes a higher posterior expression.

Some of the genes which showed higher expression levels in subplate have been previously described as associated with this compartment. Among those was Nurr1 (Nr4a2), the protein which I had originally used to identify the subplate at E15.5 (Fig 2_3 e)[118,117,321] . GABA-A receptors have been shown to be specifically present in the embryonic subplate[68] and I found one specific GABA-A receptor (GABA A alpha 5 (Gabra5)) on the microarray list. In addition, the ECM proteins fibronectin and laminin are known to be localized in the developing subplate [57,84,85] and consistently, the gene for fibronectin 1 (Fn1) and the laminin subunit alpha 4 (Lama4) were upregulated in the subplate. In agreement with previous reports[322,323], I found that Slit1 was higher expressed in the cortical plate while the Slit-receptor Robo2 was higher expressed in subplate. The cortical plate samples showed enrichment in transcripts of FoxP2, a marker of layer VI neurons[324], and Fezf2, a transcription factor specifically expressed in layer V and VI projection neurons[325,326].

3.3.3 Publicly available gene expression datasets

As a next step to validate the microarray data, I screened the publicly available gene expression datasets Gensat[327], Allen Brain Atlas[282,283] and Genepaint[328] for all 334 genes with higher expression levels in subplate. Based on the available E14.5 (Genepaint) and E15.5 (Allen Brain Atlas, Gensat) images, genes were classified into six groups (Supplementary Table S1, examples in Fig 3_3):

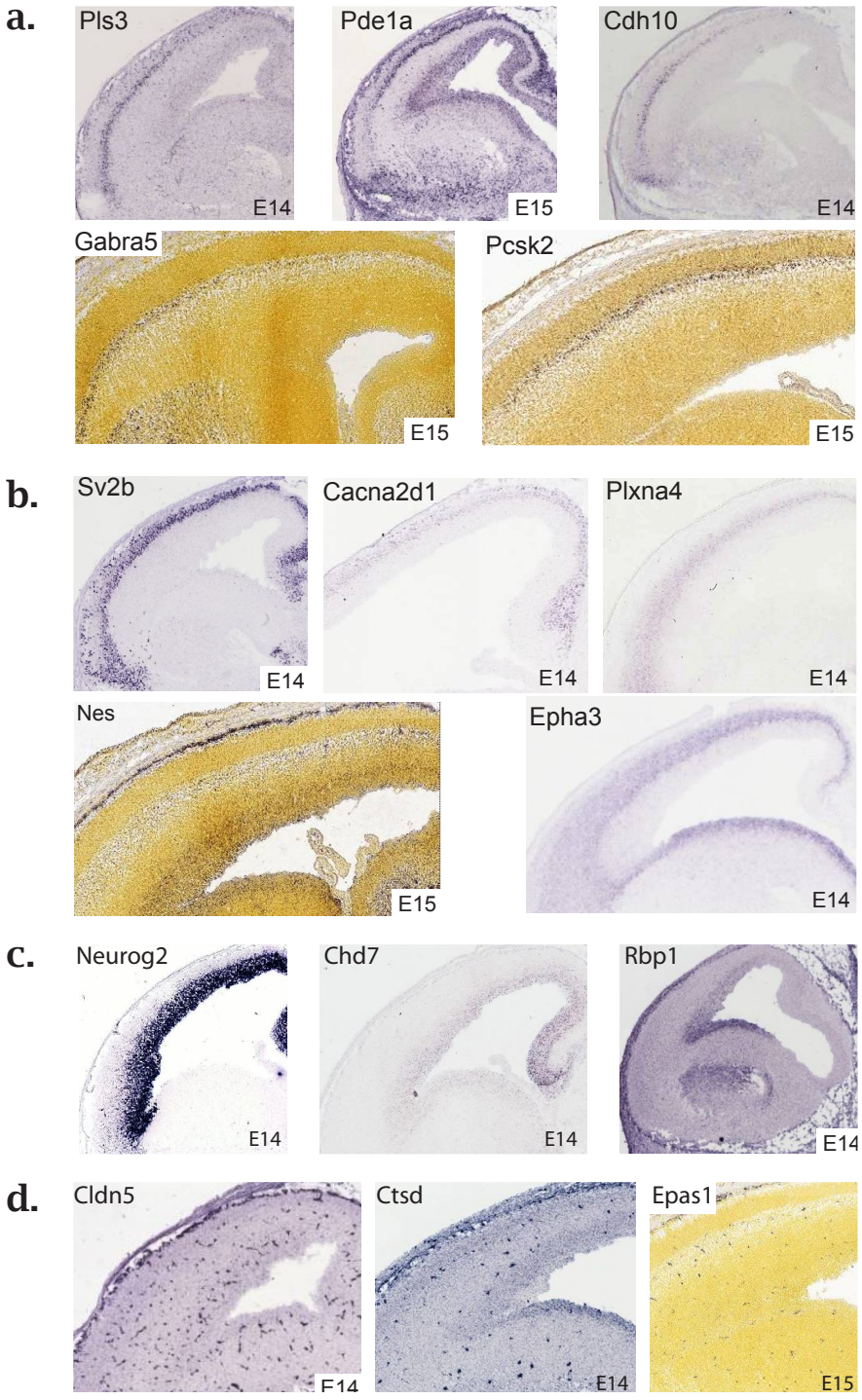

Figure 3_3. **Expression patterns of presumed subplate-enriched genes from publicly available in situ hybridization datasets.** a. Genes which are specifically expressed in subplate (Group 1). b. Genes which are possibly expressed in subplate (Group 2). Sv2b could be expressed in subplate or the lower cortical plate; Cacna2d1, Nes, Plxna4 and Epha3 are either expressed in the subplate or intermediate zone or both. C. Genes which are expressed outside of SP (Group3). Neurog2, Chd7 and Rbp1 are all strongly expressed in the ventricular and subventricular zones. d. Gene expression in blood vessels (Group 4). Blood vessels labeled by Ctsd and Epas1 appear to be denser in the subplate zone than in the cortical plate. Images for Gabra5, Pcsk2, Nes and Epas1 are from AllenBrainAtlas, all others from Genepaint.

1. Clearly and specifically expressed in subplate (10 genes, 3%, Fig 3_3 a)

2. Possibly expressed in subplate but sometimes with additional expression in the intermediate zone (68 genes, 20%, Fig 3_3 b);

3. Clearly expressed but not in subplate (75 genes, 22%, Fig 3_3 c)

4. Expressed in blood-vessels (37 genes, 11%, Fig3_3 d)

5. No or very weak expression (89 genes, 27%)

6. Data not available (56 genes, 17%).

The 75 genes in the third group were considered as false-positives and excluded from the dataset in subsequent analyses. The genes expressed in blood vessels were not excluded at this stage as previous studies have shown that the embryonic subplate can be enriched in plasma-proteins and immunoglobulins[88,87,91]. Therefore, it is conceivable that these genes are associated with subplate neurons in addition to blood vessels.

3.3.4 Quantitative RT-PCR for subplate- and cortical plate- enriched genes

For further validation of the microarray dataset, quantitative (q) RT-PCR was performed on ten genes with higher expression in subplate and on two genes with higher expression in lower cortical plate (Fig 3_4). For subplate, I chose four genes from the second group (i.e. possibly in subplate; Cacna2d1, Sema6d, Epha3 and Unc5c), four genes from the fifth group (i.e. no or weak signal; Abca8a, Cdh9, Csmd3, Kcnip4) and one genes from the sixth group (data unavailable; 2610017I09Rik). Nurr1 was included as a positive control. Quantitative RT-PCR was performed on two sample sets which had also been included in the microarray as well as on two additional sample sets specifically collected for this purpose. As described previously, the samples which had been used for the microarray contained RNA pooled from 3-4 embryos from the same litter. In contrast, the two samples newly collected for qRT-PCR were obtained from a single embryo each. The same four areas, i.e. anterior and posterior subplate and cortical plate, were collected and compared using qRT-PCR. Fold-changes were calculated for the anterior subplate (anterior subplate: anterior cortical plate) and posterior subplate (posterior subplate: posterior cortical plate) for each of the four replicates and then averaged.

For nine out of ten subplate genes and both cortical plate genes, qRT-PCR showed fold changes in the same direction as the microarray (i.e. > 1for subplate-enriched genes and < 1 for cortical-plate enriched genes). As previously reported[329], the average fold-changes were

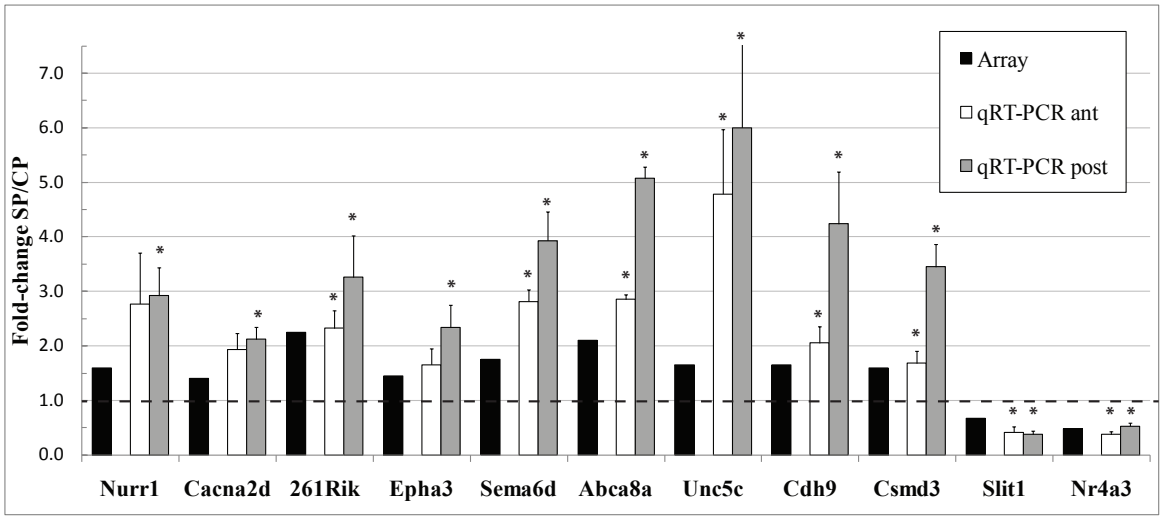

Figure 3_4.**Quantitative RT-PCR for selected subplate- and cortical plate-enriched genes.** Quantitative RT-PCR shows fold-changes in the same direction as the microarray for ten genes - eight with a higher expression in the subplate (SP) and two with a higher expression in the cortical plate (CP). Fold-changes were calculated as the ratio between anterior SP and CP and between posterior SP and CP, respectively. Error bars are SEM. Asterisks (*) indicate fold-changes which are significantly different from 1 (p-value < 0.05).

generally more pronounced than those found by the array, with a maximal fold-change of 6.0 and an average fold-change for subplate-enriched genes of 3.1 (Fig 3_4). Fold-changes in the same directions were consistently found in all four biological replicates and in both anterior and posterior comparisons for all ten genes. However, the exact value of the fold-changes was relatively variable between replicates with an average relative standard error of ~ 20%. Consequently, most but not all fold-changes were significantly different from 1 (p-value < 0.05; see Fig 3_4). The remaining subplate gene (Kcnip4) could not be sufficiently amplified with the designed primers to perform quantitative analysis.

3.3.5 Gene ontology analysis

Based on these preliminary confirmation methods, a shorter list containing 259 potentially subplate-enriched genes was compiled where confirmed false-positive genes (i.e. group 3) were omitted. A gene ontology enrichment analysis was performed on this list using the Database for Annotation, Visualization and Integrated Discovery (DAVID)[318]. Overrepresented terms associated with subplate-enriched genes were identified for biological processes and pathways.

At the level of biological processes, ten terms are significantly enriched in subplate genes (Table 3_2). Seven terms are possibly associated with neuronal development: cell adhesion, negative regulation of transcription, actin cytoskeleton organization, cell morphogenesis/ axogenesis, cell motion, cation homeostasis and activation of phospholipase C activity. The

	Enriched term	Nb.	Gene symbols
Biological processes (GO_BP)	Cell adhesion (Biological adhesion, cell-cell adhesion, homophilic cell adhesion)	18	Cd93, F11r, Antxr1, Cdh10, Cdh12, Cdh18, Cdh9, Cldn5, Fn1, Emcn, Igfbp7, Lama4, Nrp1, Omg, Pcdh8, Pcdh18, Robo2, Vtn
	Negative regulation of transcription (negative regulation of RNA metabolic process, negative regulation of gene expression)	12	Bcl6, Cited2, Dnmt3a, Bhlhe41, Cux1, Hhex, Hba-x, Id3, Sirt1, Satb2, Tle1, Zhx1
	Actin cytoskeleton organization (Actin filament organization)	7	Bcl6, Limch1, Aif1, Antxr1, Lcp1, Pls3
	Cell morphogenesis/axonogenesis (neuron projection morphogenesis, cell morphogenesis involved in neuron differentiation)	10	Bcl6, Lhx2, Slitrk3, B3gnt2, Antxr1, Cck, Nrp1, Nr4a2, Robo2, Syne2
	Cell motion (cell migration, neuron migration)	10	Fcer1g, Lhx2, B3gnt2, Cck, Gja1, Nrp1, Nr4a2, Robo2, Satb2, Syne2
	Cation homeostasis (homeostatic process)	7	Alas2, Apoe, Aqp11, Hexb, Ptger3, Slc4a4, Slc8a1
	Activation of phospholipase C activity	3	Htr2a, Rnase4, Ptger3
	Erythrocyte differentiation and homeostasis (erythrocyte development)	7	Bpgm, Bcl6, Lyn, Alas2, Epas1, Hba-x, Hba-a1
	Blood vessel development (vasculature development, blood vessel morphogenesis)	10	Cited2, Egfl7, Sox18, Rnas4, Apoe, Emcn, Epas1, Gja1, Lama4, Nrp1
	Positive regulation of immune response (Positive regulation of immune system process, regulation of adaptive immune response)	6	Fcer1g, Lyn, B2m, C1qb, C1qc, Pnp
Pathways (KEGG, Panther)	Axon guidance	8	Epha3, Lrrc4c, Nrp1, Plxna4, Robo2, Sema6d, Unc5c, Unc5d
	Focal adhesion	9	Jun, 2900073G15Rik, Ccnd1, Ccnd2, Fn1, Lama4, Mapk10, Myl9, Vtn
	Muscarinic acetylcholine receptor 2 and 4 signaling pathway	5	Cacna2d1, Gng11, Gng5, Snap23, Vamp8
	5HT2 type receptor mediated signaling pathway	5	Htr2a, Gng11, Gng5, Snap23, Vamp8
	Cadherin signaling pathway	7	Lyn, Cdh9, Cdh10, Cdh12, Cdh18. Pcdh8, Pcdh18

Table 3_2: **Gene ontology terms associated with subplate-enriched genes.** This table lists terms describing biological processes and pathways linked to the E15.5 subplate-enriched genes which are significantly overrepresented compared to a background (p-value <0.05). Similar terms were clustered into annotation groups. Numbers of genes and gene symbols associated with each term are given.

remaining three terms are probably linked to the presence of blood vessels in the subplate zone: erythrocyte differentiation and homeostasis, blood vessel development and positive regulation of immune response.

The term "cell adhesion" is linked to 18 genes of which six are cadherins or protocadherins. This gene cluster also contains the ECM proteins fibronectin (Fn1) and laminin (Lama4)

With the term "negative regulation of transcription", 12 genes are associated. These include several transcription factors such as cut-like homeobox 1(Cux1), Cbp/p300-interacting transactivator 2 (Cited2) and basic helix-loop-helix protein 41 (Bhlhe41) which can mediate both gene activation and repression. In addition, several genes in this cluster are specifically involved in transcriptional repression including B-cell lymphoma 6 (Bcl6) and Zinc finger and homeobox 1(Zhx1). Finally, a few genes are involved in epigenetic modification of the genome, for example the histone deacetylase sirtuin 1 (Sirt1)

Seven genes were connected to the process of "actin cytoskeleton organization" including the L- and T-plastins (Lcp1 and Pls3).

The two terms "cell morphogenesis/axogenesis" and "cell motility" were associated with 10 genes each, 7 of which were linked to both terms. These include the transcription factors Nurr1 and LIM homeobox 2 (Lhx2) and the guidance cue receptors neuropilin 1 (Nrp1) and roundabout homologue 2 (Robo2).

Seven genes are involved in "cation homeostasis" including two members of the solute carrier family (Slc8a1 and Slc4a4).

Finally, the term "activation of phospholipase C activity" appears to be enriched in subplate and is linked to three genes: the serotonin receptor Htr2a, the prostaglandin e3 receptor (Ptger3) and the RNAse 4/5 which has been shown to be able to activate phospholipase C in endothelial cells[330].

At the level of pathways, five terms were significantly overrepresented: axonal guidance, focal adhesion, muscarinic acetylcholine receptor signalling, 5HT2 receptor signalling and cadherin signalling.

Among the seven genes associated with "axonal guidance" are primarily guidance cue receptors including the semaphorin receptors Plxna4 and Nrp1, the ephrin receptor Epha3 and the netrin receptors Unc5c and Unc5d.

"Focal adhesion" describes pathways through which cells adhere to the ECM. Associated with this term were Fn1 and Lama4 which code for ECM proteins and two components

of the cytoskeleton, the intermediate filament vimentin (Vtn) and the myosin light chain 9 (Myl9).

Signalling through two G-protein-coupled receptors, the muscarinic acetylcholine receptor and the serotonergic 5HT2 receptor, appear to be significantly enriched in subplate. Two G-proteins are associated with these pathways (Gng5, Gng11) as well as two proteins involved in general vesicular release (Snap23, Vamp8).

Finally, the cadherin signalling pathway is overrepresented in subplate due to the enrichment in six cadherins and protocadherins.

3.3.6 Anterior-posterior gradient of subplate-enriched genes

The experimental design of this microarray study allows me to investigate whether genes are expressed in an anterior-posterior gradient. As the primary aim of this study is to investigate subplate, I compared the transcript levels of the 259 subplate-enriched genes in the anterior versus posterior subplate (Fig 3_2). I found that only 11 of these genes had higher expression levels in the anterior subplate and 4 in the posterior subplate (Table 3_3). Of the 11 genes stronger expressed in the anterior subplate, good quality public gene expression images was available for five. For two of these genes –Gabra5 and Pls3 – these images show a larger number of labelled cells in the anterior subplate than in the posterior subplate confirming the result of the microarray (Fig 3_3 a). Additionally, Cdh9 has been described as a marker for the frontal cortex, at least in the adult mouse[331]. Of the four genes stronger expressed in the posterior cortex on the microarray, publicly available gene expression data confirms this gradient for two of them, Nes and Pde1a (Fig 3_3 a, b).

3.4 Discussion

3.4.1 Experimental design of the gene expression study

In this chapter I performed a microarray screen to investigate the gene expression patterns in the developing E15.5 subplate. The microarray experiment was planned and performed following a rigorous experimental design. All four cell populations which would be compared (i.e. anterior and posterior subplate and anterior and posterior cortical plate) were collected from the same sections. Secondly, a relatively large number of dissected cell groups (~90 strips) were pooled together for each replicate. Increasing the amount of collected tissue reduced the bias that can be introduced by an exceptional aberrant sample, for example caused by imprecise microdissection. In addition, samples were pooled from 3 to 4 embryos from the same litter which should decrease variation caused by individual differences between

Anterior high		Posterior high	
Atp1b1	ATPase, Na+/K+ transporting, beta 1 polypeptide	C3ar1	complement component 3a receptor 1
Cdh12	Cadherin 12	***Nes***	nestin
Cdh18	Cadherin 18	***Pde1a***	phosphodiesterase 1A
Cdh9	Cadherin 9	Slc4a4	solute carrier family 4a4
Fam84a	family with sequence similarity 84, A		
Gabra5	GABA A receptor, subunit alpha 5		
Gm10001	Predicted gene		
Kcnip4	Kv channel interacting protein 4		
Nt5dc2 /Stab1	5'-nucleotidase domain containing 2		
Pls3	plastin 3 (T-isoform)		
Ptn	pleiotrophin		

Table 3_3: **Subplate enriched genes with an anterior-posterior gradient.** Expression levels of all subplate-enriched genes were compared between samples of the anterior and posterior subplate using the microarray data. Eleven subplate-enriched genes had a higher anterior expression and four genes a higher posterior expression. Genes for which publicly available in situ hybridization data confirms the expression gradient are highlighted (italics, bold).

animals such as body weight or sex. Finally, the microarray was performed using four biological replicates from four different litters of time-mated pregnant mice. As RNA quality has been shown to have an important influence on subsequent gene expression studies[308], only undegraded RNA with a RIN > 7.5 was used.

The relative abundance of transcripts was analyzed using a combination of the relative recent NuGEN Ovation™ Pico system and the Affymetrix ST 1.0 mouse microarrays. The NuGEN system was chosen because it has been developed specifically for low quantities of starting material (0.5 – 50ng of total RNA) and uses a linear amplification method, i.e. only the original transcript is replicated and not its copies. Linear amplification is usually preferred to exponential amplification because it has a higher fidelity and less amplification bias[332,333]. In addition, transcription and amplification are initiated both at the poly-A tail and randomly throughout the whole transcript. This approach reduces bias towards the 3'end of the transcript[334] and ensures that even partially degraded and non-polyadenylated transcripts will be successfully amplified.

The Affymetrix ST 1.0 arrays cover 28,869 well-annotated mouse genes with an average of 27 probes of per gene. Unlike on previous arrays, the probes are covering the entire length of the transcript and not only the 3' end. This again ensures that also alternatively spliced, truncated and partially degraded transcripts can be detected. Positive and negative controls were introduced and analyzed at various steps along the protocol to assure correct behaviour.

Besides these technical control points, several criteria can give insight into the quality of the microarray experiment and will be discussed in the following sections.

3.4.2 Correlation between replicates

A correlation analysis can serve as an initial quality control of the microarray data. Ideally, the differences in gene expression between the four biological replicates will be much smaller than the differences between the four cell populations. Consequently, the data of all four replicates for a given cell group will have the greatest correlation. This appeared to be largely the case for my microarray data (Fig 3_1), indicating that the samples of the different replicates were collected and microdissected with consistency.

In addition, the correlation analysis also shows a moderate correlation between the anterior and posterior subplate and anterior and posterior cortical plate, respectively. This suggests that the differences between cells in subplate and cortical plate are more pronounced than the differences between anterior and posterior areas within the same layer. This observation at E15.5 is consistent with previous findings on the P8 subplate[95].

3.4.3 Number and fold-changes of differentially expressed genes

Another criterion for evaluating the quality of a microarray can be the number of genes which are differentially expressed above a statistical threshold. Of course this strongly depends on the type of experiment, but it has been suggested that for most studies, between a hundred and a few thousand genes should be differentially expressed [335]. I found that over 300 genes were higher expressed in the subplate than in the cortical plate using a relatively stringent fold-change of ≥ 1.4 and a p-value < 0.05. The fold-changes were moderate with an average fold-change of 1.7 and about 20% of the genes with a fold-change ≥ 2.0. One possible explanation for these relatively low fold-changes is that the microdissected tissues are very heterogeneous containing postmigratory and migrating neurons, glia, ECM, fibres and blood vessels. The extracted RNA thus not only originates from the cell populations of interest (i.e. subplate or cortical plate neurons) but also from tangentially and radially migrating neurons, epithelial cells, glia and even dendrites and axons which can also contain some transcripts[336,337]. This is particularly relevant as it is known that not all of these components are evenly distributed in the subplate and the cortical plate zone at this age. For example, the embryonic subplate zone contains a large number of monoaminergic and thalamocortical afferents[70,63,77] as well as migrating interneurons[93] which are almost completely absent from the cortical plate at this stage. Inversely, the cortical plate contains dendrites extending from subplate neurons[74,75]. The differential presence of these components will likely dilute the true differences between subplate neurons and cortical plate neurons.

A second possible explanation for the low fold-changes lies in the technical challenge to precisely identify and isolate the subplate zone and the cortical plate zone in an E15.5 brain. While cresyl violet staining allows localizing the densely-packed cortical plate, the borders of the subplate zone are not distinguishable (Fig 2_2). Based on Nurr1 immunohistochemistry, I defined subplate as a 40µm band directly below the cortical plate. However, this definition is somewhat arbitrary as the width of subplate may vary across the anterior-posterior and medial-lateral axis of the developing cortex. Taking these observations together, it becomes clear that the microdissected samples cannot be considered as pure populations but as enriched in subplate and cortical plate neurons.

3.4.4 Confirmation by quantitative RT-PCR

Quantitative RT-PCR is an alternative method to measure gene expression levels and was used to further assess the quality of the microarray data. I successfully amplified 11 out of 12 genes selected for such validation with qRT-PCR. The analysis was performed on four replicates - two which had already been used for the microarray and two which had been newly collected. The two freshly collected samples were derived from individual embryos (and not from a pool of several embryos as for the microarray samples). For all four replicates, first-strand cDNA was prepared without any additional amplification. qRT-PCR showed fold-changes in the same direction as for the microarray consistently in all four replicates for all 11 amplified genes. First of all, this suggests that the technical singularities of the microarray experiment (e.g. amplification of the cDNA, normalization of data) did not introduce substantial bias or errors. Secondly, as all enrichments were found consistently in all four replicates, it appears that the sample preparations, in particular the microdissections, were performed consistently between different samples. Finally, this result suggests that at least for the 11 investigated genes, variations in gene expression between individual animals are relatively low.

3.4.5 Presence of marker genes

Another important quality control of a microarray dataset is the presence of marker genes, i.e. genes previously reported to be expressed in the studied cell population at the given age. As described in the results, I found several genes on the gene enrichment lists which had previously been associated with the subplate or the cortical plate, respectively. For subplate these include Nurr1[117], Fn1[57], Lama4[85] and Robo2[322],[323] and for the cortical plate Slit1[323], Fezf2[326] and FoxP2[324]. The differential expression of these genes in the samples confirms that the collected cell populations were indeed enriched in subplate and cortical plate cells, respectively. However, the microarray screen failed to detect a few previously reported subplate markers including MAP2, calbindin (Calb1), calretinin (Calb2) and the recently identified Hpca

and Eaac1. However, publicly available gene expression data suggests that in the E14/ E15 mouse cortex MAP2 transcripts are both present in the subplate and the cortical plate while calbindin and calretinin are not expressed in the developing cortex with the exception of the marginal zone (not shown). The absence of Eaac1 and Hpca in the microarray screen could be considered as a false negative result even though their presence in the subplate has only been shown at E12 and 14 but not at E15[153].

3.4.6 Publicly available gene expression databases

Publicly available gene expression databases such as AllenBrain Atlas, Genepaint and Gensat provide in situ hybridization images for a large number of genes and are extremely useful to get an initial assessment of a gene expression pattern. However, these datasets are generated by high-throughput methods and are not optimized for individual genes. This mainly leads to a large number of false-negative results, i.e. genes that show no or a very weak expression pattern when with a more optimized protocol they could be detected more clearly. In addition, on Genepaint and Gensat, which are the two databases with the most embryonic gene expression data, the expression patterns are often very difficult to localize as no counterstain is provided for the sections.

Gene expression data from at least one database was available for the large majority of subplate genes (278 out of 334). Based on these patterns, a quarter of the genes appeared to be expressed in a band below the cortical plate. However, with the available images, it was often impossible to assess with certainty whether this band included the subplate or the intermediate zone or both (Fig 3_3 b). I only found ten genes which appeared to be most likely specifically expressed in subplate (Fig 3_3 a).

A fifth of the genes had a clear expression pattern not involving subplate (Fig 3_3 c). The large majority of these were expressed in a large band around the ventricles, probably including both the ventricular zone (VZ) and subventricular zone (SVZ). Only a handful showed expression in the cortical plate. These genes were considered as false-positives and were excluded from the dataset for further analyses. However, for almost all of these genes, in situ hybridization data was only available from E14.5 embryos, and I cannot completely rule out the possibility that at least some of these genes could be expressed in subplate one day later at E15.5.

RNA probes for about 10% of genes labelled blood vessels throughout the entire brain (Fig 3_3 d). As it has been shown that subplate is enriched in immunoglobulin-like genes as well as plasma proteins, these genes were not considered as false-positives at this stage. On the other hand, on many images it appeared that the subplate zone contained a denser network

of blood vessels than the cortical plate. This is consistent with the described ventral-to-dorsal gradient of blood vessel development in the telencephalon[338]. The differential presence of blood vessels in subplate and cortical plate at this stage could explain why subplate samples show higher levels of genes expressed in endothelial or blood cells. In contrast to this view, however, a recent study reports that the embryonic subplate and intermediate zones are less vascularised than the cortical plate[339].

The remaining third of the genes showed very weak or no expression in the embryonic brains. Due to the limitations of the publicly available in situ hybridization data outlined above, I did not classify these genes as false-positives even though it is likely that many of them are indeed not or very weakly expressed in the embryonic cortex.

Taken together, the comparison of the microarray data with publicly available gene expression images suggests that at least a proportion (approximately 1/4) of the identified genes is expressed in the subplate. For most genes, however, further data will be needed in order to refine these expression patterns (in particular to distinguish between expression in the subplate and the intermediate zone). Indeed, it is very possible that the microdissected subplate samples were contaminated to some extent with cells or fibres from the intermediate zone as there is no clear borders between the two visible on a cresyl violet stain.

3.4.7 Conclusion on the quality of the microarray

I have assessed the quality of the microarray screen using several different criteria. Most importantly, I have found that this approach does allow identifying genes specifically expressed in the subplate at this early stage of development. This appears to be true for both previously reported genes (e.g. Nurr1, fibronectin) as well as new genes (e.g. Cdh10, Cdh18, Gabra5). However, the microarray list also contains an important number of false-positive results and further confirmation methods will be needed to analyze the gene list further.

3.4.8 Genes enriched in subplate

Functional categories

Based on the microarray and publicly available gene expression data, I have compiled a list of over 250 genes with assumed higher expression in the subplate. An ontology enrichment analysis was performed on these genes in order to gain some insight into possible molecular functions and pathways underlying the development and function of the embryonic subplate. Ten biological processes and five pathways were associated with the subplate-enriched genes (Table 3_2).

The subplate gene list contains a relatively large number of cadherins and protocadherins which are primarily underlying the enrichment in the term "cell adhesion" and "cadherin signalling pathway" . Besides maintaining appropriate cell-cell contacts, cadherins have been shown to be implicated in many other functions such as axon guidance, synapse formation and even cell fate determination[340,341,342,343.]

Genes associated with regulation of transcription constitute an interesting group as they could potentially be directly involved in the specification of subplate identity. Among the genes in this group are several transcription factors as well as some molecules involved in epigenetic modification. However, at least two of the transcription factors - Satb2 and Cux1 - have been shown to be important for the determination of cell fate and morphology of upper layer neurons, respectively[344,345,346]. This suggests that some of these genes might not be expressed in postmigratory subplate neurons but in radially migrating cells destined to the upper layers.

Subplate appears to be enriched in proteins involved in "actin cytoskeleton organization" including L- and T-plastin. Rearrangements of the cytoskeleton are among others important in cell migration and in the growth of dendrites and axons. Consistently, the terms "cell morphogenesis/axogenesis", "cell motility" and the pathway "axon guidance" are also overrepresented. All of these terms are associated with at least some receptors for guidance cues such as semaphorin, ephrin and netrin receptors. The association of axogenesis and axonal guidance with subplate-enriched genes is consistent with a role of subplate cells in pioneering the corticofugal pathway as well as in the guidance of thalamocortical afferents.

The subplate zone is known to be rich in ECM proteins such as laminin, fibronectin and chondroitin sulfate proteoglycans [57,85,86]. Consistently, the gene ontology analysis indicated an overrepresentation of genes involved in focal adhesion, i.e the binding between cells and the ECM.

Several genes involved in the activation of G-protein coupled receptors and the phospholipase C pathway appear to be differentially expressed in subplate leading to enrichment in the terms "phospholipase C activation" as well as "muscarinic acetylcholine receptor 2 and 4 signalling pathway" and "5HT2 type receptor mediated signalling pathway". The embryonic subplate receives the first inputs of monoaminergic (including serotonergic) fibres which form a dense network within subplate at E15[70,77]. Consistently, the serotonergic receptor Htr2a is preferentially expressed in the embryonic subplate according to the microarray data. Similarly, subplate has been shown to be selectively innervated by cholinergic fibres and to express nicotinergic and muscarinic acetylcholine receptors, at least in the neonatal rat[80,81,82].

Finally, a few terms enriched in the subplate are linked to endothelial and blood cells. As

outlined above, it is possible that the embryonic subplate contains a denser network of blood vessels compared to the overlying cortical plate. In addition, subplate cells have been shown to specifically produce some plasma proteins and immunoglobulin-like proteins normally associated with blood cells[87,88,89]. The role of these proteins in subplate remains to be elucidated.

Anterior-posterior gradients of subplate-enriched genes

In addition to the gene ontology analysis, I have investigated whether subplate-specific genes appear to be expressed in an anterior-posterior gradient. This could give some insights into the molecular mechanisms that are important in setting up the initial topography of thalamocortical axons. Interestingly, I found that only a very small proportion of the genes enriched in subplate are expressed in an anterior-posterior gradient (~6%; 15 out 259). This is consistent with my finding of a relatively high correlation between anterior and posterior subplate samples (Fig 3_1). Moreover, 11 out of 15 were higher expressed in the anterior subplate than in the posterior subplate and only 4 genes were higher expressed in the posterior subplate. Brain development proceeds in an anterio-lateral to posterio-medial gradient[185]. Therefore, it is very possible that at least some of the gradients could be related to a difference in maturation between the anterior and the posterior subplate.

These observations argue against an important and specific involvement of genes expressed in the subplate in the set-up of a topographic map. Consistently, it has been proposed that it is the timing of the outgrowth of the subplate and thalamocortical fibres which could determine the sequences in which the two fibre systems interact rather than the presence of specific guidance molecules[176]. However, I have here only analyzed anterior-posterior gradients for subplate-specific genes. Further analysis of all genes with an anterior-posterior gradient at E15.5 (whether expressed in subplate, cortical plate or both) could possibly be better suited to identify genes involved in the establishment of the cortical topography. For instance, it has been shown that the fibroblast growth factor 8 (Fgf8), which is expressed both in subplate and cortical plate, provides a positional cue for thalamocortical innervations (probably by regulating expression of guidance molecules such as ephrins and semaphorins). For the establishment of the correct thalamic topography, the expression of Fgf8 has to be matched between the subplate and cortical plate[192]. Finally, in order to obtain enough RNA starting material for the microarray analysis, relatively long tissue strips were microdissected and pooled from different medio-lateral positions of the cortex. These samples thus likely contain transcripts from several putative anterior and posterior cortical areas, respectively (i.e M1 and S1 for the anterior samples and V1 and A1 for the posterior samples). A more precise microdissection of individual cortical areas might be necessary to detect differentially expressed genes underlying arealization.

3.5 Conclusion

A microarray gene expression study has led to the identification of many genes with a higher expression in the embryonic E15.5 subplate than cortical plate. Several of them appear to be specific to this compartment while others will have to be further analyzed by other methods. Preliminary results suggest that some of the identified genes could play a role in the differentiation of subplate cells (Nurr1, Sox18), the growth of neurites (L-and T-plastin) and the guidance of axons (Sema6d, Epha3, Unc5c and Unc5d).

Chapter 4 Further validation of selected subplate-specific genes

4.1 Introduction

As described in the previous chapter, I have performed a gene expression analysis of the E15.5 subplate using laser capture microdissection and microarray analysis. The result was a list of over 300 genes which are higher expressed in the E15.5 subplate than in the lower cortical plate. Using publicly available in situ hybridization data, I excluded a set of genes which show a strong expression outside of subplate as false-positives and thus reduced the number of genes to 259. For about a third of these genes, publicly available data suggests that they are expressed in a cell band below the cortical plate. Further confirmation is needed to assess whether these cells are localized in the subplate or in the intermediate zone or both. For most of the remaining genes, in situ hybridization data is unavailable or the available data shows no or very weak expression. It is not feasible in the scope of this study to attempt to verify the expression of all of these genes. I therefore chose to further validate a subset of 23 genes (Table 4_2) based on one or several of the following criteria: 1) Promising expression pattern on the publicly available databases; 2) High expression levels and fold-changes; 3) Associated with presumed subplate-relevant functions.

Among the selected genes are several cadherins, a class of molecules important in a variety of function including tissue organization, axon guidance, synapse formation and even cell differentiation[340,343,341]. I further included molecules involved in neurite growth and guidance such as plastins (Pls3) and receptors for semaphorin, ephrin and netrin (Sema6d, Plxna4, Nrp1, Unc5c, Unc5d). Some genes were associated with cell differentiation (Sema6d, Nrp1, Neurod1). Other genes were chosen for their involvement in neurotransmission such as the synaptic release machinery (Sv2b), receptors for neurotransmitters (Gabra5) or ion channels (Kcnt2, Slc8a1). Finally, I also included three genes with unknown or hypothetical function as they constitute an important group on the microarray list and could give some insight into previously unknown mechanisms taking place in subplate (1190002N15Rik, Csmd3).

The aim of this chapter is to verify the subplate-specific expression of a subset of genes in wild-type mouse at E15.5 using immunohistochemistry or in situ hybridization. In addition, I will also study expression patterns in the reeler mutant mouse, where the relative position of the subplate and the cortical plate is reversed and a corresponding change in the subplate associated gene expression would be expected.

4.2 Methods

4.2.1 Tissue preparation

For *in situ hybridization*, heads from E15.5 C67/Bl6 (n=3) and E15.5 *reeler* mice (n=3) were embedded in O.C.T compound (Tissue-Tek) and flash-frozen. For immunohistochemistry, E15.5 brains from C57/Bl6 (n=3) and E15.5 brains (n=2) from *reeler* mice were immersion-fixed in 4% PFA for at least 24h. Reeler mutant mice (Orleans mutant allele, Reln [rl-Orl]) were provided by Prof André M Goffinet (Université Catholique de Louvain, Brussels, Belgium) and have been previously described[347,348].

4.2.2 In situ hybridization

For riboprobe generation, total RNA of E15.5 whole cortex was extracted, and first-strand cDNA was synthesized using Superscript III reverse transcriptase and random hexamers (Invitrogen) according to manufacturer's instruction. DNA fragments were amplified using the sets of gene-specific forward and reverse primers specified in Table 4_1. The resulting PCR products were ligated into the pST-Blue 1 plasmid (Novagen). The antisense and sense (a negative control) cRNA probes were transcribed using either SP6 or T7 RNA polymerase with digoxygenin (DIG)-labeled RNA mixture (Roche).

Fresh-frozen tissue was sectioned to 16µm on a cryostat (Jung CM3000; Leica, Germany). Sections were postfixed with 4% PFA for 20min, deproteinized with 0.1N HCl for 5min, acetylated with acetic anhydride (0.25% in 0.1M triethanolamine hydrochloride) and prehybridized at RT for at least 1h in a solution containing 50% formamide, 10mM Tris (pH 7.6), 200µg/ml E.coli tRNA, 1x Denhardt's solution, 10% dextran sulfate, 600mM NaCl, 0.25% sodium dodecyl sulfate, and 1mM ethylenediaminetetraacetic acid. The sections were hybridized in the same buffer with the DIG-labelled probes overnight at 66-68°C. After hybridization, sections were washed to a final stringency of 30mM NaCl/ 3mM sodium citrate at 66-68°C and blocked with 1% blocking reagent (Roche) for at least 1h. After overnight incubation with anti-DIG–alkaline phosphatase antibody 1:2000 (Roche), nitro blue tetrazolium chloride/5-bromo-4-chloro-3-indolyl-phosphate (NBT/BCIP, Roche) in NTM buffer (100mM NaCl, 100mM Tris-HCl, pH 9.5, 50mM MgCl2) was applied for approximately 4 – 24h. As a negative control, sections were labeled with sense cRNA probe and processed in parallel (see Fig4_1 for all negative controls for the genes shown in Fig 4_2).

Gene	Forward primer	Reverse primer	Probe length (bp)
Pls3	tcgggaagaaagaaccttcc	tccgattcttctagccatcg	601
Epha3	gtcatccagcttgtgggaat	ccgttaagccaatcaccagt	608
Abca8a	ccagacctgggaattgagaa	gttgcatgccagggtaaagt	621
Cdh9	cacagccagtgttcctgaaa	gaacacaggggctcatcta	658
Csdm3	cagcaacaaaaactggctca	tcactccaagcagcaaacac	663
Unc5c probe 1	tggggtatcctcaggacaaa	aacacagaaatgggcaaagg	616
Unc5c probe 2	ttgggcctgaagattactgg	gttcttggattggaggacca	680
Slc8a1	ggaccaacagctggagagag	aggagcacaaacagggaaga	643
Zdhhc2	ggacaaatggtctgcctgat	ttccaatcggaaggttgttc	586
Gabra5	tgactgctcacttccacctg	gagaggtggccccttttatc	645
Ogfrl1	gaaggaaatgccaaaccaaa	caaatcgcaggagctttctc	649
Plxna4	ggacatccccagctacaaga	ctgtcctcagctcctcatcc	632
Cdh10	acgagcgactcaaagagcat	tcatttgcaagagcaagacg	563
Cdh18	agccaaggtggaaaatgatg	ctctctgtccaggcttttgg	615
Unc5d	aacgtatgccctcacaggag	cgcagatcctctgtctgatg	566
Sema6d	acttcgacgtcctgcagtct	aagcatggtgatccttgtcc	618
Nrp1	tgacagcgcaatagcaaaag	accagacggatgttttctgg	648
1190002N15Rik	tcctttgctaaaaggcttcg	ccccaaactttactgcaaaca	608
Nt5dc2	agtcccttcagctttgtgga	cagctgagtgaggccatgta	617
Cdh12	aagaccttgatgtgggcagt	caggatggtcccatctgagt	572

Table 4_1. **Primer sequences for in situ hybridization riboprobes used to validate selected subplate-enriched genes.**

4.2.3 Immunohistochemistry

Immunohistochemistry was performed on sections from 4% PFA-fixed brains cut to 40μm on a vibrating microtome (Leica). For immunohistochemistry against Sv2b, Kcnt2 and Plxna4 sections were boiled in sodium citrate (0.1M, pH 4.5) at 95°C for 8min to enhance labelling for synapse-enriched proteins[349]. All sections were quenched in 1.5% hydrogen peroxide and blocked for 2h at RT with 5% serum (Sigma) in TBS with 0.2% Triton-X100 (BDH). Sections were incubated with primary antibody in 1% donkey serum and 0.2% Triton overnight at 4°C. The following primary antibodies and dilutions were used: Anti-Sv2b 1:1000 (AB15225, Millipore); anti-Kcnt2 1:1000 (ab77512, Abcam); anti-Plxna4 1:100 (ab39350, Abcam); anti-Rcan2 1:3000 (gift M. Arbones[350]); anti-NeuroD 1:200 (sc-1086, Santa Cruz Biotechnology). Biotinylated donkey anti-rabbit antibody 1:200 (Abcam) in 1% donkey serum was applied for 2h at RT and reacted with ABC using the Vectastain Elite kit (Vector) and DAB according to the manufacturer's instructions.

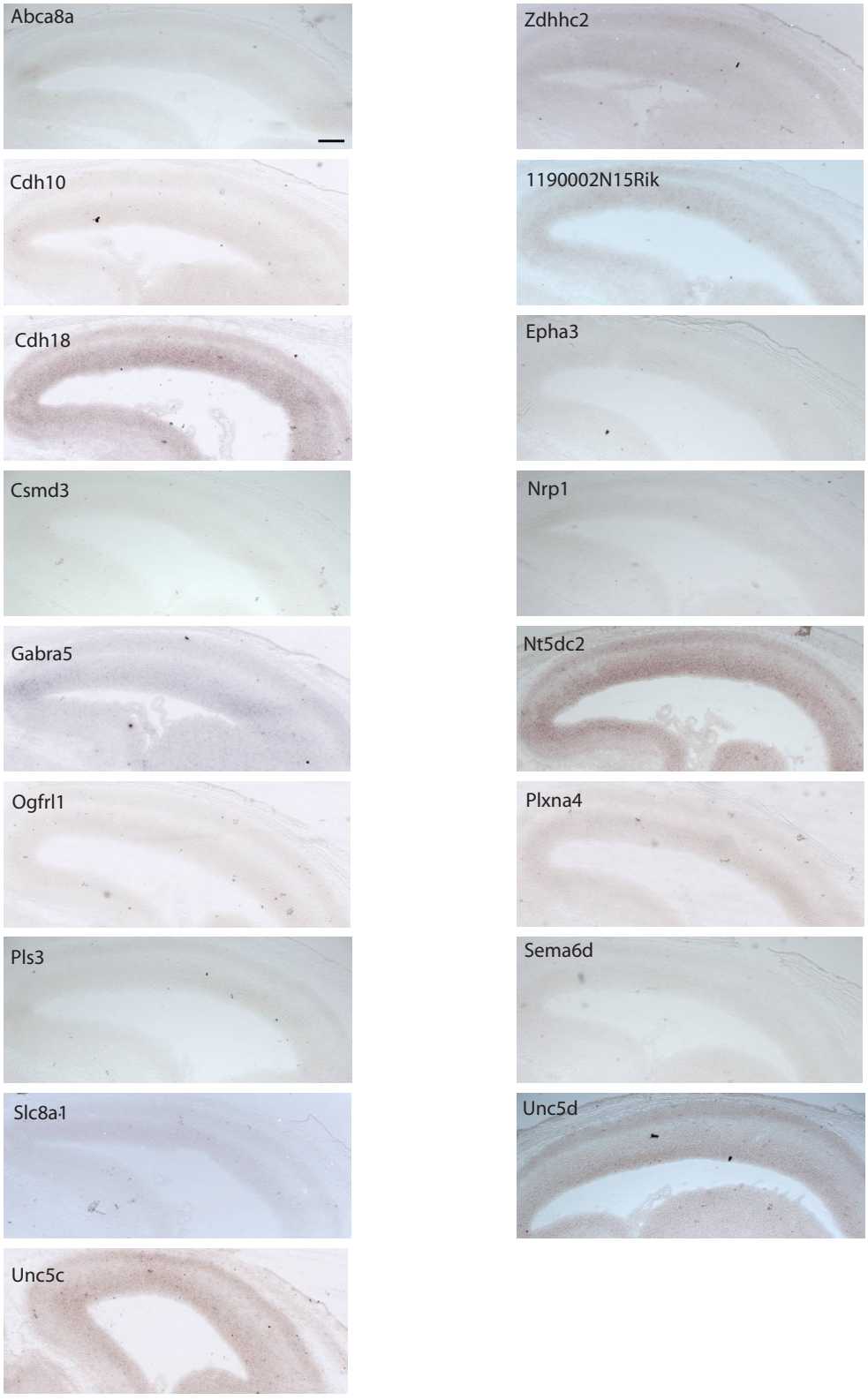

Figure 4_1. **Sense cRNA negative controls for in situ hybridization.** Panels show sagittal sections of E15.5 brains processed with sense cRNA and developed for the same length of time as sections with anti-sense cRNA (in Fig 4_2 e-n). Scalebar: 200µm.

4.3 Results

4.3.1 Expression patterns in the E15.5 mouse cortex

Using immunohistochemistry or in situ hybridization, I analyzed the expression of 23 genes from the microarray list in the E15.5 mouse cortex (Table 4_2). An expression pattern was considered as subplate-specific if it was predominantly localized in a three to four cell-wide band just below the dense cortical plate. According to this criterion, I found that 13 genes are strongly and primarily expressed in the subplate (Fig 4_2). Seven further genes were primarily expressed in the intermediate zone and/or SVZ with additional weaker expression in the subplate in some cases (Plxna4, Epha3, Nrp1; Fig 4_3).The remaining three genes were very weakly or not expressed in the E15.5 cortex (data not shown). I will focus on the 13 genes with a subplate-specific expression in the E15.5 cortex and present them according to potential functional groups.

Cadherins

The microarray screen identified four type II cadherins as well as two protocadherin as higher expressed in subplate (cadherins 9, 10, 12 and 18; protocadherin 10 and 18; Supplementary S1). **Cadherin 10** (Cdh10) and **cadherin 18** (Cdh18, aka Cdh14) showed the highest fold-changes both in anterior and posterior cortex (Cdh10: 2.4, 2.7; Cdh18: 2.7; 1.8). In situ hybridization on E15.5 brains confirmed that both Cdh10 and Cdh18 are specifically expressed in the subplate (Fig 4_2 e,f). The probes strongly labeled a substantial number of cells forming a large band in the subplate while the cortical plate appeared unlabeled. For both genes, more cells appeared to be labelled in the anterior than in the posterior subplate.

Proteins involved in axonal growth and guidance

Plastin 3 (Pls3, aka T-plastin) is an actin-bundling protein involved in neurite growth[351]. I found that in the E15.5 cortex, a riboprobe against Pls3 primarily labelled cells in the subplate (Fig 4_2 m). More cells appeared to be labelled in the anterior than in the posterior subplate where only sparse cells were visible. In the most anterior region of the cortex, a few Pls3+ cells were also seen in the lower cortical plate.

The **unc5 homologue Unc5c** (aka Unc5h3) belongs to a family of netrin receptors which mediate repulsion from a source of netrin. In the embryonic mouse CNS, Unc5c expression has been described in various structures including the spinal cord, mesencephalon, cerebellar plate and prethalamus and thalamus but to my knowledge not in cortex[352,41]. Using in situ hybridization, I found that at E15.5, Unc5c mRNA is specifically localized to the subplate

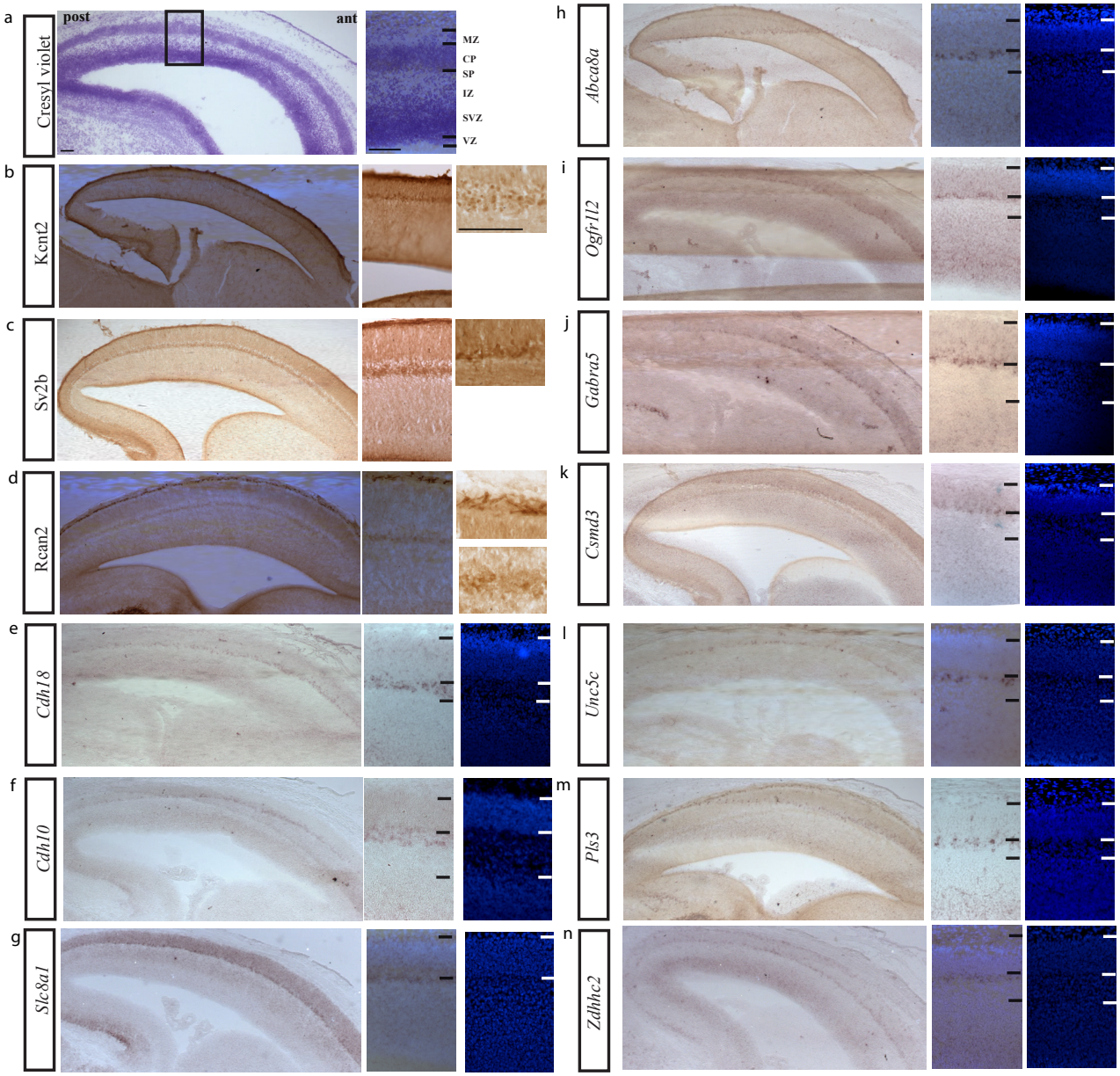

Figure 4_2. **Genes with subplate-specific expression in the E15.5 cortex**. Immunohistochemistry (b-d) or in situ hybridization (e-n) signals for 13 genes which are expressed in the E15.5 subplate (SP) but not in the overlying cortical plate (CP). Kcnt2 (b) and Rcan2 (d) show additional expression in the marginal zone (MZ). A cresyl-violet stained section is shown for reference (a). The right-most panels in (e-n) show DAPI counterstains of the same area as shown in the middle panels. Scalebars: 100µm. IZ: intermediate zone; SVZ: subventricular zone; VZ: ventricular zone.

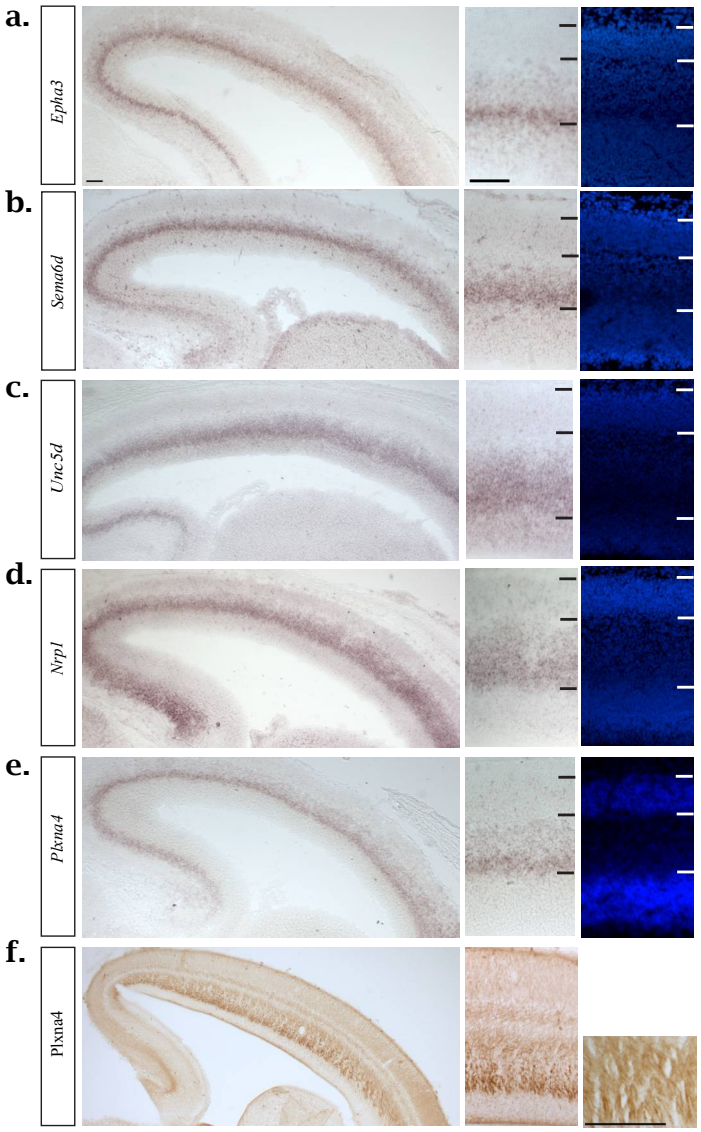

Figure 4_3. **Genes with expression in the intermediate zone in the E15.5 cortex.** In situ hybridization (a-d) and immunohistochemistry (e) signals for five genes which are primarily expressed in the E15.5 intermediate zone. Epha3 (a), Nrp1(d) and Plxna4 (e) show additional weaker expression in the subplate. The right-most panels in e-n show DAPI counterstains of the same area as shown in the middle panels. Scalebars: 100µm.

(Fig 4_2 l). Individual very strongly labelled SP cells were seen across the entire rostrocaudal expanse of the cortex.

Proteins involved in neurotransmission

The **GABA-A receptor alpha5** (Gabra5) is a subunit of the ionotropic GABA-A receptor. In the adult mouse and postnatal and adult rat brain, Gabra5 shows the highest expression in the hippocampus with an additional weaker expression in other structures including the neocortex. Immunohistochemistry against Gabra5 in adult rat was reported to prominently label neurons in layer VIb[353]. I found that in the E15.5 cortex, Gabra5 mRNA is localized in the subplate (Fig 4_2 j). Within subplate, Gabra5 appeared to be expressed in an anterior high – posterior low gradient.

The **solute-carrier 8a1** (Slc8a1, aka NCX1) is a sodium/calcium exchanger which generally exchanges 3 Na^+ for 1 Ca^{2+} [354]. Slc8a1 can be spliced into a large number of different isoforms which show differential expression in different tissue and at different developmental stages in rat[354-356]. I used a riboprobe against all splice variants of Slc8a1 and found strong staining in the E15.5 subplate (Fig 4_2 g). Subplate was clearly visible as a dark band while the cortical plate showed weaker labelling. Due to the high homology between Slc8a1 and the two other Slc8 family members (Slc8a2 and Slc8a3) I cannot exclude that the probe binds to a lesser degree to those mRNAs (probe homology with Slc8a2: 70%, Slc8a3:75%) although high stringency conditions were used for the in situ hybridization.

The gene **potassium channel subfamily T, member 2** (Kcnt2 aka Slick) encodes a sodium-activated potassium channel which is inhibited by ATP[41]. In the adult rat cortex, Kcnt2 has been shown to be primarily localized to layers II/III and V[41]. At E15.5, an anti-Kcnt2 antibody labelled a large number of cells in the subplate and fewer cells in the marginal zone. On most brains, only a few scattered Kcnt2+ cells were detected in the developing cortical plate (Fig 4_2 b) but occasionally, a larger number of cortical plate cells was labelled.

The **zinc finger, DHHC domain containing 2** (Zdhhc2 aka Dhhc2) protein is a palmitoyl acyltransferase, an enzyme which mediates post-translational protein modification by adding the fatty acid palmitate to specific cysteine residues. I found that in the E15.5 cortex, Zdhhc2 is mainly expressed in the subplate and the marginal zone with no labelling detectable in the cortical plate (Fig 4_2 n). Additional weaker staining was found in the VZ and SVZ.

The **synaptic glycoprotein vesicle 2b** (Sv2b) is one of three members of the Sv2 protein family and is involved in the Ca^{2+} regulation of neurotransmitter release[357]. Sv2b mRNA has been reported to be more strongly expressed in the upper layers of the developing cortical

plate of the E17 rat and in the entire cortex of adult rat[358]. I used an anti-Sv2b antibody on E15.5 sections and found specific labelling in the subplate and marginal zones which were clearly visible as two dark bands at low magnification (Fig 4_2 c). This observation is consistent with Genepaint gene expression data at E14 and E15 where Sv2b mRNA is also primarily localized to the subplate (Genepaint IDs EH3733 and HB596).

Proteins highly expressed in subplate with various functions

Rcan2 acts a regulator of calcineurin, a phosphatase which is highly expressed in the brain and plays key roles in neurite outgrowth, neuronal death and synaptic plasticity (reviewed in [359]). In both postnatal and adult cortex, Rcan2 is primarily expressed in interneurons although some pyramidal neurons, especially in layer VI, were also found to be Rcan2+ [350]. In the E15.5 cortex, I found Rcan2 protein primarily localized in horizontally orientated, bipolar cells in the marginal zone (Fig 4_2 d). The subplate also appeared to express Rcan2 and was visible as a dark band but the labelling was weaker than in the marginal zone. The staining in subplate was only detected in a subset of E15.5 brains. These brains generally appeared to be slightly more developed (i.e. with a thicker cortical plate), suggesting that E15.5 is the time of onset of Rcan2 expression in the subplate.

ATP-binding cassette (ABC) transporters constitute one of the largest protein superfamilies with 57 mammalian ABC genes identified so far[360]. The member **ABC transporter A8a** (Abca8a) belongs to the A family which presumably transports mainly lipids. Abca8a showed consistent fold-changes in both anterior and posterior cortex in the microarray screen (2.1 and 1.9, respectively). Using in situ hybridization, I confirmed that Abca8a is very strongly and specifically expressed in the E15.5 subplate with no staining detectable in the cortical plate (Fig 4_2 h).

CUB and Sushi multiple domains 3 (Csmd3) is a giant gene comprising 73 exons and is predicted to encode a transmembrane protein based on its amino acid sequence[361]. Csmd3 has been reported to be primarily expressed in foetal brain and testis [361]. A riboprobe designed against Csmd3 mainly labelled subplate cells in the E15.5 cortex while staining of the overlying cortical plate was much weaker (Fig 4_2 k).

The **opioid growth factor-like receptor 1** (Ogfrl1) is a largely uncharacterized protein but is partially homologous (41.7% identity in a 314 out of 464 amino acid overlap) to the opioid growth factor receptor (Ogfr). Ogfr binds the endogeneous opioid peptide met-enkephalin, an inhibitory growth molecule influencing cell proliferation and tissue organization[362][363]. In situ hybridization on E15.5 brains with a riboprobe against Ogfrl1 resulted in a strong labelling of the subplate (Fig 4_2 i). The lower cortical plate was also weakly labelled but subplate is clearly visible as a darker band.

Gene symbol	Name	Function	Expression
Specific expression in subplate			
Abca8a	ABC transporter A8a	Lipid transporter	SP
Cdh10	Cadherin 10	Type II cadherin	SP
Cdh18	Cadherin 18	Type II cadherin	SP
Csmd3	CUB and Sushi multiple domains 3	Transmembrane protein of unknown function	SP
Gabra5	GABA A receptor α5	Ionotropic GABA receptor	SP
Kcnt2	potassium channel subfamily T, member 2	Potassium channel	SP, MZ
Ogfrl1	opioid growth factor-like receptor 1	Homologous to the opiod growth factor receptor	SP
Pls3	L-plastin	Actin-bundling	SP
Rcan2	Regulator of calcineurin 2	Regulator of calcineurin	MZ, weak in SP
Slc8a1	solute-carrier 8a1	Sodium-calcium exchanger	SP
Sv2b	Synaptic vesicle 2b	Regulation of neurotransmitter release	SP
Unc5c	Unc homologue 5c	Netrin-1 receptor	SP
Zdhhc2	zinc finger, DHHC domain containing 2	Palmitoyl acyltransferase	SP
Main expression in intermediate zone/subventricular zone			
1190002N15Rik	-	Unknown	SVZ and IZ
Epha3	Eph receptor a3	Ephrin receptor	SVZ, IZ, weak in SP
Nrp1	Neuropilin 1	Receptor for VEGF and Sema3a	SVZ, IZ, weak in SP
Nt5dc2	5'-nucleotidase domain containing 2	Dephosphorylation of nucleotides	SVZ and IZ
Plxna4	Plexin a4	Sema6a receptor	SVZ, IZ, weak in SP
Sema6d	Semaphorin 6d	Guidance molecule	SVZ, IZ
Unc5d	Unc homologue 5d	Netrin-1 receptor	SVZ, IZ
No or weak expression in the cortex			
Cdh12	Cadherin 12	Type II cadherin	weak signal
Cdh9	Cadherin 9	Type II cadherin	weak signal
Neurod1	Neurogenic differentiation 1	Transcription factor	hippocampal anlage

Table 4_2. **Subplate-enriched genes selected for validation**. This table lists all 23 genes which were selected for further validation by immunohistochemistry or in situ hybridization. 13 genes were confirmed to be specifically localized in the E15.5 subplate (SP), sometimes with additional expression in the marginal zone (MZ; Rcan2, Kcnt2) ; 7 genes were primarily expressed in the intermediate zone (IZ) and subventricular zone (SVZ), sometimes with additional expression in SP (Epha3, Nrp1, Plxna4); 3 genes were not expressed in the E15.5 cortex.

4.3.2 Expression pattern of subplate-specific genes in the reeler mutant

As an additional mean of verifying the subplate-specificity of these 13 genes, I analyzed their expression patterns in the cortex of E15.5 reeler mutant mice. In these mice, the preplate fails to split and the cells normally contributing to the subplate are located underneath the pial surface[58] (Fig 4_4 a). Thalamic fibres first navigate to this mispositioned subplate (referred to as superplate) before turning back down to their targets in the cortical plate. I found that in E15.5 reeler mice the expression of the majority of subplate-specific genes was shifted to the superplate (Fig 4_4 and 4_5). *Abca8a*-, *Cdh10*-, *Cdh18*-, *Csdm3*-and *Gabra5*- positive cells were all localized in a broad band just below the cortical pial surface (Fig 4_4 b,c,d,e,h). Consistent with the sparser labelling of the subplate in wild-type animals, few but clearly labelled *Pls3*- and *Unc5c*-positive cells were visible in the superplate (Fig 4_4 f, g). In contrast, I did not find any clear labelling for *Slc8a1*, *Zdhhc2*, Sv2b or *Ogfrl1* (Fig 4_4 i, j, k and 4_5 b) in the reeler cortex, neither in the superplate nor below the cortical cells. In wild-type cortices, Kcnt2 and Rcan2 are expressed both in the subplate and the marginal zone while in the reeler cortex, Kcnt2- and Rcan2-positive cells were only visible in the superplate (Fig 4_5 a, c). The band of Kcnt2- and Rcan2-positive cells in the superplate appeared larger than the one in the marginal zone of wild-type animals, suggesting that the superplate contains both subplate and marginal zone cells positive for Rcan2 and Kcnt2. As E15.5 is the onset of Rcan2 expression in the subplate, I also analyzed P8 reeler mice for Rcan2 labelling (Fig 4_5 d, e). In the P8 wild-type cortex, Rcan2+ cells are distributed throughout the whole cortex but the subplate is clearly visible as a cell-dense band above the white matter. This band was absent in the reeler mutant brain, and did not appear to be shifted to the superplate. In contrast to the shift or absence of expression of the 13 subplate-specific genes, the expression of *neuropilin1* (*Nrp1*), which is strongly expressed in the intermediate zone, was unaffected in E15.5 reeler brains (Fig 4_4 l).

4.4 Discussion

4.4.1 Verification of expression in the E15.5 subplate

I have verified the expression patterns of 23 selected genes of the subplate microarray list using immunohistochemistry, where antibodies were available, or in situ hybridization. This subset of genes was chosen based on publicly available gene expression data, expression levels and association to subplate-relevant functions. Out of the 23 genes, 13 were primarily expressed in subplate in the E15.5 mouse brain (Table 4_2; Fig 4_2). To my knowledge, none of these genes has been previously described as specifically associated with this compartment during embryonic development. Publicly available gene expression datasets at E14.5 and/or E15.5 were available for 12 out of 13 genes but four expression patterns were difficult

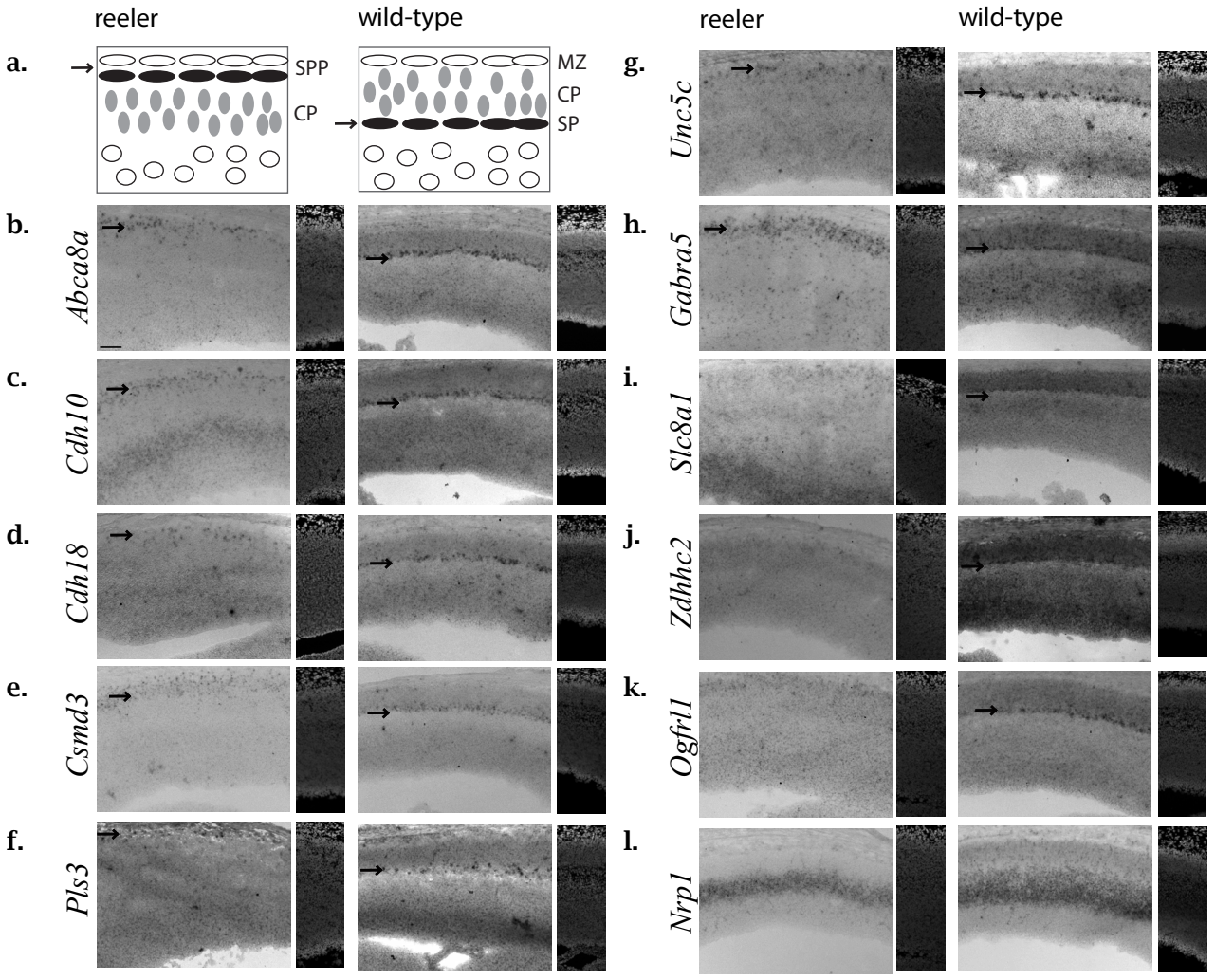

Figure 4_4. **Shifted expression of subplate-specific genes in the E15.5 reeler cortex.** a. Schema illustrating the inverted relative position of subplate (SP) and cortical plate (CP) cells in the reeler mutant. In the reeler, the preplate fails to split and remains at the top of the cortical wall as the superplate (SPP). b-l. In situ hybridization signals in the reeler and wild-type E15.5 cortex. Small panels show DAPI counterstains of the same areas. Out of ten genes with SP-specific expression in the wild-type cortex (b-k), seven are expressed in the SPP in the reeler cortex (b-h). For the remaining three genes (i-k), no clear expression pattern is visible in the reeler brain. In contrast, the expression pattern of Nrp1 (l), which is primarily localized in the intermediate zone in the wild-type cortex, remains in the same position in the reeler cortex. Scalebar: 100μm.

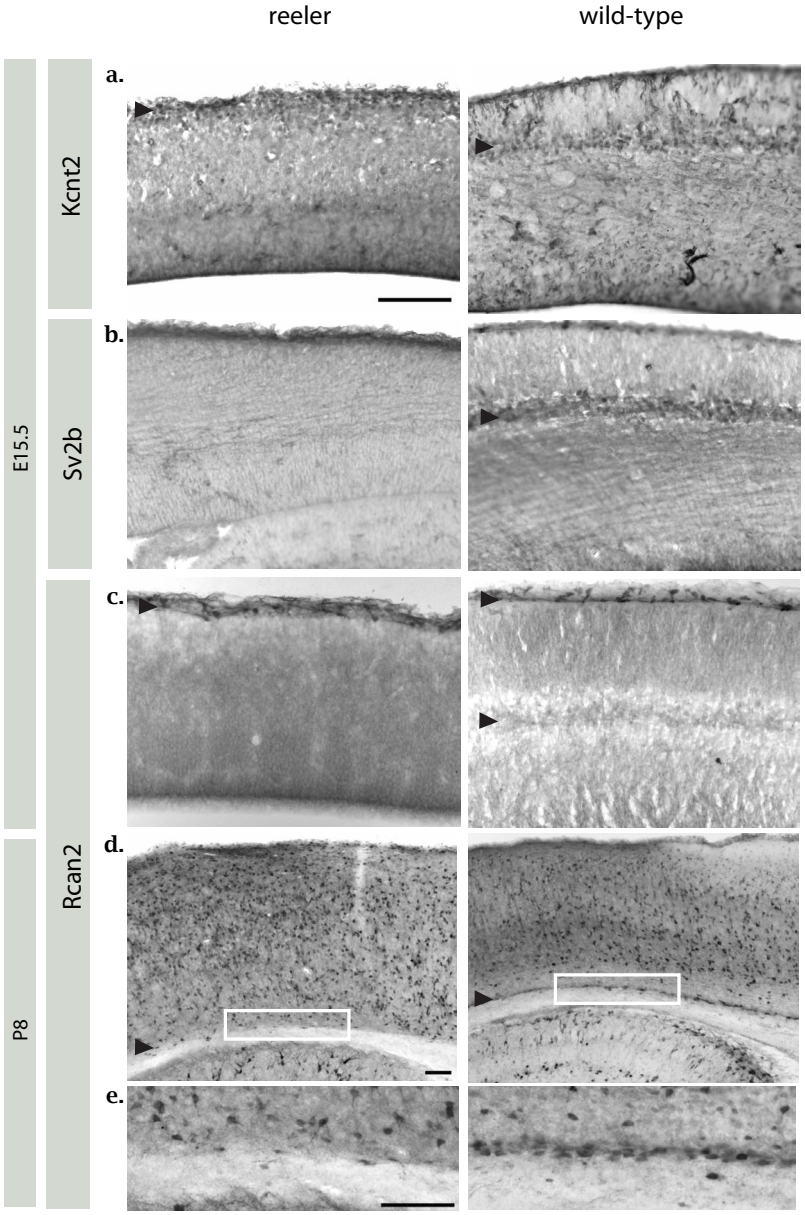

Figure 4_5. **Expression of Sv2b, Kcnt2 and Rcan2 in the reeler cortex.** Panels depict immunohistochemistry signals in the E15.5 (a-c) and P8 (d,e) reeler and wild-type cortex. a. Kcnt2 expression is localized in the subplate and the marginal zone of the wild-type cortex. In the reeler cortex, Kcnt2-positive cells are found in large numbers in superplate. b. Sv2b-positive cells are visible in the wild-type subplate but appear no longer labeled in the reeler cortex. c. Rcan2 is strongly expressed in the marginal zone and weakly in the subplate of E15.5. wild-type cortex. In the reeler, all Rcan2-positive cells are in the superplate which appears enlarged. e. In the P8 wild-type cortex but not in the reeler cortex, a band of Rcan2-positive cells is clearly visible in the subplate above the white matter. f. High magnification images of the areas delineated by a white box in e. Scalebars: 100μm.

to localize (Sv2b, *Slc8a1*, *Unc5c* and *Zdhhc2*) and two genes showed no expression (*Abca8a*, *Csmd3*). Seven of the 23 selected genes were mainly expressed in the intermediate zone and/or SVZ (Fig 4_3). Only for three of them, additional weaker expression was found in the subplate. This suggests that the microdissected subplate tissue prepared for the microarray also contained some cells from the underlying intermediate zone. This is not surprising as no clear border is visible between the subplate and the intermediate zone on the cresyl-violet stained sections used for the microdissection.

To further confirm the subplate-specific expression of the 13 newly identified genes, I analyzed their expression pattern in E15.5 cortices of reeler mutant mice. In these mice, neurons of the cortical plate do not divide the preplate into subplate and marginal zone but instead accumulate below it. The unsplit preplate remains as a single superficial layer and is referred to as the superplate. I found that 7 out of 13 genes clearly showed a shifted expression pattern from the subplate in wild-type animals to the superplate in reeler animals (*Abca8a*, *Cdh10*, *Cdh18*, *Csmd3*, *Gabra5*, *Pls3* and *Unc5c*; Fig 4_4 b-h). Within the superplate, the labelled cells appeared to be scattered and not organized into a tight layer. This shift in gene expression confirms that these genes are expressed in the subplate and not in the underlying intermediate zone or the overlying lower cortical plate. In contrast, expression of *Nrp1*, a gene primarily present in the intermediate zone, was not shifted in the reeler cortex (Fig 4_4 l). In addition, the shift suggests that the cells expressing these seven genes are residential postmigratory subplate cells and not migrating neurons present in this compartment at the time. However, I cannot exclude that tangentially migrating interneurons associated with the subplate compartment would not be shifted to the superplate. Indeed, it has been shown that at least in the postnatal reeler cortex, the position of interneurons is abnormal[364].

Two further genes – Rcan2 and Kcnt2 - are both expressed in the subplate and the marginal zone in the E15.5 wild-type cortex (Fig 4_5). In the reeler mutant, both genes are expressed exclusively in the superplate. Qualitative analysis suggests that there are more labelled cells in the superplate of the reeler cortex than in the marginal zone in the wild-type cortex. This would indicate that the superplate contains both Rcan2- and Kcnt2-positive subplate and marginal zone cells, but further quantitative analysis would be needed to confirm this observation. I did not attempt such an analysis as it should be performed on reeler and wild-type embryos from the same litter or at least on embryos from time-mated animals of the same strain which were not available at the time.

Finally, for the remaining four genes (*Ogfrl1*, Sv2b, *Slc8a1* and *Zdhhc2*) I did not find any consistent expression patterns in the reeler cortex, neither in the superplate nor in or below the cortical plate (Fig 4_4 and 4_5). One possible explanation could be that subplate-equivalent cells in the superplate do express these genes but that the expression is difficult to detect because the cells do not form a tightly-packed band as they do in the wild-type subplate. This

could be particularly the case for *Zdhhc2* and *Slc8a1* where there is a relatively high background signal even in wild-type cortices. Alternatively, it is conceivable that subplate cells in the superplate do not express these genes in the altered position. Finally, I cannot exclude that these genes are not expressed by subplate cells themselves but by other cells present in this compartment such as radially or tangentially migrating neurons.

In P8 reeler mutant brains, it was observed that the Ddc+ subplate cell population was not shifted into the superplate but remained below layer VI. In contrast, all other examined subplate populations (Cplx3+, Nurr1+, *MoxD1*+, *Ctgf*+ and *Tmem163*+ cells) were shifted as expected[117]. Among the 13 subplate-specific genes examined in reeler brains at E15.5, I did not observe any which remained expressed below the cortical plate.

4.4.2 Functional groups in the subplate-specific genes

I have identified 13 genes with a specific expression in the embryonic E15.5 subplate. These genes belong to different functional groups and could be involved in different molecular mechanisms specific to the subplate at this stage.

At E15, subplate neurons have started to establish synapses which will mature to functionality within the next few days[79]. Synaptic transmission requires the expression of a large set of proteins including neurotransmitter receptors, ion channels and the synaptic release machinery. I have confirmed the specific expression in subplate of several genes which code for proteins belonging to these functional groups. These include the ionotropic GABA receptor Gabra5, the potassium channel Kcnt2, the calcium/sodium transporter Slc8a1 and the two regulators of synaptic vesicle release Sv2b and Zdhhc2. Cadherins have also been implicated in synaptogenesis although most evidence comes from studies of type I cadherins (reviewed in [341,365]). Cadherins mediate the adhesion between the pre-and postsynaptic membranes and can be involved in the recruitment of synaptic machineries, the stabilization of neurotransmitter receptors and the regulation of synaptic plasticity. In addition, it has been suggested that the differential expression of cadherin subfamilies in the pre-and postsynaptic membranes underlies the specificity with which subpopulations of neurons connect to each other[366,367].

Subplate neurons have already extended axons into the internal capsule at E15 and these will reach the thalamus within the next few days[55,70,72,73]. The plastin Pls3 has been shown to play a crucial role in axonal growth through the interaction with F-actin[351]. Unc5c is a receptor mediating repulsion from a source of netrin-1, an important axonal guidance cue[368,369,41,42].

Cadherins have also been implicated in axonal outgrowth, fasciculation and pathfinding[340]. In particular, it has been suggested that cadherins can be used by growth cones to navigate along pre-existing pathways expressing the same type of cadherin[342,340]. As one of the presumed functions of the embryonic subplate is the guidance of thalamocortical afferents to the cortex and of corticofugal axons to the thalamus, it would be interesting to investigate whether these structures also express the same cadherins as the subplate cells (i.e. Cdh10 and Cdh18) during development. However, in contrast to type I cadherins, type II cadherins are able to establish both homophilic and heterophilic interactions[340]. Therefore, even if thalamocortical or corticofugal axons do not express the same cadherins as subplate this does not preclude that they are unable to interact.

The embryonic subplate is one of three cortical zones where interneurons migrate tangentially into the cortex, the other two being the intermediate zone and the marginal zone[93]. The regulator of calcineurin Rcan2 has been shown to be mainly expressed in interneurons in postnatal and adult mouse cortex[350]. Consistently, I have found that in the embryonic E15.5 cortex Rcan2 expressed in the marginal zone as well as the subplate. This suggests that this gene could be specifically expressed in a subtype of interneurons migrating only in the marginal zone and in the subplate but not in the intermediate zone. There is some evidence that cadherins could be also involved in tangential interneuron migration as the knock-out of the protocadherin Celsr3 causes a migration defect in calretinin-positive interneurons[370]. Similarly, netrin-1 has been shown to regulate interneuron migration in the marginal zone through the interaction with $\alpha 3\beta 1$ integrin[371], and it is conceivable that Unc5c could play a similar role in the subplate.

For some subplate-specific genes, it is difficult to hypothesize what function they could play in this compartment. For instance, Csmd3 is probably encoding a transmembrane protein but no further information is available about this gene. Abca8a is a member of the ABC transporter A subfamily which probably transports mainly lipids[372]. The A subfamily appears to be the least evolutionary conserved groups of all ABC transporters as only 7 out of 17 members are present across all vertebrate species [360]. In particular, Abca8a is only present in rodents while Abca8b is present in rodents, dog, chimp and human, indicating that there was a rodent-specific gene duplication of Abca8. There is very little known about the specific function of Abca8a but a high transport of lipids into the subplate neurons could be linked to their increased production of membrane due to axonal and dendritic growth.

4.5 Conclusion

In this chapter, I have confirmed the specific expression in the embryonic E15.5 subplate of 13 genes which have not been previously associated with this compartment at embryonic stages. These genes code for proteins associated with different functions presumed to be important for the embryonic subplate including synapse formation and maturation, axonal growth and guidance and interneuron migration.

Chapter 5 Spatiotemporal expression and co-localization of subplate-specific genes

5.1 Introduction

In the previous chapter, 13 genes have been identified which are specifically expressed in the subplate of the E15.5 mouse cortex. Some of these genes have been associated with mechanisms underlying important functions of the developing subplate such as axonal growth and guidance, synapse formation and interneuron migration. However, many genes have been associated with several functions. For example, cadherins have been suggested to be involved in cellular adhesion and tissue organization, axon guidance, synapse formation and interneuron migration[340,343,341,370]. On the other hand, for some of the genes such as Csdm3 or Ogfrl1 it is difficult to hypothesize on a possible function as they haven't been well characterized.

A developmental time-course of the expression patterns can help to better associate a gene with a possible developmental function. For example, we would expect a gene involved in the guidance of thalamocortical afferents to be expressed from E13 onwards, i.e. the time-point when thalamic axons and subplate axons meet in the internal capsule[63,174]. After E17/18, when the thalamocortical afferents grow into the cortical plate[176], such a gene could be expected to be downregulated. A gene involved in synaptic transmission, on the other hand, would be expressed from the time when subplate synapses start to become functional and potentially into adulthood.

Similarly, the analysis of extracortical expression patterns could provide some further clues about the function of a gene in cortical development. For example, cadherins have been proposed to play a role in establishing the specific connections between different structures through homophilic interactions[342,340]. Therefore, co-expression of a specific cadherin both in subplate and the thalamus could indicate that this protein is involved in matching up the two systems. In contrast, a gene involved in the general maturation of neurons could be expected to be first expressed in subplate as well as other early generated structures such as the endopiriform nucleus[373].

Finally, several of the genes specifically expressed in subplate have been proposed to be associated to interneurons or interneuron migration. Co-localization with markers of interneurons (e.g. GABA, Gad67) can help to distinguish whether these genes are expressed in migrating interneurons or postmigratory subplate neurons.

The aim of this chapter is to gain further insight into possible functions of the

subplate-specific genes by establishing a detailed developmental time-course of expression, investigating extracortical expression patterns and examining the possibility of co-localization with interneuron markers.

5.2 Methods

5.2.1 Tissue preparation

For in situ hybridization (ISH), heads from E13.5, E14.5, E15.5 and E17.5 and brains from P8 and adult C67/Bl6 mice were embedded in O.C.T (Tissue-Tek) and flash-frozen. Brains of E15.5 and P8 green fluorescent protein expression driven by glutamic acid decarboxylase 67 KDa promoter (Gad67-GFP) mice were fixed in 4% PFA for 4h (E15.5) or 24h (P8) and cryoprotected in 30% sucrose before freezing. For immunohistochemistry (IHC), E13.5, E14.5, E15.5 and E17.5 C67/Bl6 and P8 Gad67-GFP brains were immersion-fixed in 4% PFA for at least 24h. Gad67-GFP brains were provided by Sonia Rakic and Prof John Parnavelas (University College London, UK). Fixed P8 and adult brains and E17.5 brains for GABA immunhistochemistry were obtained by deeply anesthetizing with pentobarbitone (Euthatal 150 mg/kg intraperitoneally; Merial Animal Health Ltd) and perfusing through the heart with 4% PFA or with 4% PFA and 0.25% glutaraldehyde for immunohistochemistry against GABA (Agar Scientific). Further details on animal numbers and tissue preparation are listed in Table 5_1.

5.2.2 In situ hybridization

Permanent in situ hybridization was performed on coronal and sagital cryosections of E13.5, E14.5, E15.5, E17.5, P8 and adult brains as described in Chapter 4 (section 4.2.2) using the following riboprobes: Abca8a, Cdh10, Cdh18, Csmd3, Gabra5, Ogfrl1, Pls3, Slc8a1, Unc5c (probe 2) and Zdhhc2.

For co-localization, immersion-fixed Gad67-GFP brains were cut into 16µm coronal cryosections and post-fixed with 4% PFA for 10 min. Sections were treated with 2µg/ml proteinase K (Roche) in PBS for 10min at RT and deproteinized, acetylated and prehybridized as for permanent in situ hybridization. Hybridization with DIG-labelled probes and subsequent washes were performed at the lower temperature of 60°C in order to protect GFP protein structure. After blocking, sections were incubated with anti-DIG-alkaline phosphatase antibody 1:2000 (Roche) and rabbit anti-GFP antibody (1:500, Chemicon) overnight. For fluorescent color detection of probes, Fast Red (Roche) in 100mM Tris, pH 8.0, 400mM NaCl was applied for at least 6h. Sections were then incubated with donkey anti-rabbit Alexa488 1:250 (Invitrogen) in 1% donkey serum for 2h and counterstained with DAPI.

Strain	Age	Preparation	Nb	Use
C57/ Bl6 wild-type	E13.5	Immersion-fixed (PFA)	2	IHC
		Fresh-frozen	2	ISH
	E14.5	Immersion-fixed (PFA)	3	IHC
		Fresh-frozen	3	ISH
	E15.5	Immersion-fixed (PFA)	3	IHC
		Fresh-frozen	3	ISH
	E17.5	Immersion-fixed (PFA)	2	IHC
		Perfused (PFA+Gluteraldehyde)	2	IHC with GABA
		Fresh-frozen	3	ISH
	P8	Perfused (PFA)	3	IHC
		Perfused (PFA+Gluteraldehyde)	3	IHC with GABA
		Fresh-frozen	3	ISH
	Adult	Perfused (PFA)	2	IHC
		Fresh-frozen	2	ISH
Gad67-GFP C57/ Bl6	E15.5	Immersion-fixed and frozen	3	IHC and ISH
	P8	1 hemisphere immersion-fixed (PFA)	3*	IHC
		1 hemisphere immersion-fixed (PFA) and frozen	3*	ISH

Table 5_1. **Number of animals used for spatiotemporal expression and co-localization studies.** This table lists the mouse strain, developmental stage, method of tissue preparation and number of brains used for immunohistochemistry (IHC) and in situ hybridization (ISH). The asterisk (*) indicates that one hemisphere of each brain was used for IHC and the other hemisphere for ISH.

5.2.3 Immunohistochemistry

Permanent immunhistochemistry was performed on coronal and sagittal microtome sections of E13.5, E14.5, E15.5, E17.5, P8 and adult brains as described in Chapter 4 (section 4.2.3) using the following antibodies: anti-Sv2b, anti-Rcan2 and anti-Kcnt2.

For co-localization with Gad67-GFP, fluorescent immunohistochemistry against Rcan2 was performed on E15.5 16µm cryosections or P8 40 µm microtome sections. Co-localization between Rcan2 and reelin was performed on 40µm microtome sections of E15.5 brains fixed with 4% PFA and between Rcan2 and GABA on 40µm microtome sections from E17.5 and P8 brains fixed with 4% PFA and 0.25% glutaraldehyde, respectively. Cryosections were postfixed for 30min in 4% PFA and rinsed with PBS. All sections were blocked for 2h at RT with 5% serum (Sigma) in TBS with 0.2% Triton-X100 (BDH). Sections were incubated with primary antibodies in 1% serum and 0.2% Triton overnight at 4°C. Secondary antibodies were applied for 2h at RT and sections were counterstained with DAPI (Invitrogen). For combinations of primary and secondary antibodies see Table 5_2.

	Serum	Primary antibodies	Secondary antibodies
Rcan2 with Gad67-GFP	Donkey	Rcan2 1:2000 (rabbit, gift M. Arbones)	Donkey anti-rabbit Alexa568 1:500 (Invitrogen)
Rcan2 and GABA	Goat	Rcan2 1:2000; GABA 1:1000 (guinea pig, ab17413, Abcam)	Goat anti-rabbit Alexa488 1:500(Invitrogen); Goat anti-guinepig AlexaCy3 1:500 (Jackson Laboratories)
Rcan2 and Reelin	Donkey	Rcan2 1:2000; reelin 1:250 (E14, gift A. Goffinet)	Donkey anti-rabbit Alexa488 1:500 (Invitrogen); Donkey anti-mouse Alexa568 1:500 (Invitrogen)

Table 5_2: **Antibodies and sera used for Rcan2 co-localization studies.** This table lists the combinations of serum, primary antibodies and secondary antibodies used to co-localize Rcan2 with Gad67-GFP, GABA or reelin.

For co-localization, fluorescently labelled sections were imaged in a single focal plane using a single laser line scanning confocal microscope (Zeiss LSM 710). Quantification of double-labelling was performed on at least 3 sections from each brain and 3 brains.

5.3 Results

5.3.1 Temporal expression profile of subplate-specific genes in the neocortex

The expression patterns of all 13 genes which showed a subplate-specific expression at E15.5 were analyzed at additional developmental stages (E13.5, E14.5, E17.5, P8 and adult) in the neocortex (Fig 5_1, 5_2 and 5_3, Supplementary Table S2).

At E13.5, expression of *Ogfrl1*, *Zdhhc2*, *Csmd3*, *Slc8a1*, *Gabra5*, Sv2b and Kcnt2 was found in the piriform cortex and the most lateral part of the neocortex. Within the lateral neocortex, most cells labelled for Sv2b, Kcnt2, *Gabra5* and *Zdhhc2* were localized in a thin band below the developing cortical plate corresponding to the position of subplate. Labelling for *Ogfrl1*, *Csmd3* and *Slc8a1* was more diffuse and could not be attributed to a specific layer in the lateral neocortex. Rcan2+ cells were exclusively localized in the marginal zone in the entire expanse of the neocortex. No other gene was expressed in the dorsal neocortex where the split of the preplate had not yet occurred.

At E14.5, I found expression for all genes except for Rcan2 in the subplate. Again the preplate, still present in the most dorso-medial neocortex, appeared unlabelled. Within subplate, *Gabra5* and *Pls3* showed an anterior-high posterior-low gradient. *Slc8a1* and *Ogfrl1* were additionally weakly expressed in the cortical plate especially in the anterio-lateral cortex. As at E13.5, Rcan2+ cells were only found in the marginal zone but not in subplate.

At E15.5, all genes were clearly expressed in subplate as described in Chapter 4 (section 4.3.1). Several genes also showed additional expression in the most anterio-lateral cortical plate (*Unc5c*, *Csdm3*, *Cdh10*, Kcnt2 and *Ogfrl1*). *Slc8a1* was still most strongly expressed in subplate but with additional weaker expression throughout the cortical plate. Rcan2 was most strongly expressed in the marginal zone but with additional weaker expression in subplate.

At E17.5, all genes were still expressed in subplate but only *Abca8a* was exclusively localized to this layer at this stage. In addition to subplate, *Cdh18*, *Pls3* and *Zdhhc2* labelling was found in the upper half of the developing cortical plate, probably corresponding to future layer V. *Ogfrl1* was expressed in subplate and in the lower half of the cortical plate (future layer VI) in an anterior-high posterior-low gradient. Rcan2+ cells were found in the marginal zone, in subplate and very sparsely distributed throughout the cortical plate. Finally, *Csmd3*, *Slc8a1*, *Gabra5*, *Cdh10*, *Unc5c*, Sv2b and Kcnt2 were equally strongly expressed in the subplate and the entire cortical plate.

At P8, *Cdh18* and *Slc8a1* were still abundantly expressed in subplate with additional weaker expression in layers V and VI. *Pls3*, *Cdh10* and *Gabra5* were primarily expressed in subplate and layer V while *Ogfrl1* was found in subplate and layer VI. Labelling with *Unc5c* was overall weak and mostly present in layer V and upper layer VI. Interestingly, *Abca8a* labelling was absent from subplate at P8. Instead, I found expression of this gene in layer V in restricted areas of cortex as well as sometimes in layers II/III. Immunohistochemistry against Rcan2 strongly labelled a subset of cells distributed throughout all cortical layers. Subplate was still distinguishable as a darker band where many cells appeared to be weakly to moderately labelled. The remaining genes (*Zdhhc2*, *Csmd3*, Sv2b and Kcnt2) showed a widespread expression throughout the entire P8 cortex including subplate.

In adult cortices, the gene expression patterns were overall very similar to P8 with a few exceptions: *Abca8a* was no longer clearly expressed in cells of layer V but the labelling appeared as a broad dark band above the white matter; cortical expression of *Unc5c* appeared very weak and ubiquitous; finally, Rcan2 antibody labelled more pyramidal cells, in particular in layer V, than at P8.

5.3.2 Extracortical expression patterns of subplate-specific genes

A detailed analysis of the entire extracortical expression patterns of all genes would be beyond the scope of this study. I therefore limit the description to the most prominently labelled structures in the forebrain with special attention to the prethalamus (ventral thalamus) and thalamus (dorsal thalamus) and the claustroamygdalar complex (see Fig 5_4, Supplementary Table S2).

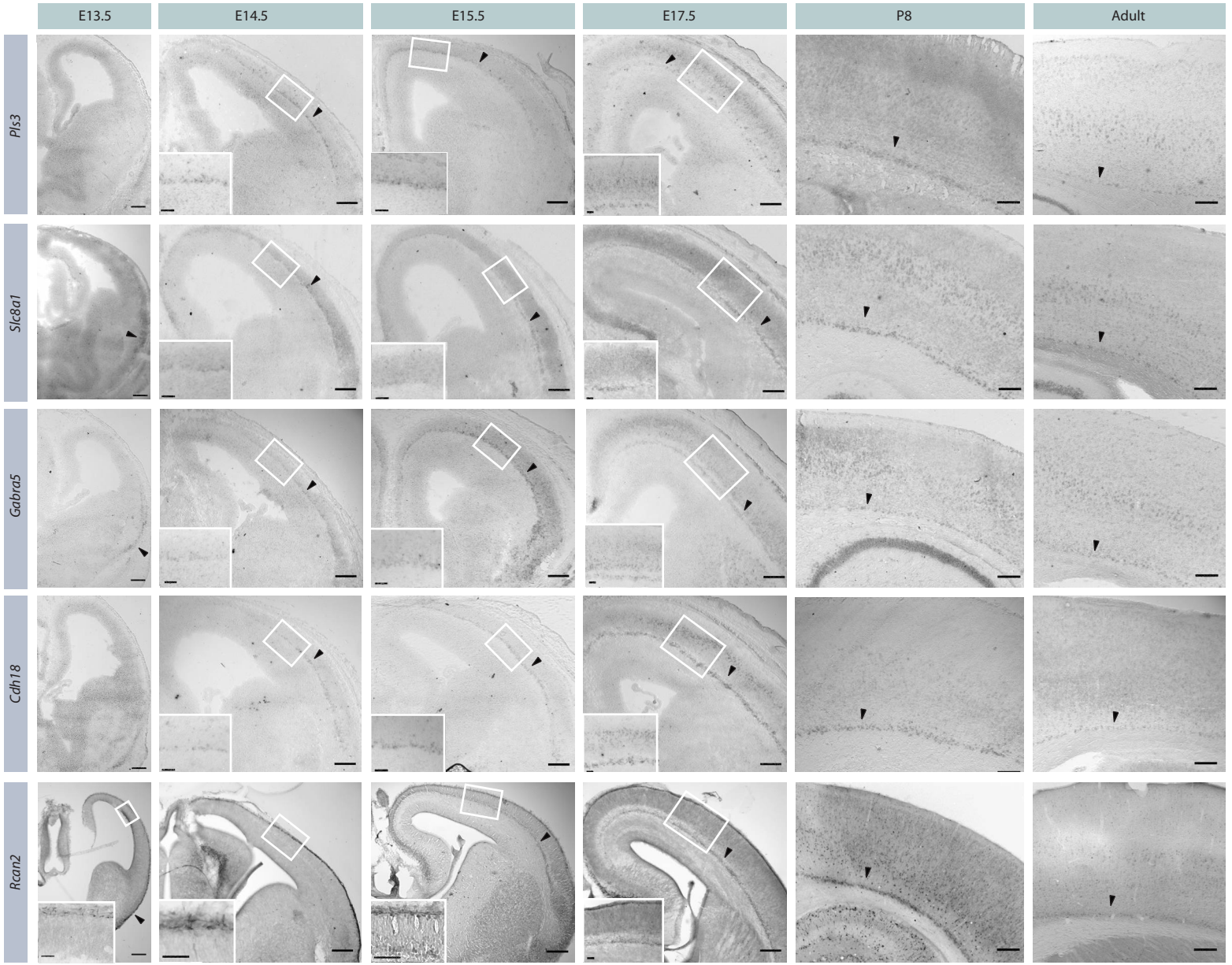

Figure 5_1

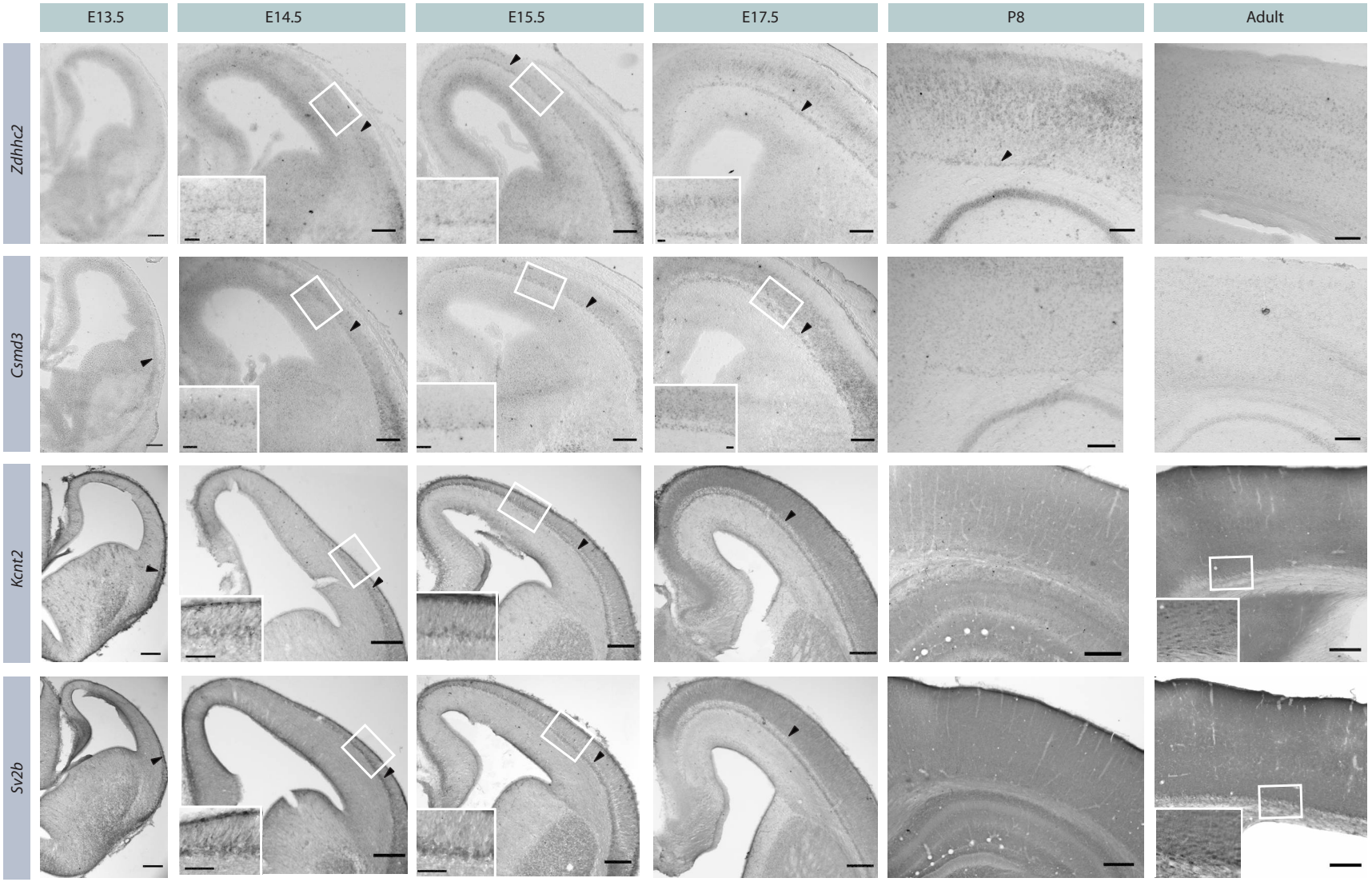

Figure 5_2

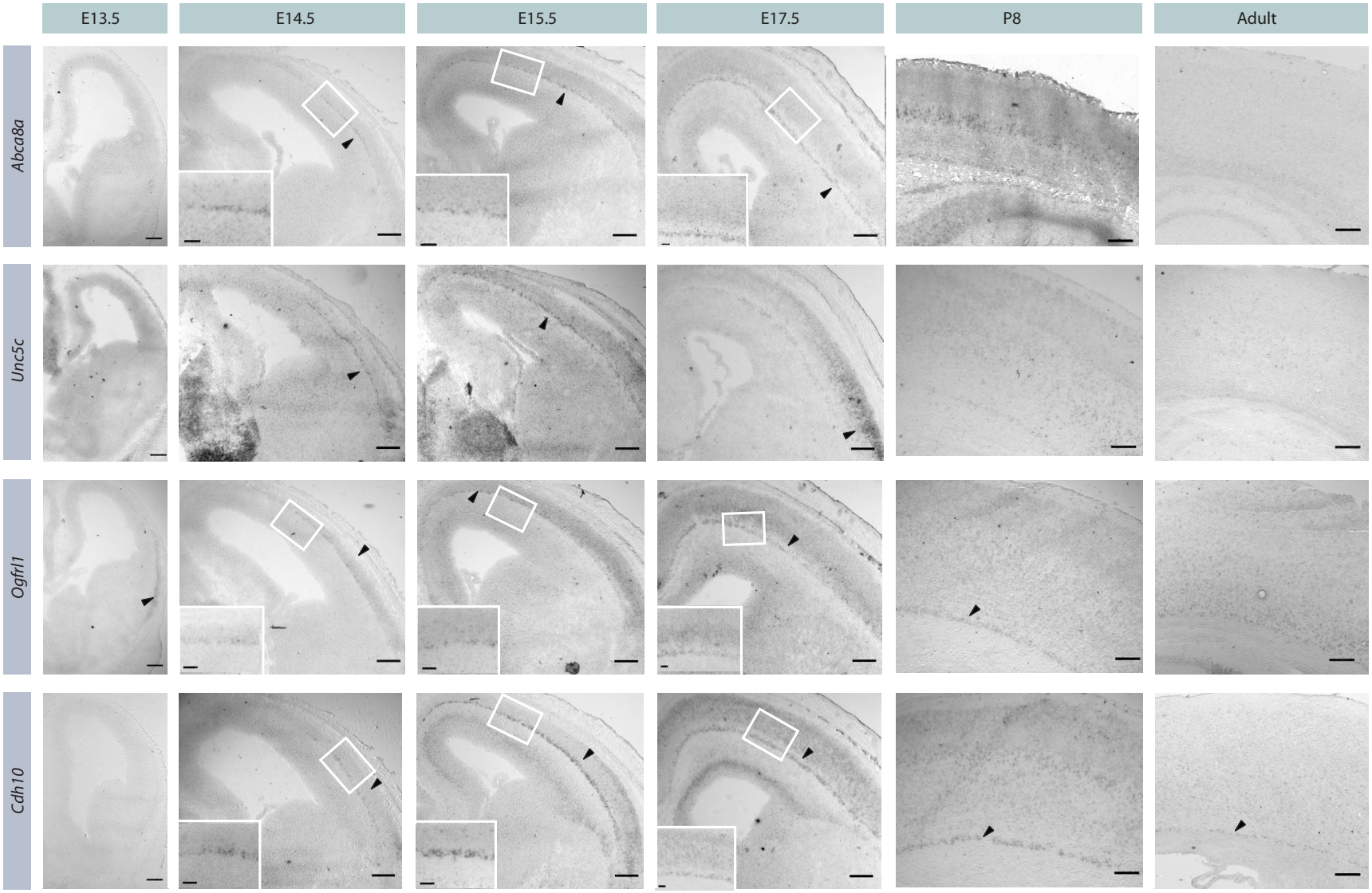

Figure 5_3

Figure 5_1. **Developmental time-course of expression of Pls3, Slc8a1, Gabra5, Cdh18 and Rcan2.** In situ hybridization or immunohistochemistry signals in the E13.5, E14.5, E15.5, E17.5, P8 and adult neocortex. At E13.5 only Gabra5 and Rcan2 are expressed in the lateral cortex (arrowheads). At E14.5 and E15.5 all genes are specifically expressed in the subplate. Rcan2 is additionally expressed in the marginal zone. Strong expression in the subplate is also visible at later developmental stages (E17.5, P8 and adult) for all genes. Scalebars: 200µm (panels); 50µm (inserts).

Figure 5_2. **Developmental time-course of expression of Zdhhc2, Csmd3, Kcnt2 and Sv2b.** In situ hybridization or immunohistochemistry signals in the E13.5, E14.5, E15.5, E17.5, P8 and adult neocortex. At E13.5 Csmd3, Kcnt2 and Sv2b are expressed in the lateral cortex (arrowheads). At E14.5 and E15.5 all genes are specifically expressed in the subplate. Kcnt2 is also expressed in the marginal zone. At later developmental stages (P8, adult), all genes become ubiquitously expressed. Scalebars: 200µm (panels); 50µm (inserts).

Figure 5_3. **Developmental time-course of expression of Abca8a, Unc5c, Ogfrl1 and Cdh10.** In situ hybridization signals in the E13.5, E14.5, E15.5, E17.5, P8 and adult neocortex. At E13.5 only Ogfrl1 is expressed in the lateral cortex (arrowhead). At E14.5 and E15.5 all genes are specifically expressed in the subplate. Cdh10 shows additional expression in the subventricular zone. At E17.5, Abca8a is still specifically expressed in the subplate, Unc5c is primarily expressed in the lateral cortical plate and Ogfrl1 and Cdh10 are equally expressed in the subplate and cortical plate. At P8, Abca8a is specifically expressed in layer V while in the adult, Abca8a expression is no longer visible. At both P8 and adult stages, Unc5c is no longer expressed while Ogfrl1 is primarily expressed in subplate and layer VI and Cdh10 in subplate and layer V. Scalebars: 200µm (panels); 50µm (inserts).

Overall, *Abca8a* showed the most restricted expression pattern as labelling was exclusively present in the subplate at E14.5 and E15.5 (Fig 5_4 a). At later stages, *Abca8a*+ cells are also found in the claustrum, endopiriform nucleus and subiculum (Fig 5_4 a'). Similarly, *Pls3* and *Ogfrl1* have a relatively restricted expression at early embryonic stages where they are only expressed in a few discrete structures including the hippocampal anlage and the olfactory bulb (Fig 5_4 g, h). *Pls3* is also expressed in the subpallial SVZ (Fig 5_4 h). At later stages, *Pls3*+ and *Ogfrl1*+ cells are found additionally in the claustroamygdalar complex and certain thalamic nuclei (Fig 5_4 g', h').

In contrast, the expression of *Gabra5*, *Slc8a1*, *Zdhhc2*, *Csmd3*, Sv2b and Kcnt2 is relatively widespread and involves many extracortical structures (Fig 5_4 d, d', e, e', f, f' j, j', k, k', m, m'). At early embryonic stages, all of these genes are expressed in the septum, the piriform cortex and some or all basal ganglia (Fig 5_4 d, e, f, j, k, m). *Gabra5*, *Zdhhc2* and *Csmd3* show additional expression in the olfactory amygdala (Fig 5_4 d, e, m) and *Gabra5*+ cells are also found in the hypothalamus (Fig 5_4 e). At late embryonic and postnatal stages, the expression of Sv2b, *Csmd3* and Kcnt2 becomes ubiquitous (Fig 5_4 d', f', k'). *Slc8a1* is expressed in the majority of forebrain structures, particularly in some septal and thalamic nuclei, but not in the striatum (Fig 5_4 j'). *Zdhhc2* is also moderately expressed in most forebrain structure but has a particularly high expression in the CA1 field of the hippocampus and the tRN in the prethalamus (Fig 5_4 m'). Expression of *Gabra5* is particularly strong in the hippocampus (Fig 5_4 e').

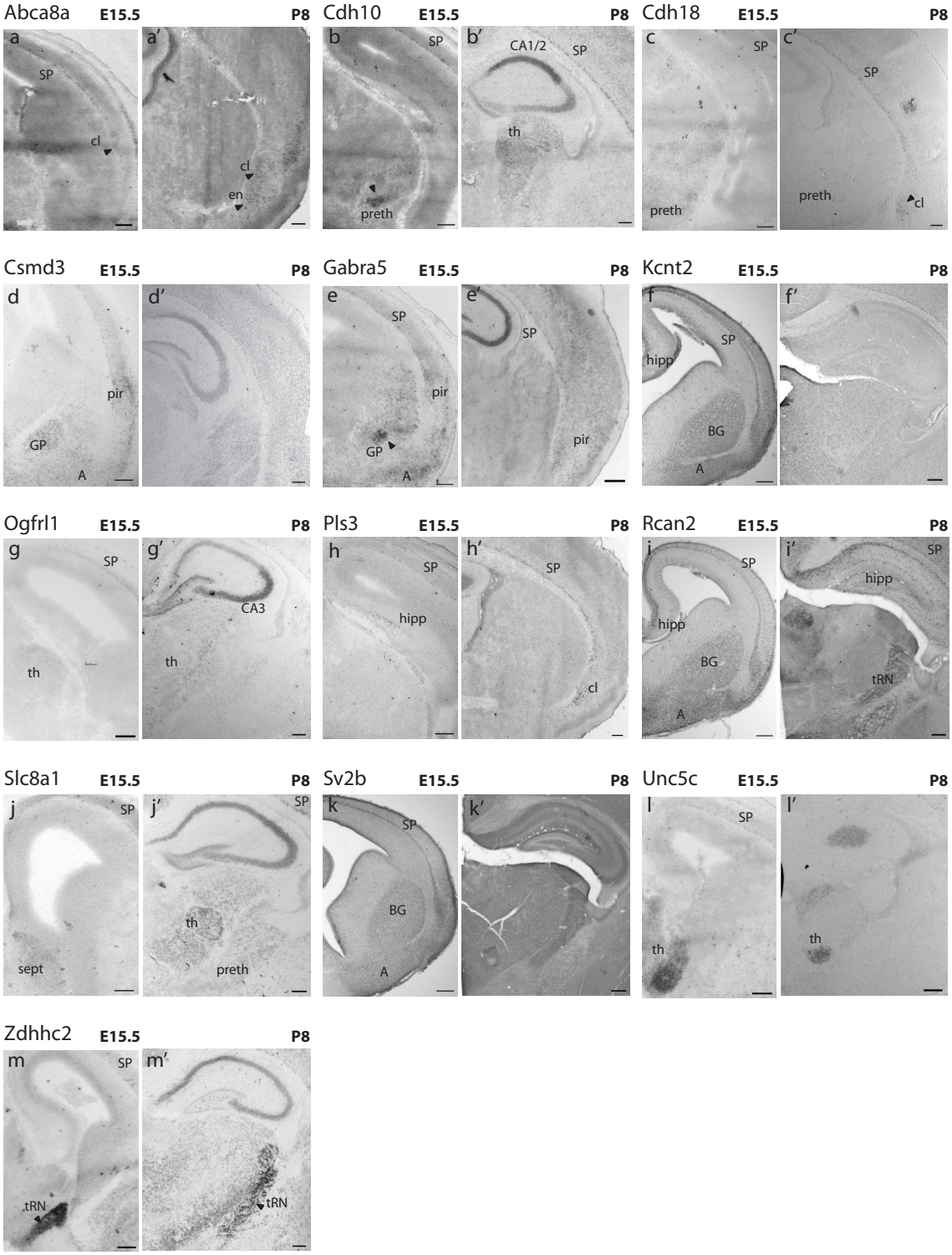

Figure 5_4. **Extracortical expression patterns of subplate-enriched genes.** In situ hybridization (a-e, g, h, j, l, m) or immunohistochemistry (f, i, k) signals at E15.5 and P8 of all 13 subplate-enriched genes. Images were selected to show extracortical areas of expression in the telencephalon and diencephalon (arrowheads and/or labeling). SP: subplate; cl: claustrum; en: endopiriform nucleus; preth: prethalamus; th: thalamus; pir: piriform cortex; GP: globus pallidus; hipp: hippocampal anlage; BG: basal ganglia; A: amygdala; tRN: thalamic reticular nucleus. Scalebar: 200μm.

In the embryonic brain, Rcan2 is strongly expressed in the hippocampal anlage and the developing prethalamus and hypothalamus (Fig 5_4 i). At postnatal stages, Rcan2+ cells are found scattered in most forebrain structures with particularly high numbers in the tRN (Fig 5_4 i'). This is consistent with their association with interneurons as the tRN mainly contains GABAergic cells[374].

In the early embryonic brain, *Unc5c* is very strongly expressed in the prethalamus, the epithalamus and the ventromedial part of the thalamus (Fig 5_4 l). At postnatal stages, the strongest expression is still found in the ventromedial thalamic nucleus and in sparse cells scattered throughout the hippocampus (Fig 5_4 l').

At E14 and E15, *Cdh10* is not expressed in the thalamus (Fig 5_4 b). From E17 onwards, however, strong labelling with *Cdh10* riboprobe is primarily found in some nuclei of the thalamus (Fig 5_4 b'). Cdh18 is expressed in the prethalamus at both embryonic and postnatal stages with no expression observable in the thalamus. (Fig 5_4 c, c') At embryonic ages, strongly labelled *Cdh18*+ cells are additionally found dispersed in the basal ganglia and the olfactory amygdala. *Cdh18* is also expressed in the claustrum throughout development.

More details on the expression patterns for each gene can be found in Supplementary Table S2 .

5.3.3 Co-localization with interneuron markers

The embryonic subplate is one of three zones where interneurons migrate tangentially from the ganglionic eminences into the cortex[93]. In order to investigate whether some of the subplate-specific genes are expressed in these interneurons, I attempted to co-localize their expression with GFP in the Gad67-GFP mouse[375]. In this transgenic line, more than 90% of cortical GABAergic cells are GFP-positive (J. Parnavelas, personal communication). Co-localization analysis was performed for Rcan2 with immunohistochemistry and for *Unc5c* and *Cdh10* with in situ hybridization (Fig 5_5, Fig 5_6).

In the E15.5 cortex, *Cdh10* and *Unc5c* are specifically expressed in the subplate but do not co-localize with Gad67-GFP (Fig 5_5). Less than 1% of *Cdh10*+ cells were found to be expressing GFP (3 double-labelled cells out of 397 *Cdh10*+ cells and 212 Gad67-GFP+ cells, n= 2 brains, Fig 5_5 a-d). *Unc5c* never co-localized with Gad67-GFP (169 *Unc5c*+ cells and 239 Gad67-GFP+ cells, n=2 brains, Fig 5_5 e-h).

Using fluorescent immunohistochemistry, Rcan2+ cells were only detected in the marginal zone of the E15.5 Gad67-GFP cortex but not in the subplate (Fig 5_6 A, B). Surprisingly,

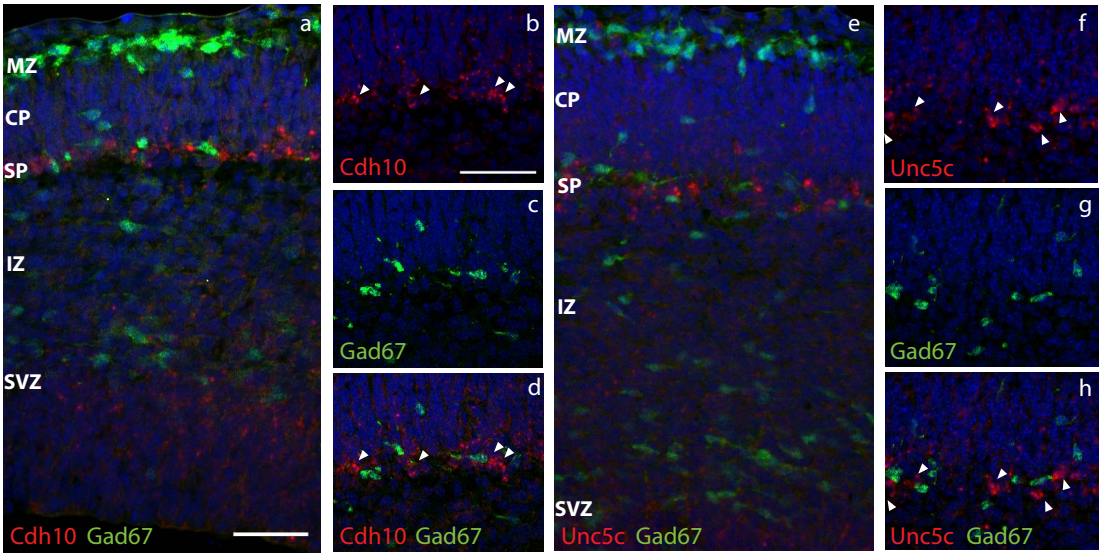

Figure 5_5. **Expression of Cdh10 and Unc5c in the Gad67-GFP cortex.** In situ hybridization against Cdh10 (a-d) and Unc5c (e-h) was performed on sections of Gad67-GFP E15.5 cortices. GFP-positive cells are primarily localized in the marginal zone (MZ), in the subplate (SP) and at the border between the intermediate zone (IZ) and subventricular zone (SVZ) corresponding to the three routes of interneuron migration (a, e).Cdh10-positive cells (a-d; arrowheads) and Unc5c-positive cells (e-h; arrowheads) are localized in the SP. No co-localization was observed between Cdh10 (red; arrowheads) and Gad67-GFP (green) (d) and between Unc5c (red; arrowheads) and Gad67-GFP (green) (h), respectively. Scalebars: 50µm.

the Rcan2+ cells in the marginal zone did not co-localize with Gad67-GFP (Fig 5_6 A). Instead, they formed a distinct band of horizontally orientated cells localized above the stream of tangentially migrating Gad67-GFP neurons (Fig 5_6 a, a'"). Based on their morphology and location, these Rcan2+ cells are most likely Cajal-Retzius cells which is further supported by their co-expression of reelin (Fig 5_6 B).

As I did not detect any Rcan2+ cells in the subplate at E15.5 using fluorescent immunohistochemistry, co-localization of Rcan2 and GABA in the E17.5 cortex was analyzed (Fig 5_6 C). At this age, Rcan2+ cells formed a distinct, cell-dense band in the subplate. In the subplate, less than 10% of Rcan2+ cells appeared to co-localize with GABA (32 double-labelled cells out of 343 Rcan2+ cells, n= 3 brains).

At P8, a dense band of Rcan2+ cells is still visible in the subplate while many Rcan2+ cells are scattered throughout the entire expanse of the cortex (Fig 5_6 D). As at E17.5, in the subplate, only a small proportion of Rcan2+ co-localized with GABA (10.5%, 9 double-labelled cells out of 106 Rcan+ cells, n= 3 brains). In contrast, in layers V and VI, the large majority of Rcan2+ were GABAergic (88.3%, 106 double-labelled cells out of 120 Rcan2+ cells, n= 3 brains) (not shown). Similar results were also found in the P8 Gad67-GFP cortex:

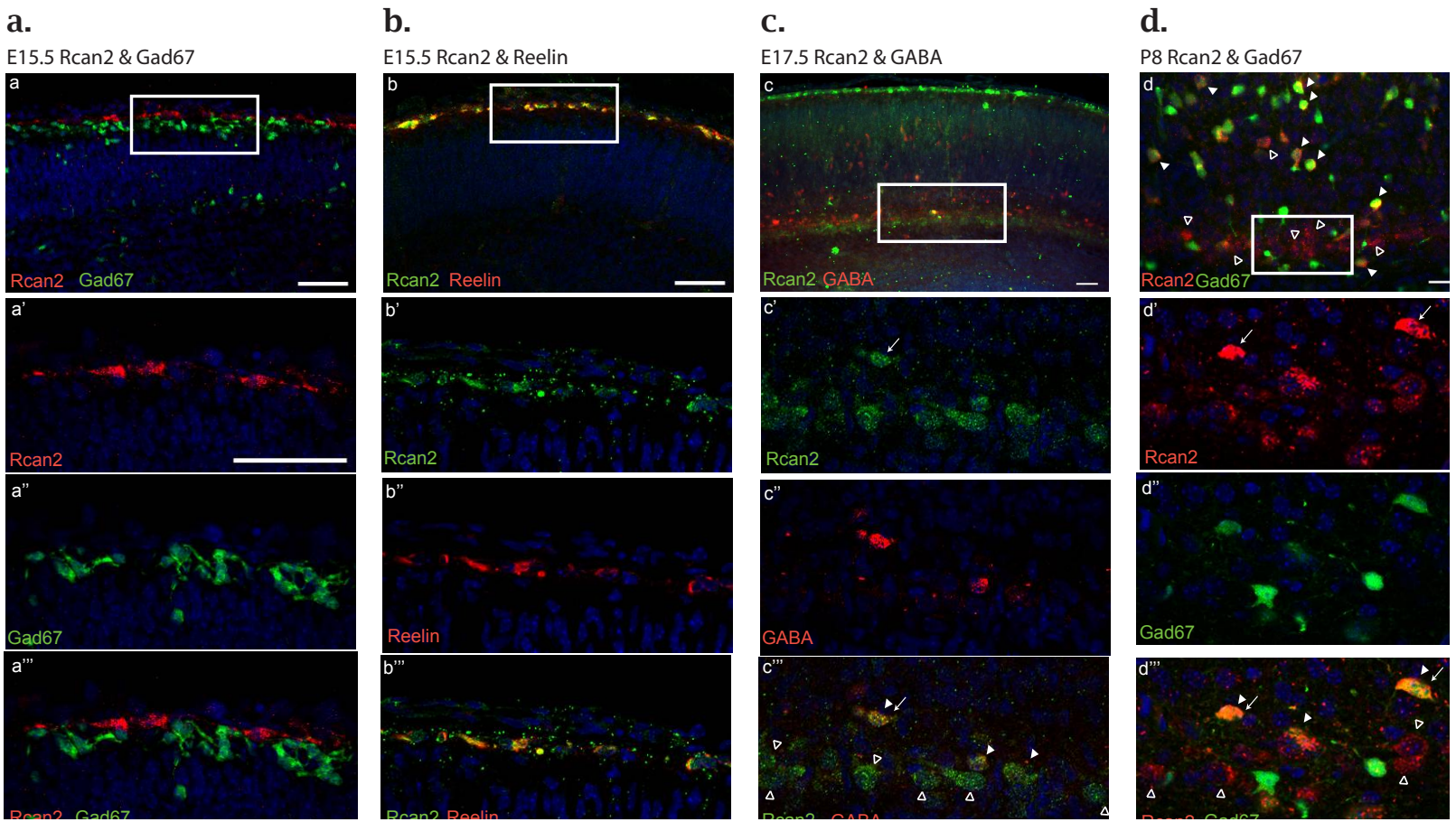

Figure 5_6. **Co-localization between Rcan2, Gad67-GFP/GABA and Reelin.** A. In the E15.5 cortex, immunohistochemistry against Rcan2 (red) primarily labels horizontally orientated cells at the outer edge of the marginal zone (a, a'). The Rcan2-positive cells are a distinct population from the Gad67-GFP-positive cells (green, a, a'') which are localized at the lower edge of the marginal zone (a'''). B. The Rcan2-positive cells in the E15.5 marginal zone (green, b') co-express reelin protein (red, b, b'', b'''). C. At E17.5, Rcan2 (green) is primarily expressed in the marginal zone and the subplate (c, c'). Sparse Rcan2-positive cells are also found within the cortical plate (arrow in c' and c'''). In the subplate, only a small proportion of Rcan2-positive cells co-express GABA (red, c'''). D. In the P8 cortex, strongly labeled Rcan2-positive cells (red) are found dispersed in all layers (d). A band of moderately labeled Rcan2-positive cells is localized within the subplate (d, d'). Only few Rcan2-positive cells in the subplate co-express Gad-67-GFP (green, d, d'''). In contrast, most Rcan2-positive cells outside of subplate (arrows in d and d''') are positive for Gad67-GFP (d, d'''). Empty arrowheads point to single-labeled Rcan2-positive cells, filled arrowheads to double-labeled Rcan2-positive cells. Scalebars: 50μm.

in the subplate, only 13.4% of Rcan2+ cells co-localized with GFP (41 out of 305 cells, n=3 brains) while in layers V and VI over 80% of Rcan2+ also expressed GFP (403 out of 499 cells, n=3 brains) (Fig 5_6 D).

5.4 Discussion

In order to gain some more insight into possible functions of the 13 subplate-enriched genes, a developmental time-course of cortical and extracortical expression was established. As subplate is one of the compartments where interneurons migrate tangentially into the cortex, I also investigated whether some of these genes co-localized with markers for GABAergic neurons. Due to technical challenges, this was only possible for three genes – Rcan2 against which a very specific antibody is available and Unc5c and Cdh10 which can be strongly and specifically labelled with riboprobes. Combining these results with findings from the literature, I will hypothesize in the following paragraphs on the possible roles these genes might play in the subplate

5.4.1 Neuronal maturation

Kcnt2, Sv2b and Csmd3 are specifically expressed in subplate at early developmental stages but from E15.5 onwards their expression expands into the entire cortical plate. These three genes also have a very widespread extracortical expression in the developing forebrain and are ubiquitously expressed in the postnatal forebrain. Most likely, Kcnt2, Sv2b and Csmd3 play a fundamental role in all forebrain neurons. Sv2b is a protein expressed in synaptic vesicles and regulates Ca^{2+}-dependent exocytosis[357]. Kcnt2 is a sodium-activated potassium channel which is inhibited by ATP and could be involved in adjusting the electric activity of a cell to its metabolic state[376]. Both functions – regulating synaptic vesicle release and controlling excitability– are fundamental to all neurons. It seems probable that Kcnt2, Sv2b and Csdm3 are first expressed in subplate because subplate neurons are born and mature earlier than neurons of the cortical plate. Similarly, it has been shown that the early embryonic subplate specifically expresses MAP2[64], a marker of mature neurons, which will later be almost ubiquitously expressed.

5.4.2 Electrophysiological properties

Gabra5 and Slc8a1 are most strongly expressed in subplate in the cortex throughout development and into adulthood, even though they show additional weaker expression in other cortical layers at later stages. The preferential expression of these two genes in subplate could indicate that Gabra5 and Slc8a1 are involved in defining some of the electrophysiologcial properties of subplate neurons.

Gabra5 is one of 18 identified subunits of the ionotropic GABA-A receptor. Outside of the cortex, Gabra5 is most strongly expressed in the hippocampus where the majority of Gabra5 subunits are localized extrasynaptically[377]. Gabra5 has therefore been suggested to mediate non-synaptic tonic inhibition[378]. However, using electron microscopy, additional Gabra5 subunits have also been found on dendritic synapses[379] and subsequently, Gabra5 has been shown to contribute to synaptic inhibition[380,381]. Although the function of Gabra5 in the cortex has not been studied it is likely that it plays a similar role in subplate as in the hippocampus.

Slc8a1 is a calcium/sodium exchanger and is involved in the control of intracellular calcium levels. Consistent with this fundamental role in cell homeostasis, Slc8a1 is widely expressed in most tissues with particular high levels in the brain, heart and kidney[382]. In the adult rat somatosensory cortex, Slc8a1 has been reported to be most strongly expressed in the deep cortical layers (V, VI and subplate) similar to my findings[383]. In contrast, the Slc8 family member Slc8a2 was evenly expressed in all cortical layers and Slc8a3 was most abundant in the upper layers. The different Slc8 isoforms might differ in their pharmacological kinetics, ligand affinity and regulation and thus confer different properties to the cell populations that differentially express them.

Zdhhc2 is specifically expressed in subplate in the early embryonic cortex, and, outside of cortex in the prethalamus. In the postnatal forebrain, a riboprobe against Zdhhc2 labels mainly the CA1 in the hippocampus, the tRN in the prethalamus and subplate and layers Va and IV in the cortex. Zdhhc2 is a palmitoyl acyltransferase, an enzyme involved in the post-translational modification of proteins. Recently, it has been suggested that Zdhhc2 could be regulating synaptic plasticity by modifying PSD95 and synaptosomal-associated proteins 23 and 25[384,385]. At early embryonic stages, some of the first connections are established within the subplate in the cortex and within the prethalamus[46]. This could explain the specific expression of Zdhhc2 in these two structures at early ages. It has been shown that subplate neurons can undergo long-term plasticity, at least in postnatal animals[114] A role of Zdhhc2 in synaptic plasticity is also consistent with its strong expression in CA1 of the hippocampus. Interestingly, Zdhhc2 remains specifically expressed in the tRN of the prethalamus while it is absent from the thalamus throughout development and in adulthood. Consistently, it has been suggested that the plasticity observed in the thalamic nuclei is mainly mediated via cortical feedback and not established in the thalamic neurons themselves[386]. The expression pattern in the tRN and subplate suggests that the contribution of this cell population to the plasticity in the thalamocortical circuitry should be further elucidated.

5.4.3 Axonal growth and maintenance

The plastin Pls3 starts to be expressed in the subplate around E14 and stays expressed strongest in subplate throughout development with an additional weaker expression in layer V and VI. Pls3 has been shown to be regulating axonal outgrowth and neurite length in motor neurons and neuronal cell lines[351]. It is plausible that Pls3 plays a similar role in cortical projection neurons in subplate and layers V and VI. This proposition is further supported by the finding that Pls3 expression in the embryonic subplate is relatively sparse indicating that only a subset of subplate cells expresses Pls3 at this stage. It would be interesting to analyze whether the Pls3-positive neurons project to different targets (e.g. to the thalamus) than Pls3-negative neurons. Pls3 is still expressed postnatally and in adulthood, when axons have been well established, which suggests that it is not only important in axonal growth but also maintenance. However, not all neurons which establish long-range connections appear to express Pls3, for example neurons in the developing thalamus are Pls3-negative. Inversely, the endopirifom nucleus which does express Pls3, projects to relatively short-range targets in the cortex[387]. It is therefore possible that Pls3 plays additional functions in the forebrain which are different from the role in axonal growth observed in motor neurons.

Cadherin 10 and Cadherin 18 are very strongly expressed in the early embryonic subplate. Cdh10 is not expressed in migrating interneurons as it does not co-localize with Gad67-GFP. Together with the finding that both Cdh10 and Cdh18 are shifted to the superplate in reeler mice, this suggests that Cdh10+ and Cdh18+ cells are postmigratory subplate neurons. Neither of these two cadherins is expressed in the developing thalamus. This does not support the idea that these molecules could directly establish the topography between individual thalamic nuclei and cortical areas through homophilic interactions between afferent and efferent axons. This is also further underlined by the fact both cadherins are expressed throughout the whole anterio-posterior and medio-lateral expanse of the cortex. A thicker band of cells is observed in the E14/E15 anterior and lateral cortex than in the posterior and medial cortex, but this is more likely related to the maturation gradient in the cortex than to topography. At later developmental stages, Cdh10 is most strongly expressed in subplate and layer V and Cdh18 in subplate and layers V and VI. These cell populations all contain neurons projecting extracortically which suggests that these cadherins could play a role in establishing and maintaining long-range connection similar to Pls3. On the other hand, unlike Pls3, Cdh10 and to a lesser extent Cdh18 are expressed in a large number of subplate cells which form a thick band below the cortical plate. This would suggest that these genes are not only expressed in the subset of cells projecting to the thalamus but in most or all subplate neurons. Cadherins could therefore play a role in the more fundamental organization of the cortex by maintaining interactions between cells in the subplate and later in other deep layers.

Unc5c is specifically expressed in subplate at E14.5 and in subplate and the lateral cortical plate at E15.5. At late embryonic and postnatal stages, Unc5c seems to be downregulated and becomes more evenly distributed. Radioactive in situ hybridization data from Gensat, which is considered more quantitative than the colorimetric method used in this study, confirms that Unc5c is expressed in the subplate and the most anteriolateral cortical plate at E15 but is absent from the P7 mouse cortex. Unc5c is a repulsive receptor for the guidance molecule netrin-1, which is strongly expressed in the mantle zone of the internal capsule[41, 42]. Recently, netrin-1 has also been shown to be present in the marginal zone of the cortex where it plays a role in the guidance of migrating interneurons[371]. It is doubtful that Unc5c in the subplate is involved in directly regulating interneuron migration as it does not co-localize with Gad67-GFP. Instead, it seems most probable that Unc5c is involved in regulating the growth of subplate projections through the internal capsule (discussed in more detail in Chapter 6, section 6.3.1).

5.4.4 Other possible functions

Abca8a is a mouse-specific ABC transporter which is postulated to transport lipids. Abca8a has an intriguing expression pattern as it is very specifically expressed in subplate at all examined embryonic stages (E13.5 – E17.5). Postnatally, the expression of Abca8a is shifted to layer V and II/III in restricted areas of the cortex and then is downregulated in adulthood. This pattern suggests that Abca8a is not involved in a general mechanism important to all neurons which its function as a lipid transporter might suggest. Instead, it more likely plays a very specific role important to subplate at embryonic stages and to some layer V and II/III cells at early postnatal stages. Without more precise details on the function of this protein it is difficult to further hypothesize what this function could be.

In the early embryonic brain, Rcan2 is primarily expressed in the marginal zone where it does not co-localize with Gad67-GFP but with reelin (Fig 5_6 B). Together with their morphology and location, this suggests that the Rcan2+ cells in the marginal zone are Cajal-Retzius cells. At late embryonic and postnatal stages, Rcan2 is expressed in subplate which is clearly visible as a labelled band above the white matter. Only 10-15% of Rcan2+ cells in the subplate are GABAergic, which corresponds approximately to two-thirds of the overall proportion of interneurons in the subplate population (15-25%)[388]. In the cortical plate, in contrast, the large majority of Rcan2+ co-express markers for interneurons (~80%) as has been previously reported[350]. Taken together, these findings show that Rcan2 is expressed in at least three different cell populations throughout development: 1) Cajal-Retzius cells; 2) Glutamatergic subplate cells; 3) Cortical interneurons in all layers including subplate. Rcan2 is a regulator of calcineurin, a phosphatase which plays key roles in regulating neurite outgrowth and guidance, neuronal death and synaptic plasticity. As Rcan2 can be involved in the regulation of

such a large number of mechanisms, it is possible that it plays very different roles in the three cell populations identified in this study.

5.5 Conclusion

A time-course of cortical and extracortical expression patterns of 13 subplate-enriched genes has helped to establish more refined hypotheses on the roles of some of these genes in subplate. While some genes are probably involved in the general maturation of cortical neurons (Kcnt2, Sv2b, Csdm3) others might in establish some of the specific electrophysiology properties of subplate (Gabra5, Zdhhc2, Slc8a1). Yet other genes are most likely involved in axonal growth and maintenance (Cdh10, Cdh18, Pls3, Unc5c).

Chapter 6 Function of Cdh10 and Unc5c in the embryonic subplate

6.1 General Introduction

A powerful and direct approach to study gene function is to decrease or completely block the gene of interest which can be achieved at three different levels: gene, transcript and protein. At the gene level, the DNA sequence or parts of it can be deleted from the genome in every cell (knock out) or in a specific cell population and/or at a specific time point (conditional knock-out) by producing transgenic animals. At the transcript level, mRNA can be blocked using RNA interference (e.g. small interfering RNAs, micro RNAs). Finally, levels of functioning proteins can be reduced with blocking antibodies or with pharmacological antagonists [389,390].

Very few studies have looked at gene function specifically in the subplate. This is partially due to the fact that subplate had been studied for a long time in non-rodent species, in particular cats and primates, where genetic technology is not readily available. In addition, even in the mouse, subplate is a difficult cell population to manipulate. So far, no transgenic model has been described which would allow to specifically delete a gene from subplate (i.e. a subplate-specific Cre-line). Moreover, subplate cells are very difficult to transfect due to their early birth-date although successful *in utero* electroporation of subplate cells has been described[192,391]. Finally, the subplate zone is not readily accessible *in vivo* (for example with blocking antibodies or pharmacological agents) due to its deep location in the cortex.

The aim of this chapter is to explore methods to gain some insight into the function of subplate-specific genes. In a first part, I use interfering RNAs against Cdh10 which are introduced into subplate using *in utero* electroporation. In a second part, I block the function of Unc5c with a blocking antibody in an embryonic slice culture system.

6.2 Part I: Cadherin 10

6.2.1 Introduction

Cdh10 is strongly and primarily expressed in the embryonic E14.5 and E15.5 subplate where Cdh10-positive cells form a thick band just below the cortical plate (Fig 4_2f and 5_3). At P8 and adult stages, Cdh10 is still strongly expressed in subplate but with additional expression in layer V (Fig 5_3). Based on this temporal expression pattern, I hypothesize that Cdh10

could have a role in axonal outgrowth and maintenance or alternatively in the general organization of the cortical layering by mediating cohesion between subplate cells (see Chapter 5 section 5.4.3). In order to investigate these hypotheses, I attempted to silence Cdh10 in subplate using RNA interference through small hairpin RNAs (shRNAs).With this method, the silencing constructs are delivered into the cells in form of DNA and subsequently transcribed into RNA. The transcript sequence is designed to loop back onto itself forming double-stranded RNA (dsRNA). This double-stranded sequence is recognized by the nuclease Dicer, which cleaves the dsRNA into 21nt-long small interfering RNA (siRNA). The siRNAs is then incorporated into the RISC nuclease complex which binds mRNA substrates through their complementarity to the siRNA and targets them for degradation[392,393,394].

The main challenge is to deliver the silencing construct into the subplate cells. Two main approaches for tissue transfection have been developed and are widely used - viral transduction or electroporation. Viral transduction can be a very efficient method to deliver DNA constructs but depending on the viral system and constructs it can take many days to achieve stable expression levels[395,396,397]. The very earliest subplate cells could be transfected is at their time of birth (E10.5-E11.5)[54]. As I want to study an effect on subplate at E14/15, this would only allow 3-5 days for transduction and stable expression to take place.

In vitro electroporation followed by slice culture is well established in our laboratory, and *in utero* electroporation has been previously described for subplate cells[192,391]. In contrast to viral transduction, gene expression starts very rapidly within 24h after electroporation. In this method, the DNA construct is most commonly injected into the lateral ventricles and a current is applied to introduce the DNA into the cells lining the ventricle. In order to transfect subplate cells, they therefore have to be electroporated at their time of birth, when they are localized at the ventricular zone[54].

The aim of this subchapter is to explore methods to transfect subplate cells with a silencing construct and to quantify the efficiency of the silencing. Further, I would like to test whether a decrease in Cdh10 expression induces any changes in the organization of the subplate layer and/or the morphology and projections of the subplate neurons.

6.2.2 Methods

Preparation of silencing constructs

Silencing constructs were prepared based on the BLOCK-iT™ shRNA Vector system using the BLOCK-iT™ U6 RNAi Entry Vector Kit (Invitrogen). The following two DNA oligo sequences targeting specifically Cdh10 were designed using the BLOCK-iT™ RNAi Designer (Invitrogen):

shCdh10_1: Top strand: caccggcacatgataagttgcatggcgaaccatgcaacttatcatgtgcc

Bottom strand: aaaaggcacatgataagttgcatggttcgccatgcaacttatcatgtgcc

shCdh10_2: Top strand: caccgcgcctgtgttatgttcaacgcgaacgttgaacataacacaggcgc

Bottom strand: aaaagcgcctgtgttatgttcaacgttcgcgttgaacataacacaggcgc

The sequences were analyzed for their specificity using BLAST and were found not to be homologues to any expressed sequences in the mouse other than Cdh10.

The top and bottom strand DNA oligos were annealed following manufacturer's instruction and the integrity of the annealed double-stranded oligos was confirmed using agarose gel electrophoresis. Chemically competent E.coli bacteria (One Shot® TOP10) were transformed with the vectors using heat-shock at 42°C for 30 sec. Positive transformants were sequenced to confirm the sequence of the oligo DNA insert. A LacZ control construct (included in the kit) was prepared in parallel in the same way.

The two Cdh10 silencing constructs were prepared (1.4μg/μ)l of each construct) as a mixture with eYFP-pCAGGS (0.7μg/μl) in TE with 0.5% fast green. The LacZ control vector (1.4μg/μl) was mixed with DsRed-pCAGGS (0.7μg/μl) in TE with 0.5% fast green. Two different reporter constructs (DsRed and eYFP) were used in order to easily distinguish between embryos transfected with control or Cdh10 silencing plasmids.

In vitro electroporation and slice culture

Time-mated C57/Bl6 mice were killed by cervical dislocation and embryos removed and decapitated at E15.5. Mixtures of DNA vectors were injected into one or both lateral ventricles using a mouth-controlled glass micropipette. Paddle electrodes (3x5mm Genepaddles, Harvard Apparatus) were placed either side of the head for electroporation with 4x100msec pulses of 38V with 100msec intervals (ECM 830 Square Wave Electroporation System, Harvard Apparatus). Half of the embryos of a litter were injected with silencing constructs and the other half with the LacZ control construct. Brains were dissected, embedded in 4% low melting point agarose (Sigma) and sectioned into 300μm slices using a vibrating microtome (Leica VT1000S). Slices were cultured on laminin/poly-L-lysine pre-coated culture inserts over 1.8ml of culture media (20mM 1M D-glucose, 1mM L-glutamine, 100units/ml penicillin, 0.1mg/ml streptomycin, in basal medium eagle and complete HBSS at 2.7:1) in six-well plates at 37°C with 5% CO_2 for 48h. The culture media was replaced once after 24h.

In situ hybridization on electroporated slices

After 48h in culture, electroporated slices were imaged on a fluorescent dissection microscope (Leica Fluo III) and then embedded in O.C.T (Tissue-Tek) and fresh-frozen. Slices were re-sectioned into 16µm sections on a cryostat (Jung CM3000, Leica). Permanent in situ hybridization was performed as described in Chapter 4 (section 4.2.2) using sense and anti-sense probes for Cdh10 and an anti-sense probe for Tbr2 (provided by Navneet Vasistha).

Dissection and RNA extraction

After 48h in culture, eYFP-positive or DsRed-positive ventricular and subventricular zones were dissected from the slices under a fluorescent dissection microscope (Leica Fluo III) using a microknife. Dissected tissues were pooled from at least 10 slices and stored in RNA stabilization solution (RNAlater, Ambion). Three replicates corresponding to slices from three different litters were prepared in this way.

RNA was extracted using TRIzol® (Invitrogen) according to manufacturer's instructions. Briefly, the tissue was homogenized in 1ml of TRIzol® and incubated for 5min at RT. After addition of 0.2 ml chloroform, samples were mixed and centrifuged at 10'000rpm for 15min at 4°C. The RNA was precipitated from the aqueous phase by adding 0.5ml of isopropanol followed by centrifugation at 10'000rpm for 10min at 4°C. The RNA was washed with 75% EtOH, air-dried and resuspended in TE.

The RNA was cleaned using the RNeasy MinElute Cleanup kit (Qiagen) according to manufacturer's instruction and an on-column DNase digestion step was performed.

Quantitative RT-PCR

The same amount of RNA (75ng) from each sample was reverse-transcribed using Superscript III Reverse Transcriptase together with 120ng of random hexamers (Invitrogen) following the manufacturer's instructions. Each reaction was performed in duplicates and pooled and no template controls were prepared in parallel. Primers were designed to amplify an intron-spanning sequence of 134nt of Cdh10 using Roche's Universal ProbeLibrary Assay design centre and Primer3 software:

Forward primer: tctgtggaaccagaaacaggt

Reverse primer: gtggtggttccagacaaacc

The qRT-PCR reaction was performed using 400nM of forward and reverse primers and Power Sybr Green reagent (Applied Biosystems) as detailed in Chapter 3 (section 3.2.6).

Each reaction was performed in triplicates and ran with no-template controls for each primer pair. The house-keeping genes Tbb2c and Actb were included on every qRT-PCR plate. LinRegPCR v11.4 software was used to calculate the starting concentration (N_0) of each sample as explained in section 3.2.6. N_0 values were normalized to the geometric mean of the relative levels of Tbb2c and Actb. Fold-changes were determined by dividing normalized N_0 values of shCdh10:shLacZ for each replicate. The average fold-changes were considered as significant if they were significantly different from 1 by $p < 0.05$ (one-sample two-sided t-test).

In utero electroporation

All experiments were performed by Dr Amanda Cheung in the laboratory of Prof Nobuhiko Yamamoto according to the guidelines laid down by the animal welfare committees of Osaka University and the Japan Neuroscience Society.

Time-pregnant ICR mice at E11.0 were anesthetized with an intraperitoneal injection of sodium pentobarbital (Nembutal, 50mg/kg body weight). Animals were kept warm during surgery and recovery from anaesthesia by placement on a heating pad. The abdomen was cleaned with 70% EtOH and a midline laparotomy was performed. Both uterine horns were exposed and kept moist with warm (37°C) PBS. For visualization of embryos, a flexible fibre cable (Leica) was placed under the uterine horn and the embryo's head was positioned close to the uterine wall by gentle pushing and rolling. DNA mixed with fast green dye was injected into one lateral ventricle via a glass micropipette controlled through a tube attached to a mouth-piece. Paddle electrodes were placed on the outside of the uterine wall on either side of the head for electroporation with 5x 50msec pulses of 25V with 950msec intervals (CUY21, Bex). Six to ten embryos were electroporated in this way and the total surgical time remained shorter than 30 min . The uterus was then placed back into the abdomen with some sterile warm PBS and the surgical incision was sutured.

Tissue preparation and immunohistochemistry

Embryos were collected at E18.5 and transcardially perfused with PBS. Brains were dissected and then assessed for expression of eYFP or DsRed under a fluorescent dissection microscope. Brains were immersion-fixed in 4% PFA over night and cut into 150µm-thick sections on a vibrating microtome (Leica). Sections were blocked with 5% donkey serum in TBS with with 0.1% Triton-X100 for 2h and incubated with anti-GFP 1:500 (A11122, Invitrogen) or anti-DsRed/RFP 1:500 (PM005, MBL) together with anti-Nurr1 1:100 (AF2156, R&D Systems) overnight. Sections were incubated with secondary antibodies – donkey anti-rabbit Alexa488 1:500 (Invitrogen) and donkey anti-goat Alexa568 1:500 (Invitrogen) or donkey anti-rabbit Alexa488 1:500 (Invitrogen) and donkey anti-goat Alexa568 1:500 (Invitrogen) – for 2h at RT and counterstained with DAPI.

Imaging and quantification

Sections were imaged on a single laser line scanning confocal microscope (Zeiss LSM 710). The entire depth and width of the cortical field containing electroporated cells was imaged by collecting z-stacks and tiled images. The confocal pinhole was set to 1.0 airy unit for the red fluorescent emission resulting in 3µm of optical section thickness. On each optical section, the lower boundary of subplate was determined based on Nurr1 labelling and DAPI counterstain. The cortex was divided into five areas: subplate (40µm), gap between subplate and cortical plate (40µm), lower cortical plate (defined by measuring the width of the entire cortical plate on each section and then divided by two), upper cortical plate, marginal zone. All electroporated cells on three sections from each brain were counted.

6.2.3 Results

Silencing of Cdh10 using shRNAs

Silencing constructs against Cdh10 were prepared as detailed above. To test their efficiency in reducing the expression level of Cdh10, an available neuroblastoma cell line (Neuro-2A) was screened for the expression of Cdh10 using RT-PCR. A 500bp-fragment of Cdh10 could not be amplified from these cells indicating that Cdh10 is not expressed in the cell line (data not shown). I next attempted to transfect the silencing constructs into subplate using E11.25 whole-head electroporation and slice culture. Due to the small size of the brain and thinness of the cerebral walls, I did not obtain enough sections of good quality to do further analyses.

In my previous gene expression analysis I found that Cdh10 is not only expressed in the embryonic subplate, but also in the SVZ at E15.5 and E17.5 (Fig 4_2 f, Fig 5_3). I therefore electroporated the silencing construct against Cdh10 at E15.5 and then analyzed its expression and knock-down effect on the cells in the SVZ two days later.

In situ hybridization against the sequence of one of the silencing constructs shows that the shRNA is clearly and strongly expressed (Fig 6_1 a, b). Slices electroporated with GFP construct alone serve as a negative control and appear unlabeled (Fig 6_1 e, f). In situ hybridization against the SVZ marker Tbr2 on adjacent sections indicates that the majority of the silencing construct is expressed in the SVZ (Fig 6_1 d). The strong binding of both sense and anti-sense riboprobes further suggests that that the sequence was successfully processed from double-stranded to single-stranded RNA (Fig 6_1, b, c).

Using qRT-PCR, I found that in the electroporated regions, the silencing construct significantly decreased the levels of Cdh10 by an average of ~30% (n= 3 replicates, p= 0.0074). This knock-down effect appears to be small but this is probably at least partly due to the fact

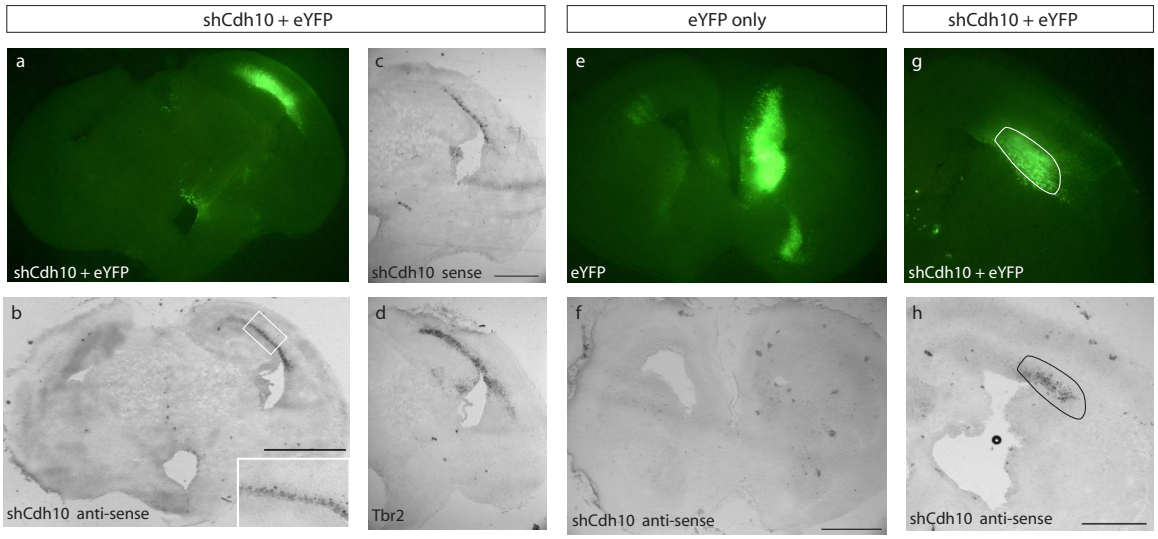

Figure 6_1. **Expression of Cdh10 silencing constructs after whole-head electroporation at E15.5.** a. A slice electroporated with Cdh10 silencing construct (shCdh10) and eYFP after 48h in culture. EYFP is clearly expressed in the lower half of the cortical wall. b. In situ hybridization against shCdh10 on a section from the same slice as shown in a. The shRNA against Chd10 is strongly expressed in the ventricular and subventricular zones (see Tbr2 expression in d) c. In situ hybridization against the complementary (sense) strand of the shRNA on an adjacent section. The sense RNA is expressed in the same location as shCdh10 indicating that the silencing construct was correctly processed into single-stranded RNA. d. In situ hybridization against Tbr2, a marker of the subventricular zone, on an adjacent section. e. A control slice electroporated with eYFP alone after 48h in culture. f. In situ hybridization against shCd10 on a section from the same slice as shown in e. No signal is detectable on the control section confirming the specificity of the RNA probe used. g. Subventricular and ventricular zones electroporated with shCdh10 and eYFP. The white outline delineates the boundary of the eYFP-positive tissue. Electroporated samples were microdissected along this boundary for qRT-PCR. h. In situ hybridization against shCdh10 on a section from the same area as shown g. The Cdh10 silencing construct is only expressed in a subset of cells within the boundary of the eYFP-positive tissue defined in g. Scalebars: 500μm.

that it was assessed on a relatively heterogeneous population of VZ and SVZ cells (see also Discussion).

In utero electroporation of shCdh10

The silencing constructs were electroporated *in utero* into E11.0 embryos by Dr Amanda Cheung and the embryos were harvested at E18.5. In total, 47 embryos in a total of 6 litters were electroporated, 10 with a LacZ control and DsRed constructs and 37 with the silencing constructs against Cdh10 and eYFP. A total of 20 embryos from 3 litters survived the electroporation and the surgery until E18.5. However, the electroporation success rate in the surviving embryos was extremely low - only one embryo was successfully electroporated with the LacZ control and two embryos with the Cdh10 silencing construct. In addition, a relatively small number of cells were transfected in each brain (approximately 50 cells per 150μm-thick cortical section).

Effect of shCdh10 on cell location and morphology

The distribution of all electroporated cells within the cortex was analyzed at E18.5. Using immunohistochemistry against Nurr1, I defined subplate as a 40µm thick band above the white matter on each section. In the control brain, almost 50% of electroporated cells were within subplate (Fig 6_2 a,i). In the brains electroporated with the Cdh10 silencing construct, an average of 15% of electroporated cells was found in the subplate zone (9.6% in brain 1 and 20.9% in brain 2) (Fig 6_2 e, i). This very preliminary finding could indicate that Cdh10 plays a role keeping the cohesion between subplate cells and thus organizing subplate into a distinct layer. However, many more experiments would be needed to corroborate this suggestion.

I also studied the cell morphology of the electroporated subplate cells. Even though immunohistochemistry against eYFP and DsRed was used, neurites were only visible for a small subset of electroporated subplate cells (examples are shown in Fig 6_2 b-d, f-h). Both for subplate cells electroporated with the control and with the silencing constructs, I found neurites extending towards the midline (Fig 6-2 b, c, f, g) and away from the midline (Fig 6_2 d, h).

6.2.4 Discussion

Efficiency of the shCdh10 silencing construct

The efficiency of the silencing construct was tested using whole-head electroporation and slice culture followed by qRT-PCR on the dissected ventricular zones. The reduction of the Cdh10 expression was tested in the E15.5 ventricular zones because these were more readily accessible than subplate even though Cdh10 expression appears stronger and more localized in subplate (Fig 4_2 f). Using this method, I found that the shRNAs significantly decreased expression of Chd10 by an average of 30%. This effect appears small but can partially be explained by the heterogeneity of the system used. The zones of electroporated cells were manually dissected as a whole piece of tissue based on the expression pattern of eYFP. Fig 6_1 shows, however, that within the boundaries of the eYFP-positive tissue, only a proportion (an estimated one-third to one-half) of cells expresses the silencing construct (Fig 6_1 g and h). It is therefore very likely that the effect on Cdh10 levels in an individual cell expressing the silencing construct would be much greater than the 30% reduction measured across the heterogeneous population.

Fluorescent-activated cell sorting could be used to obtain purer populations of electroporated cells and corroborate the silencing effect of the shRNA constructs. Alternatively, additional

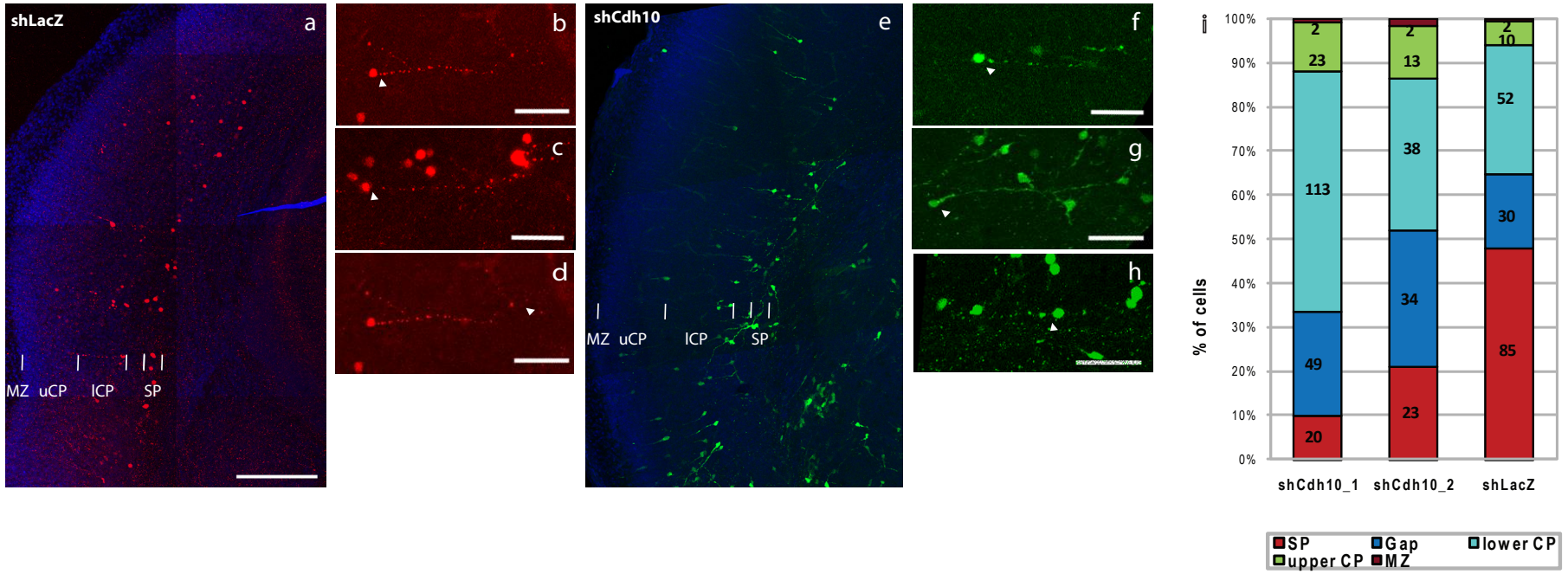

Figure 6_2. **Location and morphology of cells electroporated with control or Cdh10 silencing constructs at E11.0 in utero.** a. Section of an E18.5 brain after electroporation with LacZ control and DsRed. About half of the DsRed-positive cells (red) are localized in the subplate (SP). b-d. Examples of DsRed-positive cells within the SP zone. Electroporated cells have neurites extending towards the midline (b, c) and away from the midline (d). e. Section of an E18.5 brain after electroporation with Cdh10 silencing construct and eYFP. EYFP-positive cells are relatively widespread and only a small proportion is located within the SP. f-h. Examples of eYFP-positive cells within the SP zone. Cells electroporated with shCdh10 have similar morphologies as controls (b-d) with neurites extending towards (f, g) and away (h) from the midline. i. Numbers and proportion of electroporated cells localized in the different cortical compartments. In the two brains electroporated with Cdh10 silencing constructs (shCdh10_1 and shCdh10_2), 10% and 20% of electroporated cells are localized within the SP, respectively. In contrast, in the brain electroporated with a LacZ control construct (shLacZ), nearly 50% of electroporated cells are found within the SP. Scale-bars: 200µm (a, e), 50µm (b-d; f-h). MZ: marginal zone; uCP: upper CP; lCP: lower cortical plate.

cell lines could be screened for the expression of Cdh10 or a cell line could be stably transfected with a Cdh10 expression construct. A cell line expressing Cdh10 would provide a more homogeneous system to evaluate the effect of the silencing constructs.

Technical challenges in delivering the silencing construct to the embryonic subplate

Subplate neurons are very difficult to electroporate because of their very early birth-date between E10.5 and E11.5. I did not succeed in obtaining enough slices of electroporated E11.25 cortices with good morphology for culture. In addition, as Cdh10 is only expressed at later stages of development, a relatively long culture period of at least 4 days would be necessary. It is doubtful that all developmental processes taking place between E11 and E15 *in vivo* would be faithfully recapitulated in a culture system. It has been shown that in embryonic slice cultures, the rate of cell proliferation is decreased and neuronal migration ceases after some days[398]. On the other hand, in a recent study using E12.5 slice cultures, the splitting of the preplate and the formation of a cortical plate occurred similarly as *in vivo*[399]. This suggests that some but not all aspects of the early cortical development can be modelled in slice cultures.

Due to the technical challenges and limitations of the slice culture method, Dr Cheung tried to electroporate subplate cells *in utero* at E11.0. *In utero* electroporation of subplate cells has been successfully performed in the past by others[192,391]. However, due to the very small size of the embryos and the relative thickness of the uterine wall, this method is very challenging at this early stage. Although all mothers survived the surgery, the death and re-absorption rate of the embryos was high (approximately 50%). In addition, in embryos that survived until E18.5, the electroporation rate was very low with only 3 embryos successfully electroporated from a total of 20 surviving embryos. Further optimization of the electroporation parameters such as plasmid concentration, size and type of electrodes and voltage, number and duration of the electric pulses would be necessary in order to get more consistent expression.

Preliminary results on cell location and morphology

In the cortex electroporated with the control construct, approximately half of the transfected cells were localized within the subplate. In contrast, in the two cortices electroporated with the silencing constructs, only 10-20% of transfected cells were in the subplate zone. In both cases, the remaining cells were primarily found between subplate and the cortical plate or within the lower half of the cortical plate. This preliminary result supports the hypothesis that Cdh10 could mediate adhesion between subplate cells and thus organize these cells into a tightly packed layer. In the absence of Cdh10, subplate cells might be displaced by tangentially and radially migrating neurons and disperse within the overlying cortical plate. Indeed,

mediating cell-cell adhesion is the most fundamental function of cadherins and a role in cortical layer formation has been proposed for cadherins both in mouse[400] and ferret[401].

A very basic qualitative analysis of the cell morphology of electroporated subplate cells did not reveal any differences between control cells and cells transfected with the Cdh10 silencing construct. In both cases, I found subplate cells with neurites extending towards the midline and other cells with neurites extending away from the midline. This finding does not suggest a role of Cdh10 in the development of axons of subplate neurons. A more extensive or quantitative analysis of electroporated cells was not possible at this stage as only very few subplate cells were sufficiently labelled to visualize neurites even though immunohistochemistry was used to increase the signal of fluorescent markers. Tracing from different projection sites of subplate (e.g. internal capsule, corpus callosum, cortical plate) following *in utero* electroporation could help to analyze whether a decrease of Cdh10 alters subplate cell projections and/or morphology.

The results on cell location and morphology presented here are promising, but they have to be considered as very preliminary and many further experiments would be needed to corroborate these findings. First of all, all the analyses were only performed on three cortices, one electroporated with the control construct and two with the silencing constructs. It is likely that there is a relatively large variability in the location and size of the portion of the VZ which will be electroporated with our method. Many parameters such as plasmid concentration and volume and electric pulse strength, length and number were tightly controlled. However, other factors are more difficult to regulate including the diffusion of the injected plasmid within the ventricles or the exact position and angle of the electrodes relative to the embryonic brain.

Cortical development proceeds along an anterio-lateral to posterio-medial gradient with a 1-2 days delay of the later[185]. It is therefore conceivable that an electroporation at E11.0 targeting the most anterior portion of the ventricular zone leads to the transfection of mainly layer VI cells while an electroporation directed at the most posterior VZ would primarily transfect subplate cells. I did not find any obvious bias in the anterior-posterior or medial-lateral position of the electroporated cells in the three analyzed brains indicating that the observed differences are not caused by different electroporation sites. In addition, I counted electroporated cells on three 150 um-thick sections from each brain and thus in relatively large anterio-posterior expanse. Nevertheless, a larger number of successfully electroporated brains would allow to only quantifying cells in a defined cortical area (e.g. future somatosensory cortex) which would decrease the variability due to differences in development between areas.

Secondly, in order to be able to distinguish between control and silenced brains, two different

fluorescent marker plasmids were co-transfected with the control (DsRed) and silencing constructs (eYFP), respectively. Although these two constructs are based on the same DNA backbone, they still might differ in their transfection efficiencies or expression dynamics. In addition, immunohistochemistry with an anti-DsRed and anti-GFP antibody was used to increase the signal of the fluorescent markers. Again, the two primary antibodies as well as the secondary antibodies likely have different binding properties and fluorescent strength resulting in different numbers of neurons labeled. This might present a particular problem when analyzing the cell morphologies as different amounts of detail might be visible with the different antibodies. To prevent variability due to different fluorescent markers, it would have been preferable to use the same marker (e.g. eYFP) for both control and silencing conditions. In order to distinguish between the two, a second fluorescent marker (DsRed) could have been added in one case but not the other.

Finally, shRNAs can have non-specific effects which can mask or exaggerate the effect of the silencing of the gene of interest. First of all, off-target genes can be silenced due to partial homologies with the target sequence. It is debated how similar the sequences have to be in order for off-target silencing to occur, but a recent study has shown that as few as seven identical nucleotides can trigger down-regulation[402]. The silencing constructs against Cdh10 were therefore carefully designed and no homologous sequences were found using the Basic Local Alignment Search Tool (BLAST).

Secondly, at least certain shRNA sequences are able to trigger a cellular immune response through cytoplasmic RNA sensing receptors and activation of the interferon pathway[403,404]. These pathways most likely constitute part of the cell's protective mechanism against exogenous, usually viral, RNA. Activation of the cellular immune response by shRNAs has been shown to lead to cytotoxic cell death in cultured cortical neurons[405] and retraction of synapses and dendritic spines in hippocampal pyramidal neurons[406]. Finally, as shRNAs are processed in the same way as endogenous micro RNAs (miRNAs), their expression at high levels can lead to a saturation of the miRNA processing system. A recent study has shown that long-term high-level expression of certain shRNAs in the liver led to a downregulation of endogenous miRNAs and subsequent cell death[407]. Using DAPI counterstain to label cell nuclei, I did not notice any signs of necrosis or apoptosis in the electroporated cells but cell death should be more specifically assessed, e.g. by using TUNEL.

A shRNA against the bacterial gene LacZ was used as a control construct in this study. However, further controls for non-target effects will be necessary as these are mostly sequence-dependant. A rescue experiment where overexpression of a shRNA- resistant version of Cdh10 reverses the effect of the shRNA could give assurance that the observed changes are due to the silencing of Cdh10 alone.

6.3 Part II: Unc5c

6.3.1 Introduction

Unc5c is one of several identified receptors for the guidance molecule netrin-1[408] and is specifically and transiently expressed in the subplate of E14.5 and E15.5 cortices (Fig 4_2l, Fig 5_3, Fig 6_3 b). Other known netrin-1 receptors include Dcc (deleted in colorectal cancer), Neo1 (neogenin 1) and the Unc5 homologues Unc5a, Unc5b and Unc5d[409,410]. Dcc and Neo1 mediate chemoattraction while Unc5 homologues (upon heterodimerization with Dcc) mediate chemorepulsion from a source of netrin-1[410,411]. In the embryonic forebrain, netrin-1 is most prominently expressed in the mantle zone of the internal capsule and in the ventricular zone of the ganglionic eminences (especially the LGE)[368,42]. Additional netrin-1 expression can be found in the developing hippocampus and in the medial thalamus and hypothalamus[41,42]. A recent study has also reported the presence of netrin-1 proteins in the early embryonic marginal zone[371] (Fig 6_3 c, d).

Netrin-1 in the basal forebrain is involved in the guidance of corticofugal axons[368] and thalamocortical afferents[41,42]. In co-culture experiments, explants from the LGE had a strong growth-promoting and attractive effect on axons from E12.5 and E13.5 cortical explants. Recombinant netrin-1 protein or aggregated cells secreting netrin-1 produced a similar effect while blocking of netrin-1 with an antibody abolished the effect of the LGE[368]. These findings indicate that netrin-1 promotes the growth of cortical axons from the early embryonic cortex (E12.5 and E13.5) and contributes to their guidance through chemoattraction.

Similarly, co-cultures of thalamic explants with explants from the floor plate of the spinal cord (a source of high levels of netrin-1) showed a growth-promoting and attractive effect on thalamic axons which was abolished by netrin-1 blocking antibodies[41]. A study by Powell et al. subsequently expanded on these results[42] and found corresponding gradients of netrin-1 and netrin-1 receptors in the internal capsule and the thalamus, respectively. Netrin-1 in the internal capsule is expressed in an anterior-high to posterior-low gradient which is matched by a high expression of Dcc in the anterio-medial thalamus. Inversely, Unc5 homologues are highly expressed in the posterio-lateral thalamus. Consistently with these expression patterns, netrin-1 expressing cells had a strong attractive effect on axons from the anterior thalamus and a moderately repulsive effect on axons from the posterior thalamus. Antibody-blocking of Dcc or Unc5a/c in cultures shifted the outgrowth of anterior thalamic axons more posteriorly and of posterior axons more anteriorly, respectively[42]. Similarly, netrin-1 knock-out mice showed a profound disruption of the topography of thalamocortical axons at the PSPB. Together, these findings demonstrate that matching gradients of netrin-1 in the internal capsule and netrin-1 receptors in the thalamus contribute to the establishment of the early

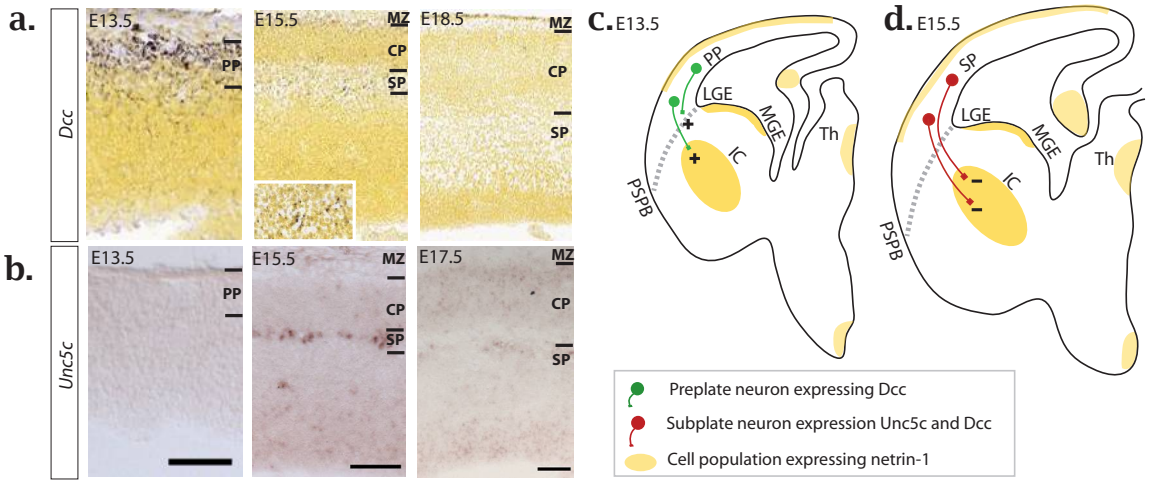

Figure 6_3. **Hypothesis on the role of netrin-1 in regulating the growth of corticothalamic subplate axons.** a. In situ hybridization signals for the netrin-1 receptor Dcc. Images are taken from AllenBrainAtlas. At E13.5, Dcc is strongly expressed in the preplate (PP) and at E15.5, weak expression is found in the subplate (SP) and in the marginal zone (MZ). At E18.5, Dcc is no longer expressed in the cortex. b. In situ hybridization signals for the netrin-1 receptor Unc5c. At E13.5, Unc5c is not expressed in the cortex while at E15.5 strongly labeled cells are found in the SP. At E17.5, Unc5c expression appears weak and uniform in the SP and cortical plate (CP). Scalebars: 100µm. c, d. Schema illustrating how netrin-1 could regulate the guidance of corticofugal SP neurons through the internal capsule (IC). Drawings depict coronal sections through the E13.5 (c) and E15.5 (d) brain. Netrin-1 (yellow) is expressed in the mantle zone of the IC, the ventricular zones of the medial and lateral ganglionic eminences (MGE and LGE), the hippocampus, marginal zone, hypothalamus and thalamus. At E13.5, corticofugal neurons in the PP express Dcc but not Unc5c (green) and axons are attracted towards netrin-1 in the IC. At E15.5, corticofugal neurons now localized in the SP express both Dcc and Unc5c (red). Netrin-1 now has a repulsive effect on corticofugal axons and their growth through the IC is temporarily arrested. PSPB: pallial-subpallial boundary; Th: thalamus.

topography of thalamic projections.

Public gene expression data and my own in situ hybridizations suggest that at E13.5 the subplate expresses Dcc but none of the other netrin-1 receptors (Fig 6_3 a, b). At E14.5 and E15.5, Unc5c is strongly expressed in the subplate and Dcc weakly without any apparent anterior-posterior gradient (Fig 6_3 a,b; Fig 4_2 l). At later developmental stages, the expression of Unc5c and Dcc appears to be downregulated in subplate (Fig 6_3 a, b). This temporal expression profile suggests that netrin-1 would first have an attractive effect on subplate cells or subplate neurites (at E13.5) followed by a repulsive effect (at E14.5/E15.5) and maybe later lose its effect completely. A very similar time-frame has been suggested for the growth of corticofugal axons from the subplate[73,72]. Corticofugal axons have been described to outgrow from subplate in the preplate stage and reach the internal capsule by E13[63,55,72]. Within the internal capsule, they slow down and "wait" for approximately two days before continuing towards the thalamus[72]. The very similar time-frames of Unc5c expression and axonal growth from subplate suggest that Unc5c and netrin-1 could play a role in mediating the

waiting period of corticofugal axons within the internal capsule (Fig 6_3 c, d).A similar role for Unc5c and netrin-1 has been described in the spinal cord, where they regulate the waiting period of primary sensory axons from the dorsal root ganglion[412].

The aim of this subchapter is to explore methods to study the growth and waiting period corticofugal subplate axons in the internal capsule and to gain some insight into whether Unc5c is involved in regulating this behaviour.

6.3.2 Methods

Carbocyanine dye tracing

Embryonic E13.5 (n=5) and E14.5 brains (n = 9) were postfixed in PFA 4% and embedded in agarose. The corticothalamic pathway at the level of the internal capsule was exposed by a cut at a 45° angle to the coronal and sagittal planes (see [413]). Small crystals of the carbocyanine dye DiI (1,1'-didodecyl-3,3,3',3'-tetra-methylindocarbocyanine perchlorate) were placed under visual guidance into the lateral cortex (2 brains at E13.5, 6 brains at E14.5) or the internal capsule (3 brains at each age). Sections were incubated at RT for 10 days. Following the incubation, the brains were re-embedded in agarose and sectioned to 70µm on a vibrating microtome (Leica VT1000S).

Thalamocortical slice cultures

Time-mated Golli-tau-eGFP mice were killed by cervical dislocation and embryos removed and decapitated at E14.5. A total of 23 brains from 3 litters were used. Brains were dissected under aseptic conditions and embedded in 4% low melting point agarose (Sigma). Brains were sectioned into 300µm thalamocortical slices at a 45° angle[413] using a vibrating microtome (Leica VT1000S). Slices were placed on laminin/poly-L-lysine pre-coated culture inserts over 1.8ml of culture media (20mM 1M D-glucose, 1mM L-glutamine, 100units/ml penicillin, 0.1mg/ml streptomycin, in basal medium eagle and complete HBSS at 2.7:1) in six-well plates at 37°C with 5% CO_2. After 1h, the culture media was replaced with either anti-Unc5a/c blocking antibody 5µg/ml (anti-rat Unc5H1, goat IgG, AF1405, R&D Systems) or control goat IgG 5µg/ml (AB-108-C, R&D Systems) in culture media. Slices were cultured for 24h.

Analysis of axonal growth

After 24h in culture, slices were fixed in PFA 4% overnight and counterstained with DAPI. Slices were imaged on a single laser line scanning confocal microscope (Zeiss LSM 710).

The entire depth of the corticothalamic fibre front was imaged by collecting z-stacks (~200-250μm total thickness). For analysis, the slice with the most advanced front of the corticofugal fibre tract from each brain was chosen. Slices from four brains were excluded as they were either damaged or appeared to be cut at a wrong angle resulting in 9 control slices and 10 slices blocked with Unc5a/c antibody. The fibre length on each slice was measured as the distance between the fibre front and lateral cortical plate at the level of the PSPB (see Fig 6_5). Two statistical tests were performed: 1) The average fibre length of all control sections and all blocked sections was compared using a unpaired, one-tailed t-test; 2) The fibre length of each blocked section was divided by the average fibre length of the control slices from the same litter. The average relative fibre length was compared to 1 using an one-sample, one-tailed t-test.

6.3.3 Results

Timing of corticothalamic axon growth

In order to establish a more detailed time-frame for corticothalamic axon growth in the early embryonic brain, fibres were traced retrogradely from the internal capsule and anterogradely from the lateral cortex using small crystals of DiI, a fluorescent lipholic carbocyanine dye which diffuses along cell membranes (Fig 6_4 A-D). After placements of DiI into the middle portion of the internal capsule at E13.5, backlabelled cells were visible in the subplate and marginal zone of the lateral cortex (Fig 6_4 a'). At E14.5, similar placements backlabelled cells in the subplate over a large expanse of the dorsolateral cortex (Fig 6_4, b'). Inversely, crystals placed into the lateral cortical wall at E13.5 labelled a bundle of corticofugal axons which had reached the middle portion of the internal capsule (Fig 6_4 c', c"). At E14.5, these corticofugal axons did not appear to have progressed further inside the internal capsule than at E13.5 (Fig 6_4 d', d"). However, at this age, DiI placed in the lateral cortical wall already backlabelled some thalamocortical fibres (Fig 6_4 d', d"). These were much less numerous and formed a thin bundle of fibres that could be traced to backlabelled cells in dorsal thalamus (Inset in d"). This indicates that after E13.5, DiI tracings will be of limited use to study corticothalamic axon growth as it will become impossible to distinguish them from thalamaocortical fibres. Therefore, I decided to use the Golli-tau-eGFP transgenic mouse model for further studies. In these animals, eGFP is expressed in the cell bodies and neurites (including corticofugal axons) of subplate and layer VI cells but not in the thalamus[72]. Additional structures and fibre systems such as the amygdala and stria terminalis (Fig 6_4 e') or the hippocampus and fornix express eGFP but these can be readily distinguished from the corticofugal fibre tract. Similar as with the DiI tracing and in agreement with a previous report[72], I found that at E14.5 eGFP-positive corticothalamic fibre front has reached the middle portion of

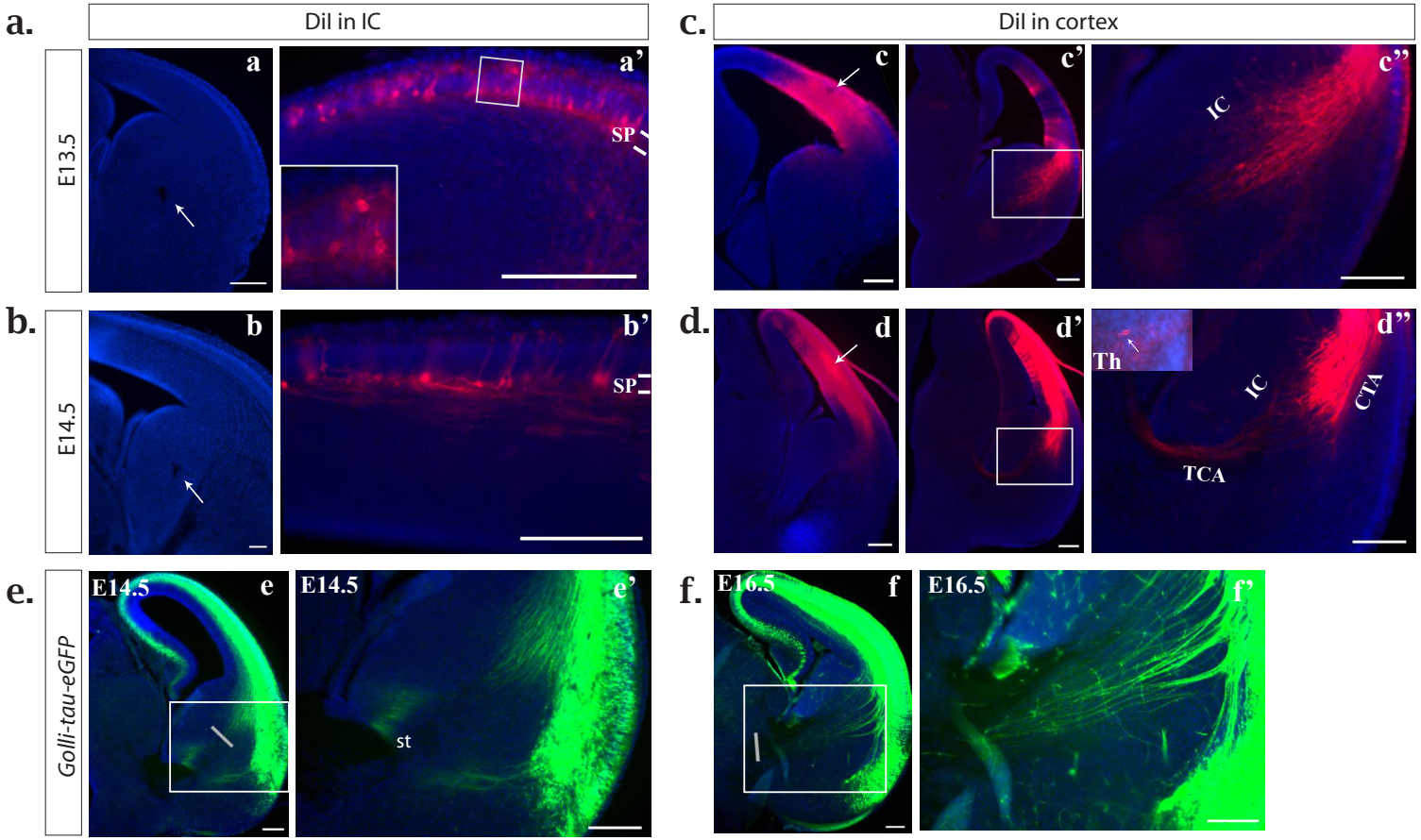

Figure 6_4. **Growth of corticothalamic axons through the internal capsule.** The progression of corticothalamic axons (CTA) through the embryonic forebrain was analyzed with DiI tracing from the internal capsule (IC; A,B) and the cortex (C, D) and in the Golli-tau-eGFP mouse where CTAs express eGFP (E, F). A. At E13.5, DiI placement in the middle portion of the IC (arrow in a) labels cells in the subplate (SP) and marginal zone of the lateral cortex (a'). B. At E14.5, the same DiI placement as in A (arrow in b) labels a large number of SP cells in the lateral and dorsolateral cortex (b'). C. DiI placement in the E13.5 dorsolateral cortex (arrow in c) labels CTAs which have reached the middle portion of the IC (c', c"). D. At E14.5, the same DiI placement as in C (arrow in d) labels both a bundle of CTAs and a bundle of thalamocortical afferents (TCA) in the IC. The insert shows a backlabeled neuron in the thalamus (Th). At E14.5 the CTAs have not progressed further inside the IC as at E13.5 (compare c', c" and d', d"). E. At E14.5, Golli-tau-eGFP-positive CTAs are within the middle portion of the IC (e, e'). F. At E16.5, Golli-tau-eGFP-positive CTAs have passed through the IC and have arrived at the border of the Th (f, f'). Light grey bars in e and f delineate the fiber front. Scalebars: 200μm. St: stria terminalis.

the internal capsule (Fig 6_4 e, e'). In contrast, by E16.5, corticofugal fibres had completely traversed the internal capsule and at least some had reached the border of the thalamus (Fig 6_4 f, f').

Together with previous findings[72], these experiments indicate the following time-course for corticothalamic axon growth: At E13.5, corticothalamic afferents have already reached deep into the internal capsule where they remain until at least E14.5 but probably E15.5 indicating a waiting period of about 48h. By E16.5, the fibres have crossed the internal capsule and have arrived at the DTB. The consistency between results of the DiI tracing and the Golli-tau-eGFP mouse further confirm that the later is a useful model to study corticothalamic axon growth.

Blocking of Unc5a/c receptors in thalamocortical slice cultures

To test whether Unc5c receptors are involved in regulating the waiting period of corticothalamic axons, thalamocortical slices of E14.5 Golli-tau-eGFP brains were cultured with a control IgG (Fig 6_5 a) or anti-Unc5a/c blocking antibody (Fig 6_5 b) for 24h. A qualitative analysis did not suggest that blocking of Unc5a/c receptors had an effect on the position of the fibre front as in both control and blocked slices fibres remained within the middle portion of the internal capsule (Fig 6_5). No fibres were found to have progressed towards the ventral part of the internal capsule or to have reached the DTB.

In addition, the length of the corticothalamic fibres in the internal capsule after culture was measured. Again, I did not find any significant difference in the fibre length between control slices (average fibre length = 299 µm ± 54; n = 9 slices) and slices blocked with antibody (322 µm ± 40; n = 10 slices) ($p = 0.24$). This remained true when only slices from the same litter were compared ($p = 0.20$).

6.3.4 Discussion

Methodological considerations and future experiments

To test the hypothesis that Unc5c is involved in regulating the waiting period of subplate corticofugal axons in the internal capsule, Unc5c receptors were inhibited in thalamocortical slices of Golli-tau-eGFP brains using a blocking antibody. This approach has several limitations that should be addressed in future experiments. First of all, the precise time-course of corticothalamic fibre growth in the culture system remains to be established. *In vivo*, Golli-tau-eGFP-positive fibres progress from within the internal capsule at E14.5 to the DTB at E16.5 (Fig 6_4 E, F). However, whether this growing pattern is recapitulated in culture, and fibres will make the same progress over 48h remains to be confirmed. Work by others on

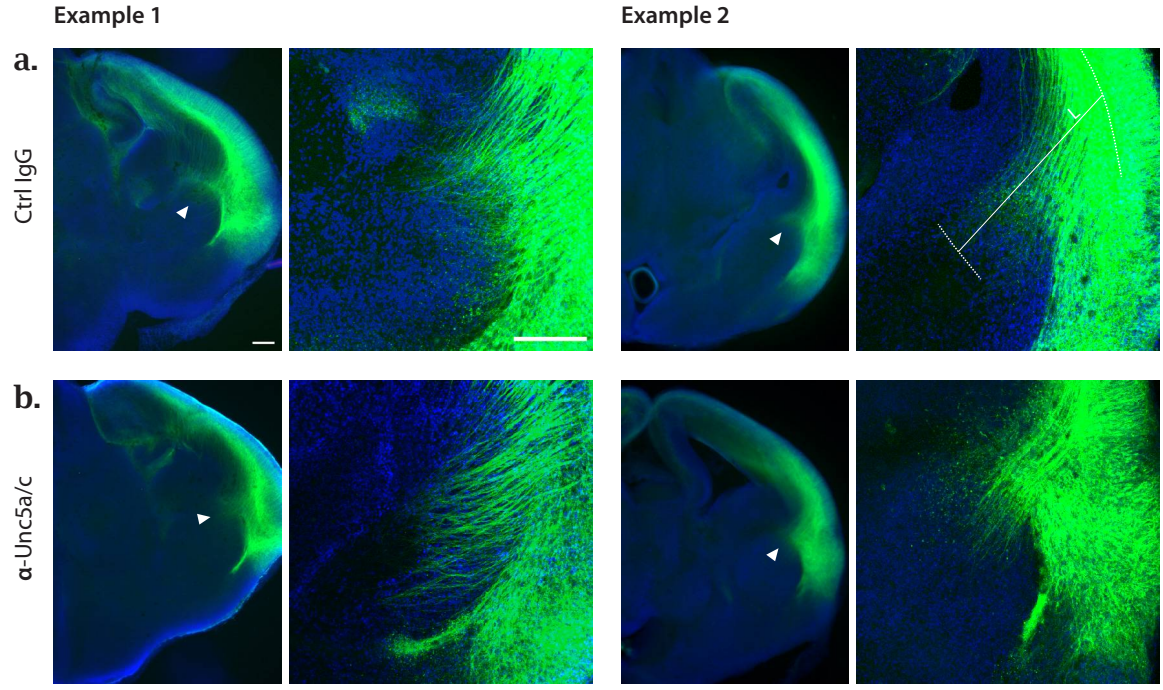

Figure 6_5. **Blocking of Unc5c receptors in E14.5 thalamocortical slice cultures.** Thalamocortical slices from E14.5 Golli-tau-eGFP brains were cultured for 24h either in the presence of a control IgG (a) or an anti-Unc5a/c blocking antibody (b). Two slices from two different brains are shown for each condition. In both control and blocked slices, the eGFP-positive corticofugal fiber front remained within the middle portion of the internal capsule (arrowheads). No fibers were found in the ventral internal capsule or at the border with the thalamus. Fiber length (L) was measured as indicated in a. Scalebars: 200µm.

similar culture systems, however, suggests that this is the case[52]. In addition, it is crucial to choose the correct angle for the thalamocortical slices in order to avoid severing the growing axon bundles. I have used a 45° cutting angle as this plane has been previously described to preserve the embryonic thalamocortical connections, even though these studies were done in slightly older brains (E18 mice and E16 rats)[413,79]. Slight differences in the cutting angle and the anterior-posterior position of the slices might explain at least in parts the variability in fibre length observed between slices (relative standard deviation of ~15%). Further testing of different angles might be necessary to determine the best cutting plane. After optimizing these parameters, further culture experiments with longer incubation times or slices from younger (E13.5) or older (E15.5) brains could complete the experiments presented here.

Secondly, the efficiency of the Unc5a/c antibody to block Unc5c receptors in the subplate has not been determined. The same antibody (at half the concentration) has shown a strong effect on the topography of thalamocortical axons in a co-culture system[42]. However, the antibody is known to have a three-time higher affinity to bind Unc5a than Unc5c receptors[42].

As thalamic axons express both Unc5a and Unc5c, it is possible that the observed effect is mostly mediated by the blocking of Unc5a and not Unc5c receptors. A higher antibody concentration might be necessary to block Unc5c receptors efficiently; however, this has to be balanced with the increasing costs of the experiment.

In parallel to manipulating Unc5c receptors, it would be interesting to directly test the effect of netrin-1 on subplate axons. A previous study has shown a strong growth-promoting and attractive effect on axons from E12.5 and E13.5 cortical explants. As Unc5c is not expressed in the cortex at E13.5 but in subplate cells at E14.5/E15.5 (Fig 5_3 and 6_3b), I would expect the effect of netrin-1 to switch from growth promoting and attracting at E12.5/E13.5 to inhibiting and repulsive at E14.5/E15.5. A simple experiment using beads soaked with recombinant netrin-1 or explants from the spinal cord floor plate with cortical explants from the Golli-tau-eGFP brain at different ages should allow verifying this prediction.

In addition, analysis of the corticothalamic fibres in E14.5 or E15.5 Unc5c knock-out brains[352] could help to further assess whether the receptor is involved in regulating the waiting period. However, Unc5c is very likely involved in the early growth and guidance of thalamocortical axons [42]. As thalamocortical fibres guide corticothalamic axons through the ventral telencephalon[176,52], it will be difficult to distinguish a direct effect of Unc5c loss on corticothalamic axons from an indirect effect on the thalamocortical fibre scaffold. This issue could be addressed using a co-culture system of Unc5c KO cortex and wild-type thalamus. It is also possible that Unc5c and netrin-1 mediate the waiting period together with other signalling systems (e.g. semaphorins)[52] and that downregulation of Unc5c is compensated by other receptors.

Alternative roles for Unc5c in the subplate

Although the temporal expression pattern of Unc5c correlates well with a role in the regulation of the waiting period of corticofugal axons, it is entirely possible that this gene is involved in a different function. Netrin-1 and netrin-1 receptors have been shown to establish the topography of thalamocortical connections through matching gradients in the internal capsule and the thalamus, respectively[42]. Both my own in situ hybridization data (Fig 4_2 l) and images from Gensat do not show an anterior-posterior gradient in Unc5c expression in the subplate. However, a more detailed analysis of the spatiotemporal expression of all netrin-1 receptors (Dcc, Neo1 and Unc5a-d) in the cortex should be performed to investigate this further.

Netrin-1 has recently been shown to regulate interneuron migration in the marginal zone through interaction with α3β1 integrin[371]. As subplate is one of the three compartments of tangential interneuron migration[93], it is possible that netrin-1 and Unc5c play a similar role in this zone. However, I have shown that Unc5c does not co-localize with Gad67-GFP, which

is expressed in 90% of cortical interneurons (Fig 5_5 e-h), suggesting that a direct role in interneuron migration is not very likely.

Finally, netrin-1 receptors, including Dcc and Unc5 homologues, are "dependence receptors", i.e. they induce cell death in the absence of their ligand[414,415]. In the developing brainstem and cerebellum of netrin-1 knock-out mice, apoptosis was significantly increased in Unc5a-, Unc5b- and Dcc-expressing cells[415]. Similarly, a recent study has shown that netrin-4 promotes cell survival in layer IV neurons of the primary sensory areas through Unc5d signaling[416]. It is therefore conceivable that Und5c is involved in regulating cell death and survival of subplate neurons. Quantification of subplate cell numbers in Unc5c- and/or netrin-1 knock-out mice could address this hypothesis.

6.4 General conclusion

Due to their early birth-date and deep location in the cortex and the absence of specific transgenic models, the murine subplate cells are a difficult population to manipulate. In this chapter, I have explored different approaches to change the expression levels or block the function of two subplate-specific genes - Cdh10 and Unc5c. After further optimization, *in utero* electroporation of gene silencing or expression constructs into subplate cells will be a useful technique to explore molecular mechanisms underlying subplate function. Initial results using shRNAs against Cdh10 suggest that this gene could be involved in organizing subplate into a distinct layer. Specific aspects of subplate development such as the establishment of thalamocortical connectivity can be effectively studied in a culture system. In this context, the Golli-tau-eGFP mouse is a useful model as corticofugal axons are strongly and specifically expressing GFP. Finally, these approaches can be completed with the analysis of transgenic animals. The identification of subplate-specific molecular markers will allow the generation of a subplate-specific *Cre* line which will constitute a very powerful tool to explore gene function in these cells.

Chapter 7 Comparison of subplate-specific genes between mouse and rat

7.1 Introduction

Gene expression analyses using microarrays at different developmental stages have led to the identification of a number of genes which are specifically expressed in the mouse subplate. The mouse (*Mus musculus*) is one of the most widely used model organisms, primarily because of the relative similarity to human, the fast breeding and the availability of gene manipulation technologies. The other commonly used rodent model species is the rat (*Rattus norvegicus*). Rats have been the prevailing model organism for pharmacological and toxicological studies and many disease models have been established in rats. Thorough physiological information is available on rats and the larger size of their organs makes them easier to manipulate, especially at very young ages. In addition, they have been the preferred species for behavioural and *in vivo* physiological studies such as recordings in freely moving animals.

Subplate has been shown to be affected in two different rat models of pathology. A model for preterm hypoxia-ischemia in P1/P2 rats led to specific cell death of subplate cells[234] (see Chapter 1 section 1.6.1 and Chapter 10). In addition, preterm hypothyroxinemia in rats (a reduction in the levels of thyroid hormones) has been suggested to cause delayed maturation of the subplate layer[417].

As rats are widely used as model organisms for many pathological studies, the aim of this chapter is to verify whether subplate cells in rats can be identified and monitored using the subplate-specific genes identified in mouse. I here compare expression patterns in the cortex of postnatal and adult mouse and rat of seven genes: Nurr1, Cplx3, *MoxD1*, *Ctgf*, *TRH*, *Tmem163* and Ddc. In addition, I also evaluate the expression of two genes which have been recently reported as subplate-specific in the perinatal rat brain - *kynurenine aminotransferase I* (*KAT-I*)[149] and progesterone receptor (PR)[418,151].

7.2 Methods

7.2.1 Animals and tissue preparation

C57/BL6 mice were obtained from the Oxford University Animal Facility and Wistar rats from Harlan Laboratories, UK. For each species, at least three brains were collected for each age (P8 and adult mouse and P0, P8 and adult rat). For in situ hybridization, animals were

killed by cervical dislocation and brains were dissected and fresh-frozen in O.C.T compound (TissueTek). For immunohistochemistry, animals were deeply anesthetized with pentobarbitone (Euthatal 150mg/kg intraperitoneally; Merial Animal Health Ltd) and perfused through the heart with 4% PFA. Brains were dissected and post-fixed in 4% PFA for 24-48h.

7.2.2 In situ hybridization and immunohistochemistry

Permanent in situ hybridization was performed on 14-16μm cryosections as detailed in Chapter 4 (section 4.2.2) using the riboprobes listed in Table 7_1. Mouse *Ctgf* and *Tmem163* probes were used both on mouse and rat as they share high sequence homology.

Permanent immunohistochemistry was performed on 40-50μm thick vibrating microtome sections as detailed in Chapter 4 (section 4.2.3) using the primary and secondary antibodies listed in Table 7_2. For co-localization between Cplx3 and Nurr1, sections were incubated with 5% donkey serum for 2h at RT and with anti-Cplx3 1:3000 and anti-Nurr1 1:100 in 1% donkey serum at 4°C overnight. Donkey anti-rabbit Alexa488(1:500) and donkey anti-goat Alexa568 (1:500) were added in 1% donkey serum for 2h before counterstaining with DAPI.

Riboprobes	**Forward primer**	**Reverse primer**
Mouse Ctgf	aagacacatttggcccagac	aagacacatttggcccagac
Mouse Tmem163	aagacacatttggcccagac	gggcaacgtcatcctaacat
Mouse MoxD1	atgcccagcaagattaccac	aaagtccagaacgctgtcgt
Mouse TRH	tggtgctgccttagattcct	ccagtgaagggactgggata
Rat MoxD1	cctgggaactgagaaaccaa	aggacgagcttgttgaagga
Rat TRH	attcatgggcagatgaggag	agtgctgaaggggtgtgact

Table 7_1. **Primer sequences for in situ hybridization riboprobes of subplate markers.**

Antibody	**Species**	**Dilution**	**Source**
Nurr1/Nr4a2	Goat	1:100 – 1:200	AF2156; R&D systems
Cplx3	Rabbit	1:3000	Gift K.Reim
Ddc	Rabbit	1:2000	ab49916, Abcam
Anti-Rabbit IgG	Donkey (biotinylated)	1:200	ab6801, Abcam
Anti-Goat IgG	Donkey (biotinylated)	1:200	ab6884, Abcam
Anti-Rabbit IgG	Donkey (Alexa Fluor488)	1:500	A21206 , Invitrogen
Anti-Goat IgG	Donkey (Alexa Fluor568)	1:500	A11057, Invitrogen

Table7_2. **Antibodies for immunohistochemistry of subplate markers.**

7.3 Results

7.3.1 Genes which are subplate-specific in both mouse and rat

For Nurr1, Cplx3, *Tmem163* and *Ctgf*, the same cortical expression patterns are found in rat as previously reported in mouse (Fig 7_1). In the P8 and adult cortex, these four genes are localized in a narrow, cell-dense band within the subplate. Nurr1 expression is restricted to subplate only in the dorsal cortex. In the lateral cortex, Nurr1+ cells are also found in layers VI, V and in a dense band below the marginal zone (Fig 7_1 a). In the subplate, Nurr1 labelling is exclusively localized in the cell nucleus. In contrast, in layers VI and V, additional labelling is visible in the processes of many cells (Fig 7_1 b). Cplx3 is exclusively expressed in subplate cells were it appears to be localized both in the cell soma and neurites (Fig 7_1 d-f). *Tmem163* is expressed both in subplate as well as layer V throughout the whole medio-lateral expanse of the cortex (Fig 7_1 j-l).

Co-localization between Cplx3 and Nurr1 in the P8 rat cortex shows that about two-thirds of Nurr1+ cells also expressed Cplx3 (67%, 904 double-labelled cells out of 1354 Nurr1+ cells, n = 3 brains). Conversely, less than half of Cplx3+ cells also had labelling with Nurr1 (42%, 524 double-labelled cells out of 1256 Cplx3+ cells, n = 3 brains). These numbers are very similar to those reported in the P8 mouse[117].

7.3.2 Mouse subplate-specific genes which are absent from the rat subplate

In the P8 mouse cortex, *MoxD1* is expressed in the subplate with sometimes an additional, weaker expression in layer V (Fig 7_2 a, b). Ddc+ cells are found in subplate, in the white matter and in the deep part of layer VI (Fig 7_2 i,j). I also examined the expression pattern of an additional gene – *thyrotropin releasing hormone* (*TRH*) – and found that it is strongly and specifically expressed in the subplate of the P8 mouse (Fig 7_2 e, f). To my knowledge, this gene has not been previously associated with subplate but has been used to label the tRN[419].

Surprisingly, in the P8 and adult rat cortex, neither *MoxD1* nor *TRH* are expressed in subplate cells even though the extracortical expression pattern is very similar to the one in the mouse (Fig 7_2 c, d, g, h). For instance, strongly labelled *MoxD1*+ cells are found in the claustrum and in the amygdaloid complex in both mouse and rat (Fig 7_2 a,c) while *TRH* is expressed in the hypothalamus and the tRN in both species (Fig 7_2 e, g). In order to confirm these differences in expression in the subplate, I generated species-specific probes for *MoxD1* and *TRH*. I used mouse probes on rat brains and vice versa (probe homology of over 90%). Both mouse and rat probes label subplate in mouse but not in rat, which indicates that the

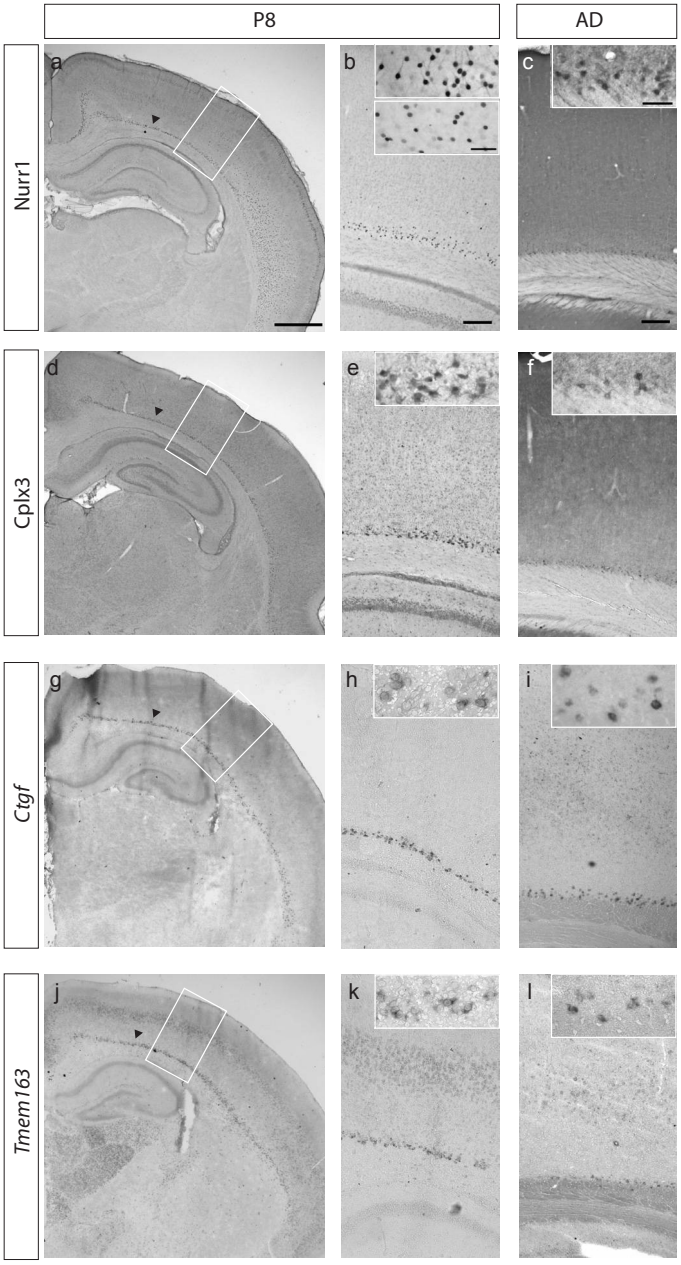

Figure 7_1. **Expression of the murine subplate markers Nurr1, Cplx3, Ctgf and Tmem163 in the rat cortex.** Immunohistochemistry (Nurr1, Cplx3) or in situ hybridization (Ctgf, Tmem163) signals in the P8 and adult (AD) rat forebrain. All four genes show very similar expression patterns as in the mouse. a-c. Nurr1+ cells are localized in the subplate in the dorsal cortex and in the subplate and layers V and VI in the lateral cortex. Top insert in b shows Nurr1+ cells in layer VI and bottom insert in subplate. Insert in c shows Nurr1+ cells in subplate. d-f. Cplx3+ cells are exclusively found in the subplate. g-i. Ctgf is strongly and specifically expressed in the subplate. j-l. Tmem163 is expressed in the subplate and layer V. Inserts in k and l show Tmem163+ cells in subplate. Scalebars: 1mm (a), 200µm (b,c) and 50µm (inserts).

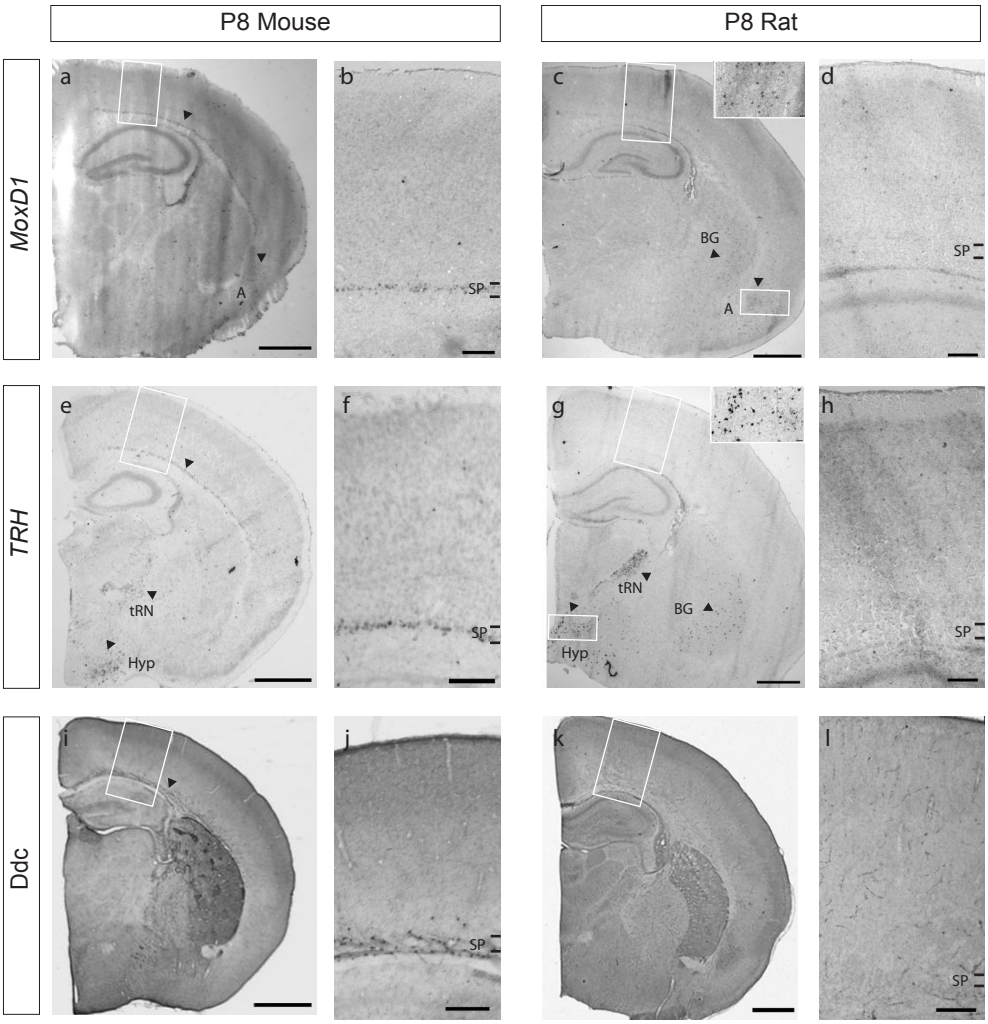

Figure 7_2. **Expression of MoxD1, Trh and Ddc in the rat and mouse cortex.** In situ hybridization (MoxD1, TRH) or immunohistochemistry (Ddc) signals in the P8 mouse and rat forebrain. All three genes are expressed in the subplate (SP) of the mouse but not the rat. a,b. In the mouse, MoxD1+ cells are localized in the SP but also in extracortical structures including the amygdala (A). c,d. In the rat, MoxD1 is not expressed by SP cells but in several extracortical structures including the basal ganglia (BG) and A (insert). e,f. In the mouse, TRH is expressed in the SP, the thalamic reticular nucleus (tRN) and the hypothalamus (Hyp). g,h. In the rat, no TRH expression is found in the SP but strongly labeled TRH+ cells are localized in the tRN, BG and Hyp (insert). i,j. In the mouse, large numbers of Ddc+ cells are found in the SP and underlying white matter. k,l. In the rat, only a few sparse Ddc+ cells are found in the SP. Scalebars: 1mm (a, c, e, g, i, k) and 200µm (b, d, f, h, j, l).

observed difference in subplate expression is not due to different isoforms or probe specificity (data not shown).

In contrast to the mouse, only very few dispersed Ddc+ cells were found in the subplate and the white matter of the P8 rat in all examined brains (n=5) (Fig 7_2 k,l). Again, the extracortical expression pattern was very similar between mouse and rat and Ddc+ cells were for instance found in the hypothalamus of both species (Fig 7_1 i, k).

7.3.3 Verification of additional potential subplate markers in rat

Two genes have been recently reported as specifically expressed in the subplate of late embryonic and early postnatal rat – PR[418,151] and KAT-I[149]. I verified whether these two genes could be used to reliably identify subplate cells in the P8 rat cortex

As previously reported, PR was strongly expressed in the P8 subplate, which is distinguishable as a dark-labeled band on images with low magnification (Fig 7_3 a). However, strong expression is also found in layers V, II/III and I while expression is lower in layers VI and IV.

In the rat, KAT-I is expressed in two different isoforms - a mitochondrial isoform (mKATI) and a cytoplasmic isoform (cKATI) – which are produced by alternative splicing and differ only in a short sequence at the 5'end. I used a pan-KATI in situ probe which targets a coding region common to both isoforms (Fig 7_3 b) as well as a riboprobe specific to mKATI (Fig 7_3 c). In the P8 rat cortex, both probes strongly labelled subplate and layer V but additional labelling was also observed in all other cortical layers (Fig 7_3 b, c). KATI expression was also analyzed in P0 cortices with very similar patterns as at P8 (data not shown).

7.4 Discussion

7.4.1 Expression of murine subplate markers in the postnatal rat subplate

Expression patterns of nine genes in the rat cortex were evaluated for their usefulness to label and monitor subplate cells in this species. I found that Cplx3 and *Ctgf* are specifically expressed in the P8 and adult rat cortex. Nurr1 is exclusively expressed in subplate in the dorsal cortex and in subplate, layers VI, V and II in the lateral cortex. *Tmem163*+ cells are found in subplate and in layer V. Expression of *Ctgf* and Nurr1 in the rat adult subplate has been previously reported[119,118]. Similar to previous studies[418,151], I found that PR is expressed in all cortical layers but shows the strongest expression in subplate and layers V, II/III and I.

I did not find any *MoxD1*+ or *TRH*+ cells and very few Ddc+ cells in subplate in the postnatal rat.

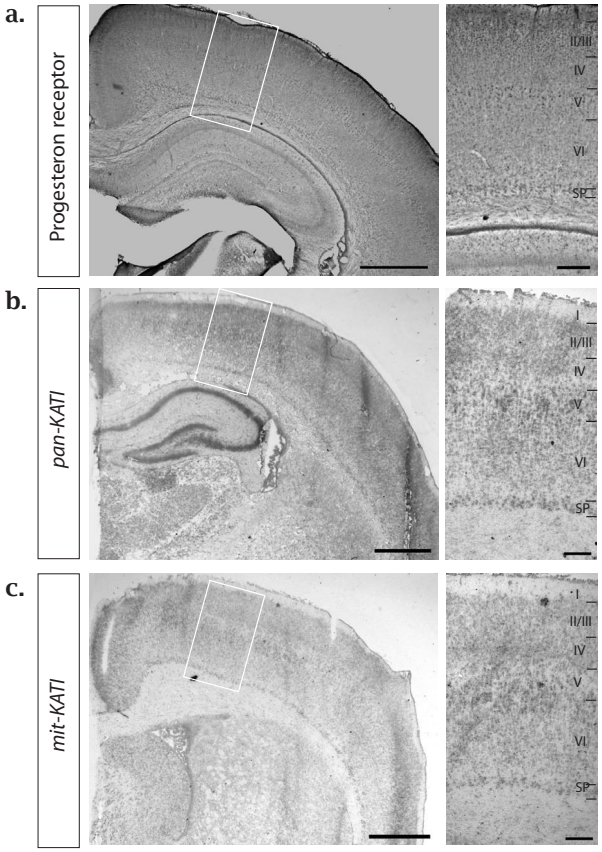

Figure 7_3. **Expression of Progesterone receptor and KATI in the P8 rat cortex.** a. Immunohistochemistry against the progesterone receptor (PR). PR is most strongly expressed in the subplate (SP) and layers V and II/III. b. In situ hybridization against both isoforms of KATI (pan-KATI). KATI is most strongly expressed in the SP and layer V but also in all other layers. c. In situ hybridization against the mitochondrial isoform of KATI (mit-KATI). Mit-KATI gives a similar labeling pattern as pan-KATI. Scalebars: 1mm (large panels) and 200μm (small panels).

Finally, in situ hybridization against *KAT-I* labelled cells in all cortical layers, both in P0 and P7 rat cortices. This is in contrast to a previous study where a polyclonal antibody raised against the entire KAT-I protein has been shown to label subplate cells specifically at least from E16 until P7 in rat[149]. As KAT-I is expressed in two different isoforms in the rat (a mitochondrial and a cytoplasmic isoform), I attempted to generate riboprobes against both isoforms of KAT-I (pan-KAT-I) as well as riboprobes specific to each isoform. I did not succeed in amplifying the cytoplasmic isoform from postnatal rat cDNA. This could be either due to technical problems or indicate that this isoform is not expressed in the cortex at this stage. I found no difference in the pattern of the pan-KAT-I or the mitochondrial KAT-I riboprobe. This suggests that it is unlikely that the observed discrepancy between *in situ hybridization* and immunohistochemistry against KAT-I is due to different isoforms visualized by the two methods.

Taken together, these results show that Nurr1, Cplx3, *Ctgf* and *Tmem163* are strongly and consistently expressed in subplate cells in the postnatal P8 and adult rat cortex. These genes could therefore be useful tools to identify and monitor subplate cells in rat.

7.4.2 Differences between mice and rats

Mice and rats are among the most commonly used model species and are often considered very similar and nearly inter-changeable. Interestingly, I found that three out of seven genes analyzed in both rodents showed species-specific differences. In the P8 and adult mouse cortex, *MoxD1* and *TRH* are specifically expressed in the subplate while many Ddc+ cells are found in subplate and in the white matter[117]. In contrast, in P8 and adult rats, *MoxD1* and *TRH* expression were completely absent in the subplate and Ddc labelling was much reduced to only a few cells. The extracortical expression patterns were very similar between the two species indicating that all riboprobes and antibodies are functional in both species.

The differences in the subplate gene expression patterns in mouse and rat are not that surprising if we consider that the mouse and rat lineages split between 12 and 24 million years ago[420]. This is roughly at the same time as the split between human and orang-utan lineages[421]. Other species-specific differences have been described for rodents such as the different distribution of acetylcholinesterase in the barrels of primary somatosensory cortex in rat compared to mouse or hamster[422]. Similarly, Krubitzer et al. have recently described important differences in cortical arealization in different rodent species and even between wild-caught and laboratory-bred rats[423]. Finally, birthdating studies in mouse and rat suggest differences in the survival of subplate cells in these two species. In mice, the large majority of subplate cells disappear during the first postnatal week[54] whereas in rats at least half of these cells persist into adulthood[112],[113] (see Chapter 1 section 1.2.3.5). However, Nurr1, Cplx3, *Ctgf*, *Tmem163, TRH* and *MoxD1* are expressed in adult mouse subplate cells[117] indicating that at least a subpopulation of subplate persist into adulthood even in mice. Similarly, rat adult subplate cells also express Cplx3, *Ctgf*, Nurr1 and *Tmem163* (Fig 7_1 c, f, i, l). It is therefore improbable that the differences observed in the expression of Ddc, *MoxD1* and *TRH* in rat and mouse are due to different survival of subplate cells in these two species. Instead, our results emphasize that rat models and mouse models are not interchangeable, and that each species has evolved many unique characteristics in the neocortex.

7.5 Conclusion

In this chapter, I have confirmed that four genes which are specifically expressed in subplate in the postnatal and adult mouse - Nurr1, Cplx3, Ctgf and Tmem163 - can also be used to label and monitor subplate cells in the postnatal and adult rat. In addition, I found several species-specific differences in the gene expression in subplate (*MoxD1*, *TRH*, Ddc) suggesting that these two rodent model organisms cannot be considered as interchangeable.

Chapter 8 Subplate in a rat model of preterm hypoxia-ischemia

8.1 Introduction

Hypoxia-ischemia in preterm infants primarily leads to injuries in the cerebral white matter. However, there is growing evidence that perinatal injury in preterms can also involve other zones including the cortical grey matter (see Chapter 1 section 1.6.1). It has been argued that the cognitive, sensory and behavioural deficits resulting from preterm injury are unlikely caused by white matter damage alone but rather reflect fundamentally abnormal brain development[424, 235]. Injury to subplate neurons could importantly contribute to the pathological consequences of an insult due to their important role in normal cortical development. The human subplate layer reaches a developmental peak at the same time as the premature brain is at the highest risk for perinatal injury (i.e. around 27 to 30 gestational weeks)[425,165]. Subplate neurons are particularly critical for the development of visual thalamocortical connections and the establishment of ocular dominance columns[175,212]. Subplate damage has therefore been proposed to underlie visual impairments which are particularly common in infants with preterm perinatal damage[426],[427].

Selective vulnerability of subplate neurons to hypoxia-ischemia has been demonstrated in a P1/P2 rat model[234]. Using ISEL, extensive cell death was observed in the ventricular zones, the white matter and the subplate four days after the hypoxia-ischemia insult. In subplate, identified by BrdU birthdating at E12.5, hypoxia-ischemia led to variable degrees of neuronal death. The average cell death rate was 45% but ranged from 20% in mild cases to nearly 90% in severe cases. Other cortical layers, although not identified by birth-dating, seemed mostly left intact except in the most severe cases where the injuries extended into layer VI. Despite a significant loss in subplate neurons following hypoxia-ischemia, no gross abnormalities in the corticothalamic and thalamocortical connections in the somatosensory and visual cortices were found. In a subsequent study using a very similar model, the authors found, however, that the ocular dominance plasticity in the visual cortex was impaired in moderate cases[428]. Similarly, recent work on the model suggests that hypoxic-ischemic damage to the subplate results in abnormal tuning characteristics in the auditory cortex[429].

In the previous chapter, I have confirmed Nurr1 and Cplx3 as two genes which reliably label two distinct yet overlapping subplate subpopulations in the early postnatal rat (see Chapter 7, section 7.3.1). The first aim of this chapter is to examine whether subplate is specifically vulnerable in a rat model of preterm hypoxia-ischemia by comparing subplate-specific markers

(Nurr1, Cplx3) and markers of other cortical layers (FoxP2, Er81) and the white matter (MBP). Secondly, I will evaluate whether the Nurr1+ and Cplx3+ subplate subpopulations are equally affected by hypoxia-ischemia or whether one subpopulation is more vulnerable than the other.

8.2 Methods

8.2.1 Hypoxia-ischemia model 1

All experiments were performed by Dr Vanessa Ginet, according to the guidelines of the Swiss Veterinary Office. Two-day-old male Sprague Dawley rats were anesthetized with 3% isoflurane and their right common carotid artery (CCA) was double- ligated and cut. Sham-operated animals underwent the same surgical procedure except that the carotid was not sectioned. After a recovery period of at least 2h with the dam, all pups except for the sham animals were placed in 6% O_2 at 35.5°C in an incubator for 1.5h (7 animals) or 2h (19 animals). Body temperature was monitored after the surgery and again after the hypoxic period and was kept stable at 35-36°C. The pups were then returned to the dam until P8 when they were killed for analysis. A total of 31 animals were used in 3 experimental series (5 sham and 26 hypoxic-ischemic).

8.2.2 Hypoxia-ischemia model 2

All experiments were performed by Ann Sheldon and approved by the University of California San Francisco Committee on Animal Research and performed in accordance with standards set forth in the Policy on Humane Care and Use of Laboratory Animals. Two-day-old male and female Sprague Dawley rats were anesthetized with 2-3% isoflurane. The right CCA was permanently coagulated with a bipolar coagulator. Sham-operated animals underwent the same surgical procedure, except that the CCA was not coagulated. Animals were returned to the dam for at least 2hr. Subsequently, pups were placed in 5.6% O_2 in chambers floating in a 37°C water bath for 1.15 to 1.45h. The pups were then returned to the dam until P8 when they were killed for analysis. One series of experiments was performed on 12 animals (2 sham and 10 hypoxic-ischemic).

Table 8_1 summarizes the main differences between Model 1 and Model 2.

8.2.3 Tissue preparation, staining and immunohistochemistry

Animals were deeply anesthetized with pentobarbitone and transcardially perfused with 4%

	Model 1	Model 2
Strain	Sprague Dawley	Sprague Dawley
Age and sex	P2, male	P2, male and female
Mean body weight (before hypoxia-ischemia) ± SD	9.2g ± 0.6	7.4g ± 0.4
Anaesthesia	3% isoflurane	2-3% isoflurane
Ischemia	Ligation and sectioning of the right CCA	Electrocoagulation of the right CCA
Hypoxia	6% O_2, 1.5-2h	5.6%, 1.15-1.45h
Temperature	35.5°C, incubator	37°C, individual floating chambers

Table 8_1. **Comparison between the two hypoxia-ischemia models.** CCA: common carotid artery. SD: standard deviation.

PFA. Brains were removed and post-fixed overnight in the same fixative. They were then sectioned into 50µm thick coronal sections on a vibrating microtome (Leica).

For cresyl violet staining, mounted and air-dried sections were rehydrated in serial alcohol dilutions with descending concentration and stained with 0.1% cresyl violet (Sigma) in H_2O for 10min. Sections were rinsed in H_20 and dehydrated through serial alcohol dilutions with ascending concentration and cleared with xylene and histoclear (Sigma).

Permanent immunohistochemistry was performed as described in Chapter 4 (section 4.2.3) using the following primary antibodies: anti-Nurr1 1:200 (AF2165; R&D Systems), anti-Cplx3 1:3000 (gift K. Reim), anti-FoxP2 1:4000; (ab16046; Abcam), anti-Er81 1:32'000 (gift T. Jessel), anti-Gad65/67 1:2000 (AB1511; Millipore), anti-NeuN 1:500 (MAB377, Chemicon), anti-calbindin 1:10'000 (D-28K, Swant) and anti-MBP 1:200 (Santa Cruz Biotechnologies).

For co-localization between MBP and isolectin B4 sections were blocked in 5% donkey serum in TBS with 0.1% Triton-X100 for 2h at RT and incubated with anti-MBP antibody at 4°C overnight. Anti-goat Alexa 488 1:500 (Invitrogen) was added together with *Griffonia Simplicifolia* isolectin B4-Texas Red 1: 200 (Vector Laboratories) in 1% donkey serum in TBS + Triton for 2h at RT before counterstaining with DAPI.

8.2.4 Quantification of cell numbers and layer thickness

Nurr1+ and Cplx3+ subplate cells were quantified in the subplate (defined as a 120µm thick layer in the P8 rat based on marker expression) across a 3.5mm long expanse of the cortex. Cells were counted blind on at least two sections at the level of S1 (Bregma -2.5) per brain. On average, about 500 Nurr1+ cells and 400 Cplx3+ cells were counted per hemisphere per

brain. Cell counts were normalized to sham controls from the same experimental series and the percentage of cell death rate calculated for each hemisphere of each brain as: %(cell death) = 1 – ((nb of cells)/ (average nb of cells in sham)). Cell death rates were tested for their statistical significance using one-sample, one-tailed t-tests ($p<0.05$). Cell death rates of Cplx3+ and Nurr1+ were compared within the same severity group using two-sample, two-tailed t-tests.

The thickness of deep layers (layers VI and V) and upper layers (layers II to IV) was measured on FoxP2-immunoreacted sections where layers VI and V are labelled. Thicknesses were measured at two points in the cortex (2mm and 3mm away from the midline) on two sections at the level of S1 (Bregma -2.5). Measurements were normalized to sham controls from the same experimental series and a reduction in thickness calculated as: reduction (thickness) = 1 – ((thickness)/ (average thickness in sham)). Thickness of upper and lower cortical layers were compared within the same severity group using t-tests.

8.3 Results

Two very similar rat models of preterm hypoxia-ischemia were prepared based on the original study by McQuillen et al.[234]. The differences between the two models are summarized in Table 8_1. Both models had similar survival rates with just over 60% for the first model (16 out of 26) and 70% for the second model (7 out of 10).

8.3.1 Histological analysis of hypoxic-ischemic brains

In the first model, a large variability in the extent of the cerebral injury was apparent. The outer gross appearance of the brain was normal in 4 cases while the ipsilateral hemisphere in the remaining cases was atrophic – mildly in 7 cases, moderately in 3 cases and severe in 4 cases.

Overall structural integrity and cell morphology was further assessed on cresyl violet stained sections, at first focusing on sections in the area S1 (Bregma -2.5) (Fig 8_1 a-c). Seven brains (45%) had normal structural and cellular morphologies at this level with no apparent lesions (Fig 8_1 a). Four further brains (25%) showed decreased cell density in the deep layers of the ipsilateral hemisphere which were in one case accompanied by several patches of dead cells and in another case by a small scar in layer V (Fig 8_1 b). Finally, five brains (30%) had extensive lesions in the ipsilateral cortical hemisphere with prominent scars, primarily localized in layer V (Fig 8_1 c). Cells below the scar (in subplate and layer VI) appeared severely degenerated while cells above the scar had normal morphologies. These severe cortical lesions were generally accompanied by a degenerated hippocampus and enlarged ventricles. In addition,

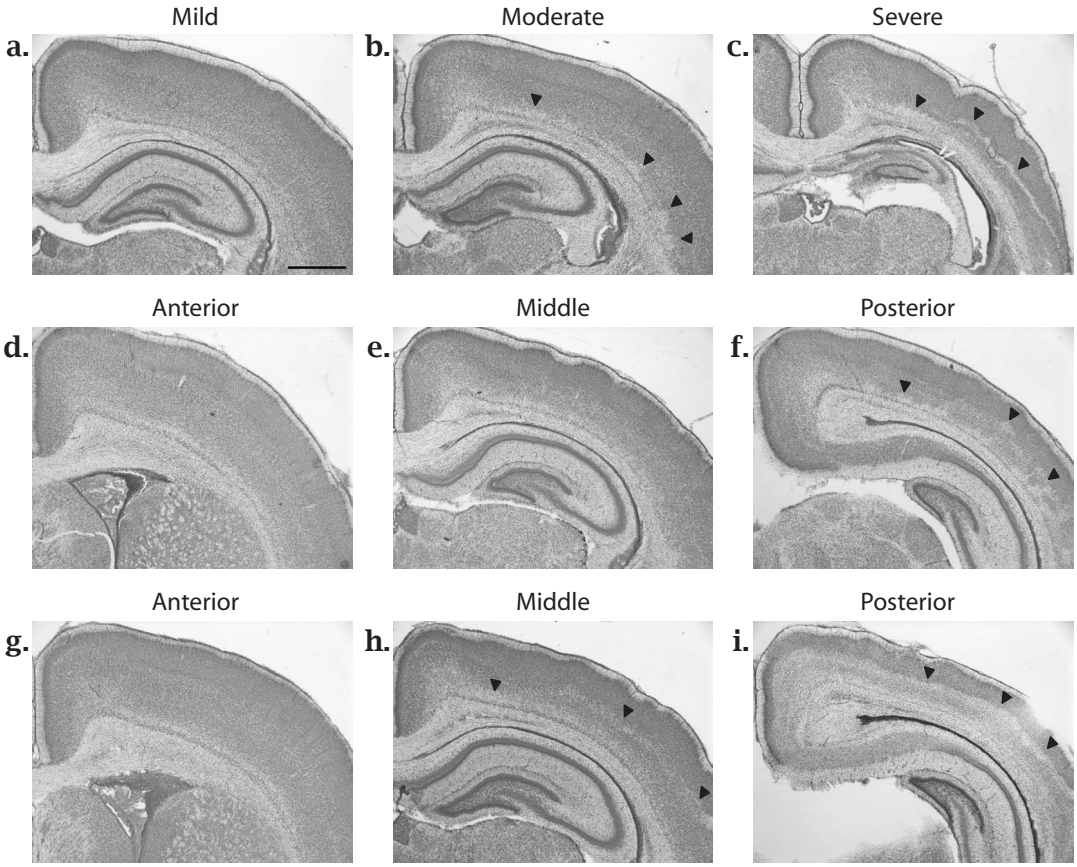

Figure 8_1. **Histological assessment of cortical injuries after hypoxia-ischemia.** Cresyl-violet stained sections from the ipsilateral hemispheres at P8 after hypoxia-ischemia at P2. a-c. Sections at the level of the somatosensory cortex in a mildly (a), a moderately (b) and a severely affected brain (c). In the mild case (a) structural and cellular morphologies appear normal. In the moderate case (b), small patches of necrotic cells and cell loss are visible in and above the subplate zone (arrowheads). In the severe case, a large band of necrotic cells spans the lower cortical layers and a prominent scar crosses the cortical wall. The hippocampus is severely degenerated (c). d-i. Sections through the anterior (d, g) , middle (e, h) and posterior (f, i) ispilateral hemisphere. Injuries appear more pronounced in the posterior than in the anterior cortex. In a first brain (d-f), the anterior region of the cortex is largely unaffected (d) while some cell loss is visible in the middle region (e, arrowhead). In the posterior cortex, in contrast, many patches of cell loss and necrosis are found in subplate and layers VI and V (f, arrhowheads). In a second brain (g-i), the histology of the anterior cortex appears again largely normal (g). In the middle regions, large areas of cell loss are visible in layers VI and V (h, arrowheads). In the posterior cortex (i), a scar crosses the entire expanse of the cortex. Scalebar: 1mm.

in the three most severe cases, the contralateral hemisphere was also affected, although to a lesser extent than the ipsilateral hemisphere. The contralateral hemispheres were most severely damaged in the region closest to the midline but also showed some atrophy, cell loss and/or small scars more laterally (not shown) .

Histological analyses on more anterior and posterior cortical areas (Bregma -0.3 and -4.3, respectively) revealed that the observed cortical lesions were usually more pronounced in the posterior regions of the brain (Fig 8_1 d-i). Figure 8_1 d-f shows an example where the

tissue appears normal in the anterior cortex, shows decreased cell density and a few patches of dead cells in the medial cortex and finally a larger lesion involving almost the entire expanse of layer V in the most posterior cortex. Similarly, scars always appeared to involve a much larger extent of the posterior cortex than the anterior cortex (Fig 8_1 g-i).

Based on this histological assessment, brains were divided into three categories: Mild (no or mild atrophy, normal histology; n= 6 brains), moderate (mild or moderate atrophy; decreased cell density or patches of dead cells at least in one area of the brain; n=5 brains) and severe (moderate or severe atrophy; presence of a scar; n = 5 brains).

In contrast to the first model, there was no apparent variability between the cases of the second model. All hypoxic-ischemic brains had a normal outer appearance and showed normal structural and cellular morphologies across the anterior-posterior expanse of the cortex (not shown). All cases in the second model were therefore classified as "mild" (n= 10 brains).

8.3.2 Subplate cell populations

The number of Nurr1+ and Cplx3+ cells were counted in the left and right hemispheres of the hypoxic-ischemic brains and compared to cell numbers in the sham-operated animals of the same series (Fig 8_2).

For the first model, I found in average no changes in subplate cell numbers in the mild cases for either subplate cell population. In the moderate cases, the number of Cplx3+ cells was significantly decreased by an average of 25% in the ipsilateral hemisphere ($p = 0.0024$) while the average number of Nurr1+ was not significantly altered ($p= 0.15$). In the ipsilateral hemisphere of the severely affected brains, both Nurr1+ and the Cplx3+ subplate cell populations were severely and high significantly decreased by an average of approximately 80% ($p < 0.001$) (Fig 8_2 c). There was no significant difference between the decrease of Nurr1+ and the Cplx3+ cell populations for any of the groups ($p>0.05$).

For the second model, where all cases had been classified as mild, no qualitative changes in subplate cells were observed in any of the hypoxic-ischemic brains either after staining with Nurr1, NeuN, Gad65/67 or calbindin (not shown).

8.3.3 Other cortical layers

To assess to what extent the injuries seen in moderate and severe cases of the first model are specific to subplate, layers VI and V were analyzed using immunohistochemistry against FoxP2 and Er81, respectively (Fig 8_3).

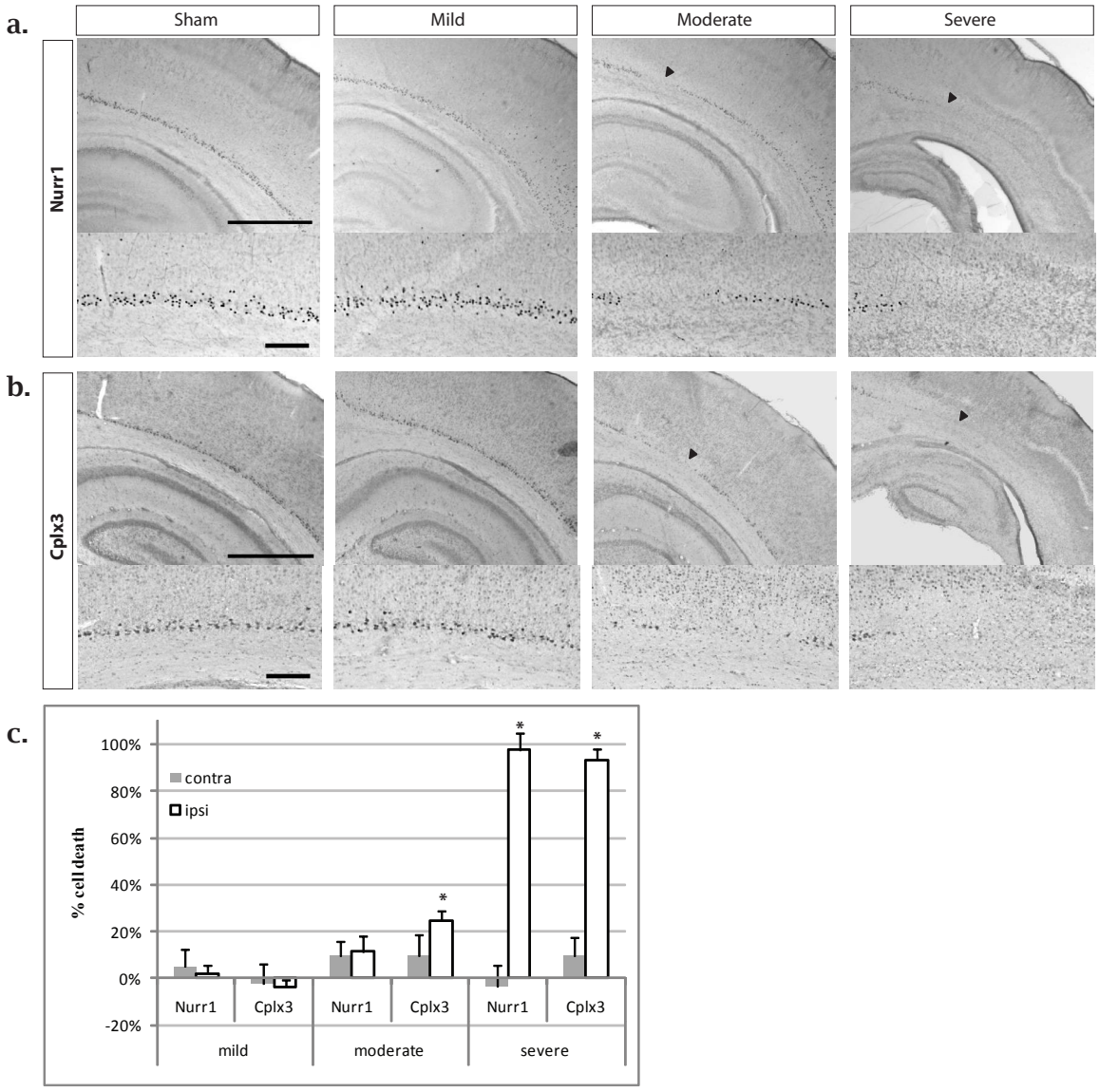

Figure 8_2. **Nurr1+ and Cplx3+ subplate cell populations after hypoxia-ischemia.** a, b. Examples of immunohistochemistry signals of Nurr1+ (a) and Cplx3+ (b) subplate cells in the ipsilateral hemisphere of sham control and mild, moderate and severe cases after hypoxia-ischemia. In the mild case, both subplate cell populations appear unaffected. In the moderate case, a few patches of cell loss are visible in the subplate with both markers (arrowheads). In the severe case, only subplate cells in the most dorsal cortex are preserved. Scalebars: 1mm (large panels); 200µm (small panels). c. Quantification of cell death of Nurr1+ and Cplx3+ in the ipsi- and contralateral hemispheres compared to sham controls. In the ipsilateral cortex of moderate cases, significant cell death was found for Cplx3+ subplate cells only (~20%) while in severe cases, a large proportion of Cplx3+ and Nurr1+ cells underwent cell death (~80%). n= 7 (mild), 5 (moderate) and 5 (severe). Error bars are SEM. Asterisks (*) indicate significant cell death compared to sham controls ($p < 0.05$).

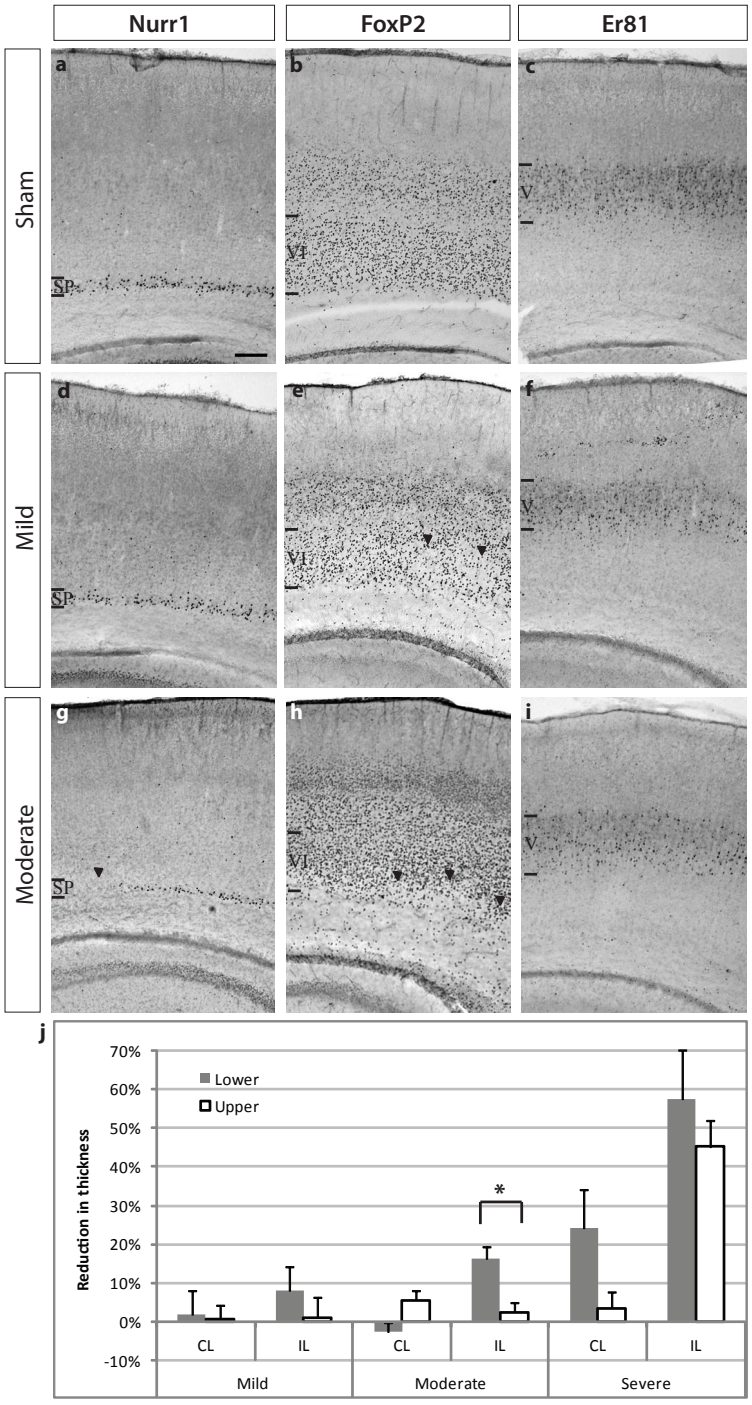

Figure 8_3. **Deep cortical layers V and VI after hypoxia-ischemia.** a-i. Examples of immunohistochemistry signals of the subplate (SP) marker Nurr1 (a, d, g), the layer VI marker FoxP2 (b, e, h) and the layer V marker Er81 (c, f, i) in the ipsilateral hemisphere of sham control and mild and moderate cases after hypoxia-ischemia. In the mild case (d-f), the Nurr1+ SP appears unaffected (d) while a few patches of cell loss are seen in the Foxp2+ layer VI (e, arrowheads). In the moderate case (g-i), cell loss is visible in the Nurr1+ SP (g) and the FoxP2+ layer VI (h) (arrowheads). Staining for Er81 in layer V appears less dense (i) than in the sham control (c). Scalebar: 200µm. j. Quantification of the reduction in thickness of upper and lower layers in the ipsilateral (IL) and contralateral (CL) cortex compared to sham controls. In the IL hemisphere of mild and moderate cases and both hemispheres of the severe cases, reduction in thickness was more pronounced for the upper layers than the lower layers. However, this difference between upper and lower layers only reached statistical significance for the IL of moderate cases (indicated by an asterisk *, $p = 0.008$). Error bars are SEM.

Qualitative analysis of the labelling showed that 11 out of 16 brains had pathological changes in FoxP2+ layer VI (Fig 8_3 e,h). These changes range from atrophy (1 brain) over patches of dead cells (5 brains) to completely degenerated cells below a scar (5 brains). Out of these eight brains, seven also showed additional pathological changes in Er81+ layer V cells (Fig 8_3 f). Correlating these observations with the changes in subplate markers, I found that 8 out of 9 brains which showed a decrease in subplate cells of more than 20% also had pathological changes in layers VI and sometimes V (Fig 8_3 g-i).Inversely, three mild cases where the Nurr1+ and Cplx3+ subplate populations were unaffected showed signs of pathology in the deep layers (Fig 8_3 d-f).

In order to determine whether lower layers (i.e. layers VI and V) are more affected than upper layers (layers IV and II/III), the thickness of the two compartments were measured in hypoxic-ischemic cases and compared to sham animals. I found that in mild, moderate and severe cases, the decrease in layer thickness was more pronounced in the infragranular layers than in the supragranular layers (Fig 8_3 j). However, this difference in vulnerability between lower and upper layers was only significant for the moderate cases (unpaired t-test, $p=0.008$).

8.3.4 White matter

As hypoxia-ischemia in preterm infants is known to primarily damage developing oligodendrocytes, I also checked for abnormal myelination using immunohistochemistry against myelin basic protein (MBP) (Fig 8_4). In the first model, a reduction of MBP+ staining was observed in 11 out of 16 brains. In mild cases, MBP+ cells and fibres appeared reduced and extended less deeply into the cortical plate (Fig 8_4 b). In severe cases, MBP+ cells appeared degenerated and almost no MBP+ fibres were present (Fig 8_4 d). Surprisingly, in several brains, MBP+ cells were found to be accumulating within lesions in the cortical plate (Fig 8_4 c). These MBP+ cells presented a characteristic morphology with large cell bodies and extensive, arborizing ramifications (insert Fig 8_4 c). These cells did not co-express the microglial marker ILB4 (Fig 8_4 e).

For the second model, no differences in MBP labelling were observed between the hypoxic-ischemic and the sham animals (not shown).

8.4 Discussion

8.4.1 Hypoxia-ischemia mainly affects deep layers but is not specific to subplate

As previously reported by others[234,428], a large variability in the severity of the hypoxic-ischemic damage between different animals was observed. For the two analyzed subplate

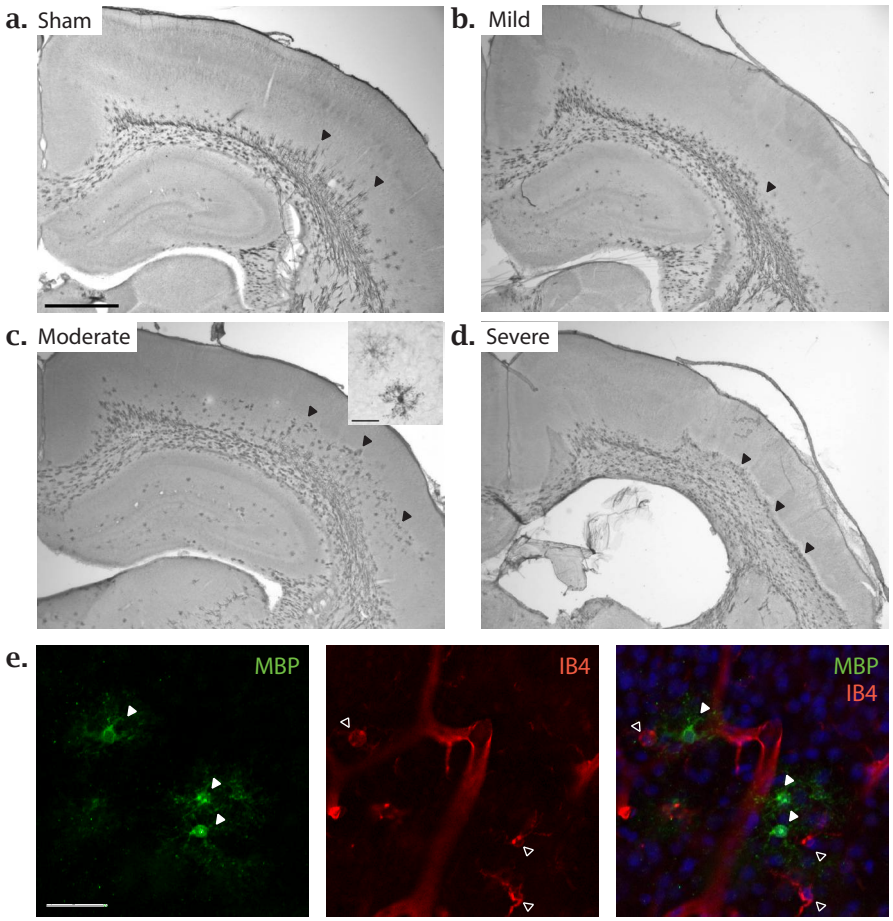

Figure 8_4. **White matter and oligodendrocytes after hypoxia-ischemia.** a-d. Examples of immunohistochemistry signals of MBP+ oligodendrocytes and cortical white matter in the ipsilateral hemisphere of sham control and mild, moderate and severe cases after hypoxia-ischemia. In the mild case (b), MBP+ cells and fibers are reduced in length in the lateral cortex compared to the sham control (arrowheads). In the moderate case (c), the lesioned area in layer V/VI is filled with MBP+ cells. The insert in c shows the morphology of two of these cells. In the severe case (d), the entire cortex below the scar contains MBP+ cells. These cells appear degenerated and do not have the same morphology as observed in c. e. Immunohistochemistry signals of MBP and IB4 within the cortical lesion. The MBP+ cells (green, filled arrowheads) filling the lesions in moderate cases (c) do not co-express the microglial marker IB4 (red, empty arrowheads) and the two cell types have very different morphologies. Scalebars: 1mm (a-d); 50μm (e and insert in c).

populations (Nurr1+ and Cplx3+ cells) no significant cell death was observed in mild cases while in moderate cases, the average decrease of Cplx3+ cells was 25%. The most severe cases showed an important decrease in the number of subplate cells of ~ 80%. The average decrease in subplate cells across all cases of the first model was ~30% for Nurr1+ cells and ~ 40% for Cplx3+ cells which is similar to the subplate cell death rate previously reported for this model (i.e. 45%)[234].

I further found that the large majority of brains with an injury in subplate also showed pathological changes in layer VI and often layer V (8 out of 9). Moreover, a few mild cases with no significant cell death in Nurr1+ or Cplx3+ subplate cells instead showed injuries in the lower layers.

The upper layers were not analyzed with specific markers but on cresyl violet stained sections they appeared intact in mild and moderate cases. Even in the most severely affected brains with prominent scars, cells in the upper layers had largely normal morphologies while cells in the lower layers below the scar were degenerated (see Fig 8_1 c). Moreover, at least in moderate cases, the thickness of the infragranular layers was significantly more reduced than the thickness of supragranular layers (Fig 8_3 j).

The increased vulnerability of the lower cortical layers is in line with two previous independent studies on comparable models of P2 and P3 rats where the authors describe columns of degenerated cells in the deep cortex involving subplate, layer VI and layer V[240, 433.] Similar to these two studies and in contrast to the work by McQuillen et al.[234], I did not find that subplate is more often or more severely affected than the deep cortical layers. McQuillen et al. report that in their model, subplate cells (labelled by BrdU birthdating at E13) are selectively affected in mild and moderate cases while only in the most severe cases, the injury extends to layer VI. However, as the authors did not analyze in detail other layers than subplate with BrdU birthdating or specific markers, it is conceivable that more subtle changes in the deep layers went undetected in some cases. On the other hand, I cannot exclude that by using Nurr1 and Cplx3 to identify subplate cells, I have analyzed different subplate subpopulations than those labelled by a pulse of BrdU at E13.

The greater vulnerability of cells in the deep layers could be linked to their more mature expression of receptors for neurotransmitters and hence a greater susceptibility to excitotoxity. Indeed, a recent study has shown that at least in culture, subplate cells express higher levels of the metabotropic mGluR3 than cells of the cortical plate[147]. Blocking of these receptors with pharmacological antagonists in subplate cells provides partial protection from glutamate-induced cell death indicating that these receptors could be linked to subplate vulnerability. Similarly, human subplate neurons in preterm infants (25-37GW) specifically express high levels of GluR2-lacking AMPA receptors[238].

In this context it is surprising that in my model injuries appeared to be more pronounced in the posterior cortex than in the anterior cortex. The cortex matures in an anterior-first posterior-last gradient[185] and I could therefore expect greater levels of neurotransmitter receptors and hence increased vulnerability in the anterior cortex. My observation suggests that neuronal maturity is only one of several parameters determining the susceptibility of a

cortical cell population to hypoxia-ischemia in this model. Other important factors are likely the density and size of blood vessels irrigating the area as well as the cells' intrinsic susceptibility to undergo apoptosis and their requirements for trophic and metabolic support. (see Chapter 1, section 1.6.1 6).

8.4.2 Different subplate subpopulations might be differentially affected

It appears that even within a given structure such as subplate not all cells are equally vulnerable to hypoxia-ischemia. This is evident from the study by McQuillen et al.,[235] where 20%-80% of subplate neurons survive the hypoxic-ischemic insult. This allows for the intriguing possibility that different subplate subpopulations show different degrees of vulnerability. In order to start to investigate this possibility, we used two markers for different, though overlapping, subplate subpopulations (about two-thirds of Nurr1+ cells express Cplx3 while half of Cplx3+ cells express Nurr1; see also Chapter 7 section 7.3.1). I found some preliminary evidence that Cplx3+ could be more susceptible to cell death than Nurr1+ cells as in moderate cases, only the number of Cplx3+ cells was significantly reduced. However, the difference in cell death between the two populations failed to reach statistical significance even though a large number of cells were counted in each brain (approximately 400 Cplx3+ cells and 500 Nurr1+ per hemisphere). Due to the large variability between animals and models, only five moderate cases were available in this study and further experiments would be needed to investigate this in more detail. It would then be interesting to extend the analysis using different markers to other subplate subpopulations including interneurons, especially once subtypes have been correlated with projection sites and electrophysiological properties (Hoerder-Suabedissen et al., in preparation)

8.4.3 White matter damage accompanies cortical lesions

In preterm infants, perinatal brain injury is known to severely affect the developing oligodendrocyte cell populations. When analyzing mature oligodendrocytes and myelination of the cortical white matter in the first model, I found that the majority of brains showed white matter abnormalities (11 out of 16). These ranged from a reduction of MBP+ cells and fibres in mild and moderate cases to an almost complete absence of MBP+ fibres and degenerated MBP+ cells in the most severe cases. Interestingly, I also observed MBP+ cells which appeared to infiltrate lesions in the deep cortical layers. Insults to the brain such as hypoxia and/or ischemia or traumatic injury activate residential microglia in and surrounding the lesioned area[430, 431, 432]. Many activated microglia are phagocytotic and engulf cellular debris and apoptotic cells. It is therefore conceivable that the MBP+ cells are microglia, which have become immunoreactive to the MBP antibody after engulfing degenerated mature

oligodendrocytes. However, I found that the MBP+ cells in the cortical lesions do not express the microglial marker IB4 which indicates that they are mature oligodendrocytes rather than microglia. Recent studies suggest that similar to other glial cells oligodendrocytes can be activated following an insult and actively modulate the inflammatory response in the brain (reviewed in [433]). It is therefore conceivable that the increase in oligodendrocytes within the cortical lesions could be part of the cerebral inflammatory response to the hypoxic-ischemic insult.

8.4.4 Consequences for interpretation of functional studies

Two recent studies have focused on understanding the functional consequences of preterm hypoxic-ischemic using rat models. In the visual cortex, hypoxia-ischemia has been shown to lead to an impairment of ocular dominance plasticity, at least in moderate cases[428]. In neurons of the auditory cortex, abnormal tuning characteristics were observed following the hypoxic-ischemic insult[429]. Based on my results and previous work, I expect that subplate damage rarely occurs in isolation. In almost all studies using the rat preterm model, damage in the cortical white matter has been described (Table 8_2). White matter injury not only involves oligodendrocytes but can also cause damage to developing axons and lead to a subsequent degeneration of projection neurons. Labelling of the thalamocortical and corticothalamic axons with DiI did not reveal any gross impairment of these pathways following hypoxia-ischemia[234], however, this does not preclude more subtle pathological changes in these connections.

In addition to the damage in white matter, I have shown here that cell degeneration in the deep layers VI and V often accompanies injuries in subplate and similar observations have been previously described[240, 434]. It appears therefore simplistic to attribute all functional impairment caused by hypoxia-ischemia to a loss in subplate neurons alone[429]. The damage in the white matter, other deep layers and subcortical structures such as the thalamic reticular nucleus[234] all need to be taken into account when interpreting functional data.

8.4.5 Variability within models and between models

In the first model here described, we observed a great variability between individual animals in the severity of the damage following the hypoxic-ischemic insult, and similar variability has been previously reported[234,428]. In the first model, the experiments were performed on littermates of male rats and great care was taken to minimize variability in animals' rearing, surgical procedures, body temperature and post-operative care. I did not find a correlation between the animals' body weight before the hypoxic-ischemic treatment and the severity of the outcome (Pearson correlation coefficient = 0.012). It is therefore likely that the inter-animal variability is linked to other parameters such as individual differences in blood pressure,

development of cerebral blood vessels and presence of collaterals.

In the second model, in contrast, the variability between animals was much reduced and I did not find any damage in either cortical grey or white matter of any of the brains analyzed. The two models are very similar (see Table 8_1) and mainly differ in the temperature maintained during the hypoxia (34°C in the first model and 37°C in the second model). A temperature reduction from 37°C to 34°C during the hypoxia has been shown to be neuroprotective as it led to a reduction in the frequency of brain injury in P7 rats[435] and provided partial protection from metabolic failure in adult rats[436]. Based on these studies, we could expect more frequent or more severe damage in our second model than in our first, but the opposite was the case.

Even though the same age (P2) and strain (Sprague-Dawley) of rats has been used for both models, the average body weight before the surgery was significantly higher in the first model (9.2 g) than in the second model (7.4 g, $p < 0.001$, unpaired t-test). A smaller body weight has been correlated with delayed thalamocortical maturation[437], and less mature brains are less vulnerable to hypoxic-ischemic insults[240]. It is therefore conceivable that the animals in the second model are less affected than those in the first model because their brains are less developed.

In addition to this current work, at least six independent studies have been conducted on models of preterm hypoxia-ischemia and their parameters and main findings are summarized in Table 8_2. Even though all models work with rats between P1-P3, the resulting injuries are different in each model. Most commonly, however, damage is observed in the periventricular white matter (five out of seven studies) and in the deep cortical layers including subplate (four studies). The many differences in outcome for these similar models indicate that many parameters including strain, exact age, body weight, sex, body temperature and duration and severity of the hypoxia can make an important difference for the animal.

The variability observed between individual animals within one model and between different models makes it more difficult to draw conclusions but also reflects the variability observed in human pathology. For instance, a recent study on hypoxic-ischemic encephalopathy in preterms describes that one-third of the infants had normal outcomes, one-third died and one-third showed impairments ranging from mild motor delays to severe cerebral palsy[438]. Animal models of preterm hypoxia-ischemia could therefore be a useful tool to further study the intrinsic and extrinsic factors determining the large variability of the outcome of a hypoxic-ischemic insult.

Age	Strain	Parameters of HI	Survival rate	White matter injury	Cortical injury	Reference
P1	Sprague Dawley	Right CCA coagulation, 6% O_2, 3.5h, 37°C	74% (23/31)	Edema and necrosis in the periventricular white matter	Neuronal loss and cystic necrosis; most severe damage in layers III-V	Sheldon et al., 1996
P2/P3	Wistar	Right CCA ligation, 5% O_2, 30min, 34°C	100% (10/10)	none	none	Towfighi et al., 1997
P2/P3	Wistar	Right CCA ligation, 5%O_2, 1h, 34°C	53% (16/30)	n.a.	columns of dead cells, sometimes fused into larger infarcts, mainly in deep cortical layers	
P2/P3	Wistar	Right CCA ligation, 5% O_2, 1.5h, 34°C	0% (0/10)	-	-	
P3	Wistar	Right CCA coagulation, 6% O_2, 30min, 37°C	91% (23/25) Sizonenko et al., 2003	loss of myelination in the intracortical white matter, clumping of fibers ; increase in early OL progenitors and numbers of mature OLs in the area of injury	Scattered or confluent columns of degenerating cells; majority of injury in deep layers (VI and SP); axonal injury in the deep and middle layers (IV, V, VI and SP)	Sizonenko et al., 2003; Sizonenko et al., 2005; Sizonenko et al., 2008
P3	Sprague Dawley	Left CCA coagulation, 6% O2, 15min, 37°C	88% (100/114)	n.a.	Neuronal death in all cortical layers plus thalamus and basal ganglia	Stadlin et al., 2003
P2	Sprague Dawley	Left CCA ligation, 6% O_2, 4h, 37°C	n.a.	Selective degeneration of late OL progenitors; increased late OL progenitors in the area of lesion; reactive OLs	n.a.	Back et al., 2001
P1/P2	Sprague Dawley	Right CCA coagulation, 5.6% O_2, 3h, 37°C	75% (48/64)	Extensive cell death in the periventricular white matter and the internal capsule (ISEL)	Moderate to near-complete death of the SP (ISEL, BrdU), other cortical layers mostly intact	McQuillen et al., 2003

Table 8_2. **Parameters and major findings of preterm hypoxia-ischemia models previously described in the literature.** HI: hypoxia-ischemia; CCA: common carotid artery; SP: subplate; BrdU: Bromodeoxyuridine; OL: oligodendrocyte; ISEL: in-situ end labeling (a method to label apoptotic cells); n.a.: not analysed.

8.5 Conclusion

In this chapter, I confirmed that subplate cells (identified by Nurr1 and Cplx3 gene expression) are affected in moderate and severe cases of a rat model of preterm hypoxia-ischemia. However, these subplate cells appear not to be more vulnerable than other deep layers or the white matter as they generally are damaged together. This should be kept in mind when interpreting functional outcome of hypoxic-ischemic models.

Chapter 9 Discussion

9.1 Summary of my major findings

The work presented in this thesis aims to contribute to our understanding of the role of subplate in normal and pathological cerebral cortical development. One of the long-term goals is to correlate the changing gene expression patterns in the subplate zone to changing properties and functions of subplate neurons or other subplate components (e.g. ECM, fibres) across several developmental stages (Fig 9_1). This approach will help us to recognize important molecular mechanisms underlying known subplate functions and could also lead to the discovery of additional, currently unknown roles for subplate cells. Moreover, these gene expression analyses can provide use with valuable molecular markers to identify and specifically manipulate subplate cell populations at different developmental stages[117]. These markers will constitute an important tool to further elucidate subplate functions in normal development and to monitor subplate cells in pathological conditions. If they can be validated for human, such markers could eventually be used in pathological diagnosis in clinical setting[439].

In the first part of my thesis, I contributed towards this larger aim by establishing a gene expression profiling of the embryonic E15.5 mouse subplate using an optimized protocol for laser capture microdissection combined with microarray analysis. This led to the identification of approximately 250 genes which are possibly higher expressed in the subplate than in the overlying lower cortical plate at E15.5. Using immunohistochemistry or in situ hybridization, I was able to confirm the enrichment of 13 genes out of 23 selected in the E15.5 subplate zone (*Abca8a*, *Cdh10*, *Cdh18*, *Csmd3*, *Gabra5*, Kcnt2, *Ogfrl1*, *Pls3*, Rcan2, *Slc8a1*, Sv2b, *Unc5c* and *Zdhhc2*). Besides *Gabra5* which has been described as preferentially localized to subplate in the adult rat[353], none of these genes has been previously associated with the subplate compartment. Publicly available gene expression datasets were available for 12 out of 13 genes but for half of them expression patterns were either difficult to localize or absent. Further evidence that these genes are indeed expressed in subplate cells was gained from analysis of reeler mutant brains. In the reeler cortex, the expression of a majority of genes (9 out of 13) was shifted in accordance with the shifted position of subplate cells while the remaining genes showed no longer any clear expression pattern.

A detailed spatio-temporal analysis of the cortical and extracortical expression profile of these identified genes allowed me to formulate more detailed hypotheses on their possible function in the embryonic subplate. While several genes likely contribute to the general maturation of subplate and other cortical neurons (Sv2b, Kcnt2 and Csmd3) others might underlie some of the distinct electrophysiological properties of subplate cells (Gabra5, Slc8a1 and

Zddhc2) or regulate axonal sprouting and growth (Pls3, Cdh10, Cdh18, Unc5c).

Cdh10 and Unc5c were chosen for further functional analysis based on their strong and specific expression in the E15.5 subplate and their interesting potential molecular function. For Cdh10, preliminary results from knock-down experiments where shRNAs were electroporated *in utero* into subplate cells suggest that this gene could play a role in organizing the subplate into a tightly packed, distinct layer separated from the rest of the cortical plate. For Unc5c, I hypothesized that it could be mediating the waiting period of subplate axons within the internal capsule as netrin-1 (the ligand of Unc5c) is strongly expressed in the mantle zone of the internal capsule[41,42]. However, preliminary results from culture experiments where slices from E14.5 Golli-tau-eGFP brains (where eGFP is expressed in neurites of subplate and some layer VI cells)[72] were incubated with a blocking antibody against Unc5a/c did not show any evidence for such a role.

The aim of the second part of my thesis was to make use of some recently identified markers for postnatal subplate cells to monitor subplate cell populations in a model of preterm hypoxia-ischemia where a selective vulnerability of subplate had been previously described[234]. In a first instance, I analyzed a range of subplate markers identified in the mouse in the postnatal and adult rat cortex as the rat is the predominantly used species for hypoxia-ischemia disease models. Cplx3, Nurr1, *Ctgf* and *Tmem163* were confirmed to be specifically expressed in the postnatal and adult rat cortex. Like in the mouse[117], Nurr1 and Cplx3 labelled distinct yet overlapping subplate subpopulations in the rat with about two-thirds of Nurr1+ cells co-expressing Cplx3 and half of Cplx3+ cells co- expressing Nurr1. Surprisingly, two further genes which are selectively expressed in the mouse subplate - *TRH* and *MoxD1* - were completely absent from subplate cells in rats. Progesterone receptor and KATI, two genes which had been described as subplate markers in the embryonic and perinatal rat[151, 149], did not show consistently specific subplate labelling in the postnatal rat in my hands.

Immunohistochemistry against Nurr1 and Cplx3 was used to monitor subplate cell numbers in hypoxic-ischemic rat brains and to compare their vulnerability to cells in other cortical layers and the white matter. In line with previous studies, deep cortical layers including subplate and the white matter were more severely affected by hypoxia-ischemia than upper cortical layers[240,434]. However, I did not find any evidence for an increased vulnerability of subplate compared to other deep layers. Comparison of Nurr1+ and Cplx3+ subplate subpopulations suggested that Cplx3+ cells could be more vulnerable than Nurr1+ cells, however, due to the large variability between individual animals further studies would be needed to corroborate this preliminary result.

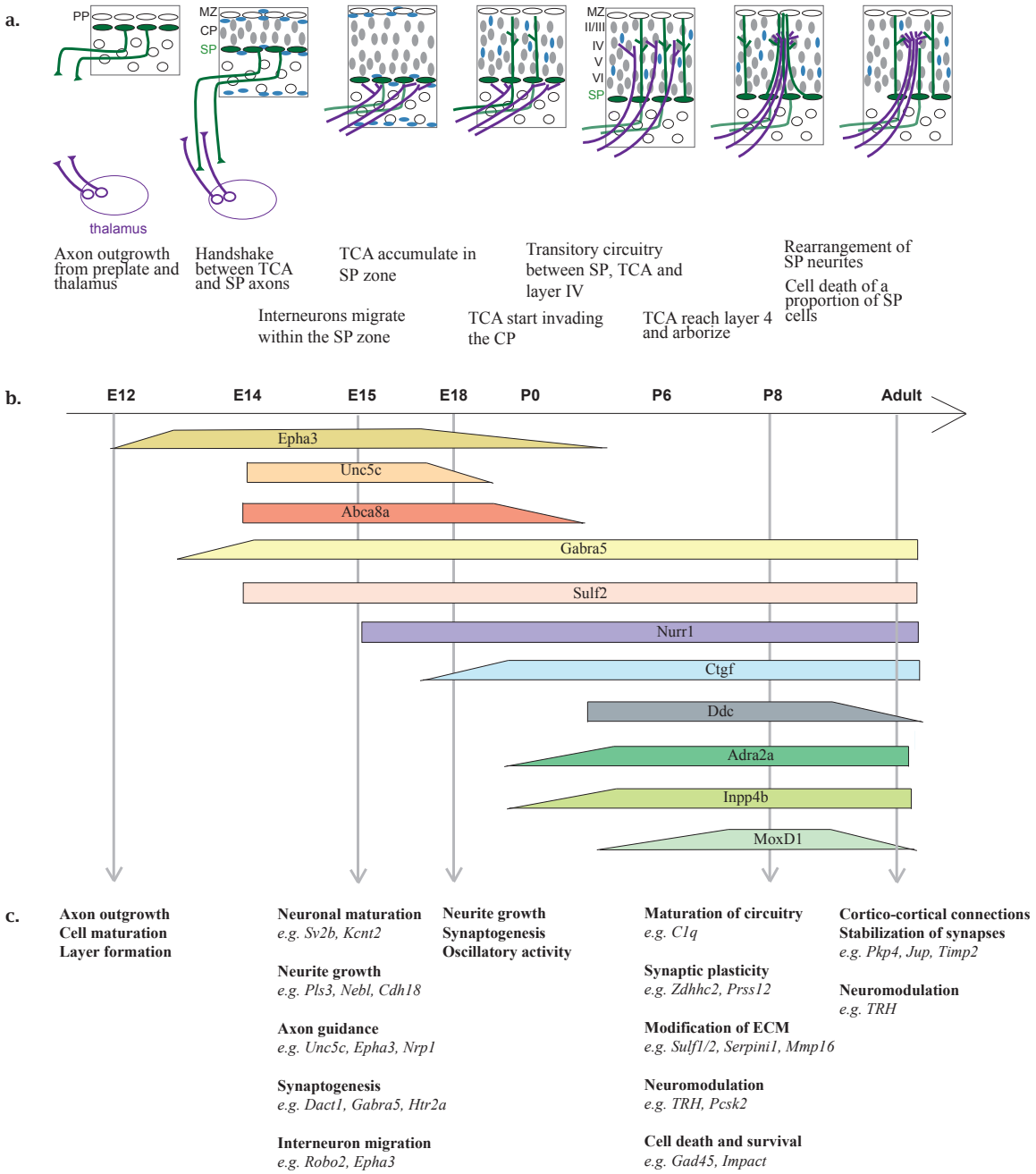

Figure 9_1. **Correlating changing expression in subplate properties and functions with gene expression** (2). This figure gives an overview how cellular and functional changes in the developing subplate (a) are correlated to gene expression (b) and molecular mechanisms (c). Findings from this thesis were used to expand and complete the illustration in Figure 1_9. a. Schema showing the development of the mouse subplate (SP) zone from E12 to adult and its integration in the cortical circuitry. b. Examples of developmental expression patterns of SP-specific genes. Gene expression in SP is very dynamic, reflecting the important developmental changes in this cell population (a). Some genes (e.g. Epha3, Abca8a, Unc5c) are expressed in the embryonic SP but downregulated in the postnatal SP. Inversely, another subset of genes (e.g. Adra2a, Moxd1) is only expressed in the postnatal SP. Yet other genes show a SP-enriched expression over a relatively long developmental period (e.g. Gabra5, Sulf2, Nurr1). c. Functions and developmental processes linked to the SP zone at E12, E15, E18, P8 and adult (the five time-points where gene expression studies have been performed). Examples of subplate-enriched genes which could be related to these mechanisms are given.

9.2 Insights from the gene expression profiling at E15.5

9.2.1 Methodological considerations

To gain insight into molecular mechanisms underlying the unique properties and functions of the embryonic subplate, I aimed to identify genes and gene pathways which are specifically expressed in subplate cells at E15.5 in the mouse. Towards this goal, strips of tissue containing anterior or posterior subplate or lower cortical plate cells were microdissected based on their position in the developing cortex (Chapter 3). The mRNA levels of nearly 30'000 genes were compared between the different samples in four replicates using microarrays-based expression analysis with statistical tests. This approach has several inherent limitations: First, gene expression levels were not compared between subplate neurons and cortical plate neurons but between entire compartments containing also mRNA from migrating neurons, glial cells, axons and dendrites and blood vessels. Second, genes identified as higher expressed in subplate than in the cortical plate are not necessarily specifically expressed in subplate as they could be equally expressed in the subplate and in the intermediate zone or any other cortical structure. Third, as a very large number of genes was compared on the microarray, the number of false-positive findings is necessarily high (i.e. a theoretical 5% for a p-value of 0.05).

The gene expression profiling resulted in a list of over 300 genes with presumed higher expression in subplate. Without a detailed analysis of every gene on this list, the exact number of false-positive findings is of course impossible to determine. However, on publicly available gene expression datasets, approximately one-fifth of the genes showed clear expression patterns which did not involve subplate at E14.5 or E15.5 suggesting that they are false-positives. Other genes on the list were found to be primarily expressed in the intermediate zone, sometimes with additional expression in the subplate (e.g. Plxna4, Nrp1). This is probably partly due to the design of the microarray study (i.e. subplate was compared with lower cortical plate but not intermediate zone) and partly due to the difficulty in distinguishing between subplate and intermediate zone on cresyl violet-stained sections for the microdissections. Finally, a few genes on the list had been previously described as associated with neurons in upper cortical layers (e.g. Tbr2, Cux1) suggesting that they are expressed in cortical plate neurons radially migrating through the subplate zone rather than subplate neurons themselves.

Taken together, these observations emphasize the importance of validating all microarray results with additional methods such as qRT-PCR and in situ hybridization or immunohistochemistry[440]. As multiple comparisons across a large number of genes underlie every microarray study, a high-rate of false-positives is an inherent problem. Many complex statistical methods have been proposed to reduce these errors, often by taking into account and correcting for the co-dependence of genes in the same pathway[441,442]. However, none of these

methods has so far prevailed and been adapted by the wider community. Even with more optimized statistical analyses in place, it will not be possible to completely eliminate false-positive results.

Shimogori et al. have recently conducted a microarray-based gene expression profiling of the developing hypothalamus. In order to confirm their microarray results, they performed high-throughput in situ hybridization against more than 1000 genes followed by high-quality, two-colour in situ hybridizations against approximately 350 selected genes[443]. As such an approach was beyond the scope of this study, publicly available gene expression databases constituted an invaluable tool for the initial assessment of gene expression patterns. However, these datasets are generated by semi-automated in situ hybridizations and are not optimized for each individual gene. Indeed, using my own optimized situ hybridization I was able to confirm two genes (Abca8a and Csmd3) as specifically expressed in subplate which do not show any expression on images from Genepaint. As publicly available gene expression data is rapidly expanding, more and higher quality images from several sources will most likely become available in the near future. In addition, algorithms which associate gene expression automatically with cortical layers and other structures are being developed and will further facilitate this task.

9.2.2 Molecular mechanisms underlying subplate functions

The main aim of the performed gene expression analysis was to gain insight into molecular mechanisms underlying known and unknown subplate properties and functions. To objectively assess the subplate-enriched gene list for functional categories, I used gene ontology analysis software (DAVID[318]) after having excluded false-positive findings (see above). Gene ontology analysis is limited by the fact that many terms associated with a given gene are very broad (e.g. development, disease, phenotype) or are not specific to any particular system, i.e. in my case to the nervous system. The later constitutes a particular challenge as many genes and proteins are pleiotropic, i.e. they play different roles in different tissues, cell types or even subcellular domains[444,445]. The discovery and incorporation of tissue- or cell-type specific gene information into ontology databases will hopefully lead to a more refined approach in the future.

Despite these limitations, gene ontology analysis revealed several functional gene groups which match well with the known characteristics and functions of the developing subplate. These include genes involved in focal adhesions (i.e. the interactions between cells and the ECM), axogenesis and axon guidance and regulation of transcription (Table 3_2). Of particular relevance are genes associated with axon guidance as this is the most clearly demonstrated role of the embryonic subplate[175,179,176] (see section 1.5.2). Out of eight genes associated with

this term, however, six appear to be expressed both in the subplate and the intermediate zone based on publicly available gene expression data and/or my own in situ hybridization analyses (Epha3, Robo2, Nrp1, Plxna4, Unc5d and Sema6d). Nevertheless, they could play a role in the establishment of thalamocortical connections as has been suggested for Epha3[446] and Robo2[322]. In addition, these guidance systems could also be involved in regulating cell migration, in particular of tangentially migrating interneurons which are present both in the intermediate zone and subplate at this stage[93]. Indeed, such a role has been previously demonstrated for Robo2[323].

Unc5c is the only one out the eight genes associated with axonal guidance which is specifically expressed in subplate at E14.5 and E15.5. Unc5c in combination with Dcc has been shown to mediate repulsion from a source of netrin-1[368]. As netrin-1 is expressed in the embryonic internal capsule, Unc5c could mediate the waiting period of subplate axons in the internal capsule (Fig 6_3). A similar role has very recently been proposed for semaphorin receptors[52]. However, preliminary experiments where I blocked Unc5c with an antibody did not show any accelerated growth of corticofugal axons in embryonic slice cultures after 24h (Fig 6_5). Additional culture experiments as well as the analysis of the timing of corticofugal axon growth in Unc5c KO mutants[352] could corroborate these findings (see section 6.3.4 for details). If additional data confirms that Unc5c is not involved in regulating the growth of corticofugal subplate axons, additional roles for Unc5c should be explored. For instance, recent studies have suggested a role of netrin-1 in guiding interneuron migration[371] and an involvement of Dcc and Unc5 receptors in regulating apoptosis[415,414,416] (see Chapter 6, section 6.3.4).

Besides axon guidance, two further functional gene categories highlighted by the gene expression ontology analysis could be of particular interest. The first is "signalling through the serotonergic receptor 5HT2". Based on the microarray analysis, the E15.5 subplate expresses high levels of the serotonergic receptor subtype 2a (Htr2a), a G-protein coupled receptor. In addition, subplate cells also appear to specifically express the G-protein subunits Gng5 and Gng11 which could be mediating the signalling through Htr2a. Monoaminergic afferents (which include serotonergic fibers) have been described to form a dense network within the subplate zone at E15[77,70], but whether they form synapses with subplate neurons has not been elucidated. The expression of Htr2a in the E15.5 subplate cells (which remains to be validated) would strongly suggest that such functional connections are present. A recent study has reported strong expression of Htr2a in the subplate as well as in pyramidal neurons in layer V and interneurons in the middle layers in young postnatal and adult rats[447]. Using electrophysiology, it should be possible to study at least in postnatal animals whether functional serotonergic inputs into subplate neurons are present, as has been previously demonstrated for glycinergic and cholinergic inputs[82,107].

The second interesting functional category is "positive regulation of immune response". There is increasing evidence that many proteins that were first discovered in the immune system are also present in the developing and adult brain under normal, non-pathological conditions (reviewed in [445]). These immune proteins are expressed in neuronal and non-neuronal cells and are believed to play non-immunological roles in the nervous system. Proposed functions for some of these immune proteins include neurite guidance (e.g. DSCAM[448,449]), activity-dependant synapse refinement (e.g. MHCI[450], C1q[451]), regulation of synaptic transmission (e.g. TNFα[452]) and structural and functional plasticity (e.g. MHCI[450,453]). Among other immune proteins, two genes coding for subunits of the complement component C1q (i.e. C1qb and C1qc) are enriched in subplate in the E15.5 microarray list (Table 3_2). C1q has been found to be expressed in the postnatal but not adult brain including the neocortex and to co-localize partially with synaptic markers, at least in the retina[451]. In the retinogeniculate pathway, C1q is necessary for synapse elimination which underlies activity-dependant synapse refinement[451]. In the immune system, C1q initiates the complement cascade leading to the lysis of bacteria and other foreign cells targeted for elimination[454]. It therefore seems that in the brain, C1q and possible other complement components mediate an analogous mechanism through which cellular materials marked for destruction are eliminated[445,455]. It should be interesting to examine whether C1q plays a similar role in the developing subplate, in particular as C1qb and C1qc appear also to be enriched in the P8 subplate according to the P8 gene expression profiling. This is the peak of neurite rearrangement observed in the barrel field of the Golli-tau-eGFP mouse model[96] and the retraction of subplate dendrites from the marginal zone[95]. This suggests that in the subplate, C1q could be involved both in the elimination of exuberant neurites and synapses as well as those subplate neurons which die through apoptosis around the end of the first postnatal week.

Out of approximately 250 genes with presumed higher expression in subplate, only a small subset was analyzed in more detail in this study (23 genes were selected of which 13 could be validated). There are many other genes with promising expression patterns and/or potentially relevant functions which could be further explored. Besides the aforementioned Htr2a, C1qb and C1qc, these include Pde1a, Psk2 and March1 which all show subplate-specific expression at E14.5/E15.5 on publicly available gene expression images (see Figure 3_3a for Pcks2 and Pde1a expression).

Pde1a is a calmodulin-dependant phosphodiesterase which preferentially hydrolyzes cyclic GMP and could thus be involved in many signalling pathways. In vascular smooth muscle cells, Pde1a appears to be regulating cell growth and survival, probably through the inhibition of beta-catenin[456], but whether Pde1a plays a similar role in the brain remains to be elucidated.

The prohormone convertase Pcsk2 (aka Pc2) has been shown to be involved in the generation of a number of different neuropeptides including choleocystokinin (Cck), neuropeptide Y (Npy), thyrotropin releasing hormone (TRH), enkephalin and vascular growth factor (Vgf)[457,458,459]. As many neuropeptides including Cck and Npy are exclusively or primarily expressed in interneurons in the neocortex[130,460,461] it would be interesting to verify whether Psck2 is expressed in GABAergic or glutamatergic neurons. Based on in situ hybridization images (Fig 3_3a), however, it seems unlikely that Psck2 is specific to interneurons for two reasons: 1) Psck2 appears to be expressed by a large proportion of subplate cells while GABAergic cells are relatively sparse in the subplate (see Fig 5_6 a); 2) At E15, Psk2-positive cells are exclusively found in the subplate and not in the marginal and intermediate zones where large populations of migrating GABAergic cells are localized. The involvement of Psck2 in the production of TRH is particularly interesting as I have shown in Chapter 7 that TRH is specifically expressed in the subplate in the postnatal and adult mouse (Fig 7_2 e,f). As a first step, potential co-localization of TRH and Psk2 should be examined. Further, as TRH is not expressed in the rat subplate, it could be informative to analyze Psck2 expression in this species. In any case, the specific expression of Psk2 in the embryonic subplate could indicate that these cells influence the developing cortical circuitry not only through synaptic input[144,145] but also neuropeptide release.

March1 is a membrane-associated ubiquitine E3 ligase. In monocytes and dendritic cells, March1 ubiquitinylates and down-regulates MHC class II proteins. As discussed above, there is increasing evidence for a role of immune proteins in brain development. MHC class I proteins have been shown to be expressed in neurons and to be spatially and temporally regulated[445]. There is currently no such data for MHC class II proteins but it could be interesting to analyze their expression in the developing cortex in relation to the expression of March1.

9.2.3 Novel embryonic subplate markers

An additional objective of the gene expression profiling was the identification of "molecular markers" which could allow us to monitor and potentially manipulate subplate cells at an early embryonic stage. An ideal marker gene should be expressed exclusively in subplate cells over a relatively long developmental period. Moreover, a specific antibody for immunohistochemistry should be available which would allow additional analyses such as combination with other markers, birth-dating or tracing. As the subplate cells are a heterogeneous population, this combinatorial approach could help to define and characterize different cell subpopulations within the embryonic subplate. Similar work has been described for the postnatal mouse subplate[117,284] and is still ongoing (Hoerder-Suabedissen et al., in preparation). Finally, the specific presence of a membrane-bound protein on subplate cells could allow us to isolate these cells using cell-sorting techniques (immunopanning, FACS) or to specifically ablate

them using immunotoxicity. In the late embryonic rat and cat, antibodies against $p75^{NTR}$ have been successfully used for these purposes. However, $p75^{NTR}$ appears not to be subplate-specific in the mouse (see also Chapter 2, section 2.1).

Out of the 13 subplate-enriched genes analyzed from the microarray screen, Abca8a, Cdh18, Gabra5 and Pls3 are the most promising potential markers for the embryonic subplate. Within the neocortex, Cdh18, and Pls3 are specifically expressed in subplate from E14.5 to E15.5, Gabra5 from E13.5 to E15.5 and Abca8a from E14.5 until at least E17.5 (Fig 5_1 and 5_3). For Gabra5, a specific antibody has been developed and described in the postnatal rat[353] while for Cdh18 and Pls3 antibodies are commercially available (anti-Cdh18, ab64869; anti-Pls3/T-plastin, ab45769; Abcam). To my knowledge, no antibody specific to Abca8a is currently available. I have briefly tested all three available antibodies and found staining of the subplate with anti-Cdh18 and anti-Gabra5 but not with anti-Pls3 (data not shown). After further optimization, these antibodies could become useful tools label and study embryonic subplate cell populations. Gabra5, Abca8a and Cdh18 are all membrane-bound proteins with extracellular domains. A specific and reliable antibody against any of these proteins might allow us to perform ablation and cell-sorting experiments on the early embryonic subplate. Finally, transgenic animals where GFP and/or *Cre* recombinase are expressed under the promoter of Gabra5, Cdh18, Abca8a or Pls3 might become available and could constitute powerful tools for the further characterization of the early embryonic mouse subplate in the future.

9.3 Comparison of subplate gene expression data across different developmental ages

Including the microarray study described in this thesis, five gene expression analyses on subplate have been performed at different developmental stages: E12[153], E15.5, E18.5[95], P8[95,117] and adult (P56, Belgard et al., submitted). Our long-term goal is to correlate the changes in gene expression patterns to changes in subplate properties and functions across development as this constitutes a powerful approach to identify molecular mechanisms important for known and unknown subplate characteristics (Fig 9_1). Similar studies have been conducted to illuminate molecular mechanisms specifying the neuronal cell types in layer V[462,463] or the development of the hypothalamus[443] or to classify neuronal populations in the forebrain[464]. An exhaustive comparison of all the subplate gene expression datasets is beyond the scope of this thesis, but I will discuss some initial insights in the following paragraphs.

9.3.1 Methodological considerations

A major obstacle for the comparison of the different subplate gene expression datasets is the fact that they were generated over a period of four years using different methods (see Table 9_1 for an overview). For the E12 study, preplate cells were purified using FACS on two different eGFP-expressing mouse lines: Pde1C-eGFP where all preplate cells express eGFP and Girk4-eGFP where only preplate cells destined for the marginal zone are eGFP-positive. By comparing gene expression in the two cell populations, genes expressed in the preplate cells destined for the subplate were indirectly deduced[153]. For all other ages, the subplate zone was dissected based on its location rather than gene expression either using laser capture microdissection (E15.5) or manual dissection (E18.5, P8, adult). However, due to smaller amounts of starting material obtained by laser microdissection, different amplification methods and microarray chips were used for E15.5 than for E18.5 and P8. The adult gene expression data was not generated by microarray but by deep sequencing (RNA-seq)[465]. These methodological differences make it impossible to directly compare raw gene expression levels across different ages. The exception are the E18.5 and P8 datasets which were generated in parallel using the same methods and for which a direct comparison is possible and has been partially completed[95]. Even though mRNA levels cannot be compared between most datasets, it will still be informative to compare lists of subplate-enriched genes across different ages.

	E12	**E15.5**	**E18.5**	**P8**	**Adult** (P56)
Isolation method	FACS	Laser capture microdissection	Manual dissection	Manual dissection	Manual dissection
Cortical area	Whole cortex	Anterior cortex	Putative S1	S1	S1
Layer comparison	Whole preplate vs MZ	SP vs lower CP	SP vs LVI	SP vs LVI	SP vs L I-III, IV, upper V, lower V, VI
Amplification method	Affymetrix Two-cycle labeling kit	NuGEN Ovation™ Pico system	Affymetrix Two-cycle labeling kit	Affymetrix Two-cycle labeling kit	none
mRNA analysis	Affymetrix Mouse 430 2.0 arrays	Affymetrix Mouse Gene 1.0 ST arrays	Affymetrix Mouse 430 2.0 arrays	Affymetrix Mouse 430 2.0 arrays	Illumina Genome Analyzer IIx RNA-Seq
p-value, fold-change	0.05; 1.5	0.05; 1.4	0.05; 1.5	0.05; 1.5	n/a
Reference	Osheroff and Hatten, 2009	My thesis	Hoerder, 2007	Hoerder-Suabedissen et al., 2009	Belgard et al., submitted

Table 9_1. **Different methods used for sample isolation and mRNA quantification in the E12, E15.5, E18.5, P8 and adult subplate gene expression analyses.** S1: primary somatosensory cortex; MZ: marginal zone; SP: subplate; CP: cortical plate; L: layer

9.3.2 Comparison of gene expression datasets

To obtain an overview of the diversity and similarities of the different datasets, I compared the entire lists of subplate-enriched genes from the five different time-points. Ideally, this should have been done on lists where false-positive genes were excluded (see above) but to verify all the genes on all the lists was beyond the scope of my study. Figure 9_2 gives an overview of the number and proportion of subplate-enriched genes which are unique to each age and shared across different ages, respectively. This comparison shows that a majority of genes (approximately 60-90%) are only enriched in subplate at one developmental time-point. This supports the viewpoint that the developing subplate is a very dynamic compartment and that different molecular mechanisms are important at different developmental stages. The E12 microarray data has the least overlap with the other datasets (only just over 10% of genes are shared at least with one other age) while the E15.5 data has the largest general overlap (more than 40% of genes are also present in at least one other dataset). This could indicate that many subplate-specific genes start to be expressed after the preplate splits i.e. around E14/E15. Indeed, a similar observation was made for subplate-specific genes identified from the E15.5 microarray: Out of 13 genes which are specifically expressed in the E14.5 and E15.5 subplate only Rcan2 was also expressed in the preplate (probably in Cajal-Retzius cells; see Chapter 5, sections 5.3.3). All other twelve genes were either not expressed in the E13.5 cortex or only in the most lateral part where the preplate had already been split into subplate and marginal zone (see Figures 5_1, 5_2 and 5_3 and section 5.3.1). However, the small overlap of the E12 datasets with those at other ages also likely reflects to some extent the different methods used as the E12 cell separation approach is very different from the one chosen for the other stages.

Not surprisingly, the largest overlap of genes was found between datasets at E15.5 and E18.5 (19% of E15.5 genes), E18.5 and P8 (13% of E18.5 genes) and P8 and adult (5% of P8 genes), respectively. It is reassuring that there is a similar overlap between data from E15.5 and E18.5 as between E18.5 and P8 as this indicates that the different methods used for subplate isolation (i.e. laser microdissection vs manual dissection) and mRNA quantification do not seem to have introduced an important bias. Only few genes appeared to be enriched in subplate samples across more than two developmental stages (see Fig 9_2): 2 genes were found to be subplate-enriched from E12 to E18.5, 13 genes from E15.5 to P8, 10 genes from E18.5 to adult and 4 genes from E15.5 to adult. These genes are particularly interesting as they are likely involved in mechanisms underlying fundamental subplate properties. Among these genes are also Nurr1 (in the E15.5, E18.5, P8 and adult datasets) and Ctgf (in the E18.5, P8 and adult datasets), two known markers for the embryonic and postnatal subplate[117]. Previously, it has been shown that Nurr1 is expressed in the subplate from E15 onwards (see also Fig 2_2) and Ctgf from E18 onwards. This corresponds very well with

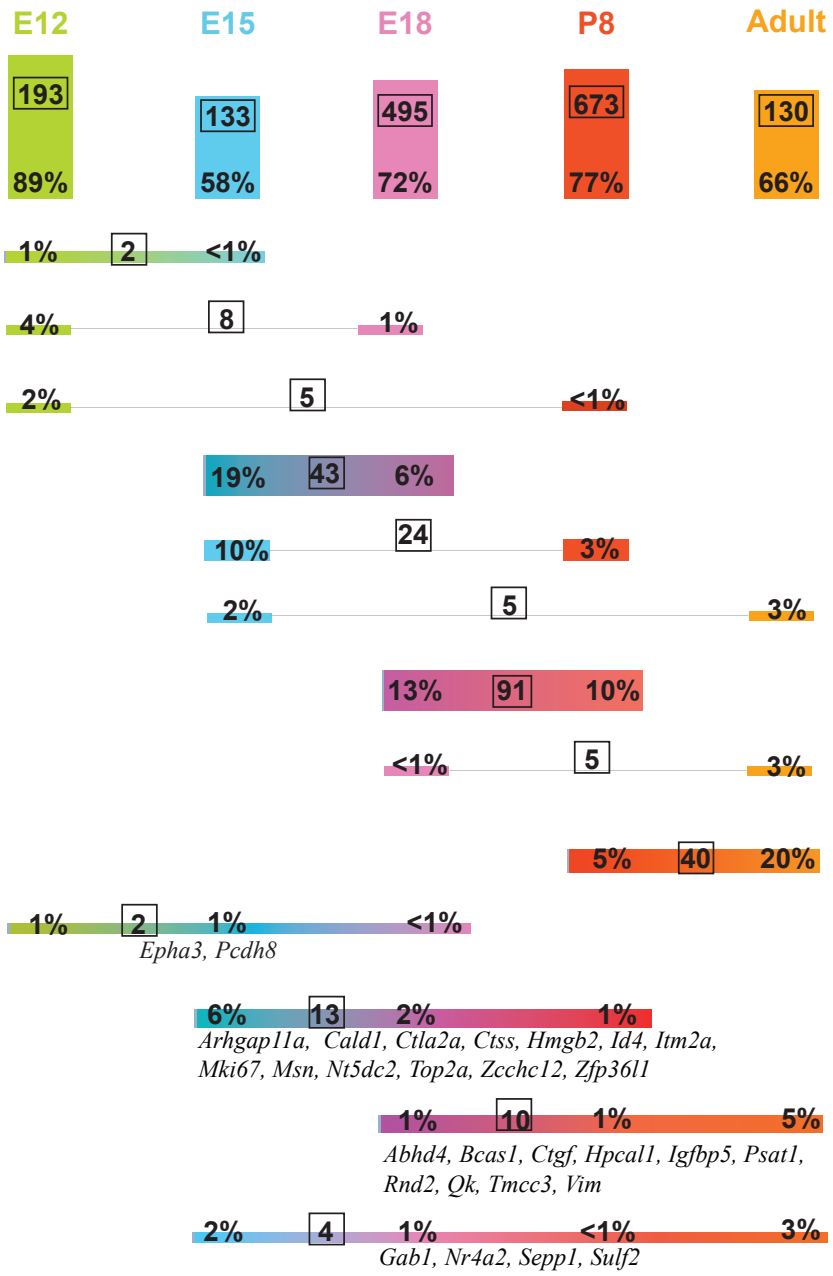

Figure 9_2. **Comparison of subplate gene expression datasets at the different developmental stages.** This schema gives an overview of numbers (boxed) and percentages of genes which are unique to each of the five datasets (E12: green; E15: blue; E18: purple; P8: red; adult: orange) and shared between two or more datasets, respectively. The thickness of the bars reflects the proportion of genes represented. The majority of genes was found in one dataset only (row 1). The largest overlap was found between the datasets of E15 and E18, E18 and P8 and P8 and adult, respectively (rows 5, 8 and 10). Only few genes were shared between more than two datasets and their names are given (rows 11-14). Percentages do not add up to 100% because a few genes with more complex distributions were omitted from the schema.

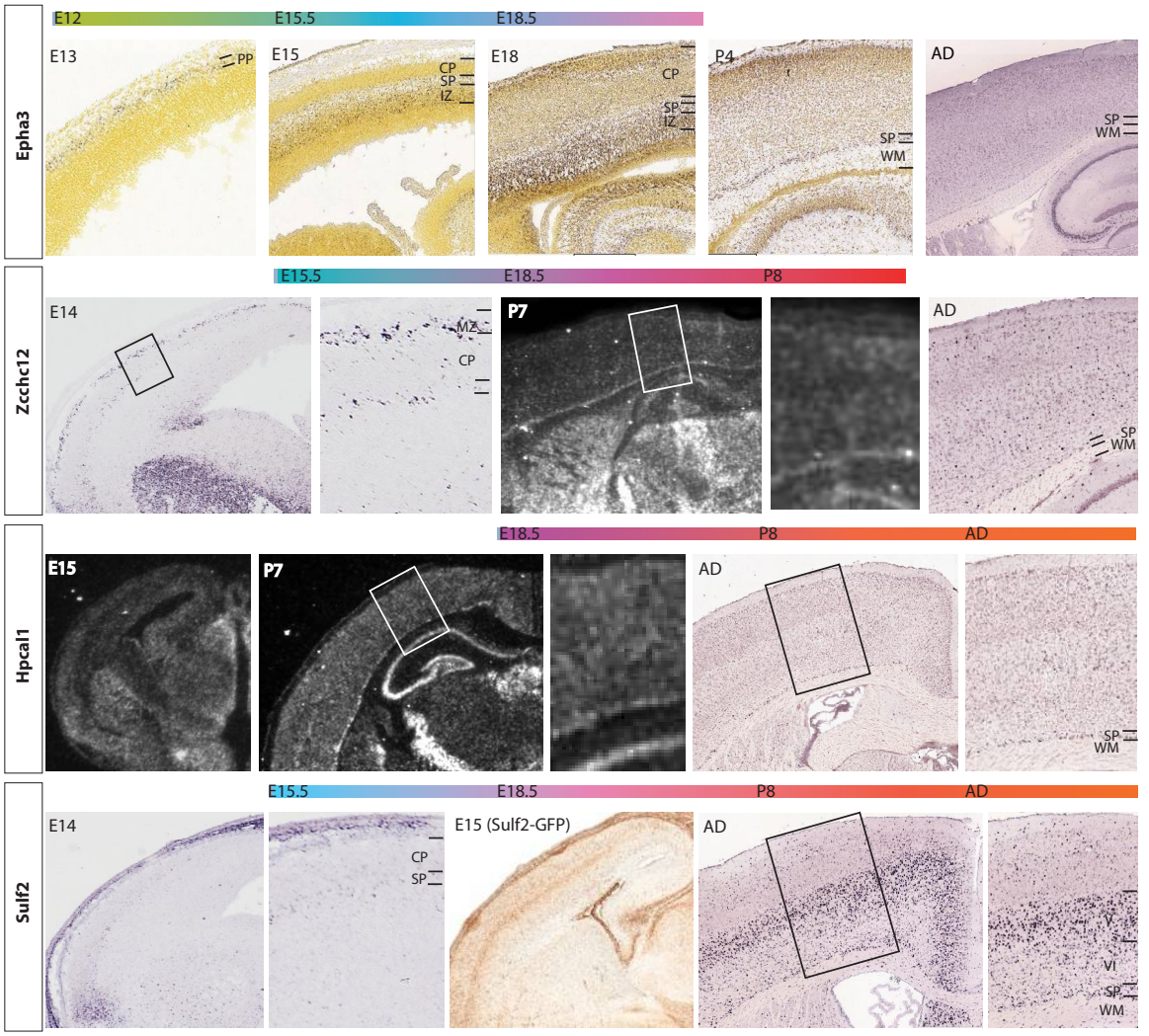

Figure 9_3. **Examples of genes with subplate-specific expression over a long developmental period.** In situ hybridization images from Genepaint (Zcchc12 E14 and Sulf2 E14), Gensat (Zcchc12 P7, Hpcal1 E15 and P7, Sulf E15) and AllenBrainAtlas (all others). Bars at the top of the panels indicate in which gene expression datasets each gene was found to be subplate-enriched. For all four genes, in situ hybridization data confirms the temporal expression profile predicted by the gene expression data.

the time-points where these genes were detected as enriched in subplate using microarray and deep-sequencing which strengthens the validity of this approach. Fig 9_3 shows public available in situ hybridization images of a few further genes with subplate-enriched expression over a relatively long developmental period. Future studies should analyze the expression patterns and functions of these genes in more detail.

9.3.3 Correlating changing gene expression with changing functions

As discussed above, the main reason to compare subplate gene expression datasets at different ages is to correlate changes in subplate functions and characteristics with changes in gene expression (Fig 9_1). Therefore, it is particularly interesting to examine genes with narrow temporal expression windows. Supplementary Table S_3 lists a set of genes from the E15.5, P8 and adult datasets which were only found to be subplate-specific at one developmental time-point. All genes listed have been validated using my own expression data, published results or public available datasets. In situ hybridization images from AllenBrainAtlas[283] of a few examples of genes with such a tight temporal regulation are shown in Fig 9_4. For instance, the beta-catenin antagonist Dact1 (from the E15.5 dataset) is strongly expressed in the preplate at E13 and weakly in the subplate and marginal zones at E15. At later developmental stages (E18, P4), Dact1 is specifically expressed in layer V and appears to be completely downregulated in the adult cortex (Fig 9_4 A). In contrast, the adrenergic receptor Adra2a and the inositol-phosphate phosphatase Inpp4b (from the P8 dataset) are not expressed in the embryonic cortex but are strongly and specifically expressed in subplate in the postnatal and adult mouse (P4, adult; Fig 9_4 C, D).

Genes which are only expressed in subplate during a particularly developmental period are likely linked to subplate properties and functions during that stage. The embryonic subplate receives early subcortical afferents including thalamocortical afferents and monoaminergic fibers[63, 70, 77] and establishes early functional synapses[71, 79]. Similarly, cells in the subplate extend some of the first corticofugal axons towards the subpallium[63, 55], and these are believed to be important in the guidance of thalamocortical afferents across the PSPB[175,179] (sections 1.2.2 and 1.5.2). Consistent with these characteristics, the E15.5 subplate shows specifically high expression of several proteins with a putative role in neurite growth, synapse formation and axonal guidance (Supplementary Table S_3; also see sections 4.3.1, 5.4.3 and 5.4.4). Among these genes is the beta-catenin antagonist Dact1 which is localized at the postsynaptic membrane and has been shown to regulate the number and length of dendritic spines in hippocampal neurons[466]. In addition, several genes involved in the regulation of the actin cytoskeleton show enriched expression in the embryonic subplate (Fmrd4a[467], Nebl[468], Pls3[351]). Rearrangements of the actin cytoskeleton likely underlie neurite extension and synapse formation and indeed, a role for Nebl and Pls3 in neurite growth has been demonstrated[468,

[351]. Finally, several receptors for guidance molecules are expressed in the embryonic subplate and intermediate zone (Plxna4, Robo2, Slitrk3, Unc5c) and could play a role in axonal growth and guidance (see above).

The early postnatal subplate cells are highly connected; they receive inputs from thalamic, monoaminergic and cholinergic afferents and project to the thalamus as well as to the ipsi- and contralateral cortex. Postnatal subplate neurons have been suggested to play a role in the synchronization of cortical activity and in the maturation and refinement of the cortical circuits. Subplate might also be involved in regulating synaptic plasticity both through direct synaptic input and the remodelling of the extracellular matrix (see Chapter 1, section 1.5.6). At least a proportion of subplate cells likely undergoes cell death around the end of the first postnatal week in mouse[54] (see Chapter 1, section 1.2.3). Several genes which could be linked to these properties of the postnatal subplate were found in the P8 microarray dataset (Supplementary Table S_3). For example, the important functional input into subplate from different systems is underlined by the specific expression of adrenergic (Adra2a), nicotinergic (Chrna4) and dopaminergic (Drd1a) receptors. A role in synaptic plasticity could be related to the high expression of the matrix metallopeptidase Mmp16 and the sulfatase Sulf1 which are both capable of degrading components of the extracellular matrix. Indeed, Sulf1 has been shown to regulate synaptic plasticity and learning, at least in the hippocampus [469]. Finally, several genes linked to the regulation of cell death and survival are specifically expressed in P8 subplate neurons including growth arrest and DNA-damage-inducible 45 alpha (Gadd45), Imprinted and ancient (Impact) and Paternally expressed 3 (Peg3).

The adult subplate has been poorly characterized but has been reported to be electrophysiologically active at least in mouse[114] and suggested to importantly contribute to cortico-cortical connectivity[110] (Chapter 1, section 1.2.4). Several genes enriched in the adult subplate appear to be adhesion proteins including neural cell adhesion molecule 1 (Ncam1), plakophilin 4 (Pkp4 aka p0071) and junction plakoglobin (Jup). The adult subplate also expresses comparatively high levels of pleiotrophin (Ptn), a growth factor which has been shown to reduce LTP in hippocampal neurons[470]. Similarly, the metalloproteinase inhibitor Timp2 which stabilizes the ECM[471] is enriched in the adult subplate. Together with the adhesion proteins, these molecules could be involved in stabilizing established cortical synapses within and outside of subplate.

Further investigations of the different datasets will be needed to gain a more comprehensive understanding of the gene expression and molecular mechanisms in subplate at different developmental stages (Fig 9_1). The preliminary analysis presented here demonstrates that this approach has the potential to lead to the discovery of important pathways underlying known and less well known subplate functions and properties.

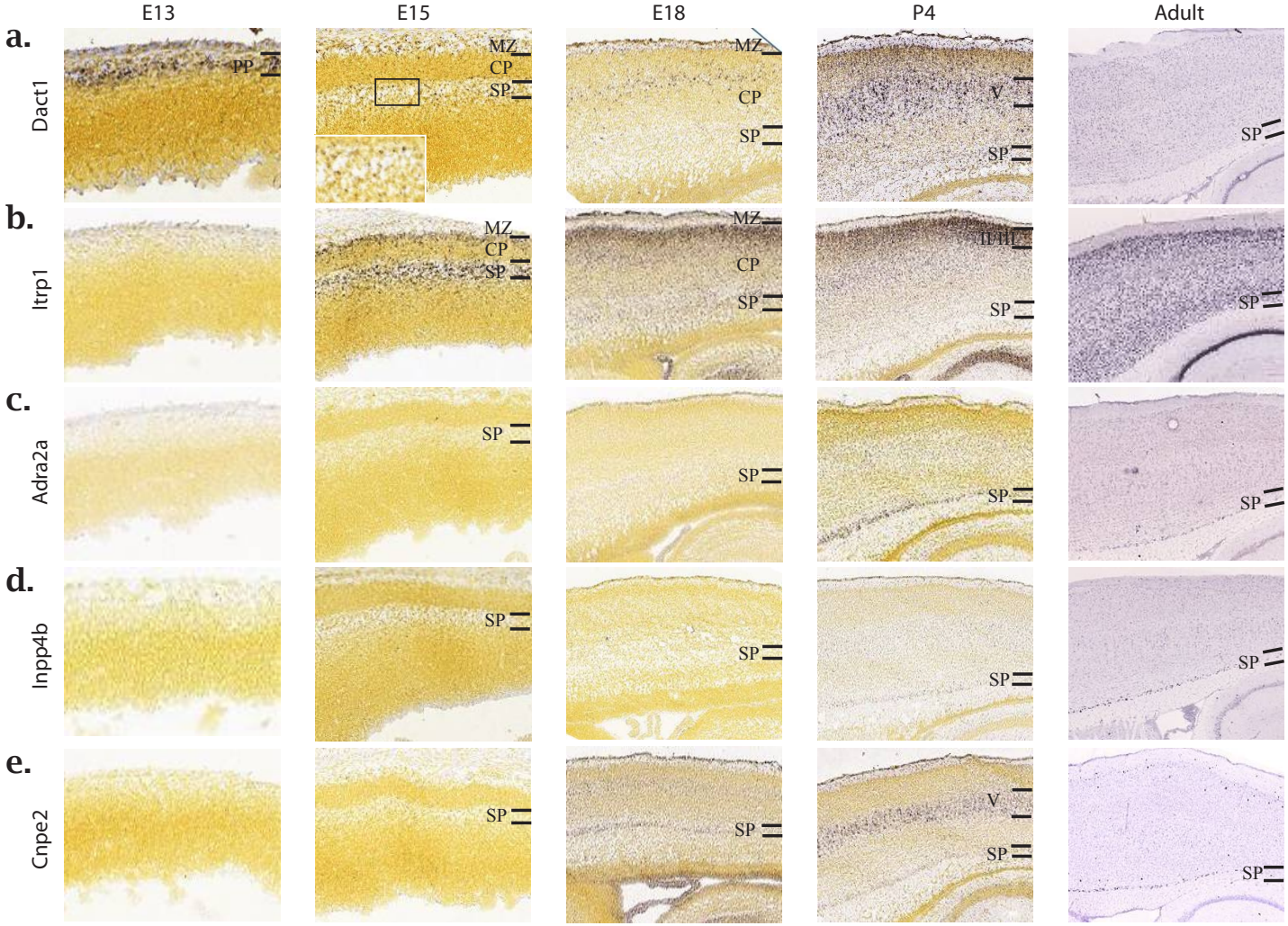

Figure 9_4. **Examples of genes with a subplate-specific expression over a short developmental period.** In situ hybridization images from AllenBrain-Atlas. a. Dact1 is strongly expressed in the E13 preplate (PP) and weakly in the E15 embryonic subplate (SP) and marginal zone (MZ). At E18 and P4, Dact1 is expressed in layer V while in the adult, expression is no longer detectable. b. Itrp1 is not expressed at E13 but strongly present in the SP and MZ at E15. At E18 and P4, the strongest expression is found in the upper cortical plate (CP) and in the adult, the expression appears uniform across all layers. c, d. Adra2a and Inpp4b are not expressed in the embryonic cortex but specifically localized to SP in the P4 and adult. e. Cnpe2 is weakly expressed in SP at E17, strongly in SP and layer V at P4 and specifically in SP in the adult.

9.4 Subplate cells in the pathological development

Subplate has been implicated in neurodevelopmental pathologies, and in particular preterm hypoxia-ischemia[424, 235, 472]. This is not very surprising if we consider that during a long period of human foetal development (from approximately 15-30 PCW), the subplate is the largest compartment in the neocortex[110]. At 15 PCW, the subplate comprises about one-third of the cortical wall in the somatosensory cortex, and continues to increase in size until the beginning of the last trimester (~25-27 PCW) when it is at least four times larger than the cortical plate[110]. It therefore seems very plausible that an insult to the developing brain during this period would also affect the subplate zone.

There is surprisingly little evidence that this is the case. Using diffusion weighted imaging (DWI), it has been shown that perinatal injury in human preterms can sometimes extend from the white matter into the subplate zone[473]. However, this observation remains anecdotal as until now, no imaging study has shown a consistent involvement of subplate in preterm hypoxic-ischemic injuries. Improved MRI technology allows to clearly distinguish the subplate from the underlying white matter and the overlying cortical plate both *in utero*, after birth and post-mortem[474,475,476,477]. More comprehensive imaging studies on subplate involvement in preterm injury using these improved methods are currently ongoing (Mary Rutherford and Petra Hüppi, personal communication).

A pathological study of preterm infants with white matter damage has shown that only a small proportion (~10%) of infants with PVL, a severe form of white matter damage, presented any neuronal loss in the cortical grey matter (this study did not distinguish between subplate and cortical plate)[230]. Gliosis (i.e. reactive astrocytes) in the cortical grey matter was found in approximately 25 % of cases. In contrast, the deep grey nuclei, in particular the thalamus and globus pallidus, and the hippocampus showed substantial neuronal necrosis in ~30% and gliosis in 50-60% of the PVL cases[230]. Similar findings were reported by a second, independent pathological study which found no generalized cell loss in the subplate of infants with PVL[232]. This suggests that substantial lesions in the cortical grey matter including the subplate are uncommon in preterm infants after a hypoxic-ischemic insult. However, a number of studies have reported more subtle changes in the subplate compartment such as an increase in markers of oxidative and nitrative stress[231], a reduction in mature chloride transporters[232] and a decrease of some markers for GABAergic neurons (Gad67, calretinin)[478].

As subplate cells are involved in fundamental developmental mechanisms, even subtle changes in this cell population could potentially have widespread consequences. For example, visual impairments, possibly due to abnormalities in the optic radiations and the visual cortex, are

particularly common in infants with preterm perinatal damage[426, 427]. As the subplate is critical for the establishment of visual thalamocortical connections and the functional modular development of the visual cortex[175, 104], it has been hypothesized that pathological changes in subplate cells could underlie these visual defects[473]. Additionally, it has been proposed that small changes in subplate neuron numbers (in particular GABAergic neurons) could lead to the functional disconnection between different cortical areas characteristic for schizophrenia[264]. Indeed, several studies have found an increase in interstitial white matter neurons at least in some cases of schizophrenia[254,255, 256,258,259,260,261] . There is no direct evidence, however, that subplate cells are causally involved in the development of either of these impairments.

Cell and slice cultures and animal models can constitute useful tools to study neuropathological mechanisms and to test some of the hypotheses outlined above. Subplate neurons in culture (immunopurified using $p75^{NTR}$ antibodies) showed an increased vulnerability to oxygen-glucose deprivation compared to other cortical neurons[147]. Similarly, in a model of P1/P2 rats, hypoxia-ischemia led to substantial and specific cell death in the white matter and subplate[234]. In subplate, an average of 40% of neurons were lost following the insult while cells in the overlying cortical appeared largely unaffected except in the most severe cases[234]. In my thesis, I aimed to extend these findings by determining the vulnerability of different cell subpopulations (defined by marker expression) in subplate and the overlying cortical layers. In contrast to the findings by McQuillen et al[234], I did not find any evidence for a selective vulnerability of subplate neurons compared to neurons in the deep cortical layers (Fig 8_3). Similar findings have been previously reported in similar hypoxia-ischemia rat models where columns of degenerated neurons extending from subplate up to layer V were commonly observed[240, 479]. This suggests, that rodent subplate neurons are not per se more susceptible to hypoxia-ischemia than other cortical neurons. Instead, the increased vulnerability of subplate and deep layer neurons compared to upper layer neurons is most likely linked to their earlier birth-date and increased maturity. It has been shown in several systems that more mature neurons are more vulnerable to excitotoxicity[239, 240,] , probably due to their increased expression levels of glutamatergic receptors and possibly their higher energy requirements. Indeed, injections of an excitotoxin in the late foetal stages of the cat induces selective cell death in subplate[175, 212] while similar injections in the newborn kitten ablates all infragranular layers[241]. In addition, the above-mentioned cell culture study has shown a higher proportion of GluR2- negative AMPA receptors - a configuration which has been linked to increased Ca^{2+} permeability and excitotoxicity[242,243,244]- on subplate neurons than on cortical plate neurons. Consistently, application of an AMPA-receptor antagonist provided greater neuroprotection from glutamate-induced excitotoxicity in subplate than in cortical plate neurons[147].

As in other species, the human subplate contains morphologically mature neurons earlier than the overlying cortical plate[480]. Neurons in the subplate also establish some of the first

synapses in the human cortex[53,110], probably both with other subplate neurons as well as thalamocortical and other subcortical afferents[165]. Consistently, subplate cells express AMPA receptors a few weeks earlier than other cortical cells[238]. These early AMPA receptors do not contain any GluR2 subunits and could thus be involved in mediating excitotoxicity (see above). However, in contrast to rodents and carnivores, primate subplate neurons are generated over a long developmental period, in parallel with neurons of the cortical plate[162,163]. Only a subset of subplate neurons (sometimes called the "presubplate") are remnants of the preplate and thus have an earlier birthdate than cortical plate neurons[481]. Therefore, not all subplate neurons in primates are necessarily more mature than neurons in the cortical plate. This difference between human and rodents might contribute to explain why a large proportion of subplate neurons undergo cell death in the rat model of hypoxia-ischemia but not in human preterms where changes in subplate cells appear to be much more subtle. Additional markers for the early and late generated subplate neurons in humans would be necessary to further study these issues.

Due to the important differences between rodent and human subplate cells in developmental history, thickness and complexity, the value of a rodent model to study subplate pathologies is debatable[481]. It could therefore be useful to investigate alternative model species . Recently, our laboratory has started to examine the subplate in the developing cortex of the pig (*Sus scrofus domestica*). The pig appears to have an elaborate subplate zone that might be subdivided into several compartments similar to the primate subplate (Wanling Tung, M.Sc. dissertation). As pigs and piglets have been relatively widely used for hypoxic-ischemic studies in the past[482,483,484], they might constitute a useful model species for futures studies of subplate injuries. Together with detailed imaging and histopathological studies in human, these animal experiments might give us a clearer insight into the role of subplate neurons in pathological development. Some of my findings on subplate gene expression in rodents might thus eventually lead to clinical translation.

Chapter 10 **Bibliography**

1. Pelvig, D.P., Pakkenberg, H., Stark, A.K. & Pakkenberg, B. Neocortical glial cell numbers in human brains. *Neurobiol. Aging* **29**, 1754-1762 (2008).
2. Azevedo, F.A.C. et al. Equal numbers of neuronal and nonneuronal cells make the human brain an isometrically scaled-up primate brain. *J. Comp. Neurol* **513**, 532-541 (2009).
3. Herculano-Houzel, S. Encephalization, neuronal excess, and neuronal index in rodents. *Anat Rec (Hoboken)* **290**, 1280-1287 (2007).
4. Watakabe, A. Comparative molecular neuroanatomy of mammalian neocortex: What can gene expression tell us about areas and layers? *Development, Growth & Differentiation* **51**, 343-354 (2009).
5. Wonders, C.P. & Anderson, S.A. The origin and specification of cortical interneurons. *Nat Rev Neurosci* **7**, 687-696 (2006).
6. Douglas, R.J. & Martin, K.A.C. Neuronal circuits of the neocortex. *Annu. Rev. Neurosci.* **27**, 419-451 (2004).
7. Brodmann, K. *Vergleichende Lokalisationslehre der Grosshirnrinde in ihren Prinzipien dargestellt auf Grund des Zellenbaues.* (Johann Ambrosius Barth Verlag: Leipzig, 1909).
8. Economo, C. & Koskinas, G. *Die Cytoarchitektonik der Hirnrinde des erwachsenen Menschen. Textband und Atlas.* (Springer: Wien, 1925).
9. Mountcastle, V.B. The columnar organization of the neocortex. *Brain* **120**, 701-722 (1997).
10. Triarhou, L.C. The Economo-Koskinas atlas revisited: cytoarchitectonics and functional context. *Stereotact Funct Neurosurg* **85**, 195-203 (2007).
11. Tomassy, G.S., Lodato, S., Trayes-Gibson, Z. & Arlotta, P. Development and regeneration of projection neuron subtypes of the cerebral cortex. *Sci Prog* **93**, 151-169 (2010).
12. O'Leary, D.D.M., Chou, S.-J. & Sahara, S. Area Patterning of the Mammalian Cortex. *Neuron* **56**, 252-269 (2007).
13. Sidman, R.L. & Rakic, P. Neuronal migration, with special reference to developing human brain: a review. *Brain Res* **62**, 1-35 (1973).
14. McConnell, S.K. & Kaznowski, C.E. Cell cycle dependence of laminar determination in developing neocortex. *Science* **254**, 282-285 (1991).
15. Frantz, G.D. & McConnell, S.K. Restriction of late cerebral cortical progenitors to an upper-layer fate. *Neuron* **17**, 55-61 (1996).
16. Desai, A.R. & McConnell, S.K. Progressive restriction in fate potential by neural progenitors during cerebral cortical development. *Development* **127**, 2863-2872 (2000).

17. Shen, Q. et al. The timing of cortical neurogenesis is encoded within lineages of individual progenitor cells. *Nat. Neurosci* **9**, 743-751 (2006).

18. Gaspard, N. et al. An intrinsic mechanism of corticogenesis from embryonic stem cells. *Nature* **455**, 351-357 (2008).

19. Mizutani, K.-ichi & Saito, T. Progenitors resume generating neurons after temporary inhibition of neurogenesis by Notch activation in the mammalian cerebral cortex. *Development* **132**, 1295-1304 (2005).

20. Fukumitsu, H. et al. Brain-Derived Neurotrophic Factor Participates in Determination of Neuronal Laminar Fate in the Developing Mouse Cerebral Cortex. *J. Neurosci.* **26**, 13218-13230 (2006).

21. Dehay, C. & Kennedy, H. Cell-cycle control and cortical development. *Nat Rev Neurosci* **8**, 438-450 (2007).

22. Seuntjens, E. et al. Sip1 regulates sequential fate decisions by feedback signaling from postmitotic neurons to progenitors. *Nat. Neurosci* **12**, 1373-1380 (2009).

23. Dehay, C., Savatier, P., Cortay, V. & Kennedy, H. Cell-Cycle Kinetics of Neocortical Precursors Are Influenced by Embryonic Thalamic Axons. *J. Neurosci.* **21**, 201-214 (2001).

24. Edgar, J.M. & Price, D.J. Radial migration in the cerebral cortex is enhanced by signals from thalamus. *Eur. J. Neurosci* **13**, 1745-1754 (2001).

25. Rash, B.G. & Grove, E.A. Area and layer patterning in the developing cerebral cortex. *Curr. Opin. Neurobiol* **16**, 25-34 (2006).

26. Bishop, K.M., Goudreau, G. & O'Leary, D.D.M. Regulation of Area Identity in the Mammalian Neocortex by Emx2 and Pax6. *Science* **288**, 344 -349 (2000).

27. Mallamaci, A., Muzio, L., Chan, C.-H., Parnavelas, J. & Boncinelli, E. Area identity shifts in the early cerebral cortex of Emx2-/- mutant mice. *Nat Neurosci* **3**, 679-686 (2000).

28. Hamasaki, T., Leingärtner, A., Ringstedt, T. & O'Leary, D.D.M. EMX2 Regulates Sizes and Positioning of the Primary Sensory and Motor Areas in Neocortex by Direct Specification of Cortical Progenitors. *Neuron* **43**, 359-372 (2004).

29. Armentano, M. et al. COUP-TFI regulates the balance of cortical patterning between frontal/motor and sensory areas. *Nat Neurosci* **10**, 1277-1286 (2007).

30. Sahara, S., Kawakami, Y., Izpisua Belmonte, J.C. & O'Leary, D.D.M. Sp8 exhibits reciprocal induction with Fgf8 but has an opposing effect on anterior-posterior cortical area patterning. *Neural Dev* **2**, 10 (2007).

31. Zembrzycki, A., Griesel, G., Stoykova, A. & Mansouri, A. Genetic interplay between the transcription factors Sp8 and Emx2 in the patterning of the forebrain. *Neural Dev* **2**, 8 (2007).

32. Miyashita-Lin, E.M., Hevner, R., Wassarman, K.M., Martinez, † S. & Rubenstein, J.L.R. Early Neocortical Regionalization in the Absence of Thalamic Innervation. *Science* **285**,

906 -909 (1999).

33. Nakagawa, Y., Johnson, J.E. & O'Leary, D.D. Graded and areal expression patterns of regulatory genes and cadherins in embryonic neocortex independent of thalamocortical input. *J. Neurosci* **19**, 10877-10885 (1999).

34. Zhou, L. et al. Maturation of "Neocortex Isole" In Vivo in Mice. *J. Neurosci.* **30**, 7928-7939 (2010).

35. Windrem, M.S. & Finlay, B.L. Thalamic ablations and neocortical development: alterations of cortical cytoarchitecture and cell number. *Cereb. Cortex* **1**, 230-240 (1991).

36. Sur, M., Angelucci, A. & Sharma, J. Rewiring cortex: the role of patterned activity in development and plasticity of neocortical circuits. *J. Neurobiol* **41**, 33-43 (1999).

37. Sharma, J., Angelucci, A. & Sur, M. Induction of visual orientation modules in auditory cortex. *Nature* **404**, 841-847 (2000).

38. López-Bendito, G. & Molnár, Z. Thalamocortical development: how are we going to get there? *Nat.Rev.Neurosci.* **4**, 276-289 (2003).

39. Garel, S. & Rubenstein, J.L.R. Intermediate targets in formation of topographic projections: inputs from the thalamocortical system. *Trends in Neurosciences* **27**, 533-539 (2004).

40. Hanashima, C., Molnár, Z. & Fishell, G. Building Bridges to the Cortex. *Cell* **125**, 24-27 (2006).

41. Braisted, J.E. et al. Netrin-1 Promotes Thalamic Axon Growth and Is Required for Proper Development of the Thalamocortical Projection. *J. Neurosci.* **20**, 5792-5801 (2000).

42. Powell, A.W., Sassa, T., Wu, Y., Tessier-Lavigne, M. & Polleux, F. Topography of thalamic projections requires attractive and repulsive functions of Netrin-1 in the ventral telencephalon. *PLoS Biol* **6**, e116 (2008).

43. Braisted, J.E., Tuttle, R. & O'Leary, D.D.M. Thalamocortical Axons Are Influenced by Chemorepellent and Chemoattractant Activities Localized to Decision Points along Their Path. *Developmental Biology* **208**, 430-440 (1999).

44. Bagri, A. et al. Slit Proteins Prevent Midline Crossing and Determine the Dorsoventral Position of Major Axonal Pathways in the Mammalian Forebrain. *Neuron* **33**, 233-248 (2002).

45. Mitrofanis, J. & Baker, G.E. Development of the thalamic reticular and perireticular nuclei in rats and their relationship to the course of growing corticofugal and corticopetal axons. *J. Comp. Neurol* **338**, 575-587 (1993).

46. Mitrofanis, J. & Guillery, R.W. New views of the thalamic reticular nucleus in the adult and the developing brain. *Trends Neurosci* **16**, 240-245 (1993).

47. Metin, C. & Godement, P. The ganglionic eminence may be an intermediate target for corticofugal and thalamocortical axons. *J.Neurosci.* **16**, 3219-3235 (1996).

48. Tuttle, R., Nakagawa, Y., Johnson, J.E. & O'Leary, D.D.M. Defects in thalamocortical

axon pathfinding correlate with altered cell domains in Mash-1-deficient mice. *Development* **126**, 1903-1916 (1999).

49. López-Bendito, G. et al. Tangential Neuronal Migration Controls Axon Guidance: A Role for Neuregulin-1 in Thalamocortical Axon Navigation. *Cell* **125**, 127-142 (2006).

50. Zhou, L., Qu, Y., Tissir, F. & Goffinet, A.M. Role of the Atypical Cadherin Celsr3 during Development of the Internal Capsule. *Cereb. Cortex* **19**, i114-i119 (2009).

51. Zhou, L. et al. Early Forebrain Wiring: Genetic Dissection Using Conditional Celsr3 Mutant Mice. *Science* **320**, 946 -949 (2008).

52. Deck, M., Mailhes, C. & Garel, S. Building reciprocal projections between the cerebral cortex and the dorsal thalamus. *FENS Abstr.* **vol.5**, 159.11 (2010).

53. Kostović, I. & Molliver, M. A new interpretation of the laminar development of cerebral cortex: synaptogenesis in different layers of neopallium in the human fetus. *Anat Rec* **178**, 395 (1974).

54. Price, D.J., Aslam, S., Tasker, L. & Gillies, K. Fates of the earliest generated cells in the developing murine neocortex. *J. Comp. Neurol* **377**, 414-422 (1997).

55. Del Rio, J.A., Martinez, A., Auladell, C. & Soriano, E. Developmental History of the Subplate and Developing White Matter in the Murine Neocortex. Neuronal Organization and Relationship with the Main Afferent Systems at Embryonic and Perinatal Stages. *Cereb. Cortex* **10**, 784-801 (2000).

56. Marin-Padilla, M. Early prenatal ontogenesis of the cerebral cortex (neocortex) of the cat (Felis domestica). A Golgi study. I. The primordial neocortical organization. *Z Anat Entwicklungsgesch* **134**, 117-145 (1971).

57. Stewart, G.R. & Pearlman, A.L. Fibronectin-like immunoreactivity in the developing cerebral cortex. *J. Neurosci* **7**, 3325-3333 (1987).

58. Caviness, V.S. Neocortical histogenesis in normal and reeler mice: a developmental study based upon [3H]thymidine autoradiography. *Brain Res* **256**, 293-302 (1982).

59. Bayer, S.A. & Altman, J. Development of layer I and the subplate in the rat neocortex. *Exp. Neurol* **107**, 48-62 (1990).

60. Miller, M.W. Cogeneration of retrogradely labeled corticocortical projection and GABA-immunoreactive local circuit neurons in cerebral cortex. *Brain Res* **355**, 187-192 (1985).

61. Fairén, A., Cobas, A. & Fonseca, M. Times of generation of glutamic acid decarboxylase immunoreactive neurons in mouse somatosensory cortex. *J. Comp. Neurol* **251**, 67-83 (1986).

62. Voigt, T., Opitz, T. & de Lima, A.D. Synchronous oscillatory activity in immature cortical network is driven by GABAergic preplate neurons. *J. Neurosci* **21**, 8895-8905 (2001).

63. De Carlos, J.A. & O'Leary, D.D. Growth and targeting of subplate axons and establishment of major cortical pathways. *J. Neurosci* **12**, 1194-1211 (1992).

64. Crandall, J.E., Jacobson, M. & Kosik, K.S. Ontogenesis of microtubule-associated protein 2 (MAP2) in embryonic mouse cortex. *Brain Res* **393**, 127-133 (1986).

65. König, N. & Marty, R. Early neurogenesis and synaptogenesis in cerebral cortex. *Bibl Anat* 152-160 (1981).

66. Blue, M.E. & Parnavelas, J.G. The formation and maturation of synapses in the visual cortex of the rat. I. Qualitative analysis. *J. Neurocytol* **12**, 599-616 (1983).

67. König, N., Roch, G. & Marty, R. The onset of synaptogenesis in rat temporal cortex. *Anat. Embryol* **148**, 73-87 (1975).

68. Cobas, A., Fairén, A., Alvarez-Bolado, G. & Sánchez, M.P. Prenatal development of the intrinsic neurons of the rat neocortex: a comparative study of the distribution of GABA-immunoreactive cells and the GABAA receptor. *Neuroscience* **40**, 375-397 (1991).

69. Ina, A. et al. Cajal-Retzius cells and subplate neurons differentially express vesicular glutamate transporters 1 and 2 during development of mouse cortex. *Eur. J. Neurosci* **26**, 615-623 (2007).

70. Crandall, J.E. & Caviness, V.S. Axon strata of the cerebral wall in embryonic mice. *Brain Res* **316**, 185-195 (1984).

71. Yuasa, S., Kitoh, J. & Kawamura, K. Interactions between growing thalamocortical afferent axons and the neocortical primordium in normal and reeler mutant mice. *Anat. Embryol.(Berl)* **190**, 137-154 (1994).

72. Jacobs, E.C. et al. Visualization of corticofugal projections during early cortical development in a τ-GFP-transgenic mouse. *Eur J Neurosci* **25**, 17-30 (2007).

73. Molnár, Z. & Cordery, P. Connections between cells of the internal capsule, thalamus, and cerebral cortex in embryonic rat. *J. Comp. Neurol.* **413**, 1-25 (1999).

74. Kristt, D.A. Acetylcholinesterase-containing neurons of layer VIb in immature neocortex: possible component of an early formed intrinsic cortical circuit. *Anat. Embryol* **157**, 217-226 (1979).

75. Divac, I., Marinković, S., Mogensen, J., Schwerdtfeger, W. & Regidor, J. Vertical ascending connections in the isocortex. *Anat. Embryol* **175**, 443-455 (1987).

76. Koester, S.E. & O'Leary, D.D. Axons of early generated neurons in cingulate cortex pioneer the corpus callosum. *J. Neurosci* **14**, 6608-6620 (1994).

77. Caviness, V.S. & Korde, M.G. Monoaminergic afferents to the neocortex: a developmental histofluorescence study in normal and Reeler mouse embryos. *Brain Res* **209**, 1-9 (1981).

78. Kageyama, G.H. & Robertson, R.T. Development of geniculocortical projections to visual cortex in rat: evidence early ingrowth and synaptogenesis. *J. Comp. Neurol* **335**, 123-148 (1993).

79. Higashi, S., Molnár, Z., Kurotani, T. & Toyama, K. Prenatal development of neural

excitation in rat thalamocortical projections studied by optical recording. *Neuroscience* **115**, 1231-1246 (2002).

80. Calarco, C.A. & Robertson, R.T. Development of basal forebrain projections to visual cortex: DiI studies in rat. *J. Comp. Neurol* **354**, 608-626 (1995).

81. Mechawar, N. & Descarries, L. The cholinergic innervation develops early and rapidly in the rat cerebral cortex: a quantitative immunocytochemical study. *Neuroscience* **108**, 555-567 (2001).

82. Hanganu, I.L. & Luhmann, H.J. Functional Nicotinic Acetylcholine Receptors on Subplate Neurons in Neonatal Rat Somatosensory Cortex. *Journal of Neurophysiology* **92**, 189 -198 (2004).

83. Hanganu, I.L., Okabe, A., Lessmann, V. & Luhmann, H.J. Cellular mechanisms of subplate-driven and cholinergic input-dependent network activity in the neonatal rat somatosensory cortex. *Cereb. Cortex* **19**, 89-105 (2009).

84. Sheppard, A.M., Hamilton, S.K. & Pearlman, A.L. Changes in the distribution of extracellular matrix components accompany early morphogenetic events of mammalian cortical development. *J. Neurosci* **11**, 3928-3942 (1991).

85. Hunter, D.D., Llinas, R., Ard, M., Merlie, J.P. & Sanes, J.R. Expression of s-laminin and laminin in the developing rat central nervous system. *J. Comp. Neurol* **323**, 238-251 (1992).

86. Oohira, A., Matsui, F., Watanabe, E., Kushima, Y. & Maeda, N. Developmentally regulated expression of a brain specific species of chondroitin sulfate proteoglycan, neurocan, identified with a monoclonal antibody IG2 in the rat cerebrum. *Neuroscience* **60**, 145-157 (1994).

87. Møllgård, K., Dziegielewska, K.M., Saunders, N.R., Zakut, H. & Soreq, H. Synthesis and localization of plasma proteins in the developing human brain. Integrity of the fetal blood-brain barrier to endogenous proteins of hepatic origin. *Dev. Biol* **128**, 207-221 (1988).

88. Sarantis, M.E. & Saunders, N.R. An immunocytochemical demonstration of alpha 2HS-glycoprotein in the developing neocortex of the rat. *Neurosci. Lett* **65**, 346-350 (1986).

89. Wang, W.Z. et al. Subplate in the developing cortex of mouse and human. *Journal of Anatomy* **217**, 368-380 (2010).

90. Dunn, J.A., Kirsch, J.D. & Naegele, J.R. Transient immunoglobulin-like molecules are present in the subplate zone and cerebral cortex during postnatal development. *Cereb. Cortex* **5**, 494-505 (1995).

91. Upender, M.B., Dunn, J.A., Wilson, S.M. & Naegele, J.R. Immunoglobulin molecules are present in early-generated neuronal populations in the rat cerebral cortex and retina. *J. Comp. Neurol* **384**, 271-282 (1997).

92. Del Rio, J.A., Soriano, E. & Ferrer, I. Development of GABA-immunoreactivity in the neocortex of the mouse. *J. Comp. Neurol* **326**, 501-526 (1992).

93. Métin, C., Baudoin, J.-P., Raki0107, S. & Parnavelas, J.G. Cell and molecular mechanisms involved in the migration of cortical interneurons. *Eur J Neurosci* **23**, 894-900 (2006).

94. Hanganu, I.L., Kilb, W. & Luhmann, H.J. Functional synaptic projections onto subplate neurons in neonatal rat somatosensory cortex. *J.Neurosci.* **22**, 7165-7176 (2002).

95. Hoerder, A. Mouse cortical subplate neurones: Molecular markers, connectivity and development. (2007).

96. Piñon, M.C., Jethwa, A., Jacobs, E., Campagnoni, A. & Molnár, Z. Dynamic integration of subplate neurons into the cortical barrel field circuitry during postnatal development in the Golli-tau-eGFP (GTE) mouse. *J. Physiol.* **587**, 1903-1915 (2009).

97. Dupont, E., Hanganu, I.L., Kilb, W., Hirsch, S. & Luhmann, H.J. Rapid developmental switch in the mechanisms driving early cortical columnar networks. *Nature* **439**, 79-83 (2006).

98. Antonini, A. & Shatz, C.J. Relation Between Putative Transmitter Phenotypes and Connectivity of Subplate Neurons During Cerebral Cortical Development. *Eur. J. Neurosci* **2**, 744-761 (1990).

99. Tomioka, R. et al. Demonstration of long-range GABAergic connections distributed throughout the mouse neocortex. *Eur. J. Neurosci* **21**, 1587-1600 (2005).

100. Higo, S., Udaka, N. & Tamamaki, N. Long-range GABAergic projection neurons in the cat neocortex. *J. Comp. Neurol* **503**, 421-431 (2007).

101. Tomioka, R. & Rockland, K.S. Long-distance corticocortical GABAergic neurons in the adult monkey white and gray matter. *J. Comp. Neurol* **505**, 526-538 (2007).

102. Friauf, E., McConnell, S.K. & Shatz, C.J. Functional synaptic circuits in the subplate during fetal and early postnatal development of cat visual cortex. *J. Neurosci* **10**, 2601-2613 (1990).

103. Friauf, E. & Shatz, C.J. Changing patterns of synaptic input to subplate and cortical plate during development of visual cortex. *J. Neurophysiol* **66**, 2059-2071 (1991).

104. Kanold, P.O. Transient microcircuits formed by subplate neurons and their role in functional development of thalamocortical connections. *Neuroreport* **15**, 2149-2153 (2004).

105. Zhao, C., Kao, J.P.Y. & Kanold, P.O. Functional excitatory microcircuits in neonatal cortex connect thalamus and layer 4. *J. Neurosci* **29**, 15479-15488 (2009).

106. Higashi, S., Hioki, K., Kurotani, T., Kasim, N. & Molnár, Z. Functional thalamocortical synapse reorganization from subplate to layer IV during postnatal development in the reeler-like mutant rat (shaking rat Kawasaki). *J. Neurosci* **25**, 1395-1406 (2005).

107. Kilb, W. et al. Glycine receptors mediate excitation of subplate neurons in neonatal rat cerebral cortex. *J. Neurophysiol* **100**, 698-707 (2008).

108. Flint, A.C., Liu, X. & Kriegstein, A.R. Nonsynaptic glycine receptor activation during

early neocortical development. *Neuron* **20**, 43-53 (1998).

109. Luskin, M.B. & Shatz, C.J. Studies of the earliest generated cells of the cat's visual cortex: cogeneration of subplate and marginal zones. *J. Neurosci* **5**, 1062-1075 (1985).

110. Kostović, I. & Rakic, P. Developmental history of the transient subplate zone in the visual and somatosensory cortex of the macaque monkey and human brain. *J. Comp. Neurol* **297**, 441-470 (1990).

111. Wood, J.G., Martin, S. & Price, D.J. Evidence that the earliest generated cells of the murine cerebral cortex form a transient population in the subplate and marginal zone. *Brain Res. Dev. Brain Res* **66**, 137-140 (1992).

112. Valverde, F., López-Mascaraque, L., Santacana, M. & De Carlos, J.A. Persistence of early-generated neurons in the rodent subplate: assessment of cell death in neocortex during the early postnatal period. *J. Neurosci* **15**, 5014-5024 (1995).

113. Robertson, R.T. et al. Do subplate neurons comprise a transient population of cells in developing neocortex of rats? *J. Comp. Neurol* **426**, 632-650 (2000).

114. Torres-Reveron, J. & Friedlander, M.J. Properties of persistent postnatal cortical subplate neurons. *J. Neurosci* **27**, 9962-9974 (2007).

115. Al-Ghoul, W.M. & Miller, M.W. Transient expression of Alz-50 immunoreactivity in developing rat neocortex: a marker for naturally occurring neuronal death? *Brain Res* **481**, 361-367 (1989).

116. Reep, R.L. Cortical Layer VII and Persistent Subplate Cells in Mammalian Brains. *Brain Behav Evol* **56**, 212-234 (2000).

117. Hoerder-Suabedissen, A. et al. Novel Markers Reveal Subpopulations of Subplate Neurons in the Murine Cerebral Cortex. *Cereb. Cortex* **19**, 1738-50 (2009).

118. Arimatsu, Y., Ishida, M., Kaneko, T., Ichinose, S. & Omori, A. Organization and development of corticocortical associative neurons expressing the orphan nuclear receptor Nurr1. *J. Comp. Neurol* **466**, 180-196 (2003).

119. Heuer, H. et al. Connective tissue growth factor: a novel marker of layer VII neurons in the rat cerebral cortex. *Neuroscience* **119**, 43-52 (2003).

120. Wang, W. et al. Comparative aspects of subplate zone studies with gene expression in sauropsids and mammals. *Cerebral Cortex* (2011).

121. Reep, R.L. & Goodwin, G.S. Layer VII of rodent cerebral cortex. *Neuroscience Letters* **90**, 15-20 (1988).

122. Vandevelde, I.L., Duckworth, E. & Reep, R.L. Layer VII and the gray matter trajectories of corticocortical axons in rats. *Anat. Embryol* **194**, 581-593 (1996).

123. Chun, J.J. & Shatz, C.J. The earliest-generated neurons of the cat cerebral cortex: characterization by MAP2 and neurotransmitter immunohistochemistry during fetal life. *J. Neurosci* **9**, 1648-1667 (1989).

124. Fonseca, M., dél Río, J.A., Martínez, A., Gómez, S. & Soriano, E. Development of calretinin immunoreactivity in the neocortex of the rat. *J. Comp. Neurol* **361**, 177-192

(1995).

125. Meyer, G., Schaaps, J.P., Moreau, L. & Goffinet, A.M. Embryonic and early fetal development of the human neocortex. *J. Neurosci* **20**, 1858-1868 (2000).

126. Naus, C.C., Miller, F.D., Morrison, J.H. & Bloom, F.E. Immunohistochemical and in situ hybridization analysis of the development of the rat somatostatin-containing neocortical neuronal system. *J. Comp. Neurol* **269**, 448-463 (1988).

127. Eadie, L.A., Parnavelas, J.G. & Franke, E. Development of the ultrastructural features of somatostatin-immunoreactive neurons in the rat visual cortex. *J. Neurocytol* **16**, 445-459 (1987).

128. Hendry, S.H. et al. Two classes of cortical GABA neurons defined by differential calcium binding protein immunoreactivities. *Exp Brain Res* **76**, 467-472 (1989).

129. Somogyi, P. et al. Different populations of GABAergic neurons in the visual cortex and hippocampus of cat contain somatostatin- or cholecystokinin-immunoreactive material. *J. Neurosci* **4**, 2590-2603 (1984).

130. Hendry, S.H. et al. Neuropeptide-containing neurons of the cerebral cortex are also GABAergic. *Proc. Natl. Acad. Sci. U.S.A* **81**, 6526-6530 (1984).

131. Fushiki, S. & Schachner, M. Immunocytological localization of cell adhesion molecules L1 and N-CAM and the shared carbohydrate epitope L2 during development of the mouse neocortex. *Brain Res* **389**, 153-167 (1986).

132. Godfraind, C., Schachner, M. & Goffinet, A.M. Immunohistological localization of cell adhesion molecules L1, J1, N-CAM and their common carbohydrate L2 in the embryonic cortex of normal and reeler mice. *Brain Res* **470**, 99-111 (1988).

133. Seki, T. & Arai, Y. Expression of highly polysialylated NCAM in the neocortex and piriform cortex of the developing and the adult rat. *Anat. Embryol* **184**, 395-401 (1991).

134. Fukuda, T. et al. Immunohistochemical localization of neurocan and L1 in the formation of thalamocortical pathway of developing rats. *J. Comp. Neurol.* **382**, 141-152 (1997).

135. Naegele, J.R., Barnstable, C.J. & Wahle, P.R. Expression of a unique 56-kDa polypeptide by neurons in the subplate zone of the developing cerebral cortex. *Proc. Natl. Acad. Sci. U.S.A* **88**, 330-334 (1991).

136. Wolozin, B. & Davies, P. Alzheimer-related neuronal protein A68: specificity and distribution. *Ann. Neurol* **22**, 521-526 (1987).

137. Wolozin, B., Scicutella, A. & Davies, P. Reexpression of a developmentally regulated antigen in Down syndrome and Alzheimer disease. *Proc. Natl. Acad. Sci. U.S.A* **85**, 6202-6206 (1988).

138. Hamre, K.M., Hyman, B.T., Goodlett, C.R., West, J.R. & Van Hoesen, G.W. Alz-50 immunoreactivity in the neonatal rat: changes in development and co-distribution with MAP-2 immunoreactivity. *Neurosci. Lett* **98**, 264-271 (1989).

139. Miller, M.W., Murtaugh, M. & Kuhn, P.E. Developmental expression of a 56 kDa

protein isolated from rat neocortex. *Brain Res. Dev. Brain Res* **81**, 260-268 (1994).

140. Allendoerfer, K.L., Shelton, D.L., Shooter, E.M. & Shatz, C.J. Nerve growth factor receptor immunoreactivity is transiently associated with the subplate neurons of the mammalian cerebral cortex. *Proc. Natl. Acad. Sci. U.S.A* **87**, 187 -190 (1990).

141. Mackarehtschian, K., Lau, C.K., Caras, I. & McConnell, S.K. Regional Differences in the Developing Cerebral Cortex Revealed by Ephrin-A5 Expression. *Cereb. Cortex* **9**, 601 -610 (1999).

142. DeFreitas, M.F., McQuillen, P.S. & Shatz, C.J. A novel p75NTR signaling pathway promotes survival, not death, of immunopurified neocortical subplate neurons. *J.Neurosci.* **21**, 5121-5129 (2001).

143. McQuillen, P.S., DeFreitas, M.F., Zada, G. & Shatz, C.J. A novel role for p75NTR in subplate growth cone complexity and visual thalamocortical innervation. *J.Neurosci.* **22**, 3580-3593 (2002).

144. Kanold, P.O., Kara, P., Reid, R.C. & Shatz, C.J. Role of subplate neurons in functional maturation of visual cortical columns. *Science* **301**, 521-525 (2003).

145. Kanold, P.O. & Shatz, C.J. Subplate neurons regulate maturation of cortical inhibition and outcome of ocular dominance plasticity. *Neuron* **51**, 627-638 (2006).

146. McKellar, C.E. & Shatz, C.J. Synaptogenesis in purified cortical subplate neurons. *Cereb. Cortex* **19**, 1723-1737 (2009).

147. Nguyen, V. & McQuillen, P.S. AMPA and metabotropic excitoxicity explain subplate neuron vulnerability. *Neurobiology of Disease* **37**, 195-207 (2010).

148. Carter, B.D. & Lewin, G.R. Neurotrophins live or let die: does p75NTR decide? *Neuron* **18**, 187-190 (1997).

149. Csillik, A.E., Okuno, E., Csillik, B., Knyihár, E. & Vécsei, L. Expression of kynurenine aminotransferase in the subplate of the rat and its possible role in the regulation of programmed cell death. *Cereb. Cortex* **12**, 1193-1201 (2002).

150. Nozaki, K. & Beal, M.F. Neuroprotective effects of L-kynurenine on hypoxia-ischemia and NMDA lesions in neonatal rats. *J. Cereb. Blood Flow Metab* **12**, 400-407 (1992).

151. Jahagirdar, V. & Wagner, C.K. Ontogeny of Progesterone Receptor Expression in the Subplate of Fetal and Neonatal Rat Cortex. *Cereb. Cortex* **20**, 1046 -1052 (2010).

152. Sakamoto, H., Ukena, K. & Tsutsui, K. Effects of progesterone synthesized de novo in the developing Purkinje cell on its dendritic growth and synaptogenesis. *J. Neurosci* **21**, 6221-6232 (2001).

153. Osheroff, H. & Hatten, M.E. Gene expression profiling of preplate neurons destined for the subplate: genes involved in transcription, axon extension, neurotransmitter regulation, steroid hormone signaling, and neuronal survival. *Cereb. Cortex* **19 Suppl 1**, i126-134 (2009).

154. Watakabe, A. et al. Comparative Analysis of Layer-Specific Genes in Mammalian Neocortex. *Cereb. Cortex* **17**, 1918 -1933 (2007).

155. Kristt, D.A. & Molliver, M.E. Synapses in newborn rat cerebral cortex: a quantitative ultrastructural study. *Brain Res* **108**, 180-186 (1976).

156. Kostovic, I. & Rakic, P. Cytology and time of origin of interstitial neurons in the white matter in infant and adult human and monkey telencephalon. *J. Neurocytol* **9**, 219-242 (1980).

157. Mark, R.F. & Marotte, L.R. Australian marsupials as models for the developing mammalian visual system. *Trends Neurosci* **15**, 51-57 (1992).

158. Reiner, A. A comparison of neurotransmitter-specific and neuropeptide-specific neuronal cell types present in the dorsal cortex in turtles with those present in the isocortex in mammals: implications for the evolution of isocortex. *Brain Behav. Evol* **38**, 53-91 (1991).

159. Montiel, J.F. et al. Hypothesis on the dual origin of the Mammalian subplate. *Front Neuroanat* **5**, 25 (2011).

160. Molnár, Z. et al. Comparative aspects of cerebral cortical development. *Eur J Neurosci* **23**, 921-934 (2006).

161. Bayatti, N. et al. A molecular neuroanatomical study of the developing human neocortex from 8 to 17 postconceptional weeks revealing the early differentiation of the subplate and subventricular zone. *Cereb. Cortex* **18**, 1536-1548 (2008).

162. Smart, I.H.M., Dehay, C., Giroud, P., Berland, M. & Kennedy, H. Unique morphological features of the proliferative zones and postmitotic compartments of the neural epithelium giving rise to striate and extrastriate cortex in the monkey. *Cereb. Cortex* **12**, 37-53 (2002).

163. Meyer, G. Genetic control of neuronal migrations in human cortical development. *Adv Anat Embryol Cell Biol* **189**, 1 p preceding 1, 1-111 (2007).

164. Judaš, M., Sedmak, G., Pletikos, M. & Jovanov-Milošević, N. Populations of subplate and interstitial neurons in fetal and adult human telencephalon. *J. Anat* **217**, 381-399 (2010).

165. Kostovic, I. & Jovanov-Milosevic, N. The development of cerebral connections during the first 20-45 weeks' gestation. *Seminars in Fetal and Neonatal Medicine* **11**, 415-422 (2006).

166. McConnell, S.K., Ghosh, A. & Shatz, C.J. Subplate neurons pioneer the first axon pathway from the cerebral cortex. *Science* **245**, 978-982 (1989).

167. McConnell, S.K., Ghosh, A. & Shatz, C.J. Subplate pioneers and the formation of descending connections from cerebral cortex. *J. Neurosci* **14**, 1892-1907 (1994).

168. Erzurumlu, R.S. & Jhaveri, S. Emergence of connectivity in the embryonic rat parietal cortex. *Cereb. Cortex* **2**, 336-352 (1992).

169. Shatz, C.J. & Rakic, P. The genesis of efferent connections from the visual cortex of the fetal rhesus monkey. *J. Comp. Neurol* **196**, 287-307 (1981).

170. Allendoerfer, K.L. & Shatz, C.J. The subplate, a transient neocortical structure: its role

in the development of connections between thalamus and cortex. *Annu. Rev. Neurosci* **17**, 185-218 (1994).

171. Bastiani, M.J., du Lac, S. & Goodman, C.S. Guidance of neuronal growth cones in the grasshopper embryo. I. Recognition of a specific axonal pathway by the pCC neuron. *J. Neurosci* **6**, 3518-3531 (1986).

172. Kuwada, J.Y. Cell recognition by neuronal growth cones in a simple vertebrate embryo. *Science* **233**, 740-746 (1986).

173. Ghosh, A. & Shatz, C.J. Pathfinding and target selection by developing geniculocortical axons. *J. Neurosci* **12**, 39-55 (1992).

174. Molnár, Z., Adams, R. & Blakemore, C. Mechanisms underlying the early establishment of thalamocortical connections in the rat. *J.Neurosci.* **18**, 5723-5745 (1998).

175. Ghosh, A., Antonini, A., McConnell, S.K. & Shatz, C.J. Requirement for subplate neurons in the formation of thalamocortical connections. *Nature* **347**, 179-181 (1990).

176. Molnár, Z. & Blakemore, C. How do thalamic axons find their way to the cortex? *Trends Neurosci.* **18**, 389-397 (1995).

177. Miller, B., Chou, L. & Finlay, B.L. The early development of thalamocortical and corticothalamic projections. *J. Comp. Neurol* **335**, 16-41 (1993).

178. Ghosh, A. & Shatz, C.J. A role for subplate neurons in the patterning of connections from thalamus to neocortex. *Development* **117**, 1031-1047 (1993).

179. Molnár, Z., Adams, R., Goffinet, A.M. & Blakemore, C. The role of the first postmitotic cortical cells in the development of thalamocortical innervation in the reeler mouse. *J. Neurosci* **18**, 5746-5765 (1998).

180. Hevner, R.F., Miyashita-Lin, E. & Rubenstein, J.L.R. Cortical and thalamic axon pathfinding defects inTbr1,Gbx2, andPax6 mutant mice: Evidence that cortical and thalamic axons interact and guide each other. *J. Comp. Neurol.* **447**, 8-17 (2002).

181. Rakic, P. Prenatal development of the visual system in rhesus monkey. *Philos. Trans. R. Soc. Lond., B, Biol. Sci* **278**, 245-260 (1977).

182. Shatz, C.J. & Luskin, M.B. The relationship between the geniculocortical afferents and their cortical target cells during development of the cat's primary visual cortex. *J. Neurosci* **6**, 3655-3668 (1986).

183. Lund, R.D. & Mustari, M.J. Development of the geniculocortical pathway in rats. *J. Comp. Neurol* **173**, 289-306 (1977).

184. Catalano, S.M., Robertson, R.T. & Killackey, H.P. Early ingrowth of thalamocortical afferents to the neocortex of the prenatal rat. *Proc Natl Acad Sci U S A* **88**, 2999-3003 (1991).

185. Bayer, S.A. & Altman, J. *Neocortical Development*. (Raven Press: New York, 1991).

186. Naegele, J.R., Jhaveri, S. & Schneider, G.E. Sharpening of topographical projections and maturation of geniculocortical axon arbors in the hamster. *J. Comp. Neurol* **277**, 593-607 (1988).

187. Connolly, M. & Van Essen, D. The representation of the visual field in parvicellular

and magnocellular layers of the lateral geniculate nucleus in the macaque monkey. *J. Comp. Neurol* **226**, 544-564 (1984).

188. Nelson, S.B. & LeVay, S. Topographic organization of the optic radiation of the cat. *J. Comp. Neurol* **240**, 322-330 (1985).

189. Lozsádi, D.A., Gonzalez-Soriano, J. & Guillery, R.W. The course and termination of corticothalamic fibres arising in the visual cortex of the rat. *Eur. J. Neurosci* **8**, 2416-2427 (1996).

190. Emerling, D.E. & Lander, A.D. Laminar specific attachment and neurite outgrowth of thalamic neurons on cultured slices of developing cerebral neocortex. *Development* **120**, 2811-2822 (1994).

191. Molnár, Z. & Blakemore, C. Development of signals influencing the growth and termination of thalamocortical axons in organotypic culture. *Exp. Neurol* **156**, 363-393 (1999).

192. Shimogori, T. & Grove, E.A. Fibroblast Growth Factor 8 Regulates Neocortical Guidance of Area-Specific Thalamic Innervation. *J. Neurosci.* **25**, 6550-6560 (2005).

193. Fukuchi-Shimogori, T. & Grove, E.A. Neocortex Patterning by the Secreted Signaling Molecule FGF8. *Science* **294**, 1071 -1074 (2001).

194. Dufour, A. et al. Area Specificity and Topography of Thalamocortical Projections Are Controlled by ephrin/Eph Genes. *Neuron* **39**, 453-465 (2003).

195. Kanold, P.O. & Luhmann, H.J. The Subplate and Early Cortical Circuits. *Annual Review of Neuroscience* **33**, 23-48 (2010).

196. Luhmann, H.J., Kilb, W. & Hanganu-Opatz, I.L. Subplate Cells: Amplifiers of Neuronal Activity in the Developing Cerebral Cortex. *Front Neuroanat* **3**, 19 (2009).

197. Sun, J.-J. & Luhmann, H.J. Spatio-temporal dynamics of oscillatory network activity in the neonatal mouse cerebral cortex. *Eur. J. Neurosci* **26**, 1995-2004 (2007).

198. Sheikh, A. & Kanold, P. Subplate neurons promote the formation of barrels within rat primary somatosensory cortex. *2010 Neuroscience Meeting Planner* **33.10**,

199. Lischalk, J.W., Easton, C.R. & Moody, W.J. Bilaterally propagating waves of spontaneous activity arising from discrete pacemakers in the neonatal mouse cerebral cortex. *Dev Neurobiol* **69**, 407-414 (2009).

200. Garaschuk, O., Linn, J., Eilers, J. & Konnerth, A. Large-scale oscillatory calcium waves in the immature cortex. *Nat. Neurosci* **3**, 452-459 (2000).

201. Yang, J.-W., Hanganu-Opatz, I.L., Sun, J.-J. & Luhmann, H.J. Three patterns of oscillatory activity differentially synchronize developing neocortical networks in vivo. *J. Neurosci* **29**, 9011-9025 (2009).

202. Cang, J. et al. Development of precise maps in visual cortex requires patterned spontaneous activity in the retina. *Neuron* **48**, 797-809 (2005).

203. Demas, J. et al. Failure to maintain eye-specific segregation in nob, a mutant with abnormally patterned retinal activity. *Neuron* **50**, 247-259 (2006).

204. Ohshiro, T. & Weliky, M. Subplate neurons foster inhibition. *Neuron* **51**, 524-526 (2006).

205. Markram, H., Lübke, J., Frotscher, M. & Sakmann, B. Regulation of Synaptic Efficacy by Coincidence of Postsynaptic APs and EPSPs. *Science* **275**, 213 -215 (1997).

206. Rivera, C. et al. The K+/Cl- co-transporter KCC2 renders GABA hyperpolarizing during neuronal maturation. *Nature* **397**, 251-255 (1999).

207. Rivera, C. et al. BDNF-induced TrkB activation down-regulates the K+-Cl- cotransporter KCC2 and impairs neuronal Cl- extrusion. *J. Cell Biol* **159**, 747-752 (2002).

208. Lein, E.S., Finney, E.M., McQuillen, P.S. & Shatz, C.J. Subplate neuron ablation alters neurotrophin expression and ocular dominance column formation. *Proc. Natl. Acad. Sci. U.S.A* **96**, 13491 -13495 (1999).

209. Mountcastle, V.B. Modality and topographic properties of single neurons of cat's somatic sensory cortex. *J. Neurophysiol* **20**, 408-434 (1957).

210. Hubel, D.H. & Wiesel, T.N. Ferrier lecture. Functional architecture of macaque monkey visual cortex. *Proc. R. Soc. Lond., B, Biol. Sci* **198**, 1-59 (1977).

211. Woolsey, T.A. & Van der Loos, H. The structural organization of layer IV in the somatosensory region (SI) of mouse cerebral cortex. The description of a cortical field composed of discrete cytoarchitectonic units. *Brain Res* **17**, 205-242 (1970).

212. Ghosh, A. & Shatz, C.J. Involvement of subplate neurons in the formation of ocular dominance columns. *Science* **255**, 1441-1443 (1992).

213. Shatz, C.J. & Stryker, M.P. Ocular dominance in layer IV of the cat's visual cortex and the effects of monocular deprivation. *J. Physiol.* **281**, 267-283 (1978).

214. Van der Loos, H. & Woolsey, T.A. Somatosensory Cortex: Structural Alterations following Early Injury to Sense Organs. *Science* **179**, 395 -398 (1973).

215. Grossberg, S. & Seitz, A. Laminar Development of Receptive Fields, Maps and Columns in Visual Cortex: The Coordinating Role of the Subplate. *Cereb. Cortex* **13**, 852 -863 (2003).

216. Feldman, D.E. Timing-based LTP and LTD at vertical inputs to layer II/III pyramidal cells in rat barrel cortex. *Neuron* **27**, 45-56 (2000).

217. Dityatev, A. & Fellin, T. Extracellular Matrix in Plasticity and Epileptogenesis. *Neuron Glia Biology* **4**, 235-247 (2008).

218. Dityatev, A., Schachner, M. & Sonderegger, P. The dual role of the extracellular matrix in synaptic plasticity and homeostasis. *Nat. Rev. Neurosci* **11**, 735-746 (2010).

219. Mataga, N., Nagai, N. & Hensch, T.K. Permissive proteolytic activity for visual cortical plasticity. *Proc. Natl. Acad. Sci. U.S.A* **99**, 7717 -7721 (2002).

220. Pizzorusso, T. et al. Reactivation of ocular dominance plasticity in the adult visual cortex. *Science* **298**, 1248-1251 (2002).

221. Matsumoto-Miyai, K. et al. Coincident pre- and postsynaptic activation induces dendritic filopodia via neurotrypsin-dependent agrin cleavage. *Cell* **136**, 1161-1171 (2009).

222. Berger, P. et al. Neuronal depolarization enhances the transcription of the neuronal serine protease inhibitor neuroserpin. *Mol. Cell. Neurosci* **14**, 455-467 (1999).

223. Inder, T.E. & Volpe, J.J. Mechanisms of perinatal brain injury. *Semin Neonatol* **5**, 3-16 (2000).

224. Khwaja, O. & Volpe, J.J. Pathogenesis of cerebral white matter injury of prematurity. *Arch. Dis. Child. Fetal Neonatal Ed* **93**, F153-161 (2008).

225. Volpe, J.J. Neurobiology of periventricular leukomalacia in the premature infant. *Pediatr. Res* **50**, 553-562 (2001).

226. Back, S.A., Riddle, A. & McClure, M.M. Maturation-dependent vulnerability of perinatal white matter in premature birth. *Stroke* **38**, 724-730 (2007).

227. Peterson, B.S. et al. Regional brain volume abnormalities and long-term cognitive outcome in preterm infants. *JAMA* **284**, 1939-1947 (2000).

228. Srinivasan, L. et al. Quantification of deep gray matter in preterm infants at term-equivalent age using manual volumetry of 3-tesla magnetic resonance images. *Pediatrics* **119**, 759-765 (2007).

229. Isaacs, E.B. et al. Hippocampal volume and everyday memory in children of very low birth weight. *Pediatr. Res* **47**, 713-720 (2000).

230. Pierson, C.R. et al. Gray matter injury associated with periventricular leukomalacia in the premature infant. *Acta Neuropathol* **114**, 619-631 (2007).

231. Folkerth, R.D., Trachtenberg, F.L. & Haynes, R.L. Oxidative injury in the cerebral cortex and subplate neurons in periventricular leukomalacia. *J. Neuropathol. Exp. Neurol* **67**, 677-686 (2008).

232. Robinson, S., Mikolaenko, I., Thompson, I., Cohen, M.L. & Goyal, M. Loss of cation-chloride cotransporter expression in preterm infants with white matter lesions: implications for the pathogenesis of epilepsy. *J. Neuropathol. Exp. Neurol* **69**, 565-572 (2010).

233. Volpe, J.J. Encephalopathy of Prematurity Includes Neuronal Abnormalities. *Pediatrics* **116**, 221-225 (2005).

234. McQuillen, P.S., Sheldon, R.A., Shatz, C.J. & Ferriero, D.M. Selective vulnerability of subplate neurons after early neonatal hypoxia-ischemia. *J. Neurosci* **23**, 3308-3315 (2003).

235. McQuillen, P.S. & Ferriero, D.M. Selective vulnerability in the developing central nervous system. *Pediatric Neurology* **30**, 227-235 (2004).

236. Catalano, S.M., Chang, C.K. & Shatz, C.J. Activity-Dependent Regulation of NMDAR1 Immunoreactivity in the Developing Visual Cortex. *J. Neurosci* **17**, 8376 -8390 (1997).

237. Talos, D.M. et al. Developmental regulation of alpha-amino-3-hydroxy-5-methyl-4-isoxazole-propionic acid receptor subunit expression in forebrain and relationship to regional susceptibility to hypoxic/ischemic injury. I. Rodent cerebral white matter and cortex. *J. Comp. Neurol* **497**, 42-60 (2006).

238. Talos, D.M. et al. Developmental regulation of alpha-amino-3-hydroxy-5-methyl-4-isoxazole-propionic acid receptor subunit expression in forebrain and relationship to regional susceptibility to hypoxic/ischemic injury. II. Human cerebral white matter and cortex. *J. Comp. Neurol* **497**, 61-77 (2006).

239. Catsicas, S. & Clarke, P.G. Spatiotemporal gradients of kainate-sensitivity in the developing chicken retina. *J. Comp. Neurol* **262**, 512-522 (1987).

240. Towfighi, J., Mauger, D., Vannucci, R.C. & Vannucci, S.J. Influence of age on the cerebral lesions in an immature rat model of cerebral hypoxia-ischemia: a light microscopic study. *Brain Res. Dev. Brain Res* **100**, 149-160 (1997).

241. Innocenti, G.M. & Berbel, P. Analysis of an experimental cortical network: II). Connections of visual areas 17 and 18 after neonatal injections of ibotenic acid. *J Neural Transplant Plast* **2**, 29-54 (1991).

242. Friedman, L.K. & Velísková, J. GluR2 hippocampal knockdown reveals developmental regulation of epileptogenicity and neurodegeneration. *Brain Res. Mol. Brain Res* **61**, 224-231 (1998).

243. Sanchez, R.M. et al. Decreased glutamate receptor 2 expression and enhanced epileptogenesis in immature rat hippocampus after perinatal hypoxia-induced seizures. *J. Neurosci* **21**, 8154-8163 (2001).

244. Jensen, J.B., Lund, T.M., Timmermann, D.B., Schousboe, A. & Pickering, D.S. Role of GluR2 expression in AMPA-induced toxicity in cultured murine cerebral cortical neurons. *J. Neurosci. Res* **65**, 267-277 (2001).

245. Habgood, M.D. et al. Cerebral blood flow in the anaesthetized immature sheep fetus and the response to hypercapnia. *Exp. Physiol* **76**, 495-505 (1991).

246. Volpe, J.J. Brain injury in premature infants: a complex amalgam of destructive and developmental disturbances. *Lancet Neurol* **8**, 110-124 (2009).

247. Price, D.J. & Lotto, R.B. Influences of the thalamus on the survival of subplate and cortical plate cells in cultured embryonic mouse brain. *Journal of Neuroscience* **16**, 3247-3255 (1996).

248. McGrath, J., Saha, S., Chant, D. & Welham, J. Schizophrenia: A Concise Overview of Incidence, Prevalence, and Mortality. *Epidemiologic Reviews* **30**, 67 -76 (2008).

249. Lewis, D.A. & Levitt, P. Schizophrenia as a disorder of neurodevelopment. *Annu. Rev. Neurosci* **25**, 409-432 (2002).

250. Wright, P., Takei, N., Rifkin, L. & Murray, R. Maternal influenza, obstetric complications, and schizophrenia. *Am J Psychiatry* **152**, 1714-1720 (1995).

251. Limosin, F., Rouillon, F., Payan, C., Cohen, J.-M. & Strub, N. Prenatal exposure to influenza as a risk factor for adult schizophrenia. *Acta Psychiatr Scand* **107**, 331-335 (2003).

252. Zornberg, G.L., Buka, S.L. & Tsuang, M.T. Hypoxic-Ischemia-Related Fetal/Neonatal Complications and Risk of Schizophrenia and Other Nonaffective Psychoses: A

19-Year Longitudinal Study. *Am J Psychiatry* **157**, 196-202 (2000).

253. Dalman, C. et al. Signs of asphyxia at birth and risk of schizophrenia: Population-based case--control study. *The British Journal of Psychiatry* **179**, 403-408 (2001).

254. Akbarian, S. et al. Distorted distribution of nicotinamide-adenine dinucleotide phosphate- diaphorase neurons in temporal lobe of schizophrenics implies anomalous cortical development. *Archives of General Psychiatry* **50**, 178-187 (1993).

255. Anderson, S.A., Volk, D.W. & Lewis, D.A. Increased density of microtubule associated protein 2-immunoreactive neurons in the prefrontal white matter of schizophrenic subjects. *Schizophr. Res* **19**, 111-119 (1996).

256. Kirkpatrick, B., Conley, R.C., Kakoyannis, A., Reep, R.L. & Roberts, R.C. Interstitial cells of the white matter in the inferior parietal cortex in schizophrenia: An unbiased cell-counting study. *Synapse* **34**, 95-102 (1999).

257. Kirkpatrick, B., Messias, N.C., Conley, R.R. & Roberts, R.C. Interstitial cells of the white matter in the dorsolateral prefrontal cortex in deficit and nondeficit schizophrenia. *J. Nerv. Ment. Dis* **191**, 563-567 (2003).

258. Eastwood, S.L. & Harrison, P.J. Interstitial white matter neurons express less reelin and are abnormally distributed in schizophrenia: towards an integration of molecular and morphologic aspects of the neurodevelopmental hypothesis. *Mol Psychiatry* **8**, 821-831 (0000).

259. Eastwood, S.L. & Harrison, P.J. Interstitial white matter neuron density in the dorsolateral prefrontal cortex and parahippocampal gyrus in schizophrenia. *Schizophr. Res* **79**, 181-188 (2005).

260. Connor, C.M., Guo, Y. & Akbarian, S. Cingulate White Matter Neurons in Schizophrenia and Bipolar Disorder. *Biological Psychiatry* **66**, 486-493 (2009).

261. Rioux, L., Nissanov, J., Lauber, K., Bilker, W.B. & Arnold, S.E. Distribution of Microtubule-Associated Protein MAP2-Immunoreactive Interstitial Neurons in the Parahippocampal White Matter in Subjects With Schizophrenia. *Am J Psychiatry* **160**, 149-155 (2003).

262. Akbarian, S. et al. Altered distribution of nicotinamide-adenine dinucleotide phosphate-diaphorase cells in frontal lobe of schizophrenics implies disturbances of cortical development. *Arch. Gen. Psychiatry* **50**, 169-177 (1993).

263. Akbarian, S. et al. Maldistribution of interstitial neurons in prefrontal white matter of the brains of schizophrenic patients. *Arch. Gen. Psychiatry* **53**, 425-436 (1996).

264. Kostović, I., Judaš, M. & Sedmak, G. Developmental history of the subplate zone, subplate neurons and interstitial white matter neurons: relevance for schizophrenia. *Int. J. Dev. Neurosci* (2010).doi:10.1016/j.ijdevneu.2010.09.005

265. Hashimoto, T. et al. Development of the brainstem and cerebellum in autistic patients. *J Autism Dev Disord* **25**, 1-18 (1995).

266. Raymond, G.V., Bauman, M.L. & Kemper, T.L. Hippocampus in autism: a Golgi

analysis. *Acta Neuropathol* **91**, 117-119 (1996).

267. Bailey, A. et al. A clinicopathological study of autism. *Brain* **121**, 889 -905 (1998).

268. Kemper, T.L. & Bauman, M. Neuropathology of infantile autism. *J. Neuropathol. Exp. Neurol* **57**, 645-652 (1998).

269. Fatemi, S.H. et al. Purkinje cell size is reduced in cerebellum of patients with autism. *Cell. Mol. Neurobiol* **22**, 171-175 (2002).

270. Casanova, M.F., Buxhoeveden, D.P., Switala, A.E. & Roy, E. Minicolumnar pathology in autism. *Neurology* **58**, 428-432 (2002).

271. Casanova, M.F., Buxhoeveden, D.P., Switala, A.E. & Roy, E. Neuronal Density and Architecture (Gray Level Index) in the Brains of Autistic Patients. *Journal of Child Neurology* **17**, 515 -521 (2002).

272. Mukaetova-Ladinska, E.B., Arnold, H., Jaros, E., Perry, R. & Perry, E. Depletion of MAP2 expression and laminar cytoarchitectonic changes in dorsolateral prefrontal cortex in adult autistic individuals. *Neuropathol. Appl. Neurobiol* **30**, 615-623 (2004).

273. Hutsler, J.J., Love, T. & Zhang, H. Histological and magnetic resonance imaging assessment of cortical layering and thickness in autism spectrum disorders. *Biol. Psychiatry* **61**, 449-457 (2007).

274. Simms, M.L., Kemper, T.L., Timbie, C.M., Bauman, M.L. & Blatt, G.J. The anterior cingulate cortex in autism: heterogeneity of qualitative and quantitative cytoarchitectonic features suggests possible subgroups. *Acta Neuropathol* **118**, 673-684 (2009).

275. Avino, T.A. & Hutsler, J.J. Abnormal cell patterning at the cortical gray-white matter boundary in autism spectrum disorders. *Brain Res* **1360**, 138-146 (2010).

276. Piven, J. et al. Magnetic resonance imaging evidence for a defect of cerebral cortical development in autism. *American Journal of Psychiatry* **147**, 734-739 (1990).

277. Fatemi, S.H. et al. Reelin signaling is impaired in autism. *Biological Psychiatry* **57**, 777-787 (2005).

278. Zhang, H. et al. Reelin gene alleles and susceptibility to autism spectrum disorders. *Mol. Psychiatry* **7**, 1012-1017 (2002).

279. Skaar, D.A. et al. Analysis of the RELN gene as a genetic risk factor for autism. *Mol Psychiatry* **10**, 563-571 (2004).

280. Serajee, F.J., Zhong, H. & Mahbubul Huq, A.H.M. Association of Reelin gene polymorphisms with autism. *Genomics* **87**, 75-83 (2006).

281. Chen, E.Y., Mufson, E.J. & Kordower, J.H. TRK and p75 neurotrophin receptor systems in the developing human brain. *J. Comp. Neurol* **369**, 591-618 (1996).

282. Lein, E.S. et al. Genome-wide atlas of gene expression in the adult mouse brain. *Nature* **445**, 168-176 (2007).

283. Allen Developing Mouse Brain Atlas [Internet] Seattle (WA): Allen Institute for Brain

Science. ©2009. Available from: http://developingmouse.brain-map.org.

284. Hoerder-Suabedissen, A., Kousha, O., García-Moreno, F. & Molnár, Z. GFP-expression in subplate cells in the Edg2-GFP and CTGF-GFP mouse. *Winter Meeting of the Anatomical Society of Great Britain and Ireland* (2010).

285. Espina, V. et al. Laser-capture microdissection. *Nat. Protocols* **1**, 586-603 (2006).

286. Emmert-Buck, M.R. et al. Laser capture microdissection. *Science* **274**, 998-1001 (1996).

287. Clément-Ziza, M., Munnich, A., Lyonnet, S., Jaubert, F. & Besmond, C. Stabilization of RNA during laser capture microdissection by performing experiments under argon atmosphere or using ethanol as a solvent in staining solutions. *RNA* **14**, 2698-2704 (2008).

288. Wang, H. et al. Histological staining methods preparatory to laser capture microdissection significantly affect the integrity of the cellular RNA. *BMC Genomics* **7**, 97 (2006).

289. Kube, D.M. et al. Optimization of laser capture microdissection and RNA amplification for gene expression profiling of prostate cancer. *BMC Mol. Biol* **8**, 25 (2007).

290. Kerman, I.A., Buck, B.J., Evans, S.J., Akil, H. & Watson, S.J. Combining laser capture microdissection with quantitative real-time PCR: effects of tissue manipulation on RNA quality and gene expression. *J. Neurosci. Methods* **153**, 71-85 (2006).

291. Vincent, V.A.M., DeVoss, J.J., Ryan, H.S. & Murphy, G.M. Analysis of neuronal gene expression with laser capture microdissection. *J. Neurosci. Res* **69**, 578-586 (2002).

292. Araki, K.Y., Sims, J.R. & Bhide, P.G. Dopamine receptor mRNA and protein expression in the mouse corpus striatum and cerebral cortex during pre- and postnatal development. *Brain Res* **1156**, 31-45 (2007).

293. Fernández-Medarde, A. et al. Laser microdissection and microarray analysis of the hippocampus of Ras-GRF1 knockout mice reveals gene expression changes affecting signal transduction pathways related to memory and learning. *Neuroscience* **146**, 272-285 (2007).

294. Paulsen, S.J. et al. Gene expression profiling of individual hypothalamic nuclei from single animals using laser capture microdissection and microarrays. *J. Neurosci. Methods* **177**, 87-93 (2009).

295. Bitoun, E., Finelli, M.J., Oliver, P.L., Lee, S. & Davies, K.E. AF4 is a critical regulator of the IGF-1 signaling pathway during Purkinje cell development. *J. Neurosci* **29**, 15366-15374 (2009).

296. Lu, L. et al. Gene expression profiling of Lewy body-bearing neurons in Parkinson's disease. *Exp. Neurol* **195**, 27-39 (2005).

297. Cantuti-Castelvetri, I. et al. Effects of gender on nigral gene expression and parkinson disease. *Neurobiol. Dis* **26**, 606-614 (2007).

298. Arion, D., Unger, T., Lewis, D.A. & Mirnics, K. Molecular markers distinguishing

supragranular and infragranular layers in the human prefrontal cortex. *Eur. J. Neurosci* **25**, 1843-1854 (2007).

299. Byne, W. et al. Schizophrenia and sex associated differences in the expression of neuronal and oligodendrocyte-specific genes in individual thalamic nuclei. *Schizophr. Res* **98**, 118-128 (2008).

300. Liang, W.S. et al. Altered neuronal gene expression in brain regions differentially affected by Alzheimer's disease: a reference data set. *Physiol. Genomics* **33**, 240-256 (2008).

301. Bernard, R. et al. Gene expression profiling of neurochemically defined regions of the human brain by in situ hybridization-guided laser capture microdissection. *J. Neurosci. Methods* **178**, 46-54 (2009).

302. Ordway, G.A., Szebeni, A., Duffourc, M.M., Dessus-Babus, S. & Szebeni, K. Gene expression analyses of neurons, astrocytes, and oligodendrocytes isolated by laser capture microdissection from human brain: detrimental effects of laboratory humidity. *J. Neurosci. Res* **87**, 2430-2438 (2009).

303. Pietersen, C.Y., Lim, M.P. & Woo, T.-U.W. Obtaining high quality RNA from single cell populations in human postmortem brain tissue. *J Vis Exp* (2009).doi:10.3791/1444

304. Chu, T.T., Liu, Y. & Kemether, E. Thalamic transcriptome screening in three psychiatric states. *J. Hum. Genet* **54**, 665-675 (2009).

305. Micke, P., Ostman, A., Lundeberg, J. & Ponten, F. Laser-assisted cell microdissection using the PALM system. *Methods Mol. Biol* **293**, 151-166 (2005).

306. Kihara, A.H., Moriscot, A.S., Ferreira, P.J. & Hamassaki, D.E. Protecting RNA in fixed tissue: an alternative method for LCM users. *J. Neurosci. Methods* **148**, 103-107 (2005).

307. Schroeder, A. et al. The RIN: an RNA integrity number for assigning integrity values to RNA measurements. *BMC Mol. Biol* **7**, 3 (2006).

308. Fleige, S. & Pfaffl, M.W. RNA integrity and the effect on the real-time qRT-PCR performance. *Mol. Aspects Med* **27**, 126-139 (2006).

309. Bulfone, A. et al. T-brain-1: a homolog of Brachyury whose expression defines molecularly distinct domains within the cerebral cortex. *Neuron* **15**, 63-78 (1995).

310. Clément-Ziza, M. et al. Evaluation of methods for amplification of picogram amounts of total RNA for whole genome expression profiling. *BMC Genomics* **10**, 246 (2009).

311. Singh, R. et al. Microarray-based comparison of three amplification methods for nanogram amounts of total RNA. *Am J Physiol Cell Physiol* **288**, C1179-1189 (2005).

312. Klur, S., Toy, K., Williams, M.P. & Certa, U. Evaluation of procedures for amplification of small-size samples for hybridization on microarrays. *Genomics* **83**, 508-517 (2004).

313. Nygaard, V. et al. Limitations of mRNA amplification from small-size cell samples. *BMC Genomics* **6**, 147 (2005).

314. Shinozaki, K. et al. Absence of Cajal-Retzius cells and subplate neurons associated with defects of tangential cell migration from ganglionic eminence in Emx1/2 double

mutant cerebral cortex. *Development* **129**, 3479 -3492 (2002).

315. Denaxa, M., Chan, C.-H., Schachner, M., Parnavelas, J.G. & Karagogeos, D. The adhesion molecule TAG-1 mediates the migration of cortical interneurons from the ganglionic eminence along the corticofugal fiber system. *Development* **128**, 4635 -4644 (2001).

316. Ramakers, C., Ruijter, J.M., Deprez, R.H.L. & Moorman, A.F.M. Assumption-free analysis of quantitative real-time polymerase chain reaction (PCR) data. *Neuroscience Letters* **339**, 62-66 (2003).

317. Ruijter, J.M. et al. Amplification efficiency: linking baseline and bias in the analysis of quantitative PCR data. *Nucleic Acids Res.* **37**, e45 (2009).

318. Dennis, G. et al. DAVID: Database for Annotation, Visualization, and Integrated Discovery. *Genome Biol* **4**, P3 (2003).

319. Ashburner, M. et al. Gene ontology: tool for the unification of biology. The Gene Ontology Consortium. *Nat. Genet* **25**, 25-29 (2000).

320. Kanehisa, M. & Goto, S. KEGG: kyoto encyclopedia of genes and genomes. *Nucleic Acids Res* **28**, 27-30 (2000).

321. Wang, W.-Z., Oeschger, F.M., Lee, S. & Molnár, Z. High quality RNA from multiple brain regions simultaneously acquired by laser capture microdissection. *BMC Mol Biol* **10**, 69-69 (2009).

322. López-Bendito, G. et al. Robo1 and Robo2 Cooperate to Control the Guidance of Major Axonal Tracts in the Mammalian Forebrain. *J. Neurosci.* **27**, 3395-3407 (2007).

323. Andrews, W.D., Barber, M. & Parnavelas, J.G. Slit-Robo interactions during cortical development. *J. Anat* **211**, 188-198 (2007).

324. Ferland, R.J., Cherry, T.J., Preware, P.O., Morrisey, E.E. & Walsh, C.A. Characterization of Foxp2 and Foxp1 mRNA and protein in the developing and mature brain. *J. Comp. Neurol* **460**, 266-279 (2003).

325. Inoue, K., Terashima, T., Nishikawa, T. & Takumi, T. Fez1 is layer-specifically expressed in the adult mouse neocortex. *Eur. J. Neurosci* **20**, 2909-2916 (2004).

326. Chen, B., Schaevitz, L.R. & McConnell, S.K. Fezl regulates the differentiation and axon targeting of layer 5 subcortical projection neurons in cerebral cortex. *Proc. Natl. Acad. Sci. U.S.A* **102**, 17184 -17189 (2005).

327. The Gene Expression Nervous System Atlas (GENSAT) Project NINDS Contract # N01NS02331 to The Rockefeller University (New York, NY). Available from: http://www.ncbi.nlm.nih.gov/projects/gensat.

328. Visel, A. GenePaint.org: an atlas of gene expression patterns in the mouse embryo. *Nucleic Acids Research* **32**, 552D-556 (2004).

329. Faux, C. et al. Differential gene expression in migrating cortical interneurons during mouse forebrain development. *J. Comp. Neurol* **518**, 1232-1248 (2010).

330. Bicknell, R. & Vallee, B.L. Angiogenin activates endothelial cell phospholipase C. *Proc Natl Acad Sci U S A* **85**, 5961-5965 (1988).

331. Bedogni, F. et al. Tbr1 regulates regional and laminar identity of postmitotic neurons in developing neocortex. *Proc. Natl. Acad. Sci. U.S.A* **107**, 13129 -13134 (2010).

332. Van Gelder, R.N. et al. Amplified RNA synthesized from limited quantities of heterogeneous cDNA. *Proc. Natl. Acad. Sci. U.S.A* **87**, 1663-1667 (1990).

333. Li, J., Adams, L., Schwartz, S.M. & Bumgarner, R.E. RNA amplification, fidelity and reproducibility of expression profiling. *Comptes Rendus Biologies* **326**, 1021-1030 (October).

334. Boelens, M. et al. Microarray amplification bias: loss of 30% differentially expressed genes due to long probe - poly(A)-tail distances. *BMC Genomics* **8**, 277 (2007).

335. Huang, D.W., Sherman, B.T. & Lempicki, R.A. Systematic and integrative analysis of large gene lists using DAVID bioinformatics resources. *Nat. Protocols* **4**, 44-57 (2008).

336. Job, C. & Eberwine, J. Localization and translation of mRNA in dendrites and axons. *Nat. Rev. Neurosci* **2**, 889-898 (2001).

337. Mohr, E. & Richter, D. Axonal mRNAs: functional significance in vertebrates and invertebrates. *J. Neurocytol* **29**, 783-791 (2000).

338. Vasudevan, A., Long, J.E., Crandall, J.E., Rubenstein, J.L.R. & Bhide, P.G. Compartment-specific transcription factors orchestrate angiogenesis gradients in the embryonic brain. *Nat Neurosci* **11**, 429-439 (2008).

339. Stubbs, D. et al. Neurovascular congruence during cerebral cortical development. *Cereb. Cortex* **19 Suppl 1**, i32-41 (2009).

340. Redies, C. Cadherins in the central nervous system. *Progress in Neurobiology* **61**, 611-648 (2000).

341. Salinas, P.C. & Price, S.R. Cadherins and catenins in synapse development. *Curr. Opin. Neurobiol* **15**, 73-80 (2005).

342. Treubert-Zimmermann, U., Heyers, D. & Redies, C. Targeting Axons to Specific Fiber Tracts In Vivo by Altering Cadherin Expression. *J. Neurosci.* **22**, 7617-7626 (2002).

343. Tai, C.-Y., Kim, S.A. & Schuman, E.M. Cadherins and synaptic plasticity. *Curr. Opin. Cell Biol* **20**, 567-575 (2008).

344. Britanova, O. et al. Satb2 is a postmitotic determinant for upper-layer neuron specification in the neocortex. *Neuron* **57**, 378-392 (2008).

345. Alcamo, E.A. et al. Satb2 regulates callosal projection neuron identity in the developing cerebral cortex. *Neuron* **57**, 364-377 (2008).

346. Cubelos, B. et al. Cux1 and Cux2 Regulate Dendritic Branching, Spine Morphology, and Synapses of the Upper Layer Neurons of the Cortex. *Neuron* **66**, 523-535 (2010).

347. Goffinet, A.M. Events governing organization of postmigratory neurons: Studies on brain development in normal and reeler mice. *Brain Research Reviews* **7**, 261-296 (1984).

348. Takahara, T. et al. Dysfunction of the Orleans reeler gene arising from exon skipping due to transposition of a full-length copy of an active L1 sequence into the skipped

exon. *Hum. Mol. Genet* **5**, 989-993 (1996).

349. Gil, O.D., Leigh Needleman & George W. Huntley Developmental patterns of cadherin expression and localization in relation to compartmentalized thalamocortical terminations in rat barrel cortex. *J. Comp. Neurol.* **453**, 372-388 (2002).

350. Porta, S., Martí, E., de la Luna, S. & Arbonés, M.L. Differential expression of members of the RCAN family of calcineurin regulators suggests selective functions for these proteins in the brain. *Eur. J. Neurosci* **26**, 1213-1226 (2007).

351. Oprea, G.E. et al. Plastin 3 Is a Protective Modifier of Autosomal Recessive Spinal Muscular Atrophy. *Science* **320**, 524-527 (2008).

352. Przyborski, S.A., Knowles, B.B. & Ackerman, S.L. Embryonic phenotype of Unc5h3 mutant mice suggests chemorepulsion during the formation of the rostral cerebellar boundary. *Development* **125**, 41-50 (1998).

353. Fritschy, J.M. & Mohler, H. GABAA-receptor heterogeneity in the adult rat brain: differential regional and cellular distribution of seven major subunits. *J. Comp. Neurol* **359**, 154-194 (1995).

354. Philipson, K.D., Quednau, B.D. & Nicoll, D.A. The sodium/calcium exchanger family-SLC8. *Pflügers Archiv European Journal of Physiology* **447**, 543-548 (2004).

355. Wakimoto, K. et al. Expression of Na+/Ca(2+) exchanger (NCX1) gene in the developmental mouse embryo and adult mouse brain. *Comp. Biochem. Physiol. B, Biochem. Mol. Biol* **130**, 191-198 (2001).

356. Quednau, B.D., Nicoll, D.A. & Philipson, K.D. Tissue specificity and alternative splicing of the Na+/Ca2+ exchanger isoforms NCX1, NCX2, and NCX3 in rat. *Am. J. Physiol* **272**, C1250-1261 (1997).

357. Janz, R., Goda, Y., Geppert, M., Missler, M. & Südhof, T.C. SV2A and SV2B function as redundant Ca2+ regulators in neurotransmitter release. *Neuron* **24**, 1003-1016 (1999).

358. Bajjalieh, S.M., Frantz, G.D., Weimann, J.M., McConnell, S.K. & Scheller, R.H. Differential expression of synaptic vesicle protein 2 (SV2) isoforms. *J. Neurosci* **14**, 5223-5235 (1994).

359. Shibasaki, F., Hallin, U. & Uchino, H. Calcineurin as a multifunctional regulator. *J. Biochem* **131**, 1-15 (2002).

360. Li, G., Shi, P. & Wang, Y. Evolutionary dynamics of the ABCA chromosome 17q24 cluster genes in vertebrates. *Genomics* **89**, 385-391 (2007).

361. Shimizu, A. et al. A novel giant gene CSMD3 encoding a protein with CUB and sushi multiple domains: a candidate gene for benign adult familial myoclonic epilepsy on human chromosome 8q23.3-q24.1. *Biochem. Biophys. Res. Commun* **309**, 143-154 (2003).

362. Zagon, I.S., Verderame, M.F. & McLaughlin, P.J. The biology of the opioid growth factor receptor (OGFr). *Brain Res. Brain Res. Rev* **38**, 351-376 (2002).

363. Zagon, I.S., Wu, Y. & McLaughlin, P.J. Opioid growth factor and organ development in rat and human embryos. *Brain Res* **839**, 313-322 (1999).

364. Hevner, R.F., Daza, R.A.M., Englund, C., Kohtz, J. & Fink, A. Postnatal shifts of interneuron position in the neocortex of normal and reeler mice: evidence for inward radial migration. *Neuroscience* **124**, 605-618 (2004).

365. Arikkath, J. & Reichardt, L.F. Cadherins and catenins at synapses: roles in synaptogenesis and synaptic plasticity. *Trends Neurosci* **31**, 487-494 (2008).

366. Takeichi, M. The cadherin superfamily in neuronal connections and interactions. *Nat. Rev. Neurosci* **8**, 11-20 (2007).

367. Williams, M.E., de Wit, J. & Ghosh, A. Molecular mechanisms of synaptic specificity in developing neural circuits. *Neuron* **68**, 9-18 (2010).

368. Métin, C., Deléglise, D., Serafini, T., Kennedy, T.E. & Tessier-Lavigne, M. A role for netrin-1 in the guidance of cortical efferents. *Development* **124**, 5063-5074 (1997).

369. Masuda, T. et al. Netrin-1 Acts as a Repulsive Guidance Cue for Sensory Axonal Projections toward the Spinal Cord. *J. Neurosci.* **28**, 10380-10385 (2008).

370. Ying, G. et al. The protocadherin gene Celsr3 is required for interneuron migration in the mouse forebrain. *Mol. Cell. Biol* **29**, 3045-3061 (2009).

371. Stanco, A. et al. Netrin-1–α3β1 integrin interactions regulate the migration of interneurons through the cortical marginal zone. *Proc. Natl. Acad. Sci. U.S.A* **106**, 7595-7600 (2009).

372. Kim, W.S., Weickert, C.S. & Garner, B. Role of ATP-binding cassette transporters in brain lipid transport and neurological disease. *Journal of Neurochemistry* **104**, 1145-1166 (2008).

373. Bayer, S.A. & Altman, J. Development of the endopiriform nucleus and the claustrum in the rat brain. *Neuroscience* **45**, 391-412 (1991).

374. De Biasi, S., Frassoni, C. & Spreafico, R. GABA immunoreactivity in the thalamic reticular nucleus of the rat. A light and electron microscopical study. *Brain Research* **399**, 143-147 (1986).

375. Tamamaki, N. et al. Green fluorescent protein expression and colocalization with calretinin, parvalbumin, and somatostatin in the GAD67-GFP knock-in mouse. *J. Comp. Neurol.* **467**, 60-79 (2003).

376. Bhattacharjee, A. et al. Slick (Slo2.1), a rapidly-gating sodium-activated potassium channel inhibited by ATP. *J. Neurosci* **23**, 11681-11691 (2003).

377. Brünig, I., Scotti, E., Sidler, C. & Fritschy, J.-M. Intact sorting, targeting, and clustering of gamma-aminobutyric acid A receptor subtypes in hippocampal neurons in vitro. *J. Comp. Neurol.* **443**, 43-55 (2002).

378. Caraiscos, V.B. et al. Tonic inhibition in mouse hippocampal CA1 pyramidal neurons is mediated by α5 subunit-containing γ-aminobutyric acid type A receptors. *Proc. Natl. Acad. Sci. U.S.A* **101**, 3662-3667 (2004).

379. Serwanski, D.R. et al. Synaptic and nonsynaptic localization of GABA-A receptors containing the alpha5 subunit in the rat brain. *J. Comp. Neurol.* **499**, 458-470 (2006).

380. Zarnowska, E.D., Keist, R., Rudolph, U. & Pearce, R.A. GABAA receptor alpha5 subunits contribute to GABAA,slow synaptic inhibition in mouse hippocampus. *J. Neurophysiol* **101**, 1179-1191 (2009).

381. Vargas-Caballero, M., Martin, L.J., Salter, M.W., Orser, B.A. & Paulsen, O. alpha5 Subunit-containing GABA(A) receptors mediate a slowly decaying inhibitory synaptic current in CA1 pyramidal neurons following Schaffer collateral activation. *Neuropharmacology* (2009).doi:10.1016/j.neuropharm.2009.11.005

382. Kofuji, P., Hadley, R.W., Kieval, R.S., Lederer, W.J. & Schulze, D.H. Expression of the Na-Ca exchanger in diverse tissues: a study using the cloned human cardiac Na-Ca exchanger. *Am. J. Physiol* **263**, C1241-1249 (1992).

383. Papa, M. et al. Differential expression of the Na+-Ca2+ exchanger transcripts and proteins in rat brain regions. *J. Comp. Neurol* **461**, 31-48 (2003).

384. Noritake, J. et al. Mobile DHHC palmitoylating enzyme mediates activity-sensitive synaptic targeting of PSD-95. *J. Cell Biol.* **186**, 147-160 (2009).

385. Greaves, J., Gorleku, O.A., Salaun, C. & Chamberlain, L.H. Palmitoylation of the SNAP25 protein family: specificty and regulation by DHHC palmitoyl transferases. *J Biol Chem* **285**, 24629-38 (2010).

386. Kaas, J.H. Is most of neural plasticity in the thalamus cortical? *Proc Natl Acad Sci U S A* **96**, 7622-7623 (1999).

387. Behan, M. & Haberly, L.B. Intrinsic and efferent connections of the endopiriform nucleus in rat. *J. Comp. Neurol* **408**, 532-548 (1999).

388. Clancy, B., Teague-Ross, T.J. & Nagarajan, R. Cross-species analyses of the cortical GABAergic and subplate neural populations. *Front Neuroanat* **3**, 20 (2009).

389. Luo, L., Callaway, E.M. & Svoboda, K. Genetic dissection of neural circuits. *Neuron* **57**, 634-660 (2008).

390. Callaway, E.M. A molecular and genetic arsenal for systems neuroscience. *Trends in Neurosciences* **28**, 196-201 (2005).

391. Shimogori, T. & Masaharu Ogawa Gene application with in utero electroporation in mouse embryonic brain. *Development, Growth & Differentiation* **50**, 499-506 (2008).

392. Paddison, P.J., Caudy, A.A., Bernstein, E., Hannon, G.J. & Conklin, D.S. Short hairpin RNAs (shRNAs) induce sequence-specific silencing in mammalian cells. *Genes & Development* **16**, 948 -958 (2002).

393. Scherr, M. & Eder, M. Gene silencing by small regulatory RNAs in mammalian cells. *Cell Cycle* **6**, 444-449 (2007).

394. Rao, D.D., Vorhies, J.S., Senzer, N. & Nemunaitis, J. siRNA vs. shRNA: Similarities and differences. *Advanced Drug Delivery Reviews* **61**, 746-759 (2009).

395. Federico, M. *Lentivirus gene engineering protocols.* (Humana Press: 2003).

396. Teschemacher, A.G., Paton, J.F.R. & Kasparov, S. Imaging living central neurones using viral gene transfer. *Adv. Drug Deliv. Rev* **57**, 79-93 (2005).

397. Teschemacher, A.G. et al. Targeting specific neuronal populations using adeno- and lentiviral vectors: applications for imaging and studies of cell function. *Experimental Physiology* **90**, 61 -69 (2005).

398. Götz, M. & Bolz, J. Formation and preservation of cortical layers in slice cultures. *J. Neurobiol.* **23**, 783-802 (1992).

399. Voss, A.K. et al. C3G regulates cortical neuron migration, preplate splitting and radial glial cell attachment. *Development* **135**, 2139 -2149 (2008).

400. Hertel, N. & Redies, C. Absence of Layer-Specific Cadherin Expression Profiles in the Neocortex of the Reeler Mutant Mouse. *Cerebral Cortex* (2010).doi:10.1093/cercor/bhq183

401. Krishna-K, Nuernberger, M., Weth, F. & Redies, C. Layer-Specific Expression of Multiple Cadherins in the Developing Visual Cortex (V1) of the Ferret. *Cereb. Cortex* **19**, 388 -401 (2009).

402. Lin, X. et al. siRNA-mediated off-target gene silencing triggered by a 7 nt complementation. *Nucleic Acids Research* **33**, 4527 -4535

403. Bridge, A.J., Pebernard, S., Ducraux, A., Nicoulaz, A.-L. & Iggo, R. Induction of an interferon response by RNAi vectors in mammalian cells. *Nat. Genet* **34**, 263-264 (2003).

404. Kenworthy, R. et al. Short-hairpin RNAs delivered by lentiviral vector transduction trigger RIG-I-mediated IFN activation. *Nucleic Acids Res* **37**, 6587-6599 (2009).

405. Bauer, M. et al. Prevention of interferon-stimulated gene expression using microRNA-designed hairpins. *Gene Ther* **16**, 142-147 (2009).

406. Alvarez, V.A., Ridenour, D.A. & Sabatini, B.L. Retraction of Synapses and Dendritic Spines Induced by Off-Target Effects of RNA Interference. *J. Neurosci.* **26**, 7820-7825 (2006).

407. Grimm, D. et al. Fatality in mice due to oversaturation of cellular microRNA/short hairpin RNA pathways. *Nature* **441**, 537-541 (2006).

408. Leonardo, E.D. et al. Vertebrate homologues of C. elegans UNC-5 are candidate netrin receptors. *Nature* **386**, 833-838 (1997).

409. Livesey, F.J. Netrins and netrin receptors. *Cell. Mol. Life Sci* **56**, 62-68 (1999).

410. Moore, S.W., Tessier-Lavigne, M. & Kennedy, T.E. Netrins and their receptors. *Adv. Exp. Med. Biol* **621**, 17-31 (2007).

411. Bradford, D., Cole, S.J. & Cooper, H.M. Netrin-1: Diversity in development. *The International Journal of Biochemistry & Cell Biology* **41**, 487-493 (2009).

412. Watanabe, K. et al. Dorsally derived netrin 1 provides an inhibitory cue and elaborates the "waiting period" for primary sensory axons in the developing spinal cord. *Development* **133**, 1379-1387 (2006).

413. Molnar, Z. et al. Normal development of embryonic thalamocortical connectivity in

the absence of evoked synaptic activity. *J.Neurosci.* **22**, 10313-10323 (2002).

414. Goldschneider, D. & Mehlen, P. Dependence receptors: a new paradigm in cell signaling and cancer therapy. *Oncogene* **29**, 1865-1882 (2010).

415. Llambi, F., Causeret, F., Bloch-Gallego, E. & Mehlen, P. Netrin-1 acts as a survival factor via its receptors UNC5H and DCC. *EMBO J* **20**, 2715-2722 (2001).

416. Takemoto, M. et al. Laminar and Areal Expression of Unc5d and Its Role in Cortical Cell Survival. *Cereb Cortex* (2011).doi:10.1093/cercor/bhq265

417. Berbel, P. et al. Role of Late Maternal Thyroid Hormones in Cerebral Cortex Development: An Experimental Model for Human Prematurity. *Cereb Cortex* **20**, 1462-1475 (2010).

418. López, V. & Wagner, C.K. Progestin receptor is transiently expressed perinatally in neurons of the rat isocortex. *J. Comp. Neurol.* **512**, 124-139 (2009).

419. Mitrofanis, J. Patterns of antigenic expression in the thalamic reticular nucleus of developing rats. *J. Comp. Neurol* **320**, 161-181 (1992).

420. Gibbs, R.A. et al. Genome sequence of the Brown Norway rat yields insights into mammalian evolution. *Nature* **428**, 493-521 (2004).

421. Glazko, G.V. & Nei, M. Estimation of divergence times for major lineages of primate species. *Mol. Biol. Evol* **20**, 424-434 (2003).

422. Sendemir, E., Erzurumlu, R.S. & Jhaveri, S. Differential expression of acetylcholinesterase in the developing barrel cortex of three rodent species. *Cereb. Cortex* **6**, 377-387 (1996).

423. Campi, K.L. & Krubitzer, L. Comparative studies of diurnal and nocturnal rodents: differences in lifestyle result in alterations in cortical field size and number. *J. Comp. Neurol* **518**, 4491-4512 (2010).

424. Volpe, J.J. Subplate neurons--missing link in brain injury of the premature infant? *Pediatrics* **97**, 112-113 (1996).

425. Kostović, I., Judaš, M., Radoš, M. & Hrabač, P. Laminar Organization of the Human Fetal Cerebrum Revealed by Histochemical Markers and Magnetic Resonance Imaging. *Cereb. Cortex* **12**, 536 -544 (2002).

426. Cioni, G. et al. Cerebral visual impairment in preterm infants with periventricular leukomalacia. *Pediatr. Neurol* **17**, 331-338 (1997).

427. Lanzi, G. et al. Cerebral visual impairment in periventricular leukomalacia. *Neuropediatrics* **29**, 145-150 (1998).

428. Failor, S. et al. Neonatal Cerebral Hypoxia-Ischemia Impairs Plasticity in Rat Visual Cortex. *J. Neurosci.* **30**, 81-92 (2010).

429. Wess, J.M. & Kanold, P.O. Neonatal cerebral hypoxia-ischemia impairs development of functional responses in auditory cortex. *40th Annual Neuroscience Meeting* **671.2**,

430. Stoll, G. Inflammation and glial responses in ischemic brain lesions. *Progress in*

Neurobiology **56**, 149-171 (1998).

431. Bona, E. et al. Chemokine and inflammatory cell response to hypoxia-ischemia in immature rats. *Pediatr. Res* **45**, 500-509 (1999).

432. Nagata, N. Repetitive intermittent hypoxia-ischemia and brain damage in neonatal rats. *Brain and Development* **22**, 315-320 (2000).

433. Zeis, T. & Schaeren-Wiemers, N. Lame Ducks or Fierce Creatures? - The Role of Oligodendrocytes in Multiple Sclerosis. *J Mol Neurosci* **35**, 91-100 (2008).

434. Sizonenko, S.V. et al. Selective cortical alteration after hypoxic-ischemic injury in the very immature rat brain. *Pediatr. Res* **54**, 263-269 (2003).

435. Yager, J., Towfighi, J. & Vannucci, R.C. Influence of mild hypothermia on hypoxic-ischemic brain damage in the immature rat. *Pediatr. Res* **34**, 525-529 (1993).

436. Oakden, E., Chiswick, M., Rothwell, N. & Loddick, S. The influence of litter size on brain damage caused by hypoxic-ischemic injury in the neonatal rat. *Pediatr. Res* **52**, 692-696 (2002).

437. Hoerder-Suabedissen, A., Paulsen, O. & Molnár, Z. Thalamocortical maturation in mice is influenced by body weight. *J. Comp. Neurol* **511**, 415-420 (2008).

438. Logitharajah, P., Rutherford, M.A. & Cowan, F.M. Hypoxic-ischemic encephalopathy in preterm infants: antecedent factors, brain imaging, and outcome. *Pediatr. Res* **66**, 222-229 (2009).

439. Hevner, R.F. Layer-specific markers as probes for neuron type identity in human neocortex and malformations of cortical development. *J. Neuropathol. Exp. Neurol* **66**, 101-109 (2007).

440. Lewandowski, N.M. & Small, S.A. Brain Microarray: Finding Needles in Molecular Haystacks. *J. Neurosci* **25**, 10341 -10346 (2005).

441. Ge, Y., Sealfon, S.C. & Speed, T.P. Multiple testing and its applications to microarrays. *Stat Methods Med Res* **18**, 543-563 (2009).

442. Jeanmougin, M. et al. Should we abandon the t-test in the analysis of gene expression microarray data: a comparison of variance modeling strategies. *PLoS ONE* **5**, e12336 (2010).

443. Shimogori, T. et al. A genomic atlas of mouse hypothalamic development. *Nat. Neurosci* **13**, 767-775 (2010).

444. Stearns, F.W. One hundred years of pleiotropy: a retrospective. *Genetics* **186**, 767-773 (2010).

445. Boulanger, L.M. Immune proteins in brain development and synaptic plasticity. *Neuron* **64**, 93-109 (2009).

446. Kudo, C., Ajioka, I., Hirata, Y. & Nakajima, K. Expression profiles of EphA3 at both the RNA and protein level in the developing mammalian forebrain. *J. Comp. Neurol* **487**, 255-269 (2005).

447. Weber, E.T. & Andrade, R. Htr2a Gene and 5-HT(2A) Receptor Expression in the Cerebral Cortex Studied Using Genetically Modified Mice. *Front Neurosci* **4**, (2010).

448. Chen, B.E. et al. The molecular diversity of Dscam is functionally required for neuronal wiring specificity in Drosophila. *Cell* **125**, 607-620 (2006).

449. Ly, A. et al. DSCAM is a netrin receptor that collaborates with DCC in mediating turning responses to netrin-1. *Cell* **133**, 1241-1254 (2008).

450. Huh, G.S. et al. Functional requirement for class I MHC in CNS development and plasticity. *Science* **290**, 2155-2159 (2000).

451. Stevens, B. et al. The Classical Complement Cascade Mediates CNS Synapse Elimination. *Cell* **131**, 1164-1178 (2007).

452. Beattie, E.C. et al. Control of synaptic strength by glial TNFalpha. *Science* **295**, 2282-2285 (2002).

453. McConnell, M.J., Huang, Y.H., Datwani, A. & Shatz, C.J. H2-K(b) and H2-D(b) regulate cerebellar long-term depression and limit motor learning. *Proc. Natl. Acad. Sci. U.S.A* **106**, 6784-6789 (2009).

454. Williams, L.W., Burks, A.W. & Steele, R.W. Complement: function and clinical relevance. *Ann Allergy* **60**, 293-300 (1988).

455. Rosen, A.M. & Stevens, B. The role of the classical complement cascade in synapse loss during development and glaucoma. *Adv. Exp. Med. Biol* **703**, 75-93 (2010).

456. Nagel, D.J. et al. Role of nuclear Ca2+/calmodulin-stimulated phosphodiesterase 1A in vascular smooth muscle cell growth and survival. *Circ. Res* **98**, 777-784 (2006).

457. Vishnuvardhan, D., Connolly, K., Cain, B. & Beinfeld, M.C. PC2 and 7B2 null mice demonstrate that PC2 is essential for normal pro-CCK processing. *Biochem. Biophys. Res. Commun* **273**, 188-191 (2000).

458. Zhang, X. et al. Neuropeptidomic analysis establishes a major role for prohormone convertase-2 in neuropeptide biosynthesis. *J. Neurochem* **112**, 1168-1179 (2010).

459. Nillni, E.A., Aird, F., Seidah, N.G., Todd, R.B. & Koenig, J.I. PreproTRH(178-199) and two novel peptides (pFQ7 and pSE14) derived from its processing, which are produced in the paraventricular nucleus of the rat hypothalamus, are regulated during suckling. *Endocrinology* **142**, 896-906 (2001).

460. Burgunder, J.M. & Young, W.S. Cortical neurons expressing the cholecystokinin gene in the rat: distribution in the adult brain, ontogeny, and some of their projections. *J. Comp. Neurol* **300**, 26-46 (1990).

461. Gallopin, T., Geoffroy, H., Rossier, J. & Lambolez, B. Cortical Sources of CRF, NKB, and CCK and Their Effects on Pyramidal Cells in the Neocortex. *Cereb.Cortex* **16**, 1440 -1452 (2006).

462. Arlotta, P. et al. Neuronal subtype-specific genes that control corticospinal motor neuron development in vivo. *Neuron* **45**, 207-221 (2005).

463. Molyneaux, B.J. et al. Novel Subtype-Specific Genes Identify Distinct Subpopulations

of Callosal Projection Neurons. *J. Neurosci* **29**, 12343 -12354 (2009).

464. Sugino, K. et al. Molecular taxonomy of major neuronal classes in the adult mouse forebrain. *Nat. Neurosci* **9**, 99-107 (2006).

465. Marguerat, S. & Bähler, J. RNA-seq: from technology to biology. *Cell. Mol. Life Sci* **67**, 569-579 (2010).

466. Okerlund, N.D. et al. Dact1 is a postsynaptic protein required for dendrite, spine, and excitatory synapse development in the mouse forebrain. *J. Neurosci* **30**, 4362-4368 (2010).

467. Ikenouchi, J. & Umeda, M. FRMD4A regulates epithelial polarity by connecting Arf6 activation with the PAR complex. *Proc. Natl. Acad. Sci. U.S.A* **107**, 748-753 (2010).

468. Deng, X.A., Norris, A., Panaviene, Z. & Moncman, C.L. Ectopic expression of LIM-nebulette (LASP2) reveals roles in cell migration and spreading. *Cell Motil. Cytoskeleton* **65**, 827-840 (2008).

469. Kalus, I. et al. Differential involvement of the extracellular 6-O-endosulfatases Sulf1 and Sulf2 in brain development and neuronal and behavioural plasticity. *J. Cell. Mol. Med* **13**, 4505-4521 (2009).

470. del Olmo, N. et al. Pleiotrophin inhibits hippocampal long-term potentiation: a role of pleiotrophin in learning and memory. *Growth Factors* **27**, 189-194 (2009).

471. Gomez, D.E., Alonso, D.F., Yoshiji, H. & Thorgeirsson, U.P. Tissue inhibitors of metalloproteinases: structure, regulation and biological functions. *Eur. J. Cell Biol* **74**, 111-122 (1997).

472. Ferriero, D.M. & Miller, S.P. Imaging selective vulnerability in the developing nervous system. *J. Anat* **217**, 429-435 (2010).

473. McQuillen, P.S. & Ferriero, D.M. Perinatal subplate neuron injury: Implications for cortical development and plasticity. *Brain Pathology* **15**, 250-260 (2005).

474. Maas, L.C. et al. Early laminar organization of the human cerebrum demonstrated with diffusion tensor imaging in extremely premature infants. *Neuroimage* **22**, 1134-1140 (2004).

475. Perkins, L. et al. Exploring cortical subplate evolution using magnetic resonance imaging of the fetal brain. *Dev. Neurosci* **30**, 211-220 (2008).

476. Corbett-Detig, J. et al. 3D global and regional patterns of human fetal subplate growth determined in utero. *Brain Struct Funct* **215**, 255-263 (2011).

477. Kostovic, I. & Vasung, L. Insights from in vitro fetal magnetic resonance imaging of cerebral development. *Semin. Perinatol* **33**, 220-233 (2009).

478. Robinson, S., Li, Q., DeChant, A. & Cohen, M.L. Neonatal loss of γ–aminobutyric acid pathway expression after human perinatal brain injury. *J Neurosurg* **104**, 396-408 (2006).

479. Sizonenko, S.V. et al. Developmental changes and injury induced disruption of the radial organization of the cortex in the immature rat brain revealed by in vivo diffusion

tensor MRI. *Cereb.Cortex* **17**, 2609-2617 (2007).

480. Mrzljak, L., Uylings, H.B., Kostovic, I. & Van Eden, C.G. Prenatal development of neurons in the human prefrontal cortex: I. A qualitative Golgi study. *J. Comp. Neurol* **271**, 355-386 (1988).

481. Suárez-Solá, M.L. et al. Neurons in the White Matter of the Adult Human Neocortex. *Front Neuroanat* **3**,

482. Foster, K.A. et al. An improved survival model of hypoxia/ischaemia in the piglet suitable for neuroprotection studies. *Brain Research* **919**, 122-131 (2001).

483. Björkman, S.T., Miller, S.M., Rose, S.E., Burke, C. & Colditz, P.B. Seizures are associated with brain injury severity in a neonatal model of hypoxia-ischemia. *Neuroscience* **166**, 157-167 (2010).

484. Sullivan, S.M., Björkman, S.T., Miller, S.M., Colditz, P.B. & Pow, D.V. Morphological changes in white matter astrocytes in response to hypoxia/ischemia in the neonatal pig. *Brain Res* **1319**, 164-174 (2010).

Appendix

Gene symbol	Ant SP: Ant CP	Post SP: Post CP	Gene expression database
1190002N15Rik	1.5		2 (GP: IZ, maybe SP)
2010011I20Rik	1.4	1.4	3 (GP: VZ, SVZ)
2610017I09Rik	2.2	2.3	6 (n/a)
2810004N23Rik		1.4	5 (GP: unclear signal)
2810417H13Rik	2.0	2.0	3 (GP: SVZ)
2900073G15Rik	1.4	1.4	5 (GP: weak signal)
A130022J15Rik		1.7	4 (GP: blood vessels)
Abca8a	2.2	2.0	5 (GP: no signal)
Acsl5	1.4		5 (GP: weak signal)
Adamts1		1.4	2 (GP: SP and/or IZ)
Aif1	3.5	2.6	6 (n/a)
Akr1b3 /Gm6644	1.6	1.6	2 (GP: SVZ, IZ, maybe SP)
Alas2	1.7	1.7	4 (GP: blood vessels)
Ankrd37 /Lrp2bp		1.4	5 (GP: no signal)
Antxr1	1.7		5 (GP: no signal)
Anxa3	1.5		4 (GP: blood vessels)
Apobec1	1.4		5 (GP: weak signal)
Apod	2.0	2.8	4 (GP: blood vessels)
Apoe		1.4	4 (AB/GS: blood vessels)
Aqp11		1.4	5 (GP: no signal)
Arhgap11a	1.7	1.6	2 (GP: SP and VZ/SVZ)
Arhgdib		2.4	5 (GP/GS: weak, unclear signal)
Arl4a	1.5		6 (n/a)
Atp1a1	1.5		2 (AB: weak in SP)
Atp1b1		1.4	2 (GP: weak in SP?)
B230307C23Rik		1.5	6 (n/a)
B2m	2.6	2.6	5 (GP: no signal)
B3gnt2	1.6	1.7	5 (GP/AB: no signal)
BC017612		1.6	5 (GP: no signal)
BC028528	2.4	2.2	5 (GP: unclear signal)
Bcl6	1.5	1.9	5 (GP/GS: CP; AB: SP/IZ)
Bcl7b	1.4		5 (GP: no signal)
Bhlhe41	5.4		6 (n/a)
Birc5	1.5		3 (GP: SVZ, VZ)
Bola3		1.7	5 (GP: no signal)
Bpgm	2.1	1.6	5 (GP: weak signal)
C1qb		1.5	4 (GP/AB: blood vessels)
C1qc	3.0	4.7	4 (GP: blood vessels)
C3ar1		2.0	4 (GP: blood vessels)

Gene symbol	Ant SP: Ant CP	Post SP: Post CP	Gene expression database
Cacna2d1	1.3	1.5	2 (GP: SP and/or CP?)
Calcrl	1.4		5 (GP/GS: no signal)
Cald1	1.3	1.4	5 (GP: no signal)
Casc5		1.4	5 (GP: no signal)
Casp8	1.8	1.8	3 (GP/GS: VZ/SVZ; AB: no signal)
Cav1	2.0	1.8	3 (GP: VZ/SVZ, blood vessels)
Cck	1.6		2 (GP/GS: SP or lower CP; AB: only subcortical)
Ccnd1	1.6		6 (n/a)
Ccnd2	2.0	1.5	2 (GP: SVZ/VZ and IZ or SP)
Cd164	1.6		3 (GP/AB: SVZ/VZ)
Cd53		1.9	4 (GP: blood vessels)
Cd63	1.6	1.5	3 (GP: SVZ/VZ, blood vessels; AB: SVZ/VZ)
Cd93	2.0	1.4	6 (n/a)
Cdh10	2.4		1 (AB: in SP; GP: in SVZ and SP)
Cdh12	1.9	1.6	2 (AB: weakly in SP; GP: CP)
Cdh18	3.1	2.0	1 (GS: weakly in SP)
Cdh9	1.8	1.5	5 (GP: weak signal)
Cfh		1.5	3 (GS: SVZ/VZ, CP; GP: blood vessels)
Cflar		1.9	2 (GP: SP or lower CP; GP/AB: no signal)
Chchd3	1.4		2 (GP: SP or IZ, SVZ/IZ; GP: no signal)
Cited2		1.5	2 (GP. SP or IZ, SVZ; AB: unclear signal)
Ckap2		1.4	3 (GP: VZ/SVZ)
Cks2		1.6	2 (GP: VZ/SVZ, IZ, maybe SP)
Cldn5	1.4	1.7	4 (GP: blood vessels)
Clic1		1.4	3 (GP: SVZ/VZ; GS: unclear signal)
Coro2b		1.4	5 (GP: weak signal)
Cpsf4		1.4	2 (GP: SP and VZ/SVZ; GS: no signal)
Crabp1		1.7	2 (GP: preplate; GS: SP or IZ in GFP)
Crim1	1.4		2 (GP: very weak in SP; GS: SP or IZ in GFP)
Crtac1 /Golga7b	1.4		2 (GP: preplate, SP; AB: maybe weak in SP)
Csdc2	1.4		2 (AB: VZ, SVZ, SP?)
Csmd3		1.6	5 (GP: no signal)
Cspp1	1.8		3 (GP: VZ, SVZ, CP)
Ctla2a	1.8	1.6	3 (GP: CP and SVZ)
Ctsd		1.4	4 (GP: blood vessels)
Ctss	3.6	4.9	4 (GP: blood vessels; AB: no signal)
Cux1/Cutl1	1.9	2.1	2 (AB: VZ, SVZ, IZ, maybe SP; GP/GS: mostly VZ, SVZ)
Cux2		1.5	3 (GP, AB, GS: mainly in IZ)

Gene symbol	Ant SP: Ant CP	Post SP: Post CP	Gene expression database
Cxcr4		1.4	3 (GP, AB, GS: only outside cortex)
Cyth3	1.5		6 (n/a)
Dact1	1.6		2 (GP: preplate, SP; AB: poster SP or IZ)
Dap		1.4	6 (n/a)
Dbi	2.1	2.1	3 (GP/AB: SVZ/VZ)
Decr1		1.4	6 (n/a)
Dennd4a	1.7		6 (n/a)
Dlx1as	1.3	1.5	6 (n/a)
Dnajc15		1.6	6 (n/a)
Dnajc3	1.5		5 (GP: unclear signal)
Dnmt3a	1.4	1.3	5 (GP/GS/AB: unclear signal)
Dok5	1.4		3 (GS: CP)
Dpp10	1.5		2 (GP: MZ, SP, IZ)
E130006D01Rik		1.5	5 (GP: no signal)
Egfl7		1.4	4 (GP: blood vessels)
Eltd1	1.6		4 (GP: blood vessels)
Emcn	1.4	1.8	4 (GP: blood vessels)
Eomes		1.6	3 (GP, GS, AB: SVZ/VZ)
Epas1	1.4		4 (GP: blood vessels)
Epha3	1.5	1.4	2 (GP, AB: in IZ, SVZ, VZ maybe SP)
Erbb2ip	1.7	1.7	2 (GP: SP, IZ, SVZ, VZ)
F11r		1.6	5 (GP: unclear signal)
Fabp7	2.7	2.2	3 (GP: VZ/SVZ)
Fam162b		1.8	6 (n/a)
Fam84a	1.5		2 (GS: SP or IZ in GFP animal)
Fbrs		1.6	6 (n/a)
Fcer1g		1.6	5 (GP, GS: unclear signal)
Fcrls	2.6	1.8	6 (n/a)
Flrt3	1.7	2.5	3 (GP: IZ)
Fn1	1.6	1.4	4 (GP: blood vessels)
Frmd4a		1.5	2 (GP: SP or IZ)
Fstl5	1.6		3 (GS, GP: VZ/SVZ, maybe CP)
Ftl1 / Gm10252 / Ftl2	1.4	1.5	5 (GS, GP: unclear signal)
Fuz	1.4		5 (GP: no signal)
Fzd1		1.4	3 (AB, GP: IZ; GS: no signal)
Fzd2		1.4	3 (AB, GP, GS: SVZ/VZ)
G530012D18Rik	3.2	3.1	6 (n/a)
Gab1	1.4		3 (GP: SVZ/VZ)

Gene symbol	Ant SP: Ant CP	Post SP: Post CP	Gene expression database
Gabra5	2.1	1.9	1 (AB: sparsely in SP)
Galnt7	1.4		2 (GP: SP or IZ)
Gatm	1.8		5 (GP: unclear signal)
Gbe1	1.6		3 (GP: VZ/SVZ; GS: no signal)
Gimap6	1.4		5 (GP: unclear signal)
Gja1	2.0		4 (GP: blood vessels; AB/GS: no signal)
Gkap1		1.5	6 (n/a)
Glt28d2	1.6	1.3	5 (GP: no signal)
Gm10001	1.4		6 (n/a)
Gm3579	1.4		6 (n/a)
Gm5226	1.5	1.6	6 (n/a)
Gm5263		1.5	6 (n/a)
Gm8681	1.9	2.7	6 (n/a)
Gmfg	1.4		5 (GP: no signal)
Gnai2	1.4	1.4	3 (GP: VZ/SVZ, blood vessels; GS:VZ/SVZ)
Gng11	1.9	2.0	5 (GP: weak signal)
Gng12		1.4	3 (GP/GS: VZ/SVZ)
Gng5		1.4	2 (GP: unclear signal; GS: GFP in SP or lower CP)
Grb10		1.4	3 (GP, GS: VZ/SVZ)
Gspt2		1.4	2 (GP: maybe in SP/IZ)
Gstk1		1.6	5 (GP: no signal)
Gstm5	1.7	1.6	3 (GP: SVZ/VZ)
Gvin1		1.4	5 (GP: no signal)
H19	1.8	1.6	3 (GP: ventral VZ/SVZ, blood vessels)
H2afx		1.4	3 (GP: SVZ, some blood vessels)
Hadha	1.4		3 (GP: VZ/SVZ, CP)
Hba-a1 /Hba-a2	1.7	1.5	4 (GP: blood vessels)
Hba-x	2.1	2.2	6 (n/a)
Hbb-b1 /Hbb-b2	1.4		4 (GP: blood vessels)
Hbb-y	2.2	3.1	4 (GP: blood vessels)
Heg1	1.4	1.6	3 (GP: VZ, SVZ, IZ, blood vessels)
Hexb		2.2	5 (GP: no signal)
Hhex	1.5		5 (AB: CP/SP; GP: no signal)
Higd1b		2.6	6 (n/a)
Hist1h2bk / Gm11277	1.5	1.4	6 (n/a)
Hist1h2bm	1.4		6 (n/a)
Hmgb2	2.0	2.9	2 (GP: VZ, SVZ, SP?)
Htr2a	1.5		5 (GP/GS: no signal)

Gene symbol	Ant SP: Ant CP	Post SP: Post CP	Gene expression database
Id3	1.5	1.4	4 (GP/AB: blood vessels)
Id4	1.4		3 (GP, AB: VZ/SVZ; GS: no signal)
Ide	1.5		3 (GP: VZ, SVZ)
Ier3		1.7	5 (GP, GS: no signal)
Ifitm3	1.8		5 (GP: no signal)
Ifngr1	1.4		2 (GP: SVZ and SP/lower CP)
Igf2	1.5	1.5	4 (GP, GS, AB: blood vessels)
Igfbp7	2.4	2.2	6 (n/a)
Ing2	1.4		5 (GP: no signal)
Insm1	1.5	1.3	3 (GP: SVZ, VZ, IZ)
Itm2a	2.0	1.6	4 (GP: blood vessels)
Itpr1		1.4	2 (GP/AB: SP, MZ, IZ?)
Jph1	1.9	1.7	5 (GP: unclear signal)
Jun		1.4	2 (AB: VZ, SVZ, SP; GS/GP: VZ, SVZ)
Kbtbd11	1.6	1.7	2 (GP: strongest in SP?)
Kcnab1	2.0	1.4	1 (AB: SP)
Kcnip4	2.3		5 (GS, GP: no signal)
Kcnj8	1.9	2.0	5 (GP: unclear signal)
Kcnt2	2.2	1.9	6 (n/a)
Kif11	1.5		3 (GP: VZ, SVZ)
Kif1c	1.5		2 (GP: SP or lower CP)
Lama4	1.4	1.6	4 (GP: blood vessels)
Lca5	1.5		3 (GP: CP, SVZ, VZ)
Lcp1	2.3		4 (GP: blood vessels)
Lhx2		1.7	2 (GP/AB:VZ, SVZ, IZ, SP)
Limch1		1.4	5 (GS: unclear signal)
Lmo2		1.6	4 (GP: blood vessels; GS: unclear signal)
Lmo4	1.4		3 (AB: CP, SP; GP/GS: mostly subcortical)
Lpar1	1.4		3 (GS: VZ, SVZ)
Lrrc4c	1.4		6 (n/a)
Lrrc6		1.5	5 (GP: no signal)
Lrrn3	1.3	1.4	3 (GP, GS, AB: SVZ/VZ)
Luzp2	2.2		5 (GP: no signal)
Ly86		2.4	5 (GP: no signal)
Lyn	1.4	1.4	5 (GS: no signal)
Lyz2	1.3	1.4	5 (GS: unclear signal)
Maff	1.5		5 (GP: no signal)
Mapk10	1.4		5 (AB, GS: unclear signal; GP: CP)
March1	1.4		2 (GP: SP?)

Gene symbol	Ant SP: Ant CP	Post SP: Post CP	Gene expression database
Mctp1	1.6		5 (GP: no signal)
Mdk		2.0	3 (GP/GS: VZ/SVZ)
Mfsd2a		1.5	6 (n/a)
Mgat4a	1.4		5 (GP: no signal)
Mir196a-2		1.5	6 (n/a)
Mki67	1.4	1.8	4 (GP: blood vessels, VZ/SVZ)
Mlec	1.4		6 (n/a)
Mpeg1	2.2	2.3	4 (GP: blood vessels)
Mrc1		1.4	5 (GP: no signal)
Mrpl48	1.4	1.3	5 (GP: unclear signal)
Msn	1.7	1.8	3 (GP/GS: VZ, SVZ, blood vessels)
Myl9	1.6	1.5	5 (GP: no signal)
Myo1b		1.5	3 (GP, GS: VZ/SVZ)
Nap1l5	1.5		2 (MZ, SP)
Ncapg	1.3	1.4	3 (GP: SVZ, VZ)
Nebl	1.4		2 (GP: preplate, SP and/or lower CP)
Nes	1.5	2.4	2 (AB/GS: VZ, SVZ, IZ, SP)
Neto1	3.0	1.5	3 (GS: olfactory bulb)
Neurod1	1.6	1.4	2 (AB: SVZ; GP: SVZ, IZ, SP)
Neurog2	1.4	1.8	3 (GS: VZ, SVZ)
Nhlh1		1.5	2 (GS: GFP in SP; GP: IZ; AB: no signal)
Nhsl1	1.6	1.3	5 (GP: weak)
Nid2 /2700060E02Rik		1.4	3 (GP: VZ, SVZ, CP)
Nr4a2/Nurr1	1.6		1 (AB, GS, GP: SP and ventricular zones)
Nrarp	1.7		3 (GS: VZ, SVZ)
Nrp1	2.0	2.0	2 (GS, AB, GP: IZ and SP?
Nt5dc2 /Stab1	1.4	1.5	2 (GP: IZ, SP)
Nusap1 / Oip5	1.4		3 (GP: VZ, SVZ)
Odz1	1.4		4 (GP: weak signal)
Ogfrl1		1.6	1 (GP: SP)
Omg	1.4		5 (GP/GS: no signal)
Ostf1		1.4	5 (GP, GS, AB: weak signal)
Palmd	1.5	1.8	2 (GS: VZ, SVZ, IZ, maybe SP)
Pcdh18	1.6		6 (n/a)
Pcdh8		1.5	5 (GP: no signal)
Pcsk2	1.5		1 (AB/GP: SP)
Pde1a	1.8	1.6	1 (GP: VZ, SVZ, SP; AB: no signal)

Gene symbol	Ant SP: Ant CP	Post SP: Post CP	Gene expression database
Pde5a		1.4	5 (GP, AB:unclear signal)
Pdzrn3		1.4	2 (GP, GS: SP and/or IZ)
Pid1	1.4		6 (n/a)
Pla2g16		1.4	6 (n/a)
Plac9	1.4		5 (GP: weak signal)
Plk1	1.6		3 (GP: VZ, SVZ)
Pls3	1.4		1 (GP: SP)
Plxna4	1.7	1.7	2 (GP: IZ, SP)
Pnp	1.8	1.7	5 (GP: unclear signal)
Pou3f2	1.3	1.4	2 (GS, AB: ubiquitous but weaker in CP; GP: unclear signal)
Ppic	1.5	1.9	5 (GS: no clear signal)
Ppp1r1a		1.5	3 (GP, GS: VZ/SVZ)
Ppp2r1b	1.4	1.4	2 (GP: SP and/or IZ)
Prdm8		1.4	3 (GP: SP and CP)
Psmb10		1.4	3 (GP: CP, SP)
Ptchd1	1.6		6 (n/a)
Ptger3		1.4	5 (GP, GS: weak or no signal)
Ptn	1.4	1.6	2 (GS: GFP in SP; GP: VZ)
Ptpla		1.5	6 (n/a)
Ptprk	1.5		3 (GP, GS: SVZ; AB: IZ)
Rab31	1.4		5 (GP: weak signal)
Ralb		1.5	4 (GP: blood vessels)
Ramp2	1.6		4 (GP: blood vessels)
Rasgrp3		1.4	3 (GS: VZ, SVZ; GP: weak signal)
Rbms1	1.4		3 (GS: only subcortical expression)
Rbms3	1.4		6 (n/a)
Rbp1	1.5	1.5	3 (GP, GS: VZ, SVZ)
Rcan2	1.7		1 (GS: SP)
Rgs10	1.7	2.6	5 (GP, GS, AB: no or weak signal)
Rgs2	1.4	1.7	5 (GS, GP: no signal)
Rgs5	2.6	2.0	4 (GS: blood vessels)
Rnase4 / Ang	1.4	1.4	5 (GP: no signal)
Rnasel	1.4		5 (GP: weak signal)
Rnf217	1.6		6 (n/a)
Robo2	1.6	1.9	2 (GP: IZ, SP?)
Rras2	1.6		3 (GP: VZ, SVZ, blood vessels)
Satb2	1.4	1.9	2 (GP: IZ, SP?)
Scrn1	1.4		3 (GP, GS: VZ, SVZ, IZ)

Gene symbol	Ant SP: Ant CP	Post SP: Post CP	Gene expression database
Sema3a		1.4	3 (GP: IZ, SVZ, VZ)
Sema6d	1.7	1.8	2 (GP: IZ, SP?)
Sepp1	2.4	2.6	5 (GP, GS: unclear signal)
Serf2		1.4	5 (GP: unclear signal)
Serpine2	2.1	1.7	3 (GP: not expressed in cortex)
Serpinh1		1.6	3 (GP, GS: VZ, SVZ, blood vessels)
Sirt1	1.4		5 (GP, GS: no signal)
Slc17a6		1.8	3 (GP, AB: IZ)
Slc25a37	1.4		5 (GP: no signal)
Slc25a40		2.4	6 (n/a)
Slc2a1	1.5	1.6	4 (GS, AB: blood vessels; GP: no signal)
Slc35b4	1.4		2 (GP: IZ, SP, MZ?)
Slc4a4	1.4	1.8	6 (n/a)
Slc7a5	1.4		5 (GP: no signal)
Slc8a1	1.4		2 (GP: SP?)
Slitrk3	1.5	1.5	2 (GP: preplate, MZ, SP; GS: no signal)
Smc4	1.4	1.4	6 (n/a)
Smyd3	1.4		5 (GP: unclear signal)
Snap23		1.5	5 (GP: unclear signal)
Sox18	1.7		5 (GP: unclear signal)
Sparc	2.3	2.3	5 (GS, GP: unclear signal)
Sparcl1	1.4		4 (GP: blood vessels; GS: unclear signal)
Spc25	2.1		6 (n/a)
Sphkap	1.4		6 (n/a)
Stxbp6		1.4	3 (GP: VZ, SVZ, hippocampal anlage; AB: hippocampal anlage)
Sulf2	1.7	1.5	2 (GP:anterior SP?)
Sv2b	1.7		2 (GP: preplate, SP, MZ)
Syne2	1.8		2 (GP: VZ, SVZ, SP?)
Szt2	1.4		6 (n/a)
Tacc3		1.5	3 (GP: VZ, SVZ)
Tcf12	1.6	1.5	3 (GP, GS, AB: SVZ,VZ, IZ)
Tgds	1.5		5 (GP: unclear signal)
Tifa		1.5	3 (GP: VZ, SVZ, blood vessels)
Tle1		1.4	2 (GP, AB: SP, SVZ, VZ; GS: SVZ, VZ)
Tmeff2	2.0		2 (GP: SP or lower CP?)
Tmem158	1.4	1.5	6 (n/a)
Tmem176b	1.6		6 (n/a)
Tmem177		1.4	6 (n/a)

Gene symbol	Ant SP: Ant CP	Post SP: Post CP	Gene expression database
Top2a	2.0	2.0	3 (GP: VZ, SVZ, blood vessels)
Tpbg	3.7	1.7	3 (GP: VZ, SVZ)
Trps1	1.9		3 (GP, GS, AB: VZ, SVZ, olfactory bulb)
Tspan7		1.4	5 (GP: unclear signal)
Ttc28	1.3	1.5	2 (GS: IZ, SP, MZ)
Ttc39c		1.4	6 (n/a)
Ttc9	1.4		5 (GP: no signal)
Txn2		1.4	5 (GP: no signal)
Tyrobp	4.3	4.9	4 (GP: blood vessels)
Uaca	1.3	1.5	6 (n/a)
Ube2c /Tnnc2		1.5	5 (GP: no signal)
Unc5c	1.5	1.8	2 (GS: SP?)
Unc5d	2.2	1.3	2 (GP: SP or IZ)
Usp46	1.9	1.3	5 (GP: unclear signal)
Uxt	1.3	1.4	3 (GP: VZ, SVZ, maybe CP)
Vamp8	1.7		6 (n/a)
Vmn2r122	1.4		6 (n/a)
Vmn2r84	1.4		6 (n/a)
Vti1a	1.4		6 (n/a)
Vtn	2.1	1.5	4 (GP: blood vessels)
Zbtb1	1.4		3 (GP: VZ, SVZ)
Zc3h12c		1.7	5 (GP: no signal)
Zcchc12	1.5		2 (GP, GS: SP, MZ?)
Zdhhc2	2.0	2.0	2 (GP: SP or lower CP?, VZ)
Zeb1	2.0	1.5	3 (GS: VZ, SVZ)
Zfp36l1	1.6		3 (GP: VZ, SVZ)
Zfp385b	1.6		6 (n/a)
Zhx1	1.4		2 (GP, AB: VZ, SVZ, maybe SP)
Zic3		1.5	3 (GS: only extracortical; GP, AB: no signal)

Supplementary Table S_1. **Genes enriched in the E15.5 subplate based on the microarray expression analysis.** This table lists in alphabetical order all 334 genes with significantly higher mRNA levels in the subplate (SP) than the cortical plate (CP) as determined by microarray analysis (p-value > 0.05; fold-change ≥ 1.4). Publicly available in situ hybridization datasets from AllenBrainAtlas (AB), Genepaint (GP) and Gensat (GS) were used to validate this list and to assign genes to the following categories: 1: specifically expressed in SP; 2: expressed in SP and/or lower CP and/or intermediate zone (IZ) but difficult to localize; 3: clearly expressed but not in the SP; 4: expressed in blood vessels; 5: weakly or not expressed; 6: not available (n/a). SVZ: subventricular zone; VZ: ventricular zone; MZ: marginal zone;

		E13.5	E14.5	E15.5	E17.5	P8	Adult
Abca8a	*neocortex*	n.e.	SP	SP	SP	L5 in some areas of the cortex, rarely L2/3	no clear labeling but darker band in lower L6 and SP
	telencephalon	n.e.	n.e.	n.e.	claustrum	claustrum, end. n., subiculum	no clear labeling
	diencephalon	n.e.	n.e.	n.e.	n.e.	n.e.	no clear labeling
Unc5c	*neocortex*	n.e.	SP (esp. lateral)	SP and lateral CP	weak in SP and CP (esp. medio-dorsal)	weak, strongest in L5 and upper L6, very few SP cells	weak ubiquitous expression
	telencephalon	n.e.	claustrum	claustrum	claustrum, olfactory bulb	claustrum (?), sparse cells in hippocampus	weak ubiquitous expression
	diencephalon	epithalamus, thalamus (medioventral part), prethalamus	epithalamus, thalamus (medioventral part), prethalamus	epithalamus (habenular n.), thalamus (esp DLG), prethalamus	thalamus (esp. DLG),	thalamus (especially ventromedial nucleus)	weak ubiquitous expression
Slc8a1	*neocortex*	lateral cortex	strong in SP, weaker in CP	strong in SP, weaker in CP	SP and CP	strongest in SP, weaker in L5 and 6;	strongest in SP, weaker in L5 and 6
	telencephalon	piriform cortex	piriform cortex, hipp.anlage, septum	hipp.anlage, septum, GP	septum, hippocampus, GP	very widespread, particularly strong in septal nuclei, ; not expressed in striatum	very widespread, particularly in end. n., claustrum; not expressed in striatum
	diencephalon	n.e.	n.e.	thalamus	thalamus	widespread, particularly strong in some thalamic nuclei, hypothalamus	widespread, strong in some thalamic nuclei

		E13.5	E14.5	E15.5	E17.5	P8	Adult
Zdhhc2	*neocortex*	lateral SP, piriform cortex	weak in SP, piriform cortex	SP, piriform cortex	SP and upper CP	strongest in SP, L5a and L 4	entire cortex, strongest in L4
	telencephalon	septum	septum, olfactory amygdala, bed n. of stria terminalis	septum, olfactory amygdala, bed n. of stria terminalis	piriform cortex, septum, olfactory amygdala, olfactory bulb	widespread expression, strongest in the hippocampus (CA1)	widespread expression, strongest in hippocampus (CA1)
	diencephalon	n.e.	thalamus, hypothalamus	thalamus, hypothalamus	prethalamus	widespread expression, strongest in the tRN	widespread expression, strongest in the tRN
Ogfrl1	*neocortex*	lateral cortex, piriform cortex	SP, lateral CP	SP and lateral CP	SP and lower CP	SP and L6	SP and L6
	telencephalon	n.e.	n.e.	olfactory bulb, induseum griseum, hipp. anlage	olfactory bulb, hippocampus	hippocampus (CA3), claustrum, end. n., olfactory bulb (glomerular and mitral layers)	hippocampus (CA3) claustrum, end. n.
	diencephalon	n.e.	weak in thalamus	weak in thalamus	weak in thalamus	thalamic nuclei	thalamic nuclei (absent in medial, weak in lateral, strong in ventral nuclei, esp. ventroposterior th. n.)
Gabra5	*neocortex*	lateral SP, piriform cortex	SP	SP (ant-post gradient)	SP and CP (ant-post gradient)	Strongest in SP and L5	SP and L5
	telencephalon	olfactory bulb	piriform cortex, basal ganglia olfactory amygdala, olfactory bulb	piriform cortex, septum, basal ganglia, hipp. anlage, olfactory tubercule, olfactory amygdala	hippocampus, induseum griseum, olfactory bulb (mitral layer), basal ganglia	hippocampus, claustrum, piriform cortex, amygdala	hippocampus, claustrum
	diencephalon	hypothalamus	hypothalamus (?)	hypothalamus (?)	hypothalamus	hypothalamus, thalamus	thalamus (?)

		E13.5	E14.5	E15.5	E17.5	P8	Adult
Csmd3	*neocortex*	lateral cortex	SP, very lateral CP	SP, lateral CP	SP and CP	ubiquitous expression	weak ubiquitous expression
	telencephalon	piriform cortex	piriform cortex, septum, GP, olfactory amygdala	piriform cortex, olfactory amygdala, GP	strong in basal ganglia, septum, amygdala	ubiquitous expression	weak ubiquitous expression
	diencephalon	prethalamus	prethalamus, hypothalamus	hypothalamus, prethalamus	prethalamus, thalamus, hypothalamus,	ubiquitous expression	weak ubiquitous expression
Cdh10	*neocortex*	n.e.	SP	SP, anterio-lateral CP	strongest in SP, weaker in CP, SVZ	strongest in SP and upper L5	strongest in L5 and SP
	telencephalon	n.e.	piriform cortex	piriform cortex	olfactory cortex	hippocampus (CA1/2)	hippocampus (CA1/2)
	diencephalon	n.e.	n.e.	n.e.	thalamus	certain thalamic nuclei	certain thalamic nuclei ?
Cdh18	*neocortex*	n.e.	SP	SP	SP, upper CP	SP, very weak in L5 and L6	SP and L6
	telencephalon	n.e.	piriform cortex, septum, olfactory tubercle,	GP, claustrum, olfactory amygdala, substantia innominata,	GP, claustrum,	claustrum, IMLF	n/a
	diencephalon	n.e.	prethalamus	prethalamus	prethalamus (VLG)	prethalamus	n/a
Pls3	*neocortex*	lateral cortex	SP	SP, most ant CP	SP, lateral CP	strongest in SP, then in L5	strongest in SP, weaker in all other layers
	telencephalon	n.e.	n/a	olfactory bulb, hipp. anlage, piriform cortex, subpallial SVZ	hippocampus	claustrum, end. n., n. accumbens, hippocampus	claustrum, end. n., basolateral amygdala, hippocampus
	diencephalon	n.e.	n.e.?	n.e. ?	n.e. ?	thalamic nuclei (e.g. parafascicular thalamic n.)	certain thalamic nuclei

		E13.5	E14.5	E15.5	E17.5	P8	Adult
Rcan2	*neocortex*	MZ	MZ	MZ, sometimes weak in SP	SP, MZ	single cells in the whole cortex, dark band in SP	single cells in the whole cortex, dark band in SP
	telencephalon	basal ganglia	hippocampus, preoptic area	hippocampus, claustrum, basal ganglia, piriform cortex, substantia innominata, baso-lateral amygdala	hippocampus, claustrum	hippocampus, striatum, ventral pallium	endopirifform nucleus, piriform cortex, central amygdala
	diencephalon		prethalamus and hypothalamus	prethalamus and hypothalamus	thalamic and hypothalamic nuclei (e.g. paraventricular hypothalamic n.)	pavaraventricular hypothalamic nucleus, tRN, laterodorsal th. nucleus	hypothalamus
Sv2b	*neocortex*	preplate, lateral SP and MZ	SP, MZ	SP, MZ	entire cortex	entire cortex	entire cortex
	telencephalon	preoptic area, basal ganglia	preoptic area, piriform cortex, hippocampal anlage, septum	claustrum, piriform cortex, endopiriform n., basal ganglia, hippocampus	very widespread	ubiquitous	ubiquitous
	diencephalon				very widespread	ubiquitous	ubiqutious

		E13.5	E14.5	E15.5	E17.5	P8	Adult
Kcnt2	*neocortex*	preplate, lateral SP and MZ	SP, MZ	SP, MZ, sometimes in CP	entire cortex	entire cortex	entire cortex
	telencephalon	preoptic area, basal ganglia	preoptic area, piriform cortex, hippocampal anlage, septum	claustrum, piriform cortex, endopiriform n., basal ganglia, hippocampus	very widespread	ubiquitous	ubiquitous
	diencephalon				very widespread	ubiquitous	ubiquitous

Supplementary Table S_2. **Cortical and extracortical expression of subplate-enriched genes at different developmental stages.** This table lists structures in the cortex, the extracortical telencephalon and the diencephalon where subplate-enriched genes were found to be additionally expressed. This list is not exhaustive and only describes areas where expression was clearly visible on the available sections. SP: subplate; MZ: marginal zone; CP: cortical plate; L: layer; n.e.: not expressed; end. n.: endopiriform nucleus; DLG: dorsolateral geniculate nucleus; VLG: ventrolateral geniculate nucleus; tRN: thalamic reticular nucleus; hipp. anlage: hippocampal anlage; SVZ: subventricular zone; GP: globus pallidus; IMLF: interstitial nucleus of the medial longitudinal fasciculus.

E15.5		
Adamts1	a disintegrin-like and metallopeptidase with thrombospondin type 1 motif	cleavage of extracellular matrix proteins
Atp1a1	ATPase, Na+/K+ transporting, alpha 1 polypeptide	basic electrophysiological properties
Atp1b1	ATPase, Na+/K+ transporting, beta 1	basic electrophysiological properties
Cacna2d1	calcium channel, voltage-dependent, alpha2/delta subunit 1	electrophysiological properties
Cdh12	cadherin 12	layer organization, neurite growth and guidance, synapse formation
Cdh18	cadherin 18	layer organization, neurite growth and guidance, synapse formation
Cflar/C-flip	CASP8 and FADD-like apoptosis regulator	modulator/inhibitor of apoptosis
Chchd3	coiled-coil-helix-coiled-coil-helix domain containing 3	mitochondrial membrane protein; important for mitochondrial function
Cpsf4	cleavage and polyadenylation specific factor 4	mRNA processing and regulation
Csdm3	CUB and Sushi multiple domains 3	putative transmembrane protein
Dact1	dapper homolog 1, antagonist of beta-catenin	establishment of dendrites and excitatory synapses
Frmd4a	FERM domain containing 4A	scaffolding protein; could play a role in actin cytoskeleton rearrangments
Gabra5	GABA A receptor, subunit alpha 5	ionotropic GABA receptor subunit, electrophysiological properties
Ifngr1	interferon gamma receptor 1	endogeneous INF-y regulates cell proliferation; involved in inflammatory responses
Itpr1	inositol 1,4,5-triphosphate receptor 1	regulation of internal Ca2+ stores; electrophysiological properties (oscillations, plasticity)
Kcnt2	potassium channel subfamily T, member 2	potassium channel
March1	membrane-associated ring finger (C3HC4) 1	ubiquitin E3 ligase; posttranscriptional regulation
Nebl/Lasp2	nebulette	actin filament stabilization; focal adhesion
Ogfrl1	opioid growth factor receptor-like 1	similar to Ogfr which regulates cell proliferation and tissue organization
Pcsk2/Pc2	proprotein convertase subtilisin/kexin type 2	maturation of protein precursors; synthesis of neuropeptides
Pls3	plastin 3 (T-isoform)	actin cytoskeleton reorganization, neurite growth

Plxna4	plexin A4	repulsive Sema6a receptor; axonal guidance
Robo2	roundabout homolog 2	Slit receptor; axonal guidance and interneuron migration
Satb2	special AT-rich sequence binding protein 2	transcription factor; upper neuron cell fate
Slc8a1	solute carrier family 8 (sodium/calcium exchanger), member 1	calcium homeostasis, electrophysiological properties
Slitrk3	SLIT and NTRK-like family, 3	neurite outgrowth
Sv2b	synaptic vesicle glycoprotein 2 b	synaptic transmission
Tle1	transducin-like enhancer of split 1	transcriptional co-repressor
Ttc28	tetratricopeptide repeat domain 28	Unknown
Unc5c	unc-5 homolog C	repulsive netrin receptor, axon guidance
Zdhhc2	zinc finger, DHHC domain containing 2	palmitoyl transferase, synapse plasticity
P8		
5033414K04Rik	RIKEN cDNA	Unknown
6330500D04Rik	RIKEN cDNA	Unknown
Acvr2a	activin receptor IIA	receptor for BMP7 (and BMP4)
Adcy8/AC8	adenylate cyclase 8	axonal pathfinding, learning and memory formation
Adra2a	adrenergic receptor, alpha 2a	adrenergic receptor subtype
Arhgap26	Rho GTPase activating protein 26	activator of Rho GTPase; signaling pathways
BC062109	predicted gene	Unknown
Cacng5	calcium channel, voltage-dependent, gamma subunit 5	calcium channel
Camk2d	calcium/calmodulin-dependent protein kinase II, delta	Signaling pathways including receptor recycling
Cdkn2c/Ink4c	cyclin-dependent kinase inhibitor 2C	inhibitor of CDK4 and 6; cell cycle and growth regulation
Chrna4	cholinergic receptor, nicotinic, alpha polypeptide 4	cholinergic receptor
Chst2/C6ST	carbohydrate sulfotransferase 2	Sulfonation; signaling pathways
Clic1	chloride intracellular channel 1	formation of intracellular vesicles
Clic5	chloride intracellular channel 5	formation of intracellular vesicles
Cplx3	complexin 3	regulates neurotranmitter release
Drd1a	dopamine receptor D1A	dopamine receptor
E130012A19Rik	RIKEN cDNA	Unknown
E430002G05Rik	RIKEN cDNA	unknown
Etv5/ERM	ets variant gene 5	transcription factor; activated by Fgf

Gadd45a	growth arrest and DNA-damage-inducible 45 alpha	regulation of cell cycle and cell survival
Galnt10	UDP-N-acetyl-alpha-D-galactosamine:polypeptide N-acetylgalactosaminyltransferase 10	protein glycosylation; signaling pathways
Gsta4	glutathione S-transferase, alpha 4	detoxification of oxydative stress; modification of signaling pathways
Impact	imprinted and ancient	regulates response to amino acid starvation
Inpp4b	inositol polyphosphate-4-phosphatase, type II	regulates inositol phosphate signaling
Kcnip3/DREAM	Kv channel interacting protein 3, calsenilin	regulates transcription, potassium channels and the NMDA receptor
Lmbrd1	LMBR1 domain containing 1	lysosomal membrane protein
Mmp16/MT-MMP3	matrix metallopeptidase 16	Degradation of components of the extracellular matrix
Moxd1	monooxygenase, DBH-like 1	homologous to dopamine beta-hydroxylase but with unknown substrate
Oprm1	opioid receptor, mu 1	receptor for endogeneous opioids; decreases exitability
Pctk3/PCTAIRE	serine/threonine-protein kinase PCTAIRE-3	kinase with unknown substrate
Pdia5	protein disulfide isomerase associated 5	PDIs mediate protein folding in the ER
Peg3	paternally expressed 3	regulates the wnt pathway and thus proliferation, apoptosis and others
Rgs20/RGSZ1	regulator of G-protein signaling 20	regulation of cytoskeleton; regulation of mu opioid receptor
Rgs8	regulator of G-protein signaling 8	regulation of the inward rectifying K+ channel (GIRK); regulation of the muscarinic acetylcholine receptor;
Sdk2	sidekick homolog 2 (chicken)	lamina-specific synapse formation in the retina
Sema3e	semaphorin 3E	guidance cue for axons and vascular patterning
Sorcs3	sortilin-related VPS10 domain containing receptor 3	bind NGF and maybe p75ntr; regulated by neuronal activity; cell survival or plasticity
Stt3b/Simp	STT3, subunit of the oligosaccharyltransferase complex, homolog B	glycosylation of proteins
Sulf1	sulfatase 1	cleaves heparane sulfates from the extracellular matrix

Svil	supervillin	binds to the cytoskeleton; involved in cell motility and cytokynesis
Syt1	synaptotagmin I	Ca2+ sensor for neurotransmitter release
Thbs2	thrombospondin 2	synaptogenic protein
Thrsp/S14	thyroid hormone responsive SPOT14 homolog	responds to TH; TH-induced cell death
Tmem132d	transmembrane protein 132D	specific to mature oligodendrocytes?
Tnmd	tenomodulin	anti-angiogenic in connective tissues
Trh	thyrotropin releasing hormone	neuropeptide
Adult		
Atp2b4	plasma membrane calcium ATPase 4	Na+/K+-ATPase, different subunits/ isoforms are differentially expressed and probably confer different electrophysiological properties
Cntn2	Contactin-2	adhesion molecule
Cpne2	Copine 2	Ca2+-dependant phospholipid-binding protein; involved in intracellular transport
Jup	Junction plakoglobin	catenin involved in adherens junctions
Kcnab1	Voltage-gated potassium channel subunit beta-1 (Kv-beta-1)	electrophysiological properties
Ncam1	Neural cell adhesion molecule 1	cell-cell adhesion molecule, involved in neurite outgrowth and synaptogenesis
Papss1	Bifunctional 3'-phosphoadenosine 5'-phosphosulfate synthetase 1	synthesis of PAPS, the donor of sulfate (involved in sulfation, a major modification pathway)
Pkp4	Plakophilin-4	involved in adherens junctions, in particuar desmosomes
Ptn	Pleiotrophin	growth factor associated to the extracellular matrix; involved in neurite outgrowth and synaptic plasticity
Slc9a3r2	Solute carrier family 9 isoform A3 regulatory factor 2	calcium homeostasis, electrophysiological properties
Tgfa	Protransforming growth factor alpha	regulates neurogenesis and angiogenesis; also regulates expression of neurotransmitter receptors
Timp2	Metalloproteinase inhibitor 2	regulator of metalloproteinases, enzymes involved in the degradation of the extracellular matrix

Supplementary Table S_3. **Genes with age-specific subplate-enriched expression.** This table lists genes which are only present in the microarray dataset of one developmental age (E15.5, P8 or adult). Subplate-specific expression was confirmed using public available in situ hybridization data. Main functions of each gene as described in the literature are listed.